3897

THE ELECTROCHEMISTRY OF CHEMICALLY MODIFIED CONDUCTING POLYMERS

Darryl Hirst Dawson BSc. (Hons)

A thesis submitted for

the degree of

Doctor of Philosophy

Department of Chemistry

University of Warwick

Coventry CV4 7AL

October 1992

To Mum, Dad and all those people who stuck with me when times got tough for us all.

"I'm sorry. I can't do it. I'll try harder next time".

"No! Either do or do not, there is no try. You did not believe in yourself and that is why you failed. We are more than just flesh and bones we are luminous beings!"

F. Douglas

Table of Contents

List of Figures

List of Tables

Acknowledgements

I would like to thank the following people:

Prof. Phil Bartlett for his patient and excellent supervision throughout the course of this work.

SERC for financial support.

Dr. Mike Bailes and Neil Blair for their excellent computer programs.

Drs. Keith Harris, Keith Hallinan and Chris Reeve for their help with the organic synthesis presented in this work. In particular Keith Harris for being so Welsh.

Dr. Jon Farrington for his initial studies into poly(5-carboxyindole) a polymer which we will remember fondly for many years to come.

Prof. Peter Moore, Dr. Andrew Benniston and Dr. L-Y. Chung for the pyrrole crown ether monomer.

Keith Pratt for his very diligent proof reading.

Daren Caruana for his interest in things other than chemistry.

Diego Centonze for his humour, "May your glass be forever empty!"

Peter Birkin for his sense of direction.

All the other members of the electrochemistry group both past and present at the Universities of Bath and Warwick.

Declaration

The work presented in this thesis was conducted by the author. Where work by other authors has been discussed a clear indication is given in the text.

This work was conducted in the chemistry departments at Warwick and Bath Universities under the supervision of Prof. P. N. Bartlett.

Signed.....

Summary

The work described in this thesis concentrates on chemically modified heterocyclic conducting polymers based upon pyrrole, thiophene and indole monomers with particular emphasis placed upon carboxylic acid substituents. A brief description of the electrochemistry of chemically modified poly(pyrroles) is given with an explanation of the problems associated with the chemical modifications.

A reasonable understanding of the properties of chemically modified poly(thiophenes) has been achieved. In particular the properties of poly(3-thiopheneacetic acid) have been characterised in both aqueous and nonaqueous solution using standard electrochemical techniques in conjunction with reflectance FTIR studies.

Finally the understanding of poly(indole) and poly(5-carboxyindole) electrochemistry has been greatly improved especially with regards to the chemical structure of each polymer, which was elucidated from several reflectance FTIR studies. The characterisation of the electrochemical growth and the aqueous electrochemistry of poly(5-carboxyindole) are the areas in which the greatest advances have been made. The techniques of reflectance FTIR spectroscopy, UV/vis spectroscopy and impedance spectroscopy have aided the study of poly(5-carboxyindole) immensely.

More studies need to be performed before a fuller understanding of these polymeric systems is achieved and the final chapter gives suggestions for further work which will add to the information given in this thesis.

Chapter 1

Introduction

1.0 Historical Background of Conducting Polymers

Conducting polymers have become the subject of an intensive multidisciplinary research effort over the past decade after several research groups showed that trans-poly(acetylene),[1,2,3] figure 1.1, could be made to conduct by positively doping the polymer. One of the original methods of doping was by exposure to iodine vapour,[4] figure 1.2, which is believed to be responsible for a radical attack upon the polymer which initially forms radical sites, called polarons, upon the conjugated polymer backbone.[5,6] Upon further oxidation of the polymer the polarons join together to form two spinless non-radical states called solitons. Both polarons and solitons are responsible for the conductivity of the polymer using the conjugated π-bonding system as a ladder for transporting charge down the length of the polymer chain.

Original conductivities of the doped trans-poly(acetylenes) were found to be around 1000 S cm^{-1} but there has been significant effort put into the improvement of the properties,[7] both conductive and mechanical, of trans-poly(acetylene) and its derivatives by, for example, increasing its chain length, reducing the number of defects in the conjugated system and devising new polymerisation synthetic routes.[8] Conductivities have now reached values of greater than 100,000 S cm^{-1}, however the polymers suffer from instability and attack by atmospheric oxygen which limits their potential applications.

The discovery that organic polymers could be made to conduct by virtue of a π-conjugated backbone capable of delocalising and transporting charge carriers destroyed the myth that only metals and graphite systems could exhibit conductivities above the semiconductor

Figure 1.1 Structure of trans-poly(acetylene)

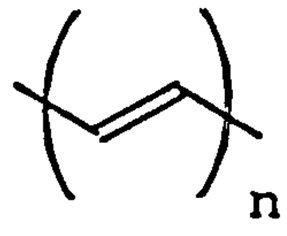

Figure 1.2 Iodine doping of trans-poly(acetylene)

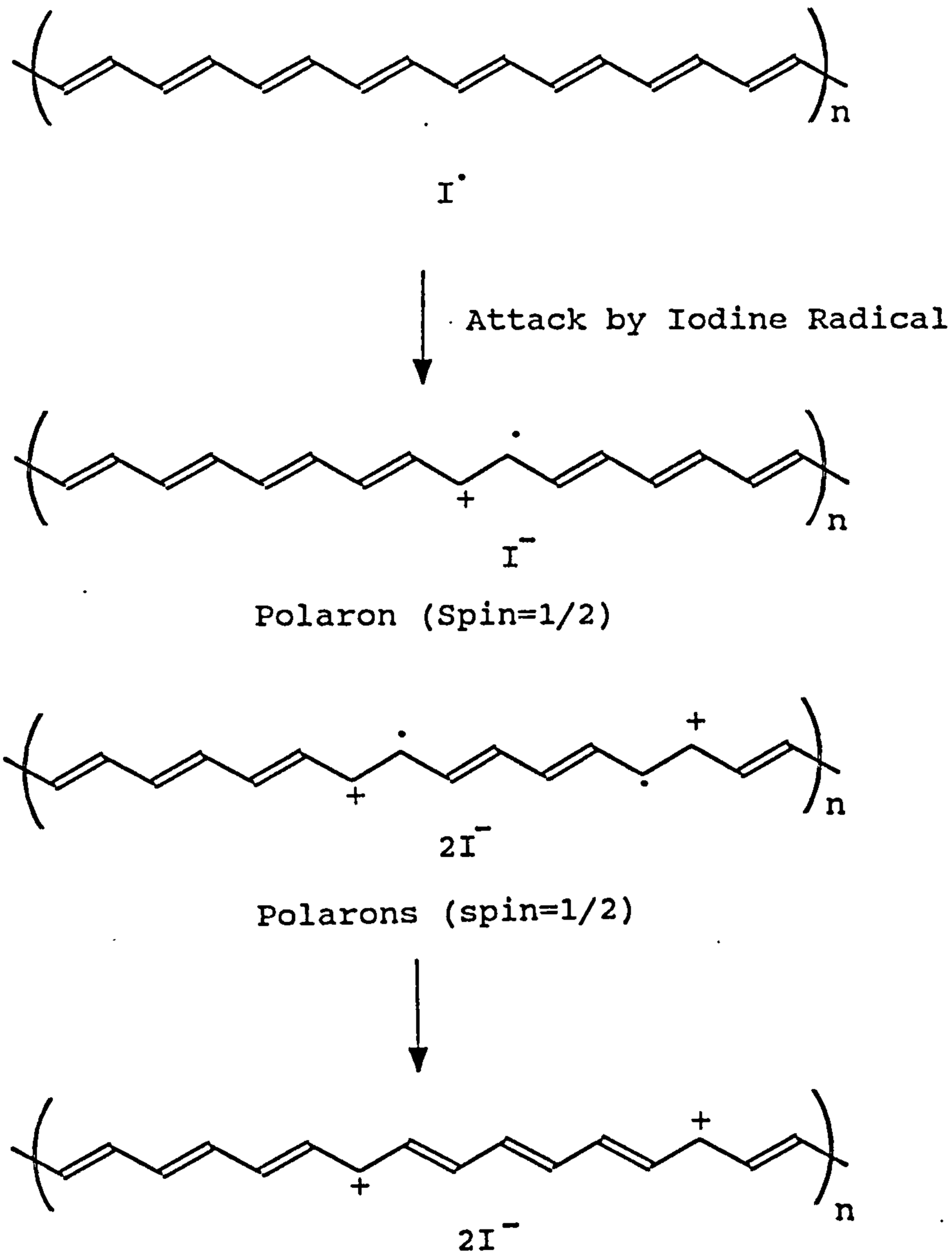

range. It is beyond the scope of this introduction to discuss further the search for more efficient conducting materials but rather to concentrate on the specific area of heterocyclic conducting polymers and the specific properties of these materials.

1.1 Heterocyclic Conducting Polymers

Conducting polymer science advanced further when it was discovered that certain heterocyclic compounds, for example pyrrole[9] and thiophene,[9] could, under the right conditions, be polymerised quite easily by oxidation of the monomer to form polymers that could be reversibly doped into the conducting state and then dedoped to an insulating state by either electrochemical or chemical means. Poly(pyrrole)[10,11,12,13] figure 1.3, initially discovered by Dall'Olio *et al.*[14] is the most studied of all the heterocyclic conducting polymers. It is bonded through the α positions of the pyrrole monomer providing an uninterrupted cis-trans π bonded conjugated network which can be oxidised into a conducting state. Regarded as one of the simplest conducting polymers it serves as a reasonable example of this class of conducting polymers.

The ease of deposition coupled with the conducting nature of the materials suggests that conducting polymers could be useful for the purpose of electrode modification. A chemically modified electrode[15] is one which has been deliberately coated with a film of foreign molecules so that the direct contact between solution species and the electrode is prevented *i.e.* electron transfer is mediated by molecules comprising the coating. Such modified electrodes lend themselves to applications such as biosensing,[16] pH determination[17] and gas sensing.[18]

The polymers formed were stable free standing films in air which displayed interesting properties other than conductivity, such as electrochromism[19] and high capacitance.[20] These polymers are generally deposited upon electrodes by electrochemical oxidation, in a suitable

solution, of the monomer which initiates the polymerisation. The polymerisation mechanisms will be discussed later in this chapter.

Some commonly studied poly(heterocycles) are shown in figure 1.4. However, there are several other more novel polymers which have been studied.

1.3 Electrochemical Polymerisation of Heterocyclic Conducting Polymers

Although heterocyclic conducting polymers can be polymerised chemically[9] by oxidising agents such as $FeCl_3$ and $Cu(ClO_4)_2$ the preferred technique, for electrochemists, is by electrochemical oxidation, and in some cases reduction, of the monomers to form radicals which then initiate the polymerisation process. The reaction mechanism for the polymerisation of heterocyclic conducting polymers is still largely unknown although several studies have been undertaken, particularly on pyrrole[13,25,26,27,28,29] and the following reaction scheme, figure 1.5, has been suggested.

The scheme shows the initial formation of a radical cation in step (a). The position or the radical site is preferentially at the α-position of the pyrrole due to a higher degree of resonance stabilisation. The position of the radical site is quite fortuitous since this is the position where a polymer bond will be formed. A polymer with bonds at the β-position would not have a continuous conjugated system; this has consequences for the conductive nature of the polymer which will be discussed later in the chapter.

Steps (b) and (c) although shown as reactions with monomers could also be thought of as reactions with polymer chains as shown by the further steps (f) and (g). Several authors[26,30,31] are sceptical as to whether step (c) takes place suggesting that two radical cations would coulombically repel each other rather than react to form a bond, but this

Figure 1.3 Chemical structure of poly(pyrrole)

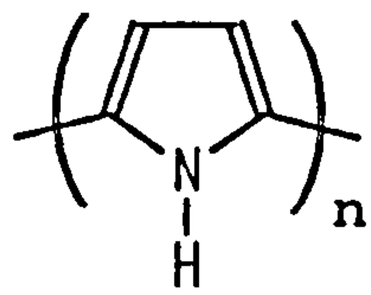

Figure 1.4 Common poly(heterocycles)

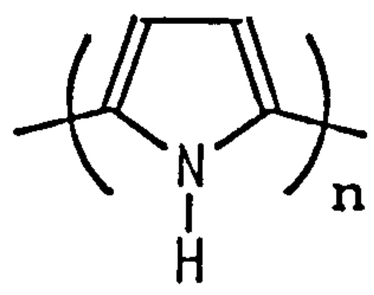

Poly(pyrrole)

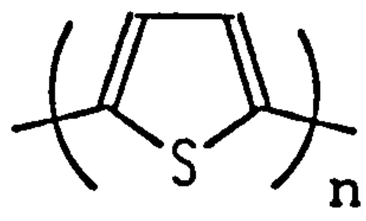

Poly(thiophene)

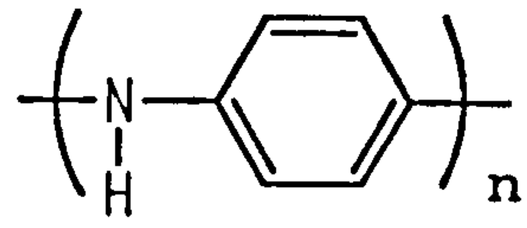

Poly(aniline)[21]

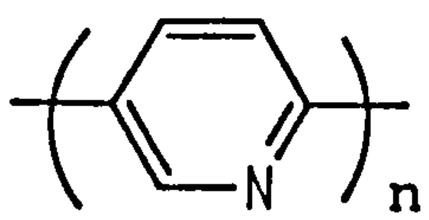

Poly(pyridine)[22]

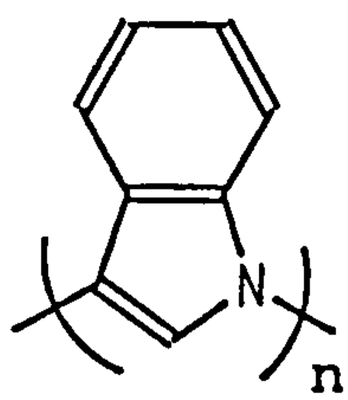

Poly(indole)[23]

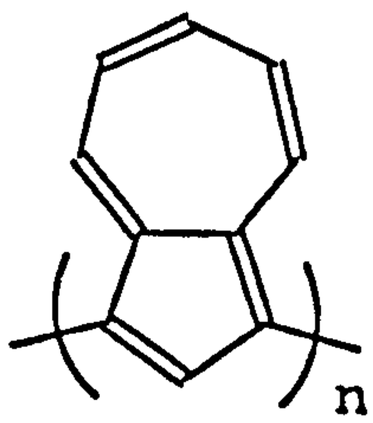

Poly(azulene)[24]

Figure 1.5 Suggested reaction mechanism for the polymerisation of poly(pyrrole)

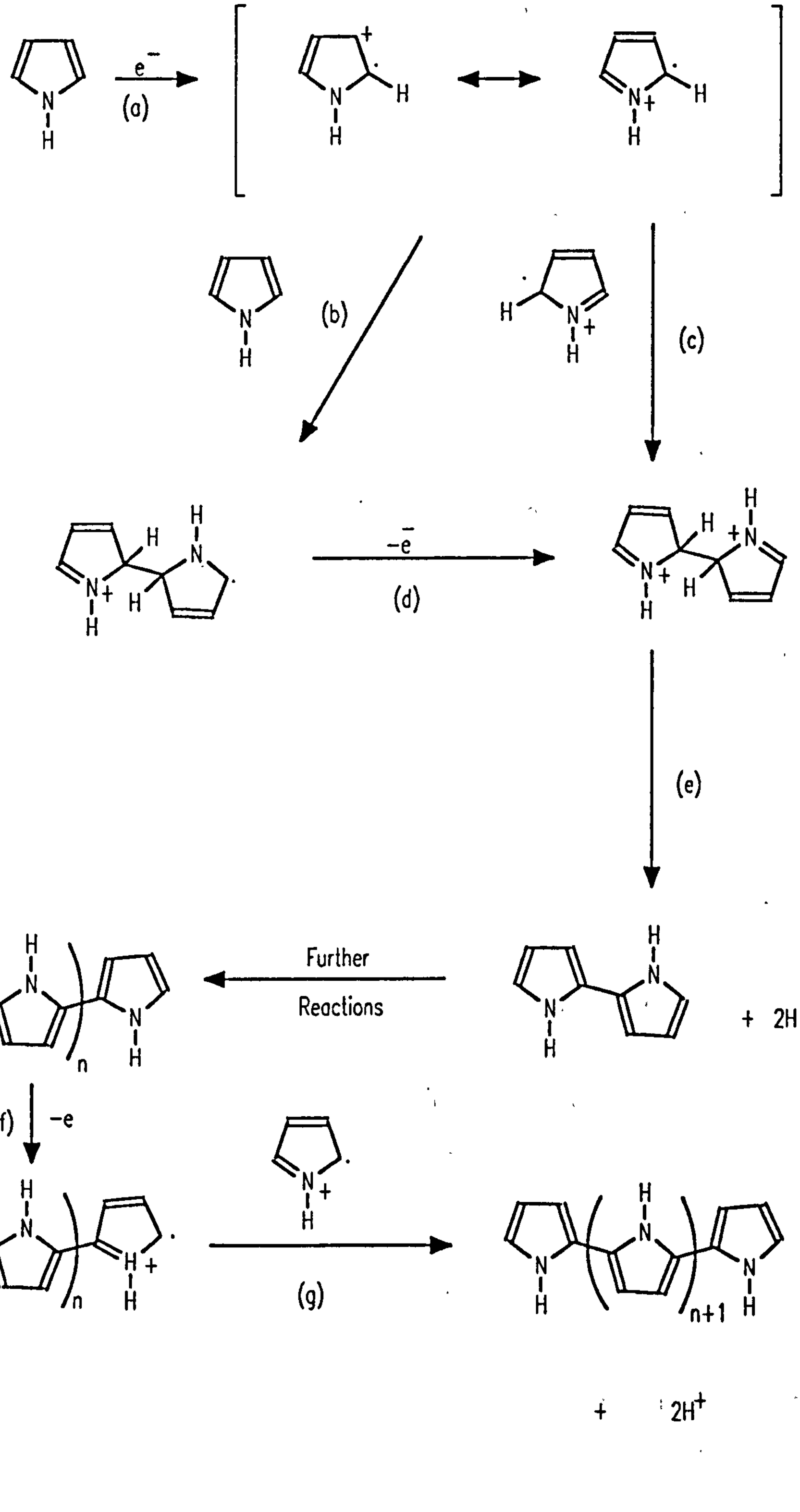

effect would be reduced by increasing the ionic strength of the growth solutions. Other authors have suggested that the radical - radical coupling is the only symmetrically allowed reaction[32] when orbital symmetry is considered. Step (b) involves the attack of a radical cation upon a neutral species followed by a further oxidative process (d) which then leads to a double deprotonation in step (e). Step (c) is also followed by step (e). The problem of determining the favoured reaction step, (b) or (c) is mainly due to the difficulty of detecting radical sites on the polymer chain during polymerisation.

One point which is generally accepted is that monomer radicals are required throughout the polymerisation and that oxidation of only the polymer in a solution containing the monomer will not result in further polymerisation. It is also accepted that large amounts of charge are consumed during the polymerisation. Two electrons per monomer unit are removed to form the polymer and charge is also taken up during the oxidation of the polymer. The amount of charge required to oxidise the polymer and the way that it is distributed in the polymer's conjugated chain will be discussed later in the chapter.

The polymerisation also depends very heavily upon the effect of the solvent[33] and the dopant[34] anion used during the growth process figure 1.6. The nucleophilicity of both the solvent and the dopant anion is the most important factor. A strongly nucleophilic species is capable of competing with the monomers in the nucleophilic attack on the polymerising radical species preventing continued polymerisation.

The susceptibility to attack by nucleophiles other than the monomer species depends greatly upon the properties of the monomer species in question. For example, pyrrole has a much lower redox half wave oxidation potential of 0.76 V vs. Ag/Ag^{+} (0.1 mol dm^{-3} in acetonitrile) than thiophene which has a value of 1.60 V against the same reference.

Figure 1.6 The effect of strong nucleophiles upon the polymerisation of poly(heterocycles)

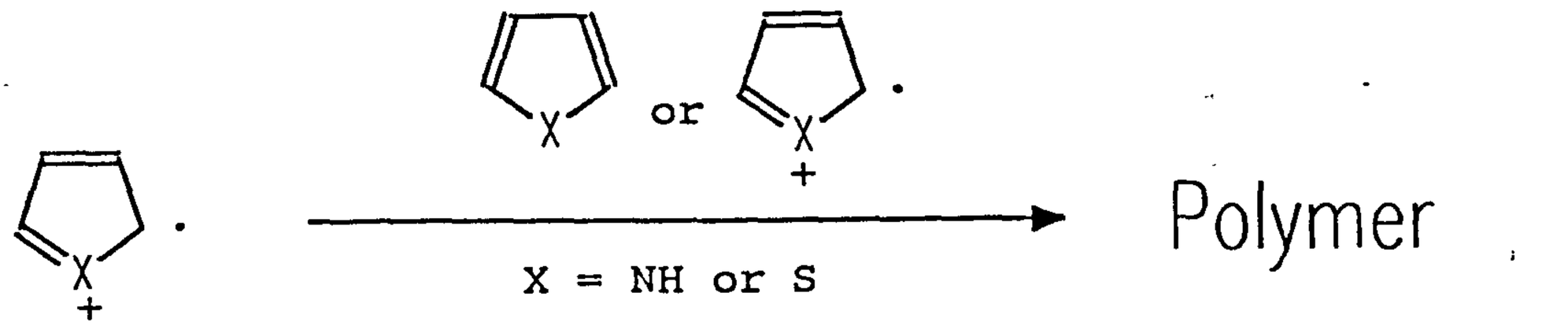

This suggests that oxidised thiophene is much more reactive than oxidised pyrrole. This is borne out in the polymerisation of the two species; pyrrole can be polymerised in both acetonitrile and water whereas thiophene cannot be polymerised under aqueous conditions. In fact the polymerisation of thiophene in acetonitrile is very sensitive to the presence of water.[35] It has been shown that traces of water (0.1 mol dm^{-3}) in acetonitrile can retard the polymerisation process by acting as a nucleophile and concentrations of greater than 1.0 mol dm^{-3} entirely prevent polymerisation.

The reactivity of the monomers can be reduced by adding electron donating substituents to the non-bonding positions but generally substituted monomers tend to behave in a similar manner to the parent monomer because the substituent cannot exert a big enough influence upon the oxidation potential.

The polymers may also be susceptible to attack from nucleophiles at the β-position after the main polymerisation is complete.[36,37] This usually occurs when the polymer has been oxidised too far, a process known as "overoxidation". After overoxidation occurs the polymer generally becomes more resistive or passive to further attempts at oxidation and reduction. Figure 1.7, shows the effect of the attack of water in acetonitrile on poly(thiophene).

1.4 Bulk Polymerisation and Electrochemical Deposition

After discussing the chemical nature of the polymerisation of heterocyclic conducting polymers the bulk behaviour of the polymerisation or electrochemical deposition must be discussed.

Electrochemical polymerisations have been performed on a variety of substrates the most popular being platinum, gold, glassy carbon and indium doped SnO_2.

Figure 1.7 The effect of "overoxidation" on poly(thiophene) in the presence of water.

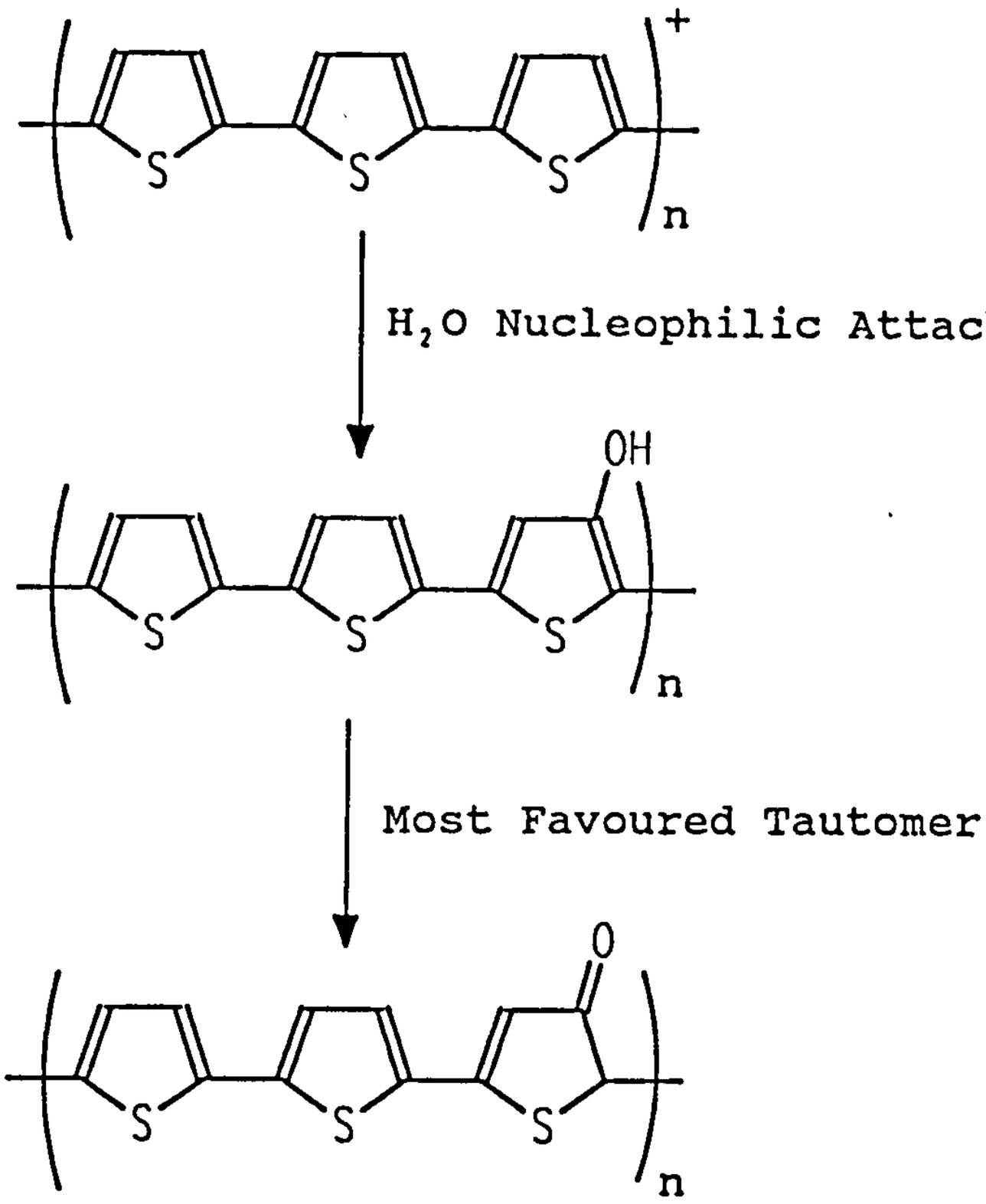

Reduction in conductivity due to disruption of conjugation and discharge of polymer

Pletcher *et al.*[35] studied the polymerisation of thiophene in acetonitrile by cyclic voltammetry and chronoamperometry at different potentials and found evidence for a nucleation process. Nucleation loops were observed during cyclic voltammetry figure 1.8, and transients recorded, figure 1.9, showed an initial rising portion with a linear $i - t^2$ relationship which can be interpreted as instantaneous nucleation and three dimensional growth. After the current peaks the transient has an $i - t^{-1/2}$ relationship which is interpreted as a film thickening process controlled by linear diffusion of the monomer to the anode.

Hillman *et al.*[38] using chronoamperometry, figure 1.10, described an initial monomer adsorbance process for the polymerisation of thiophene in acetonitrile seen as a current spike, followed by polymer nucleation resulting in a rising $i - t$ transient. As the nuclei join to form a continuous film electron transfer control results in a level $i - t$ transient.

Although these inconsistencies in results exist, due mainly to differences in growth conditions, it is generally accepted that the deposition process involves an initial three dimensional nucleation followed by a steady one dimensional growth perpendicular to the plane of the electrode, figure 1.11.

Very similar results to Hillman *et al.*[38] have been obtained for poly(pyrrole) in both acetonitrile[41] and aqueous[42] conditions. However the water content of acetonitrile has been found to affect the nucleation process. The nucleation process is retarded in very dry acetonitrile and enhanced by a 1 % increase by volume of water being added. Water is thought to act as a base[41] during the polymerisation process by removing the protons ejected during the polymer bond formation. Larger increases in water concentration have proved to be less beneficial.

Other techniques[42,43] have been used to study the nucleation process which go beyond the scope of this chapter.

Figure 1.8 Nucleation loops observed during the cyclic voltammetry at 100 mV s^{-1} of thiophene (50 mmol dm^{-3}) in acetonitrile containing TEAT (0.2 mol dm^{-3}) at a platinum electrode[35]

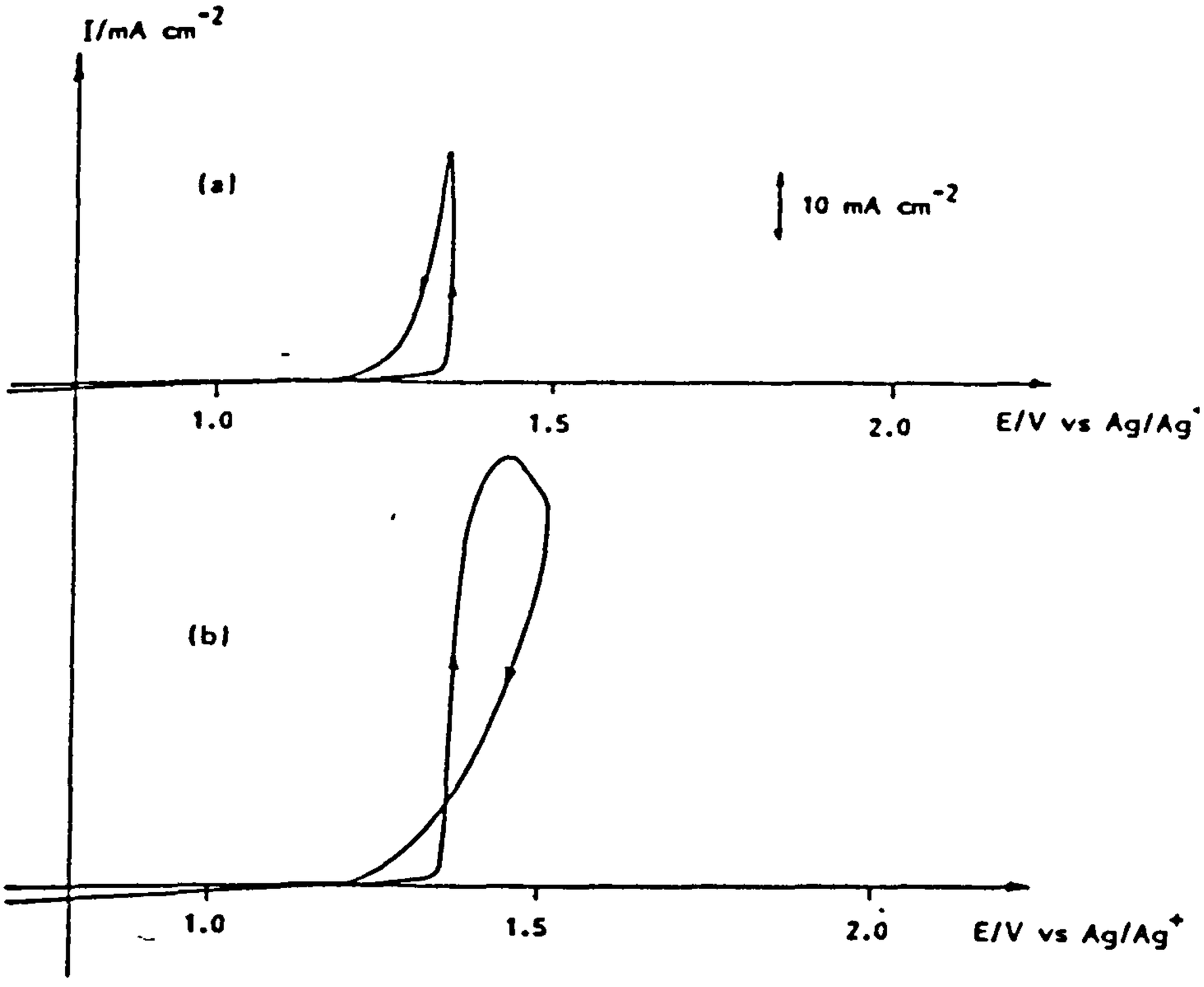

Figure 1.9 Potentiometric steps,[35] at a platinum electrode, of a thiophene (50 mmol dm^{-3}) acetonitrile solution containing TEAT (0.2 mol dm^{-3}) at various potentials vs. Ag/Ag^{+}

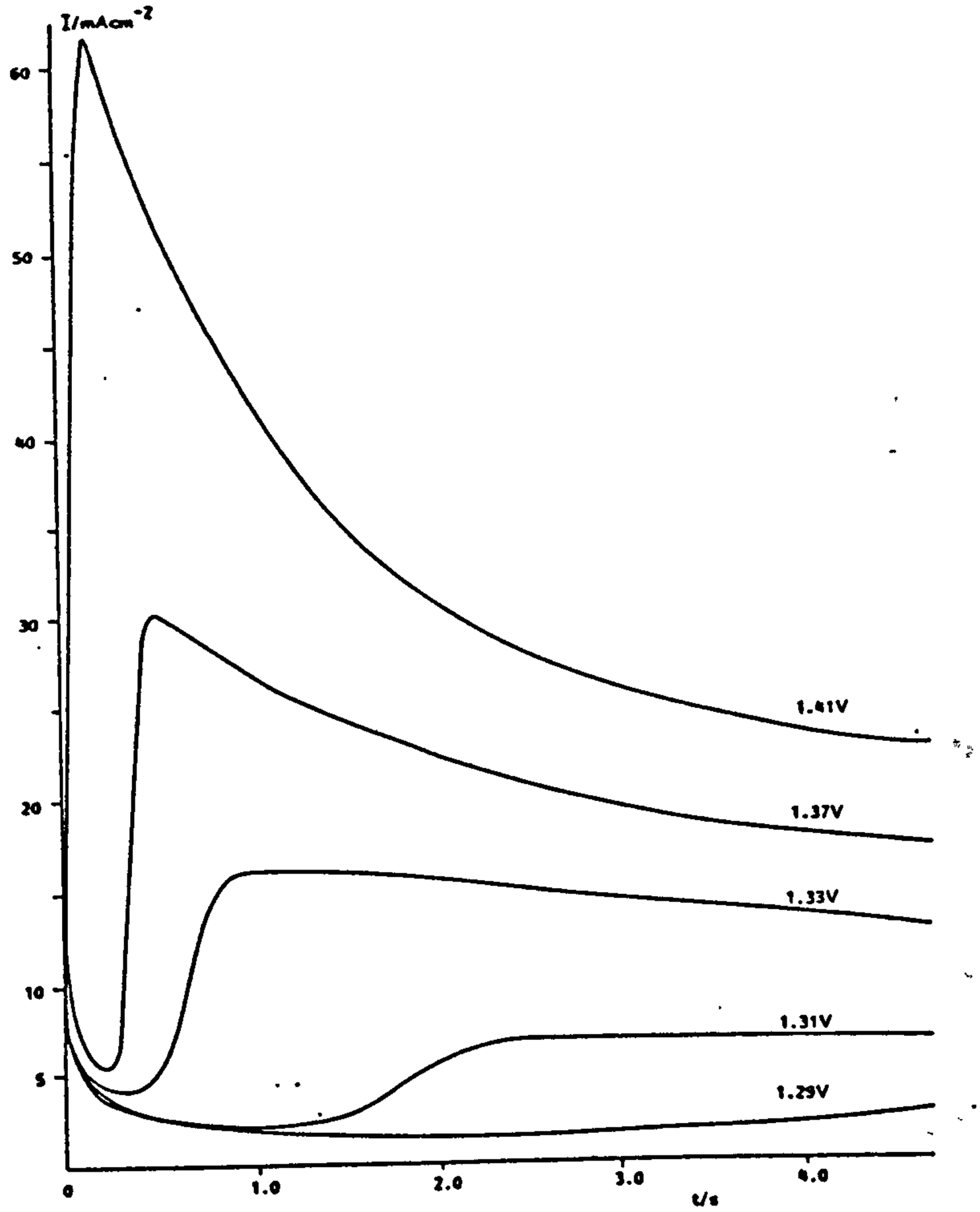

Figure 1.10 A potential step from 0.0 V to 1.8 V (vs. SCE) at a platinum electrode in a solution thiophene (50 mmol dm^{-3}) acetonitrile containing TEAT (0.1 mol dm^{-3})[38]

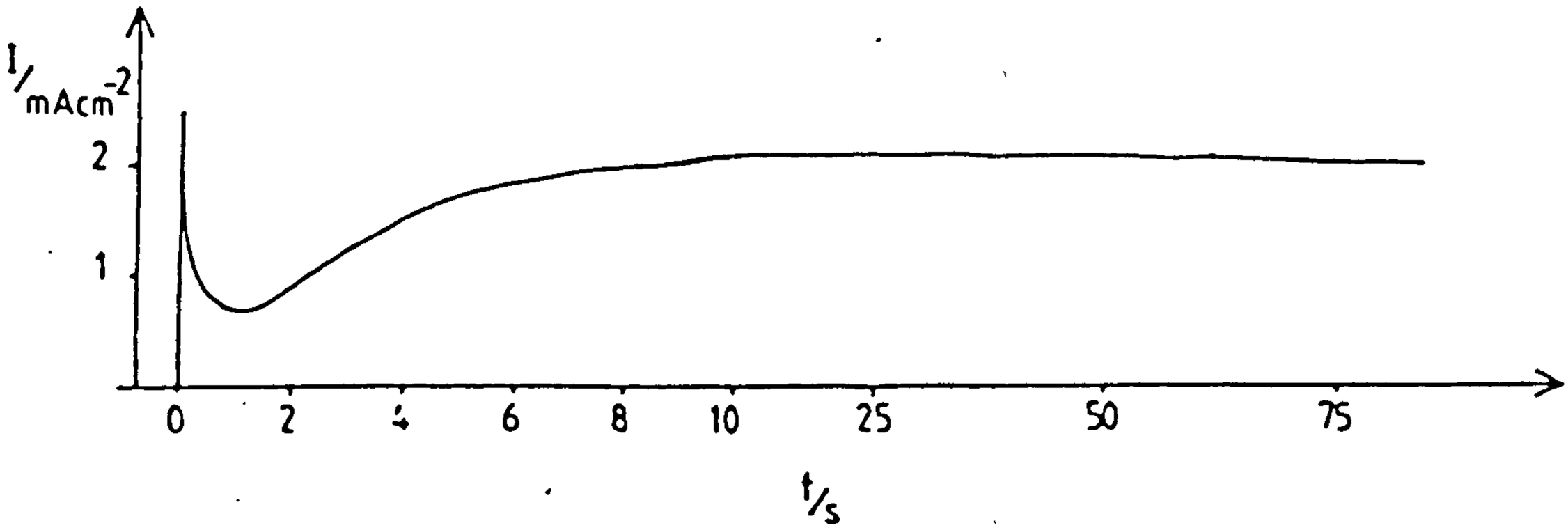

Figure 1.11 Diagrammatical representation of three dimensional nucleation followed by one dimensional growth

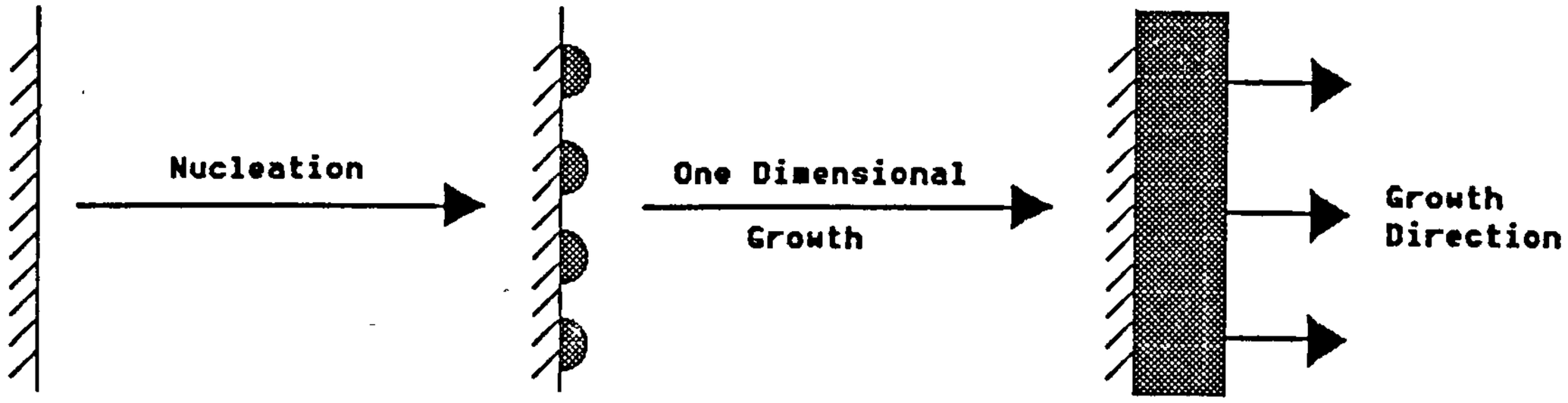

1.5 Redox Behaviour and Conductivity of Heterocyclic Conducting Polymers

As mentioned previously the requirement of a continuous π-bonded system for the conductivity of a conducting polymer is very important. Figure 1.12, shows how charge can be transferred down a chain of poly(1,4-phenylene) but not down a chain of poly(1,3-phenylene).

The redox behaviour of conducting polymers is different from the behaviour of immobilised redox couples.[44] It has been suggested that the initial oxidation of the polymers is faradaic followed by a long capacitative charging process.[45] More recent suggestions imply that several redox processes are involved which weakly interact with each other.[46] The later explanation is regarded as a more adequate description of the large potential regions observed between the onset of oxidation and complete oxidation.

Poly(1,4-phenylene) has proved to be a good model system for the aromatic type conducting polymers. The initial oxidation of this polymer produces a polaron[47,48,49] (spin = 1/2). Upon further oxidation a diionic bipolaron (spin = 0) is formed, figure 1.13.

The charge separation in the bipolaron state is determined by the offset in energy destroyed by the disruption of aromaticity in the monomers of the chain. The charged states shown in figure 1.13, are capable of transferring charge down the length of the polymer chain. Both the polaron and the bipolaron have associated energies and can be thought of as energy states which have their own place in an orbital band diagram. Figure 1.14, shows the band diagrams for typical metals, nonconducting polymers and conducting polymers.

The presence of polarons and bipolarons has been confirmed by studies of oligomeric phenylene compounds[50,51,52] which show distinct

Figure 1.12 The charge transport mechanism of poly(1,4-phenylene) as opposed to poly(1,3-phenylene)

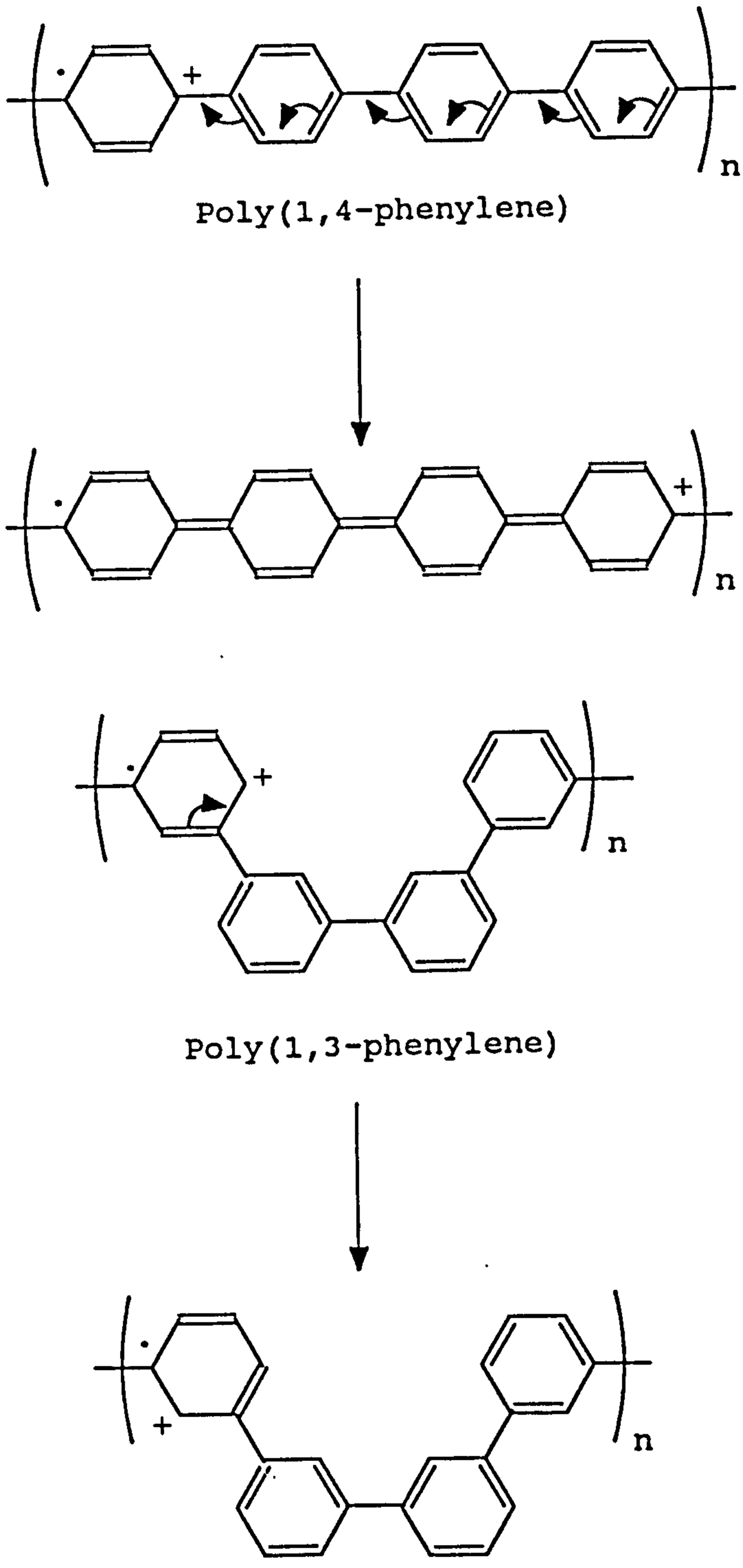

Poly(1,4-phenylene)

Poly(1,3-phenylene)

Figure 1.13 Polaron and bipolaron formation during the oxidation of poly(1,4-phenylene)

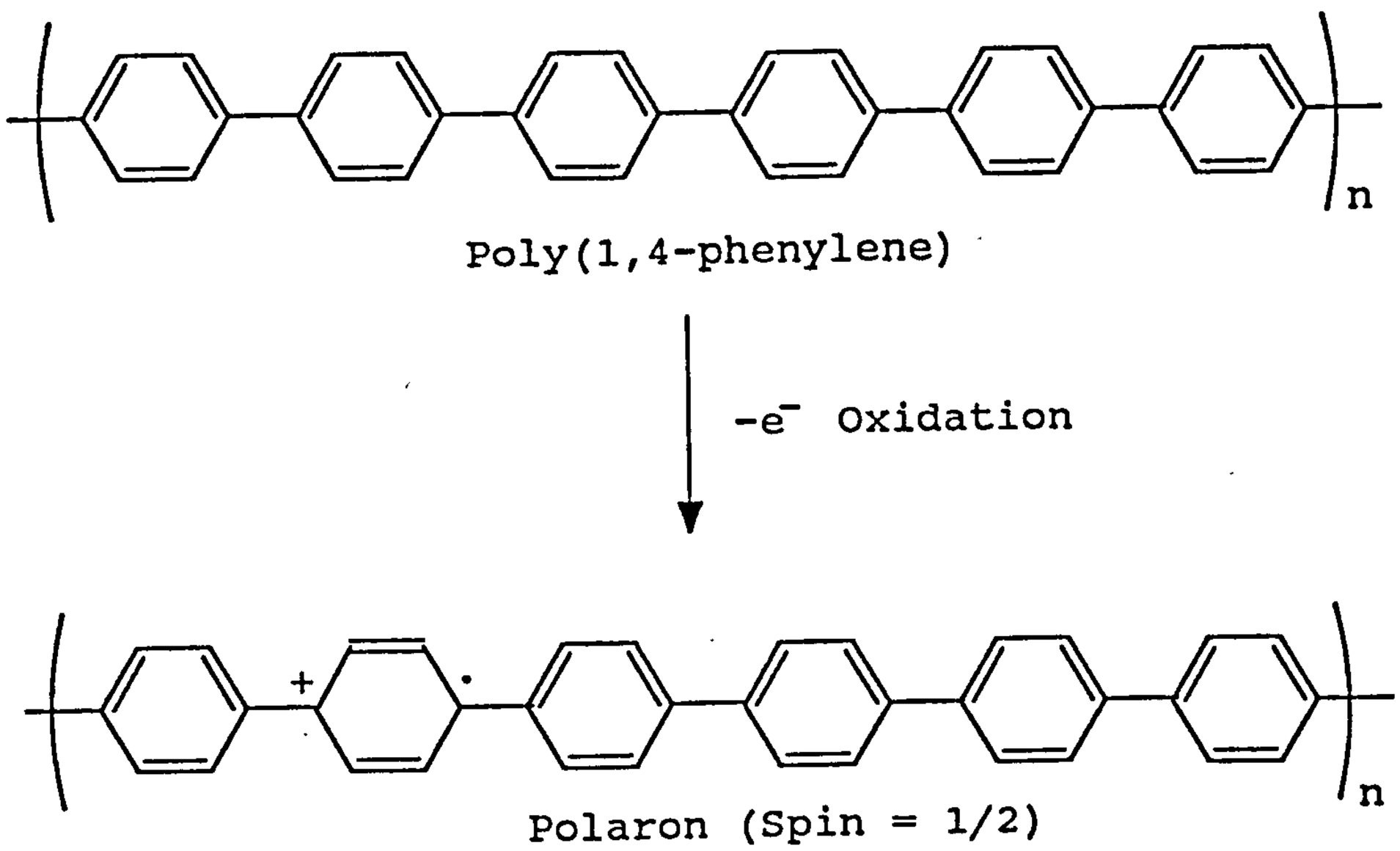

Figure 1.14 Energy band diagram for typical metals, nonconducting polymers and conducting polymers

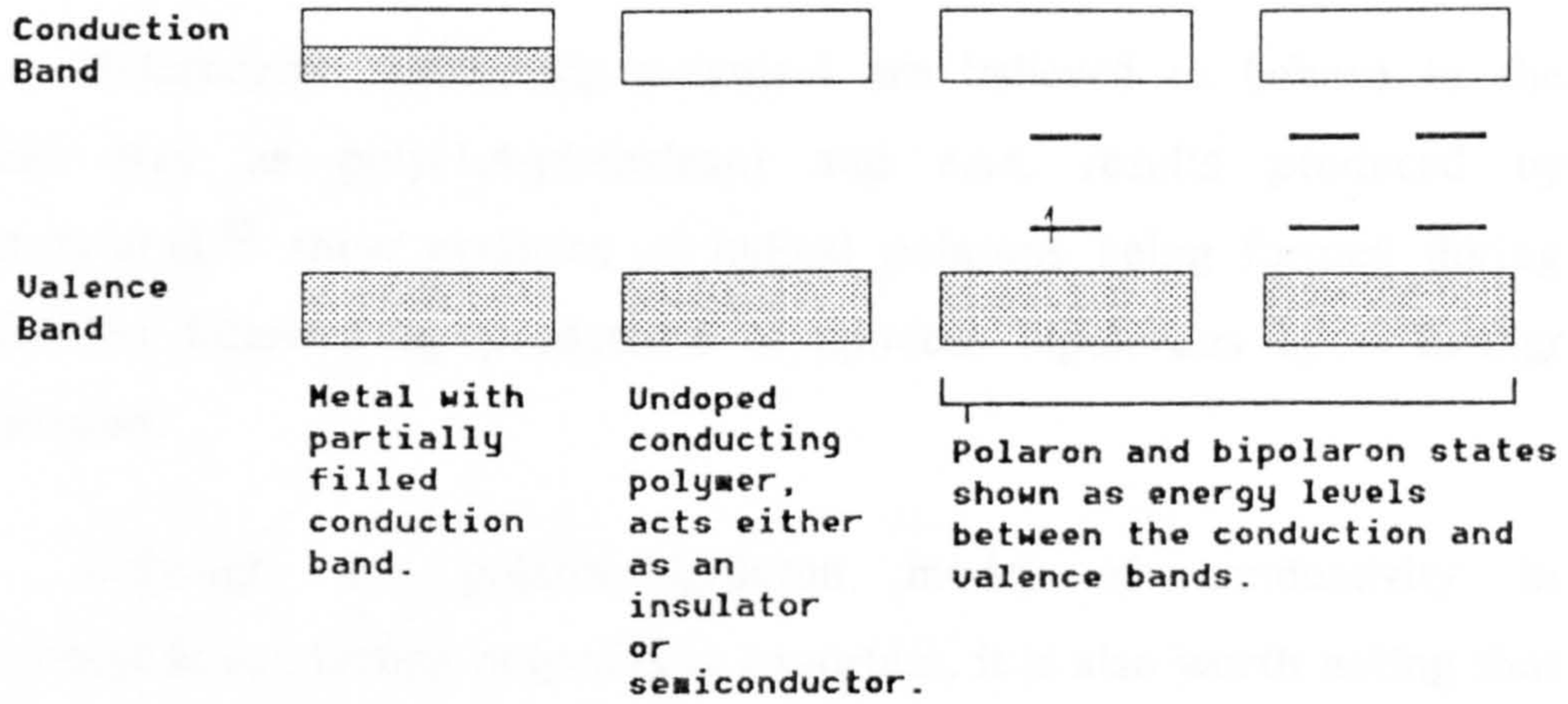

oxidation peaks during cyclic voltammetry corresponding to polaron and bipolaron formation. The reduction peaks are somewhat more negative than the oxidation peaks suggesting that a large scale structural reorganisation is involved.

Heterocyclic conducting polymers are believed to behave in the same way as poly(1,4-phenylene) and e.s.r. results produced by Albery *et al.*[53] show evidence of radical polarons being formed during oxidation followed by production of spinless bipolarons upon further oxidation.

Although the polaron/bipolaron model of conductivity in heterocyclic conducting polymers is important, it is also worth noting that other physical aspects of the polymers exert a great influence on their conductivity. Wegner *et al.* [54] have studied compounds of the type shown in figure 1.15. The size of the ring was used to attenuate the distance between each polymer chain. It was was conclusively shown that increasing the distance between the polymer chains markedly reduced the conductivity. The conductivity range of conducting polymers is shown in figure 1.16.

The overall charge taken up by the polymer, during oxidation, per monomer unit is called the dopancy (δ). For polymers such as poly(pyrrole) and poly(thiophene) the dopancy tends to lie between $\delta = 0.25$ and $\delta = 0.33$, which means that when the polymer is fully oxidised there is one charge for every three or four monomer units. However lower figures have been quoted for the dopancies. The overall charge consumed during polymerisation can now be defined in equation 1.1, from figure 1.17.

$$Q_T = (2 + \delta)me \qquad (1.1)$$

m - number of moles of monomer.

Figure 1.15 Monomers of the type studied by Wegner *et al.*[54]

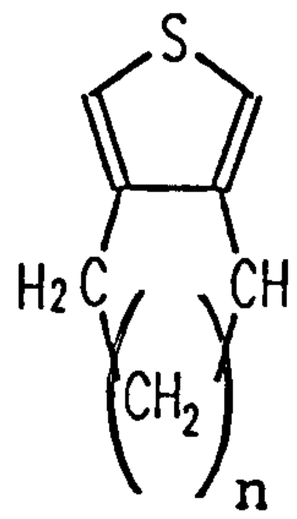

Figure 1.16 Conductivity range of conducting polymers

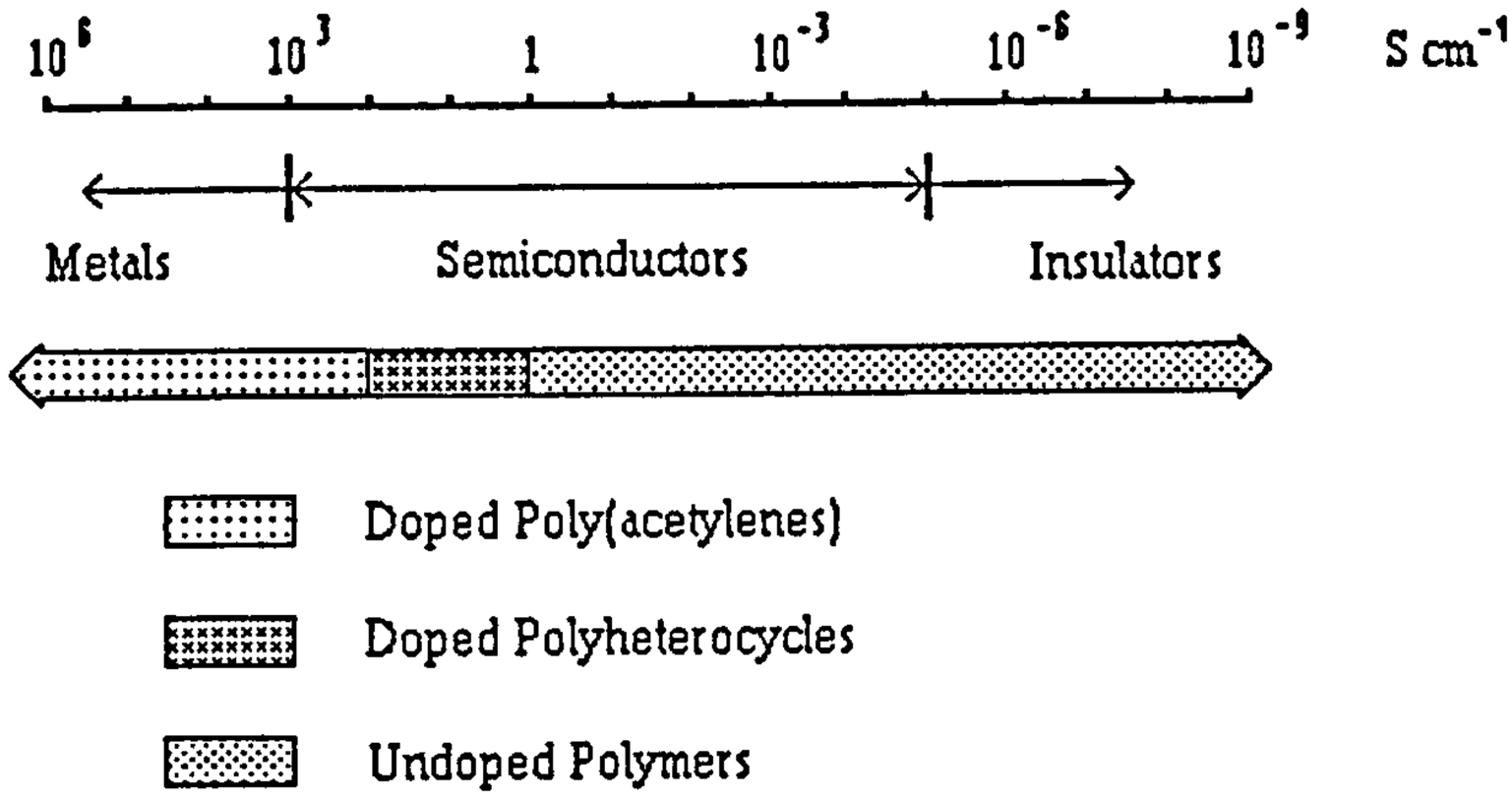

Figure 1.17 Consumption of charge during polymerisation

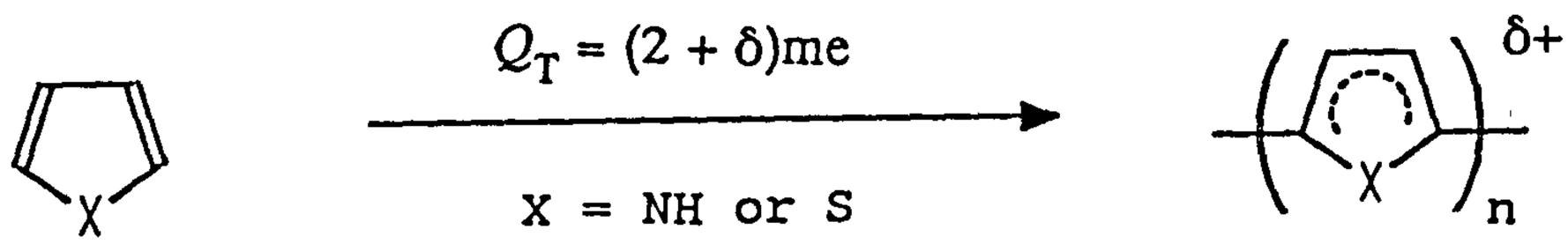

1.6 The Effect of Dopant and Solvent on the Electrochemistry of Heterocyclic Conducting Polymers

The way that charge is distributed in the polymer chain has already been discussed but an equally important aspect is the way that charge is countered in order to maintain electroneutrality. When a conducting polymer is oxidised or in other words is positively doped the dopant inevitably takes the form of anions. The dopant anions hence have a very important effect on the electrochemistry of conducting polymers. The doping behaviour can be divided into three different types;

(i) by diffusion of small anionic[34] species such as BF_4^- and ClO_4^- into the polymer matrix during oxidation and diffusion out during dedoping,

(ii) by entrapment of large anions[55] or polymeric anionic[56,57,58,59] systems in the polymer to act as a macro dopant resulting in expulsion of cations during oxidation of the polymer and their return during dedoping,

(iii) by covalently binding anionic species[60,61,62,63] to the monomers, known as "self doping" or "auto doping", resulting in behaviour similar to (ii).

The three types of processes given are highly idealised and very rarely occur independently of each other. The most common form of doping is type (i) although type (ii) is becoming more popular since the large counter ions impart their own characteristics on the films improving their overall mechanical properties especially when anionic polymers are used.

Type (iii) is probably the most electrochemically interesting class of doping. Covalent binding of sulphonates to pyrrole[60,61] and thiophene[62] have been the most commonly studied although the effects of carboxylic

acid groups on pyrrole[63] have also been investigated. Pickup[17] studied poly(3-methylpyrrole-4-carboxylic acid) finding that direct linkage of a carboxylic acid group to the ring had an inductive effect on the polymer imparting a pH dependent "self doping" effect, figure 1.18.

The choice of dopant can be very important, especially during polymerisation, but also to prevent deactivation due to blockage of the film by large cations.[64,65]

Solvents as always play a large part in the electrochemistry of conducting polymers. The nucleophilic effects of solvents on the electrochemical polymerisation of conducting polymers have already been described but other properties are also of importance when the processes of doping and dedoping are considered. Dopant ions are naturally solvated and carry solvent in and out of the polymer during doping and dedoping To facilitate doping, the polymer must already contain solvent molecules, a process known as wetting.

Poly(thiophene) is an example of a polymer that exhibits very good electrochemistry in acetonitrile but inhibited electrochemistry under aqueous conditions unless the films are thin.[66] Neutral poly(thiophene) is hydrophobic[67] with a contact angle, for a drop of pure water, of 180°. However when fully oxidised the contact angle approaches 0° and the polymer becomes hydrophilic. It has been shown that poly(3-methylthiophene)[68,69] exhibits limited aqueous electrochemistry or degradation depending on the type of dopant ion used. Anions such as NO_3^- and ClO_4^- allow a limited doping process to occur which is not fully understood but varies with the treatment and history of the polymer and anions such as SO_4^- and Cl^- allow the polymer to be oxidised only at potentials at which it will be overoxidised. The aqueous electrochemistry of the poly(thiophenes) can be improved by the substitution of poly(ether) groups[70] at the β-position but the limited behaviour of these polymers

Figure 1.18 Cyclic voltammetry at 100 mV s-1 of poly(3-methylpyrrole-4-carboxylic acid) at a platinum electrode in aqueous acetate (0.2 mol dm^{-3}) buffer containing KNO_3 (0.1 mol dm^{-3}) at various pH values[17]

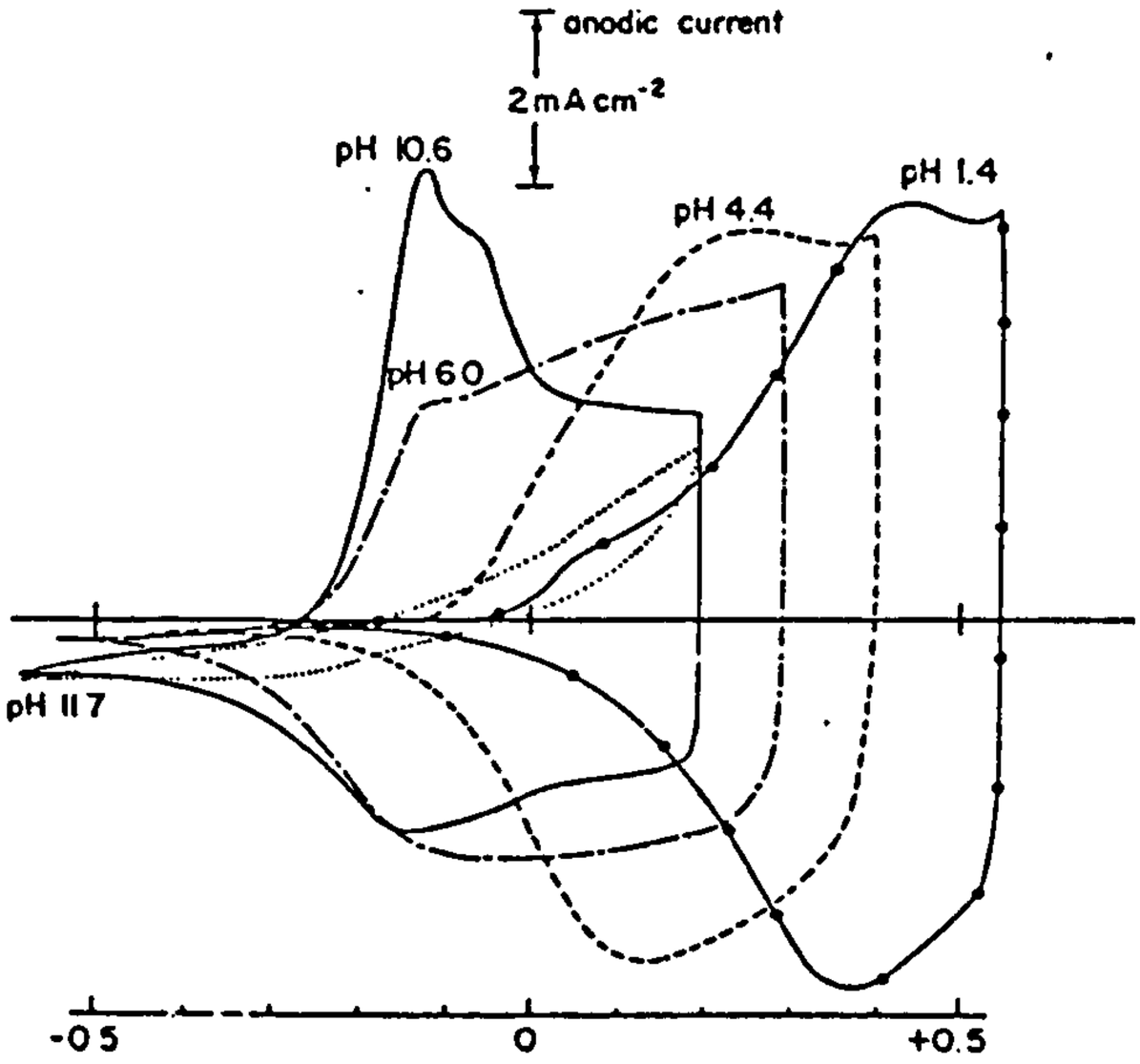

presents a barrier to their potential applications.

Most conducting polymers experience "break-in",[71,72] effects when cyclic voltammetry is performed upon them for the first time or when the polymer has been allowed to relax in one oxidation state for a finite length of time. The effect is seen as an initial retardation of the oxidation or reduction of conducting polymers during cyclic voltammetry which is associated with a reorganisation within the polymer that allows the flow of solvent and counter ions during the cycle to proceed more easily.

1.7 Substituted Heterocyclic Conducting Polymers

One of the most interesting features of heterocyclic conducting polymers is their ability to be chemically modified by covalently binding substituents to positions which are not directly involved in the polymerisation process. The substituents can alter the properties of the conducting polymers drastically which means that monomers can be chemically tailored to produce polymers to suit the specific needs of a particular application.

Pyrrole monomers are usually substituted at the nitrogen[73] position due to the ease of substitution compared to the difficult chemistry involved during the substitution of the β-position. Thiophenes in contrast cannot have substituents on the sulfur but the ease of substitution at the β-position has allowed several monomers to be synthesised.

Alkyl substituted thiophenes were probably the simplest studied substituted thiophenes.[74,75] They were largely studied as a means of improving the processability of poly(thiophenes) by increasing their solubility in organic solvents since neither poly(pyrrole) nor poly(thiophene) are soluble in any solvent. N-substituted alkyl pyrroles[19] have also been studied. Substitution was found to generally reduce the conductivity of the polymers by increasing the distance between each

monomer chain. The ease of electrochemical oxidation and reduction was found to be governed by a fine balance between the electron donating effects of the β-substituents and steric effects which reduce the planarity of the π-bonded conjugated network.[76]

As mentioned earlier the substituents have a very important effect on the polymerisation of monomers. Several β-substituted thiophenes were studied in acetonitrile,[77] figure 1.19, performing cyclic voltammetry and the results were rationalised in terms of the Hammett-Taft equation 1.2.

$$E = \rho_{\pi}\sigma + S \qquad (1.2)$$

$\rho_{\pi}\sigma$ - polar-mesomeric parameters (σ - Hammett constant)

S - steric factor

The plot shows that the steric factor S is largely constant and the reactivity of the monomers largely depends on the oxidation potential. The monomers shown outside the box, figure 1.19, do not polymerise, their higher reactivities reduce the selectivity for monomer - monomer coupling and increase the influence of side reactions with nucleophiles.

Properties other than the inductive effect of the substituent on the aromatic ring can also interfere with the polymerisation of heterocyclic conducting polymers. For example the lone pair of electrons on pyrrole-pyridine in the monomer[78] shown in figure 1.20, inhibits the electrochemistry of pyrrole and hence electropolymerisation is prevented.

Figure 1.19 Hammett-Taft plot of several β-substituted thiophenes (monomers outside the box do not polymerise)

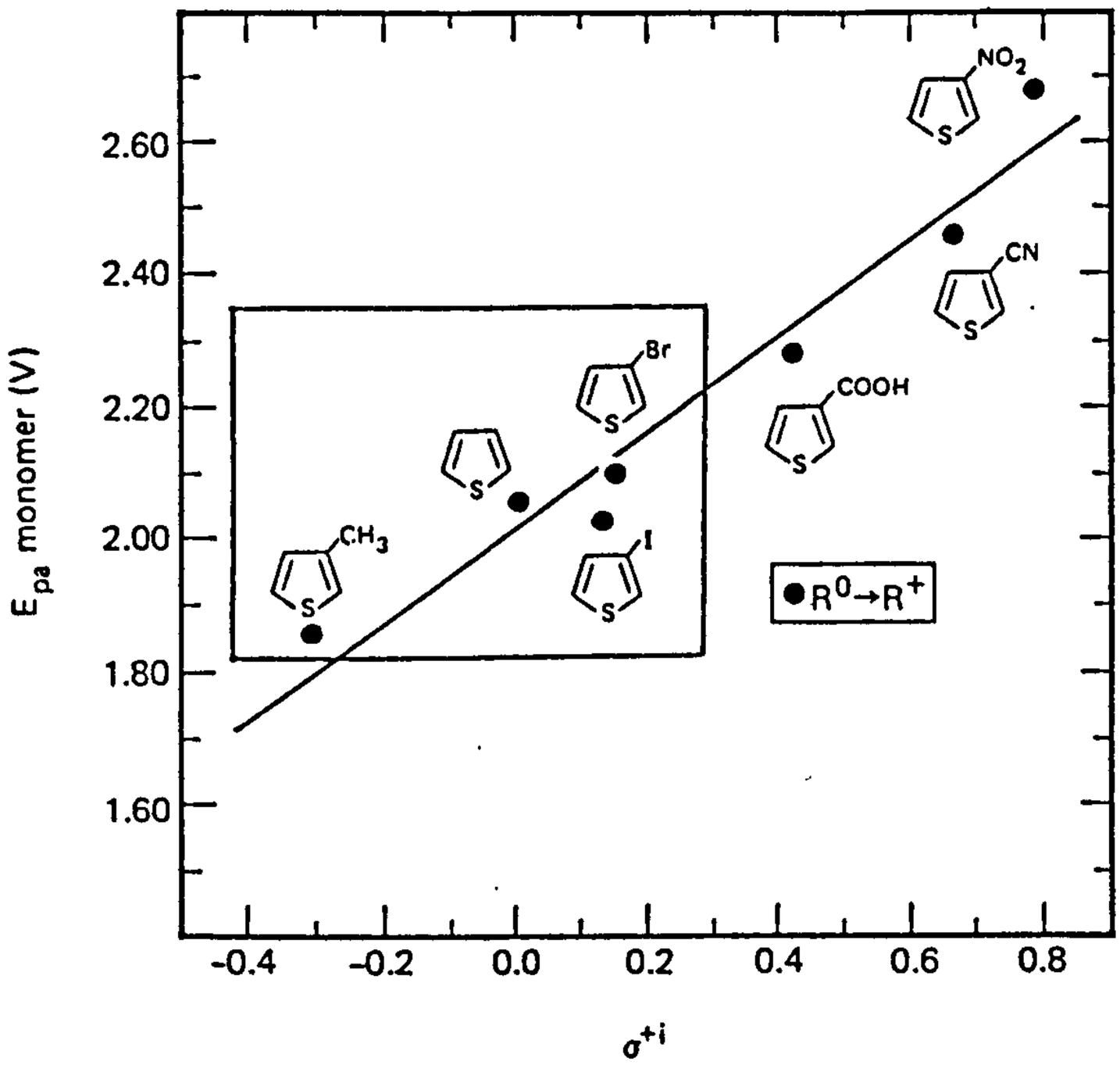

Figure 1.20 Pyrrole-pyridine monomer whose lone pair of electrons inhibits polymer formation

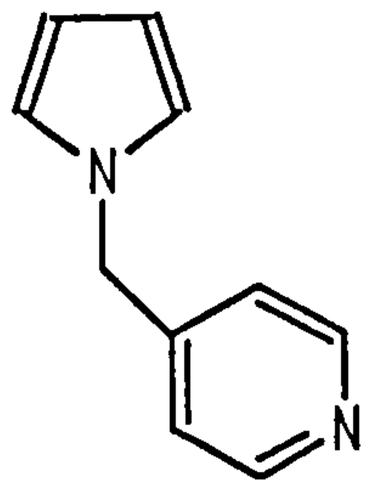

Substituent effects add another complexity to conducting polymer electrochemistry which needs to be taken into account if progress is to be made in improving these very interesting materials.

The effect of self doping substituents has already been discussed but several more exotic substituents have been studied, the most popular being ones that have their own redox behaviour such as ferrocene[79] and anthraquinone.[80] The redox substituents display electrochemical behaviour characteristic of immobilised redox couples. This behaviour is independent of the electrochemical behaviour of the conducting polymer.

The work described in this thesis concentrates on conducting polymers modified with carboxylic acid groups and their subsequent effects on the electrochemistry in aqueous solutions. Carboxylic acid modified conducting polymers have the following distinct advantages;

(i) the potential for self doping and of binding metal ions due to the ease of deprotonation,[17,81] their weakly acidic nature means that unlike sulphonates the level of deprotonation can be controlled by pH,

(ii) the variety of chemistry available to further modify the carboxylic acid groups by, for example, esterification or by carbodiimide[82,83] peptide coupling reactions,

(iii) the ease of characterisation of the conducting polymers and the further modified polymers by FT-IR due to the strong absorption of the carbonyl group in the spectrum.

Previous studies on the effects of carboxylic acid substituted monomers and polymers have been made showing their future potential as either pH sensors,[17,81] modified electrodes[84] or as precursors for more sophisticated peptide modified electrodes for biosensors.[85] However, further studies need to be undertaken to fully understand the

electrochemistry of this interesting class of modified conducting polymers.

A number of techniques, other than electrochemistry, have been used to characterise and study the conducting polymers described in this thesis, namely, FT-IR spectrometry, UV/vis spectrometry and impedance spectrometry. These three major techniques will now be discussed.

1.8 FT-IR Spectroscopy of Heterocyclic Conducting Polymers

The development of FT-IR spectroscopy using the Michelson interferometer[86] has enabled infrared spectra to be recorded in the time domain as interferograms and translated by means of a Fourier Transform to the frequency domain to give a normal infrared spectrum. The speed at which the interferograms can be collected and processed, due mainly to fewer moving parts within the spectrometer, compared to normal dispersive infrared measurements gives the technique a distinct advantage, in addition to having a higher energy throughput. Such a technique enables several interferograms to be collected and averaged before processing, increasing the signal to noise ratio[87] because the signal increases directly with the number of scans (n) while the noise only increases with $\sqrt{n}$ due to its statistical nature. An increase in the signal to noise ratio has enabled many techniques such as specular reflectance, attenuated total internal reflectance and diffuse reflectance to be developed increasing the variety of substrates which can be studied.

Specular reflectance is the main technique used throughout this thesis. The infrared beam is reflected at an angle of approximately 21° off a surface upon which the conducting polymer under investigation is deposited, figure 1.21.

The technique is ideal as a nondestructive means of studying conducting polymers on electrodes which can then go on for further study.

Figure 1.21 Specular reflectance FT-IR spectroscopy (at approx. 21°) of a sample deposited upon a reflecting surface

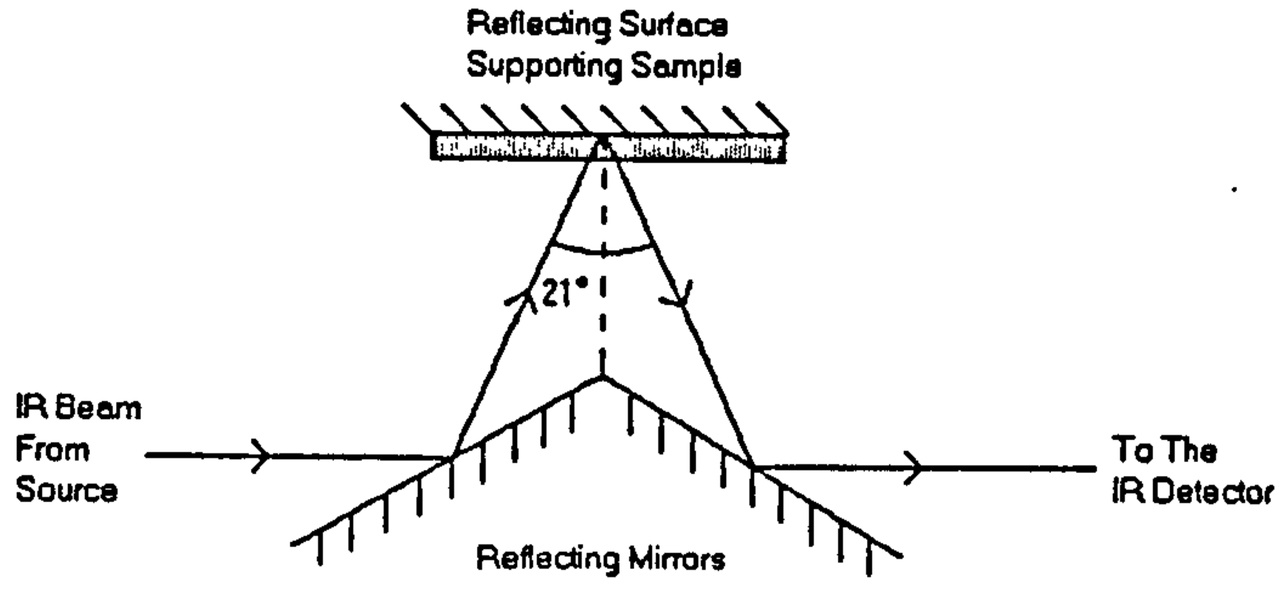

There are three areas regarding conducting polymers in which FT-IR can be of particular use;

(i) chemical characterisation of the polymer chain and the changes incurred on the structure during doping and dedoping,[88]

(ii) detection of dopant ions, *e.g.* BF_4^- at 1060 cm^{-1} and ClO_4^- at 1100 cm^{-1},

(iii) observation of very strong polaron and bipolaron bands in the near infrared region.[88] .

Poly(thiophene) and poly(3-methylthiophene)[89] have been studied showing that there are a significant number of defects in the poly(thiophene) chain due to α-β and β-β linkages as opposed to just pure α-α bonds, figure, 1.22. This was confirmed by the presence of both α (3071 cm^{-1}) and β (3055 cm^{-1}) C-H stretches in the infrared spectrum. Poly(3-methylthiophene) showed only β C-H stretches confirming its more regular bonding.

The example given shows the power of infrared spectrometry in the analysis of conducting polymers and confirms that poly(thiophene) has more defects due to the higher reactivity of the monomer during polymerisation. Many other studies[89,90] have also been reported but it is worth noting that if the polymer is oxidised the very strong polaron and bipolaron bands may obscure the structural information in the infrared spectra above 2000 cm^{-1}.

1.9 Optical Properties and UV/vis Spectrometry of Conducting Polymers

As mentioned previously some electronic transitions are observed in the near infrared spectrum[88] but another transition is observed in the visible spectrum due to π-π* transitions from the conjugated backbone of the polymer. It is thought that the electronic transitions[91,92,93,94] shown

Figure 1.22 Possible defects in poly(thiophene)

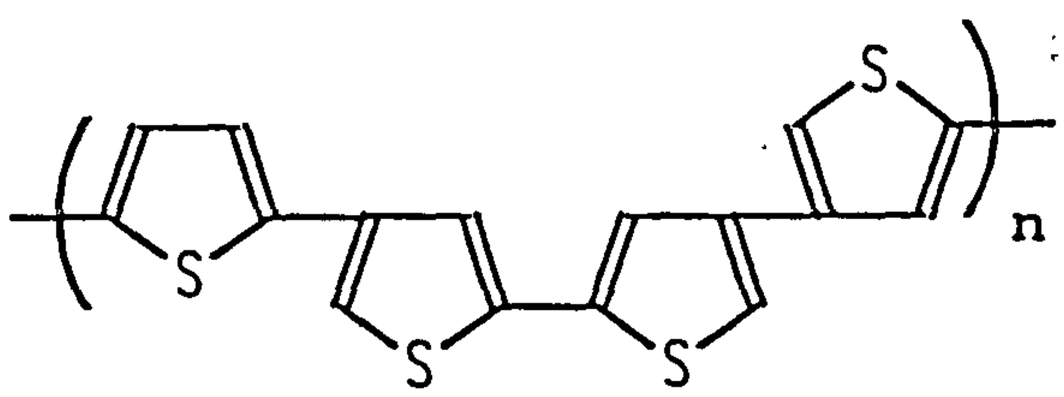

in figure 1.23 are responsible for the features of both the visible and near infrared spectra.

The π-π^* transition ($h\nu_1$) observed in the visible region of the spectrum decreases in intensity and increases in energy as the polymer is oxidised. When a polaron is formed there are three additional transitions ($h\nu_2$,$h\nu_3$,$h\nu_4$) which are observed in the near infrared region. When a bipolaron is formed there are only two additional transitions ($h\nu_2$ and $h\nu_3$) also observed in the far visible and near infrared regions. The change in the intensity of transitions during oxidation and reduction allows the doping process to be followed by UV/vis spectrometry. Near infrared studies have not been performed in this thesis.

Most UV/vis studies have been performed using optically transparent electrodes (OTE), like indium doped tin oxide (ITO) or microgrids, to facilitate the collection of normal *in situ* absorbance spectra. However, a technique called near normal incidence reflectance spectroscopy (NNIRS)[95] has also been applied to record UV/vis spectra of conducting polymers[96,97] deposited on reflecting platinum electrodes.

The results from UV/vis studies on conducting polymers are generally recorded as normal absorbance spectra although some papers[98,99] have used a technique called derivative cyclic voltabsorptometry (DCVA)[100] which involves plotting the rate of change of absorbance with potential (dA/dE) against the applied potential (E) for a specific wavelength. The technique is complimentary to cyclic voltammetry since (dA/dE) should be directly proportional to current (i) for a purely faradaic process. Capacitative effects are hence not observed and this has been of particular interest when comparing cyclic voltammograms and cyclic voltabsorptammograms of the same conducting polymer.

Figure 1.23 Possible electronic transitions occurring within conducting heterocyclic polymers

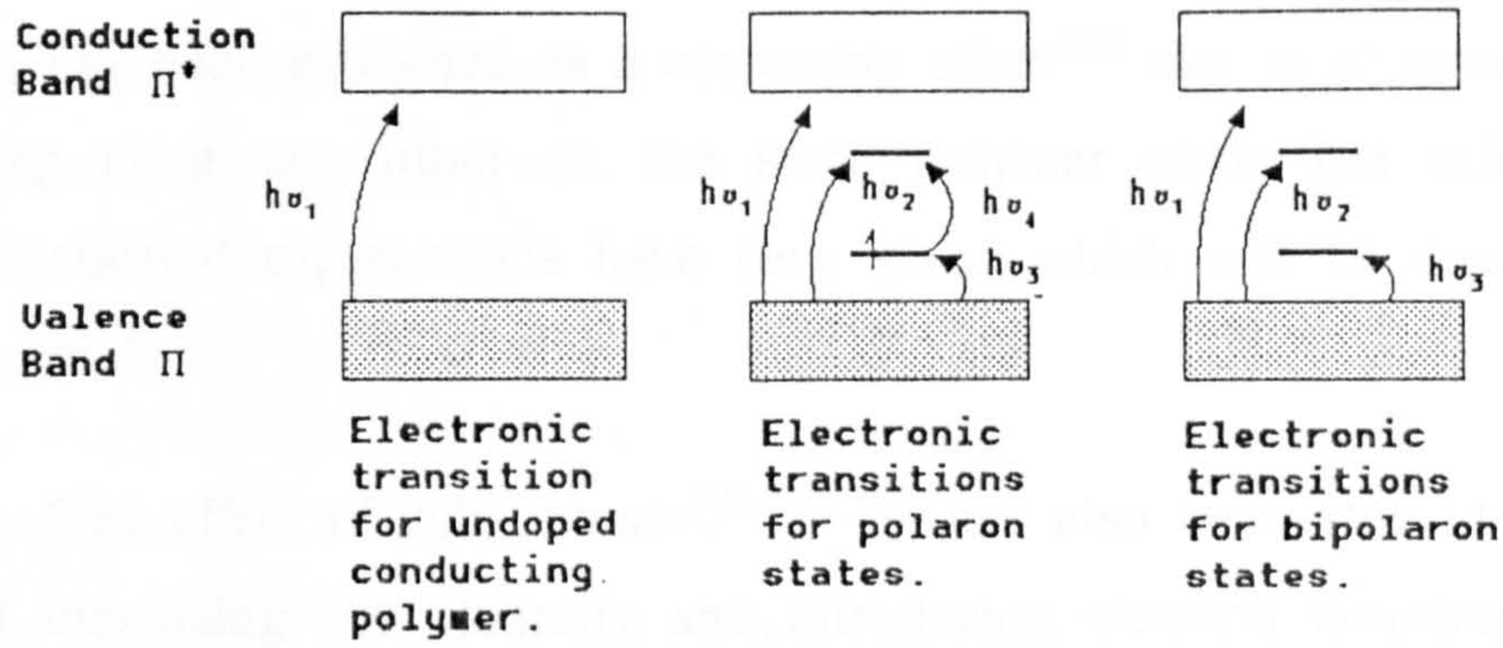

UV/vis spectrometry has enabled several groups[101,102] to study further the redox behaviour of conducting polymers. There is still some debate as to the exact behaviour especially concerning the contribution that capacitance makes to the charge passed during doping. Data fitted to the Nernst equation has yielded values of n significantly lower than 1. This has been explained as a coulombic effect[103] due to charged species acting upon one other on the same polymer chain but other more sophisticated explanations have been given which will be discussed in chapter 5.

The effect of substituents[104,105,106] has also been studied showing that increasing the planarity and introducing electron donating groups induces a bathochromic shift of the π-π^* band gap for the dedoped polymers.

1.10 Impedance Spectroscopy of Heterocyclic Conducting Polymers

Impedance spectroscopy has facilitated the study of the capacitative and resistive nature of conducting polymers. The technique measures both the in phase (Z') and 90° out of phase (Z'') impedance components of a small applied ac potential at a particular frequency. Generally the ac potential is applied across films during standard electrochemical experiments as a small (5 - 10 mV) modulation to the main applied potential. When the impedance components are measured over a range of frequencies the resistive nature of the polymers can begin to be understood. Data is usually recorded as a Nyquist plot ($-Z''$ against Z') which can also be thought of as an Argand diagram showing the vector sum of the impedance components (Z' and Z'') and the phase lag of the applied ac potential to the ac current measured. Further discussion of the technique, equipment and analysis of results are covered in standard texts[107,108] and will not be discussed further in this introduction.

Several impedance spectroscopy studies have been performed on

heterocyclic conducting polymers, mainly on poly(pyrrole)[109,110,111]. Low frequency (mHz - Hz) studies have yielded results suggesting that the oxidised polymers act as simple capacitances, but higher frequency (Hz - kHz) studies show more complex behaviour. Albery *et al.*[53] have developed a transition line model for the behaviour of conducting polymers by considering the resistances of the polymers (R_p) and the solution (R_{aq}) separated by capacitances (C_p) as described in figure 1.24.

The effect of such a model on the impedance spectrum involved a very involved and complex calculation. Real impedance data could only be compared with the model if R_p was made equal to R_{aq} otherwise a 45° "Warburg" region was observed between the onset of the low frequency capacitative behaviour and the high frequency resistance and capacitance in parallel type behaviour figure 1.25.

It has been pointed out that the resistance of the polymer depends on charge transfer between chains[54] and hence R_p is very unlikely to be equal to R_{aq} so the model was amended[112] to take this into account. Even the amended model failed to fully explain the experimental results and a "Warburg" region was still observed in the simulations. The overall nature of the impedance response of heterocyclic conducting polymers is hence still largely under debate with only low frequency studies being of any particular use.

Lower frequency studies have shown that the degree of doping affects the capacitances measured.[109] The large magnitude of the capacitances are thought to be due to the formation of a double layer at the surface of the polymer chains rather than at the bulk surface of a large piece of polymer. It has been pointed out that the redox processes have associated effects on the capacitance hence capacitative behaviour is observed throughout the oxidation of the polymer and not just near the fully oxidised region. This has lead to the conclusion that the capacitative

Figure 1.24 Transition line model for conducting polymers proposed by Albery *et al.*[53] (R_p - resistance of polymer, R_{aq} - resistance of the solution separated by C_p - capacitance)

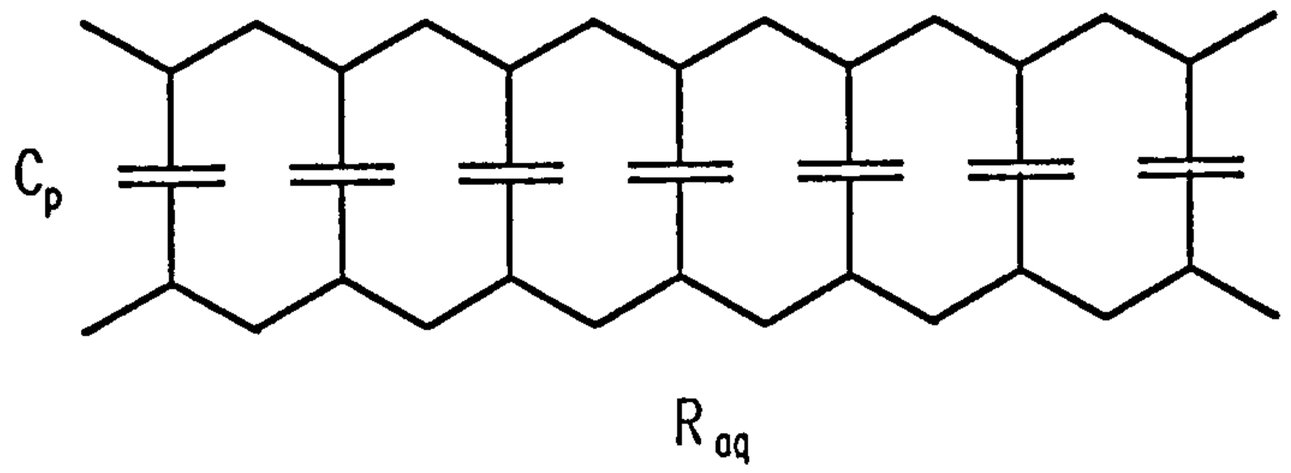

Figure 1.25 Typical prediction for a Nyquist plot of a conducting polymer using the transition line model proposed by Albery *et al.*[53]

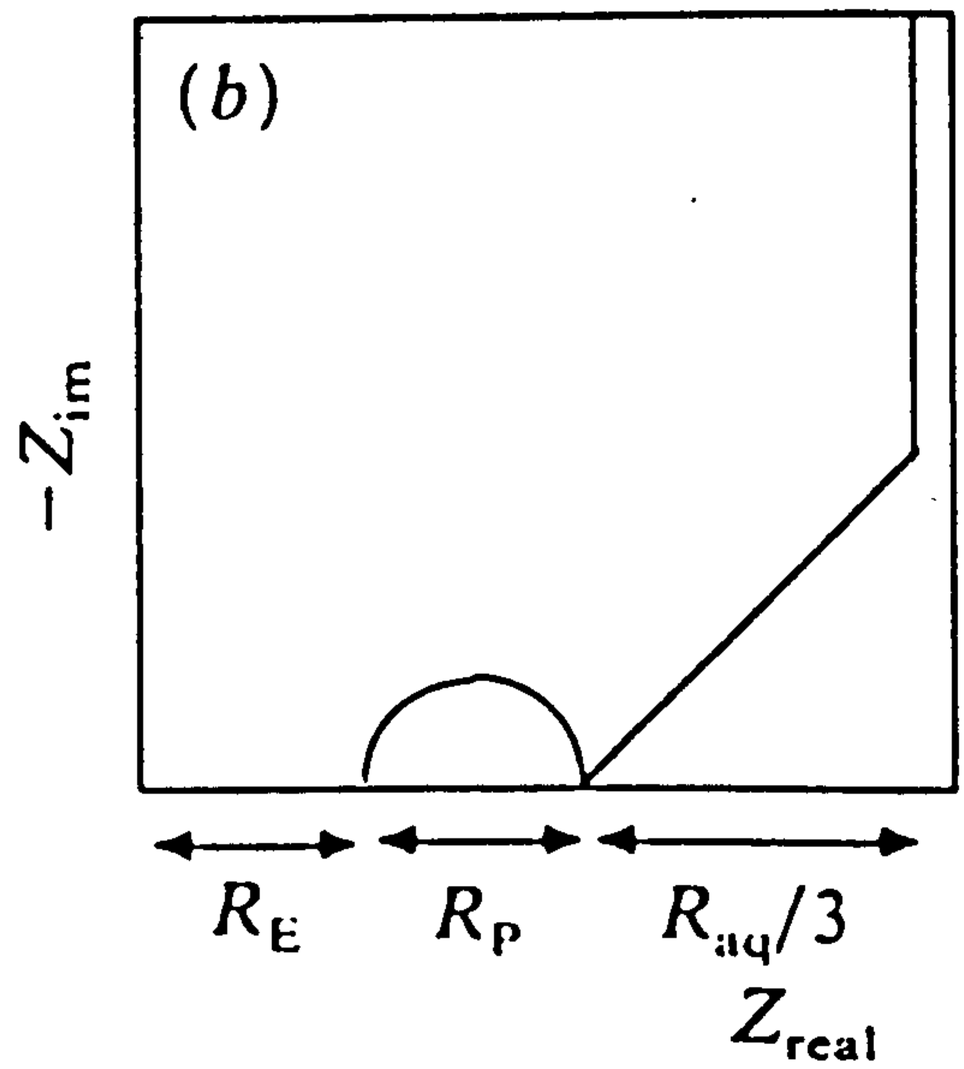

process seen in the cyclic voltammetry of conducting polymers is simply a continuation of the oxidation of the polymer. This conclusion is supported by data on the extent of the doping at particular potentials and contradicts some UV/vis DCVA results,[98] mentioned earlier, which suggest that there is a large purely capacitative region but these results may be due to deviations in the UV/vis spectrum.

The resistances of the polymers measured using this technique are found to fall very rapidly in the first stages of oxidation and then to remain low. Generally the technique is very good at low frequencies to determine the capacitances between the polymer and the solution.

1.11 Other Techniques Used to Analyse Heterocyclic Conducting Polymers

The number of analysis techniques available to conducting polymer scientists is very great and an exhaustive discussion of each would be inappropriate in this introduction. However some of the main techniques that compliment and add to the ones previously described will be briefly summarised in this section.

The quartz crystal microbalance (QCM) has been used to study the effects of cyclic voltammetry[113,114] of conducting polymers by measuring the mass of material present on the crystal. Such studies have shown the movement of both solvent and counter ions in the film during doping.

Ellipsometry has also been used to follow the growth of conducting polymers[40] and determine the thickness of the films at different oxidation states.

Nuclear magnetic resonance (NMR)[115] has proved to be a very powerful tool in studying the chemical structure of conducting polymers. The technique of magic angle spinning has enabled solid state NMR

studies to be performed on the most intractable conducting polymers,[116] but relatively large amounts of material are required. The results obtained from NMR have generally complimented the results obtained using FT-IR illustrating the usefulness of the simpler and easier FT-IR technique.

Scanning electron microscopy (SEM)[117] has been utilised to study the morphology of conducting polymers showing that poly(thiophenes) tend to have fibrous structures whereas poly(pyrroles) tend to form in spheroids. The technique can be extended further by studying the energy dispersive X-rays (EDAX) which provides information on the elemental composition of the polymers[118] by their characteristic X-ray emissions in the scanning electron microscope.

Unfortunately the final two techniques have the disadvantage of being *ex situ.*

1.12 Conclusion

A wide ranging summary of the science of conducting polymers has been given which is most relevant to the electrochemical and chemical nature of these interesting materials. However the literature on these materials is far more wide ranging and the potential applications are immense. The work undertaken in this thesis concentrates mainly on conducting polymers based on thiophene, pyrrole and indole with carboxylic acid substituents and the unique effects which those substituents impart on the electrochemistry of the polymers. The three main analysis techniques described in sections **1.8, 1.9** and **1.10** are used in conjunction with standard electrochemical techniques to study the effects of the carboxylic acid groups. Poly(indoles)[27,119,120,121] are a much less studied class of conducting polymer. The monomers show similar reactivity to thiophenes when studied using the Hammett - Taft equation (1.2). The chemical structure of the polymers is still under

debate but the widely accepted view is that bonding occurs at the 1 and 3 positions. The work in this thesis represents a significant step forward in the understanding of poly(indoles) which will be discussed in the following chapters.

Chapter 2

Experimental

2.1 Introduction

Standard electrochemical techniques have been employed in this thesis which have been summarised in several standard texts.[107,122,123,124,125,126] The three electrode system is used throughout the thesis to make electrochemical measurements. The equipment employed for electrochemical and chemical studies will now be described. All glassware was cleaned by immersion in Decon 90 solution for 24 h followed by a thorough rinse using water from a Whatman WR50 RO (Reverse Osmosis) purification system (conductivity $S \leq 1.0\ \mu S\ cm^{-1}$).

2.2 Electrodes

Platinum rotating disc electrodes (A = 0.385 cm^2) encased in Kel-F were employed in most studies. A platinum ring-disc electrode (r_1 = 0.201 cm, r_2 = 0.210 cm and r_3 = 0.227 cm) and a glassy carbon electrode (A = 0.323 cm^2) both encased in Kel-F were also employed for several studies. All electrodes were supplied by Oxford Electrodes, their areas were calculated using the mean of several randomly selected diameters measured with a travelling microscope. Initial polishing was achieved using individual Hyprocel lapping cloths (Engis) sprayed with 6 μm, 3 μm and 1μm diamond lapping spray (Engis). Before each individual experiment the electrodes were initially polished with 1 μm alumina/water slurry followed by 0.3 μm alumina/water slurry, both on medical cotton wool, to give a mirror finish. The electrodes were then washed with Whatman RO water and dried by wiping with a clean soft tissue. Indium doped tin oxide electrodes (ITO) were used for UV/vis studies, the electrode areas could not be readily measured but approximate dimensions will be quoted in the text.

All potentials were measured against a previously described[127] in-house constructed saturated calomel electrode (SCE) incorporating a low porosity ceramic frit (gift from Kent Industrial Measurements Ltd.). The reference electrodes were frequently checked against a commercial saturated calomel electrode (Radiometer) for deviations above ± 6 mV. If deviations exceeded this value the calomel electrodes were repacked and tested again before further use.

Counter electrodes were constructed from (1 × 4) cm^2 platinum gauze spot welded to 1 mm thick platinum wire which was 7 cm long. The counter electrode was regularly washed in Whatman RO water and was cleaned before each experiment by heating over a blue Bunsen flame until the platinum glowed orange and the flame had no colours corresponding to contaminants.

2.3 Electrochemical Cells

Most electrochemical studies were performed using a previously described, specifically designed electrochemical cell constructed from Pyrex®[127]. The cell is water jacketed so that solutions could be thermostatted at 25 °C ± 0.2 °C using a water bath circulator (Grant Instruments (Cambridge) Ltd. models W14 and SE15). The cell has an approximate volume of 15 cm^3 with the counter electrode placed in a second compartment behind a high porosity glass frit to prevent contamination of the bulk solution by products produced by reactions at the counter electrode. Solutions were degassed directly, for at least 20 minutes, in the cell by bubbling oxygen free nitrogen through the solution. The nitrogen was scrubbed, to remove traces of oxygen, by bubbling through a caustic solution of anthraquinone-2-sulphonate in contact with zinc amalgam, using a series of dreschel bottles and zero porosity sinter heads. If dry nitrogen was required it was subsequently passed down a sealed glass drying column consisting of Silica Gel,

activated 3 Å and 4 Å molecular sieves and sodium hydroxide pellets. After degassing a blanket of oxygen free nitrogen was passed over the solution at positive pressure to prevent diffusion of atmospheric oxygen back into the cell.

Electrochemistry in solutions of less than 5 cm^3 was performed using a small pyrex cell at ambient temperatures (20 - 25 °C). In this case the counter electrode could not be separated from the rest of the solution and the cell was only used if it was not practical to use larger volumes.

2.4 Electrochemical Equipment

Most electrochemical experiments were carried out using a commercial potentiostat with an internal voltage source (Thompson Electrochem Ltd., Ministat) capable of passing high currents by virtue of external measuring resistors. This potentiostat was coupled with an external 16-bit digital potential sweep generator with a potential range of ± 4.5 V and sweep range of 0.01 $\mu V\ s^{-1}$ to 10 $V\ s^{-1}$ (Thompson Electrochem. Ltd., Miniscan). In addition a smaller commercial potentiostat (Oxford Electrodes) with internal measuring resistors, triangular wave generator and voltage source was occasionally utilised. For ring disc electrode work an in-house constructed bipotentiostat was used with modular triangular wave generator, voltage sources and voltage followers. Rotation of the electrode was achieved using a commercial electrode rotator (Oxford Electrodes) capable of rotating a disc or ring disc electrode between 1 Hz and 50 Hz (± 0.01 Hz) while maintaining electrical contact with the potentiostat. Electrochemical data was recorded using an X-Y-t chart recorder (Bryans/Gould model: 60,000) or alternatively using a digital voltmeter (Keithley model: 197) capable of measuring both direct and ac voltage, current and resistance.

2.5 Impedance Spectroscopy Equipment

Impedance spectra were obtained by coupling a Solartron frequency response analyser (Schlumberger model: 1250) to an in-house purpose built low noise potentiostat. The applied ac voltage and ac current response were monitored using a two channel digital storage oscilloscope (Gould model: OS4020). An IBM 286 XT microcomputer linked by an RS232 serial port to the Solartron was used to collect raw data which was converted to ASCII format using a simple Turbo Pascal® (Borland) computer program for further data manipulation.

Lock-in studies were performed using a Jupiter 2000 (Black Star) frequency function generator monitored by an Apollo 100 (Black Star) universal counter-timer. The in-phase and out of phase components of the signal were monitored by a combination of a Low Noise (Lock-in) Amplifier Type 450, a Phase Sensitive Detector Type 411 and Phase Shifter Type 421 (Brookdeal Electronics) coupled to an in-house purpose built low noise potentiostat.

2.6 FT-IR Equipment

Two FT-IR spectrometers were utilised throughout the course of this thesis, the first being a Perkin Elmer 1720X (maximum resolution 2 cm^{-1}) with a purpose built computer work station, the second being a Nicolet 510P (maximum resolution 0.8 cm^{-1}) interfaced with a Philips 386 microcomputer running PCIR software (Nicolet Computers Ltd.). Standard IR techniques were used for normal chemical samples. A 21° to the normal specular reflectance accessory (Specac) was used to study deposits upon electrodes. A special electrode support was designed, figure 2.1, to hold standard size disc electrodes over the reflectance accessory.

Figure 2.1 Electrode support for the specular reflectance accessory

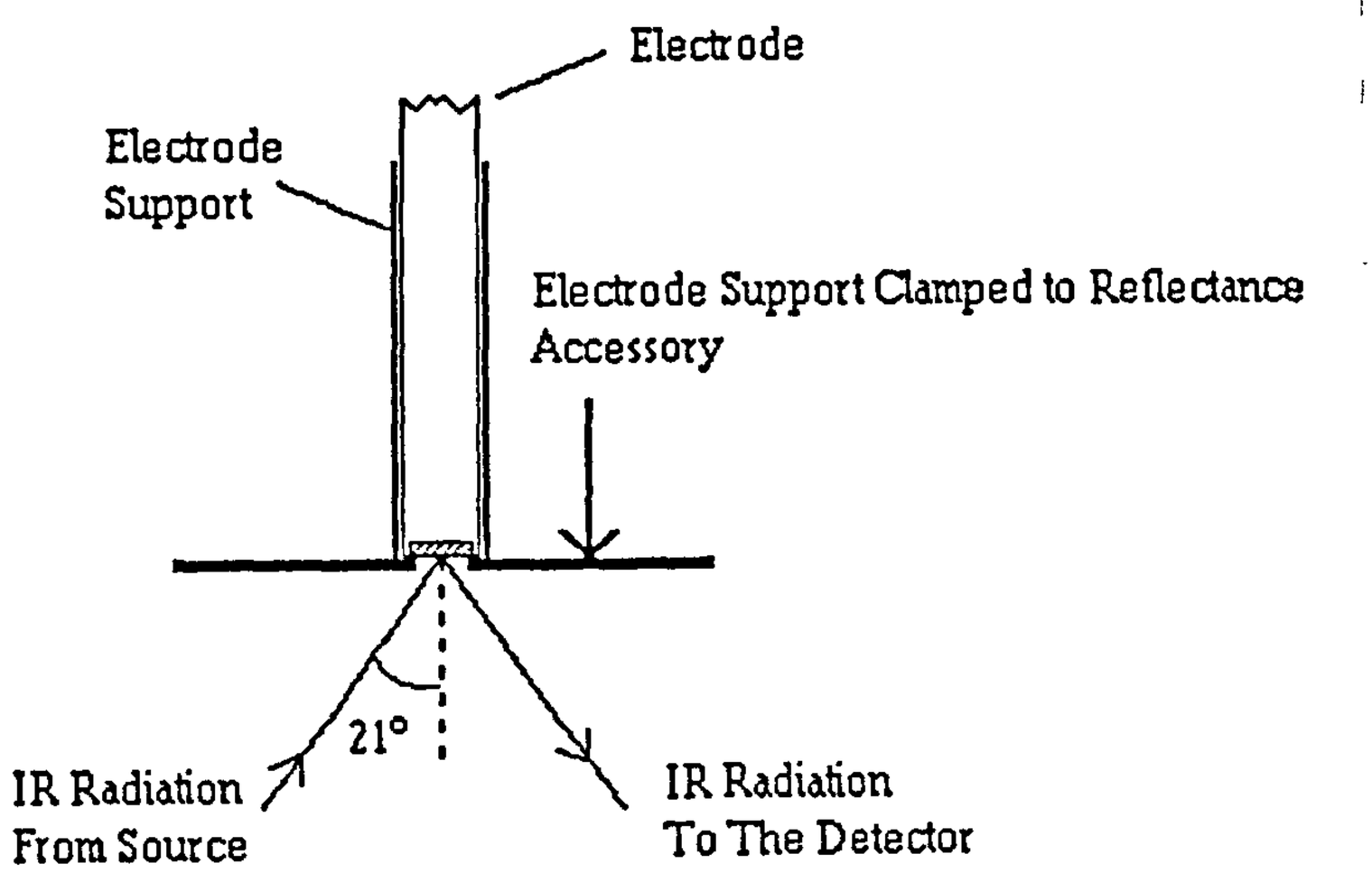

2.7 UV/Vis Equipment

In-situ UV/vis studies were carried out using a diode array UV/vis spectrophotometer (Hewlett-Packard model: 8452A) interfaced to a Hewlett-Packard 386 microcomputer with UV/vis operating software. The cell arrangement shown in figure 2.2 was used at stationary potentials, provided by a simple potentiostat (Oxford Electrodes). The cell is not suitable for potential sweeping due to the size of the working electrode and the position of the reference electrode, which creates *iR* drop effects. Indium doped tin oxide (ITO) electrodes were used as the optically transparent working electrodes, giving an optical cut out below 320 nm.

2.8 Computer Software

Electrochemical data was analysed using Sigma Plot 4.1 (Jandel Software) to produce graphs, calculate regression coefficients (r) and curve fit. PCMODEL (Serina Software) molecular modelling software was used to calculate molecular dimensions and to study theoretical monomer - monomer space filling interactions in polymer chains.

2.9 Purification and Synthesis of Chemicals

Acetonitrile (Aldrich, BDH and Rathburn, HPLC grade) was distilled over calcium hydride, under a dry nitrogen blanket, for at least 24 h and was used immediately without further storage. Tetraethylammonium tetrafluoroborate (TEAT) (Aldrich, 98 %) was recrystallised from methanol (Fisons, AnalaR) and dried under high vacuum. Aqueous solutions were prepared using water from the Whatman WR50 RO purification system pumped through a carbon filter (Whatman model: Still Plus) giving a conductivity in the range 0.1 to 1.0 $\mu S\ cm^{-1}$. Perchloric acid (Aldrich, A. C. S. Reagent) and hydrochloric acid 37% (Aldrich, AnalaR) were used to prepare acidic

Figure 2.2 Electrochemical cell arrangement for UV/vis studies

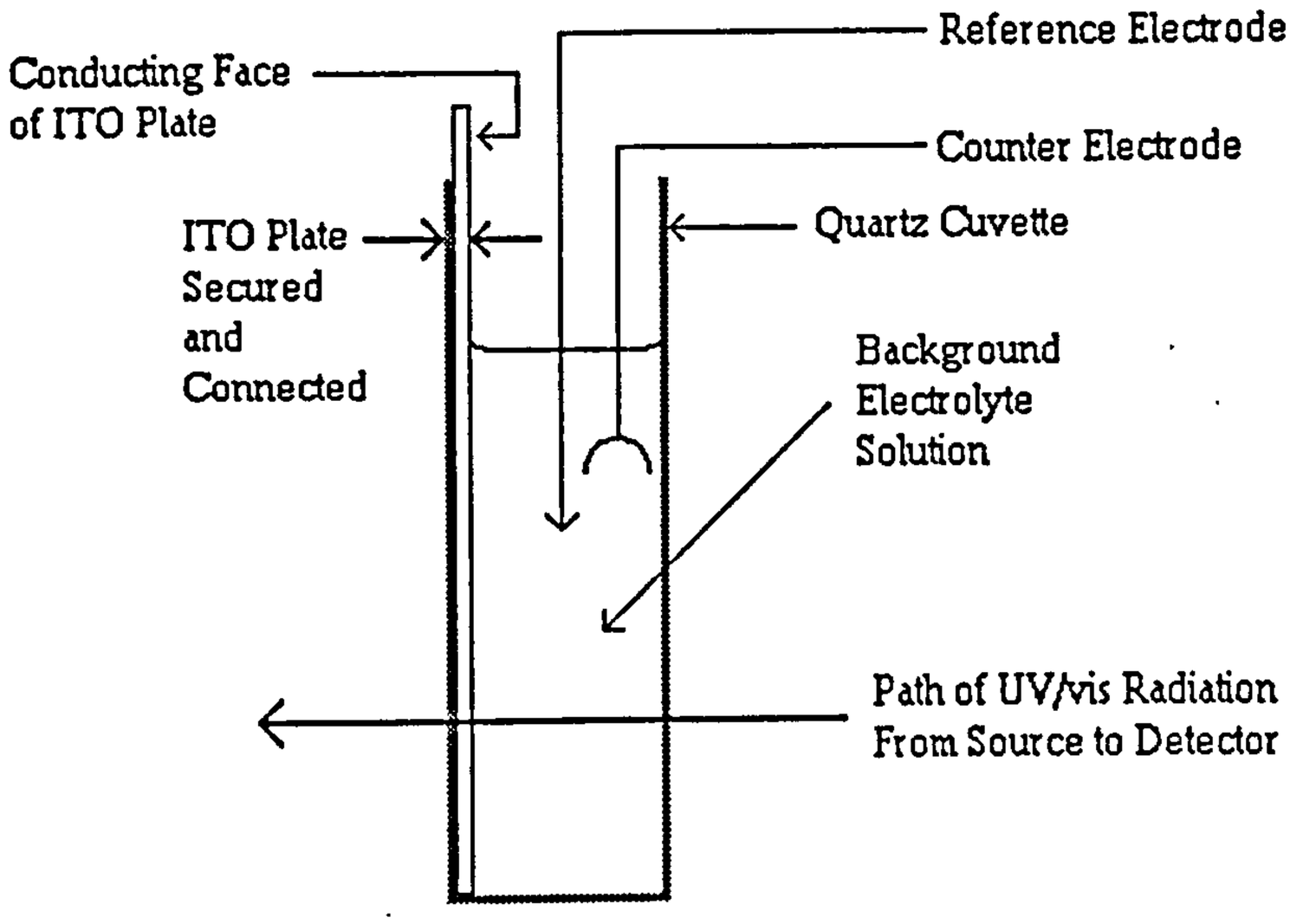

solutions. Sodium Hydroxide (Fisons, AnalaR) was used to prepare basic solutions. The McIlvaine[128] buffer was used extensively throughout the coarse of work described in this thesis. The buffers are prepared from two solution components comprising of firstly citric acid (Fisons, AnalaR) (0.1 mol dm^{-3}) and secondly di-sodium hydrogen orthophosphate (Fisons, AnalaR) (0.2 mol dm^{-3}) both with sodium chloride (Fisons, AnalaR) (0.1 mol dm^{-3}) to increase the ionic strength.

3 Å and 4 Å molecular sieves (Aldrich) were activated by heating (250 - 300 °C) under high vacuum for 24 h.

The monomers studied in this thesis are shown in figure 2.3.

1-(2-Cyanoethyl)pyrrole (I) (Aldrich, 99+ %) was used without further purification.

1-(2-Carboxyethyl)pyrrole (II) was synthesised by refluxing 1-(2-cyanoethyl)pyrrole (5g) in an aqueous potassium hydroxide solution (1.0 mol dm^{-1}) (300 cm^{-3}) with 10% ethanol for 72 h, figure 2.4. The reaction solution was then acidified using concentrated hydrochloric acid solution and extracted using diethyl ether (3 × 50 cm^{-3}). The organic phase was dried over magnesium sulfate and reduced under vacuum to yield needle crystals of 1-(2-carboxyethyl)pyrrole (I) (4.6g, 80%). The solid product was recrystallised from a minimum of distilled cyclohexane. δ_H (ppm, 270 MHz, $CDCl_3$, Me_4Si) δ 2.83 (2H, t, H^4), δ 4.21 (2H, t, H^3), δ 6.15 (2H, m, H^1), δ 6.67 (2H, m, H^2). δ_c (ppm, 67.8 MHz, $CDCl_3$, Me_4Si) δ 36.2 (C^4), δ 44.4 (C^3), δ 108.6 (C^1), δ 120.5 (C^2), δ 176.8 (C^5). m/z (EI) 139 (60%, $M^{+\cdot}$), 94 (40%, $C_4H_4NCH_2CH_2^{+\cdot}$), 80 (100%, $C_4H_4NCH_2^{+\cdot}$). I. R. (cm^{-1}, nujol mull) 1709 (s, C=O stretch), 939 (s, C-OH deformation), 722 (s, C-H pyrrole o. p. bend).

1-(-1-Benzo-15-crown-5-methylene)pyrrole (III) was a gift from Dr. A. C. Benniston and was used without further purification.

Figure 2.3 Monomers studied in this thesis

Pyrroles

(I)

(II)

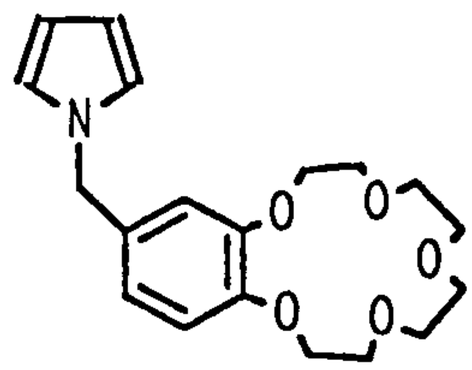

(III)

Thiophenes

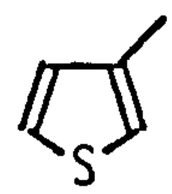

(IV)

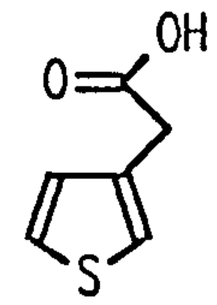

(V)

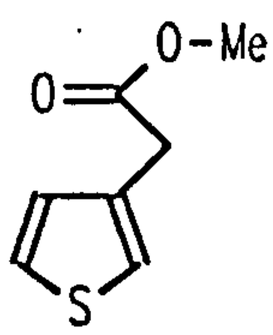

(VI)

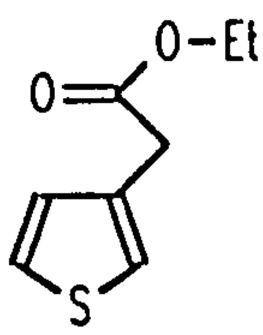

(VII)

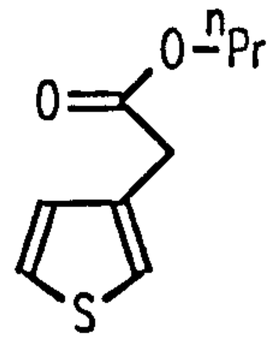

(VIII)

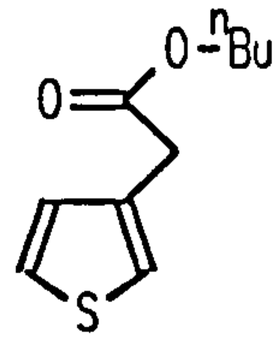

(IX)

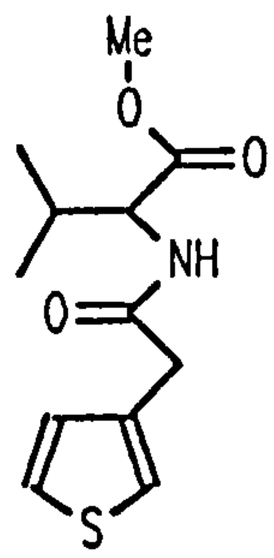

(X)

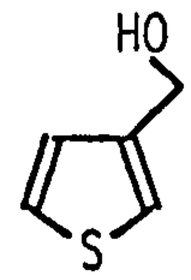

(XI)

Indoles

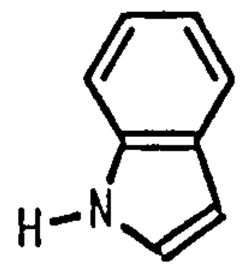

(XII)

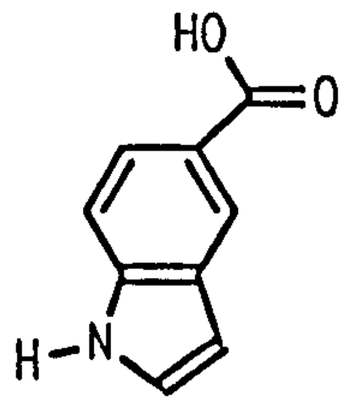

(XIII)

Figure 2.4 Synthesis of 1-(2-carboxyethyl)pyrrole

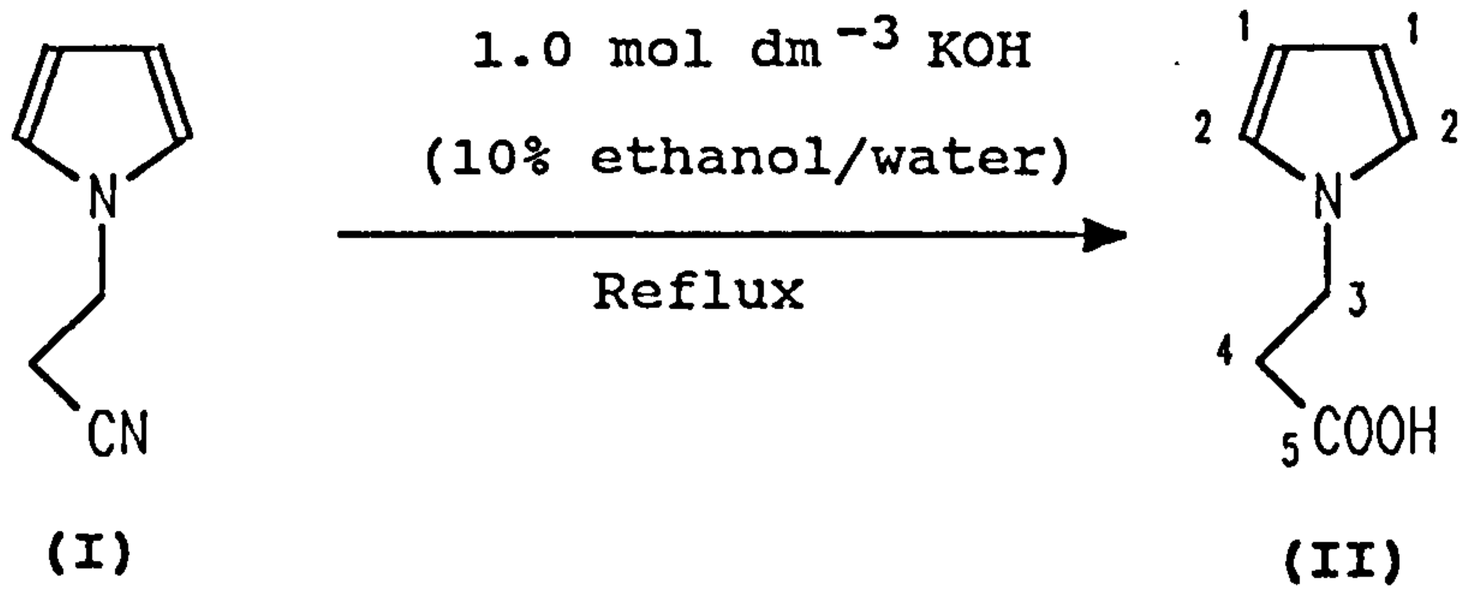

3-Methylthiophene (IV) (Aldrich, 99+ %) was distilled under reduced pressure and stored over activated 3 Å molecular sieves.

3-Thiopheneacetic acid (V) (Aldrich, 98%) was recrystallised from distilled water and dried under high vacuum. Used 3-thiopheneacetic acid (V) was recovered from acetonitrile solution and background electrolyte by reducing the solution under vacuum followed by recrystallising twice from distilled water.

Methyl(3-thiopheneacetate) (VI), ethyl(3-thiopheneacetate) (VII), n-propyl(3-thiopheneacetate) (VIII) and n-butyl(3-thiopheneacetate) were synthesised in the following manner, figure 2.5. Methanol (Fisons, AnalaR), ethanol (Aldrich, AnalaR), n-propanol (Fisons, AnalaR) and n-butanol (Fisons, AnalaR) were distilled separately over calcium hydride and used immediately without further storage. 3-Thiopheneacetic acid (V) (4×5 g) was dissolved in each of the dried alcohols (100 cm^{-3}) with a drop of concentrated hydrochloric acid and refluxed. The reactions were followed using thin layer chromatography with a 10 : 1 dichloromethane (Aldrich, Reagent Grade) : methanol system with a spray for detecting esters (1% vanillin in concentrated sulfuric acid with a trace of ethanol). After complete reaction the reaction solutions were reduced under vacuum and dissolved in diethyl ether (Fisons, Analar) (50 cm^{-3}). The organic phase was washed with saturated sodium hydrogen carbonate solution (3×30 cm^{-3}) and dried over anhydrous magnesium sulfate before being reduced under vacuum and pumped under high vacuum. The esters were obtained as clear liquids (80 - 90 % yield) and used without further purification. Methyl(3-thiopheneacetate) (VI): δ_H (ppm, 400 MHz, $CDCl_3$, Me_4Si) δ 3.65 (2H, s, H^5) δ 3.69 (3H, s, H^7) δ 7.03 (1H, c, H^3) δ 7.14 (1H, c, H^1) δ 7.27 (1H, c, H^2). δ_C (ppm, 100 MHz, $CDCl_3$, Me_4Cl) δ 35.3 (C^5) δ 51.7 (C^7) δ 122.6 (C^4) δ 125.4 (C^3) δ 128.2 (C^1) δ 133.3 (C^2) δ 171.2 (C^6). m/z (EI) 156 (80%, $M^{+\cdot}$) 97 (100%, $(C_4H_4S)CH_2^{+\cdot}$). I. R. (cm^{-1}, thin layer) 3100 (m, αC-H stretch) 2800-3000 (ms, aliphatic

C-H stretches) 1741 (vs, C=O stretch) 1440 (s, CH_3 sym. deformation) 1350-1550 (m, aromatic ring stretches) 1150 (s , CC(=O)-O stretch). (d = 1.26 g cm^{-3}). Ethyl(3-thiopheneacetate) **(VII)**: δ_H (ppm, 400 MHz, $CDCl_3$, Me_4Si) δ 1.27 (3H, t, H^8) δ 3.64 (2H, s, H^5) δ 4.15 (2H, q, H^7) δ 7.04 (1H, c, H^3) δ 7.14 (1H, c, H^1) δ 7.27 (1H, c, H^2). δ_C (ppm, 100 MHz, $CDCl_3$, Me_4Si) δ 13.9 (C^8) δ 35.7 (C^5) δ 60.6 (C^7) δ 122.5 (C^4) δ 125.4 (C^3) δ 128.2 (C^1) δ 133.5 (C^2) δ 170.8 (C^6). m/z (EI) 170 (90%, $M^{+\cdot}$) 97 (100%, $(C_4H_4S)CH_2^{+\cdot}$). I. R. (cm^{-1}, thin layer) 3100 (m, αC-H stretch) 2800-3000 (ms, aliphatic C-H stretches) 1735 (vs, C=O stretch) 1350-1550 (m, aromatic ring stretches) 1150 (s, CC(=O)-O stretch). (d = 1.27 g cm^{-3}) n-Propyl(3-thiopheneacetate) **(VIII)**: δ_H (ppm, 400 MHz, $CDCl_3$, Me_4Si) δ 0.92 (3H, t, H^8) δ 1.60 - 1.69 (2H, c, H^8) δ 3.64 (2H, s, H^5) δ 4.06 (2H, t, H^7) δ 7.04 (1H, c, H^3) δ 7.14 (1H, c, H^1) δ 7.27 (1H, c, H^1). δ_C (ppm, 100 MHz, $CDCl_3$, Me_4Si) δ 10.1 (C^9) δ 21.8 (C^8) δ 35.7 (C^5) δ 66.2 (C^7) δ 122.5 (C^4) δ 125.3 (C^3) δ 128.3 (C^1) δ 133.6 (C^2) δ 170.9 (C^6). m/z (EI) 184 (85%, $M^{+\cdot}$) 97 (100%, $(C_4H_4S)CH_2^{+\cdot}$). I. R. (cm^{-1}, thin layer) 3100 (m, αC-H stretch) 2800-3000 (s, aliphatic C-H stretches) 1735 (vs, C=O stretch) 1350-1550 (m, aromatic ring stretches) 1150 (s, CC(=O)-O stretches). (d = 1.25 g cm^{-3}). n-Butyl(3-thiopheneacetate) **(IX)**: δ_H (ppm, 400 MHz, $CDCl_3$, Me_4Si) δ 0.92 (3H, t, H^{10}) δ 1.31 - 1.40 (2H, c, H^9) δ 1.57 - 1.64 (2H, c, H^8) δ 3.64 (2H, s, H^5) δ 4.10 (2H, t, H^7) δ 7.03 (1H, c, H^3) δ 7.12 - 7.14 (H, c, H^2). δ_C (ppm, 100 MHz, $CDCl_3$, Me_4Si) δ 13.4 (C^{10}) δ 18.9 (C^9) δ 30.4 (C^8) δ 35.7 (C^5) δ 64.5 (C^7) δ 122.5 (C^4) δ 125.3 (C^3) δ 128.2 (C^1) δ 133.6 (C^2) δ 170.8 (C^6). m/z (EI) 198 (25%, $M^{+\cdot}$) 97 (100%, $(C_4H_4S)CH_2^{+\cdot}$). I. R. (cm^{-1}, thin layer) 3100 (w, αC-H stretch) 2800-3000 (s, aliphatic C-H stretches) 1736 (vs, C=O stretch) 1350-1550 (m, aromatic ring stretches) 1150 (s, CC(=O)-O stretch). (d = 1.15 g cm^{-3}).

Compound **(X)** was synthesised by stirring L-valene methyl ester hydrochloride (Aldrich) (1.17g) with distilled triethylamine (Aldrich) (0.97 cm^{-3}) in dry dichloromethane (30 cm^{-3}).

Figure 2.5 Synthesis of the 3-thiopheneacetic acid esters monomers (VI), (VII), (VIII) and (IX)

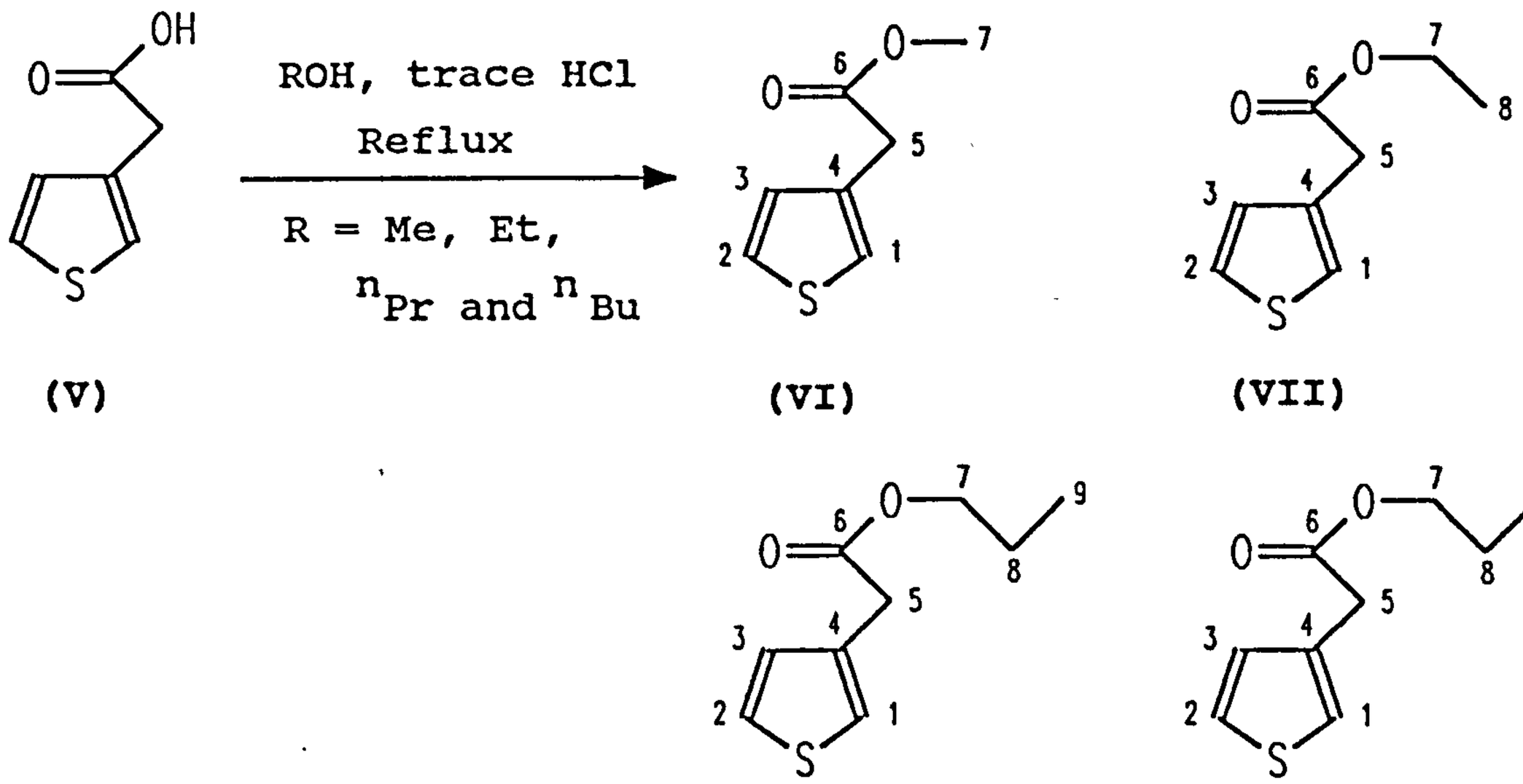

(V) (VI) (VII)

(VIII) (IX)

Figure 2.6 Synthesis of compound (X) using carbodiimide chemistry

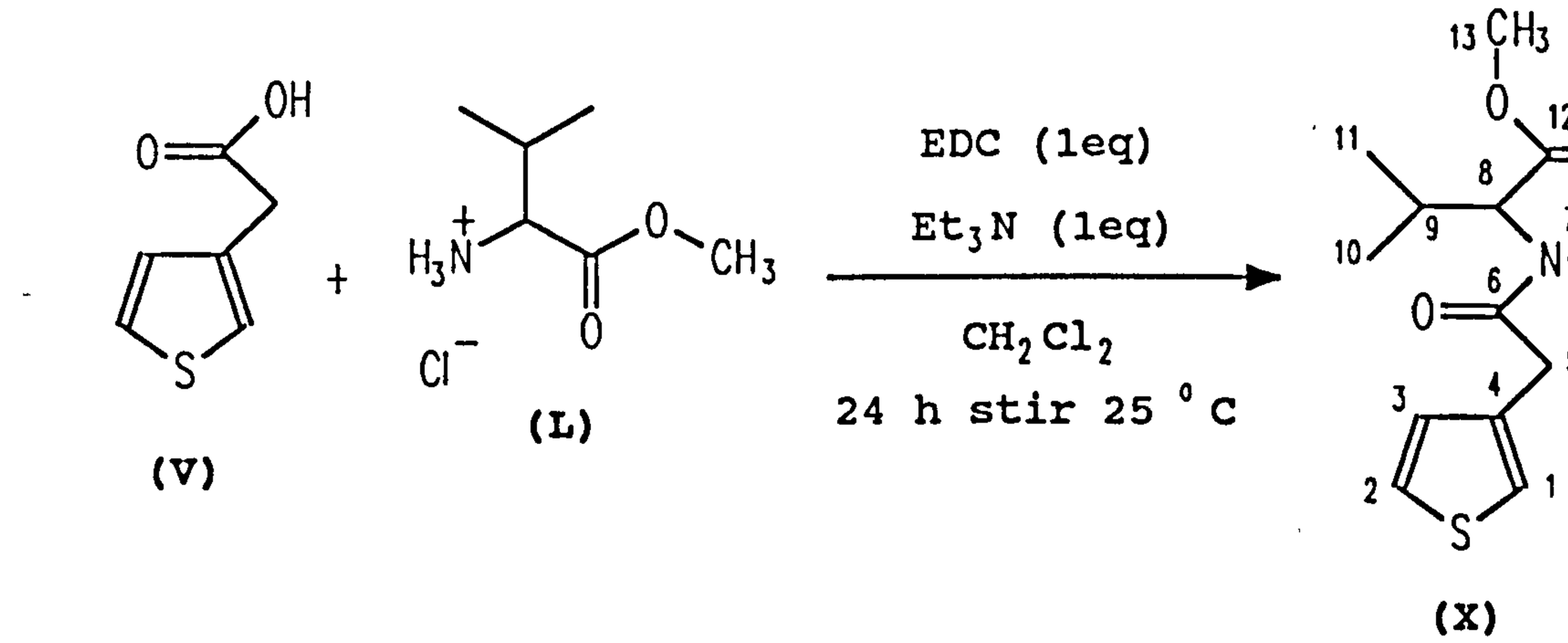

(V) (L) (X)

1-(3-Dimethylaminopropyl)-3-ethylcarbodiimide hydrochloride (Aldrich) (1.48g) and 3-thiopheneacetic acid (1.00g) were added to the reaction mixture and stirred for 24 h, figure 2.6. The reaction mixture was reduced under vacuum and the remaining solid was redissolved in ethyl acetate (Aldrich, Reagent Grade) (50 cm^{-3}) and washed with distilled water (30 cm^{-3}) and saturated sodium hydrogen carbonate solution (30 cm^{-3}) before being dried over anhydrous magnesium sulfate, reduced under vacuum and pumped dry under high vacuum to yield compound (X) (1.31g, 73%) which was used without further purification. δ_H (400 MHz, $CDCl_3$, Me_4Si) 0.76 (3H, d, $H^{(10 \text{ or } 11)}$) δ 0.85 (3H, d, $H^{(10 \text{ or } 11)}$) δ 2.07 (1H, doublet of a septet, H^9) δ 3.62 (2H, d, H^5) δ 3.68 (3H, s, H^{13}) δ 4.5 (1H, dd, H^8) δ 6.01 (1H, d, H^7) δ 7.00 (1H, c, H^3) δ 7.17 (1H, c, H^1) δ 7.32 - 7.34 (1H, c, H^2). δ_C (400 MHz, $CDCl_3$, Me_4Si) δ 17, 19 (C^{10}, C^{11}) δ 31 (C^9) δ 38 (C^5) δ 52 (C^{13}) δ 57 (C^8) δ 123 (C^4) δ 127 (C^3) δ 128 (C^1) δ 134 (C^2) δ 170, 172 (C^6C^{12}). m/z (EI) 255 (20%, $M^{+\cdot}$) 97 (100%, $(C_4H_4S)CH_2^{+\cdot}$). I. R. (cm^{-1}, nujol mull) 3290 (s, N-H stretch) 1742 (s, C=O ester stretch) 1646 (s, C=O peptide stretch) 1551 (s, N-H bend) 1215 (s, O-C-O antisym. stretch).

3-Thiophenemethanol (XI) (Aldrich, 99 %) was distilled under reduced pressure and stored over activated 3 Å molecular sieves before use.

Indole (XII) (Aldrich, 99+ %) was sublimed under reduced pressure, protected from direct light and stored at below 0 °C.

5-carboxyindole (XIII) (Aldrich, 99%) was recrystallised from a minimum of distilled water and dried under high vacuum for 48 h.

2.10 Deuteration of Indole-5-carboxylic Acid

5-carboxyindole (XIII) was deuterated[129] at the 3-position by recrystallising in deuterium oxide with a trace of concentrated

hydrochloric acid, figure 2.7. ^1H NMR data showed that the 3-position was fully deuterated and the 1-position was partially deuterated, FTIR data will be discussed in the following chapters.

Figure 2.7 Deuteration of 5-carboxyindole (XIII)

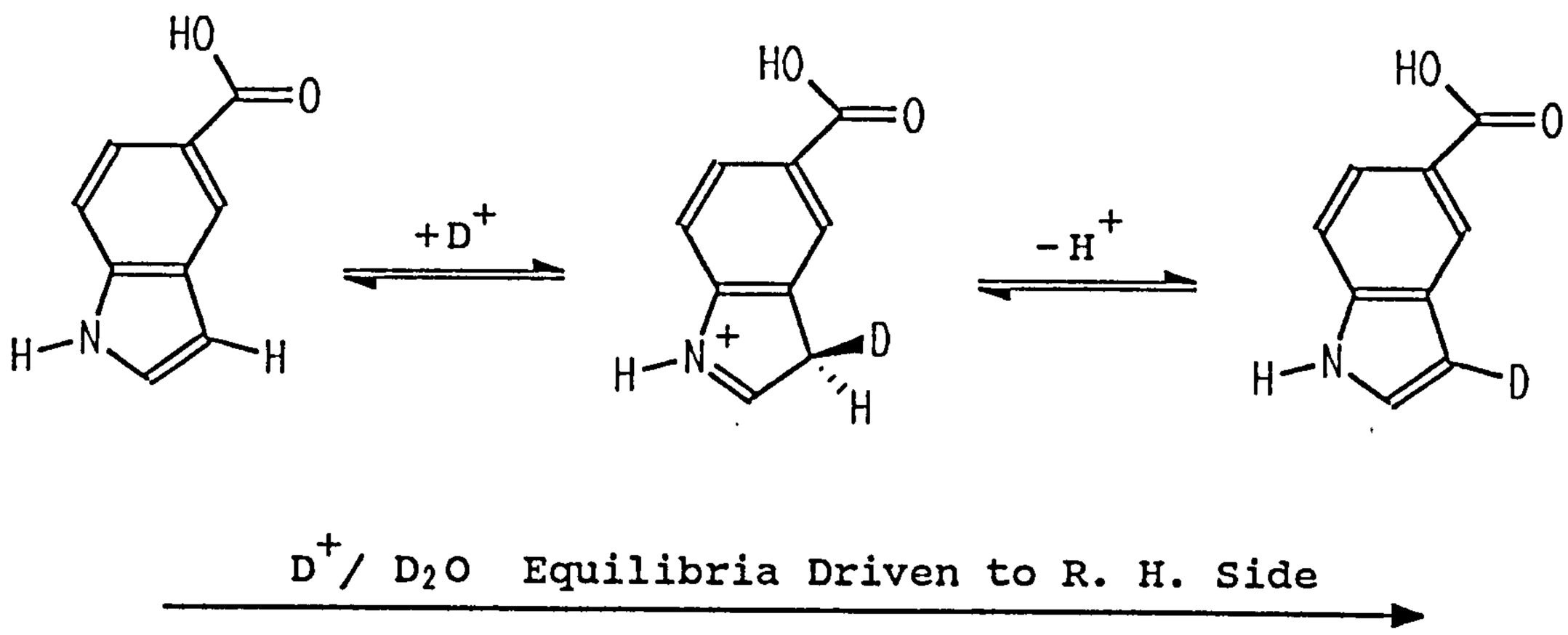

Chapter 3

Chemically Modified Poly(pyrroles)

3.1 Introduction

Poly(pyrroles) being the largest class of heterocyclic conducting polymer have been studied intensely in many different areas of application.[10,11,12,13,14] As mentioned previously

several pyrrole monomers, with carboxylic acid substituents,[17,63] have been studied but a full understanding of their particular effects has not as yet been reached. It is not the aim of this chapter to intensively study the effects of the various substituents, but rather to provide a contrast with which to compare the more complete studies performed on both poly(thiophenes) and poly(indoles). Finally, a poly(pyrrole) macrocyclic polymer (appendix 1) is described in detail and provides a further example of a novel chemically modified poly(pyrrole).

3.2 Electrochemical Polymerisation of Poly(1-(2-cyanoethyl)pyrrole) and Poly(1-(2-carboxyethyl)pyrrole)

Films of poly(1-(2-cyanoethyl)pyrrole) were grown from solutions of 1-(2-cyanoethyl)pyrrole (I) (20 mmol dm^{-3}) in acetonitrile containing TEAT (0.1 mol dm^{-1}) by potentiometrically stepping from 0 V to 1.25 V (vs. SCE) at a polished stationary platinum disc electrode (A = 0.385 cm^2). A steady i - t transient is observed after 5 s, similar to those reported by Hillman *et al.*[38] with an initial nucleation transient, figure 3.1. Films could be grown for extended periods of time ($t > 60$ s) without passivating the electrode.

Films of poly(1-(2-carboxyethyl)pyrrole) were grown from solutions of 1-(2-carboxyethyl)pyrrole (II) (20 mmol dm^{-3}) in acetonitrile containing TEAT (0.1 mol dm^{-3}) by potentiometrically stepping from 0 V to

Figure 3.1 Growth of poly(1-(2-cyanoethyl)pyrrole) by potentiometrically stepping from 0.0 V to 1.25 V (vs. SCE) in a solution of 1-(2-cyanoethyl)pyrrole (20 mmol dm^{-3}) in acetonitrile containing TEAT (0.1 mol dm^{-3}) at a stationary platinum electrode (A = 0.385 cm^2)

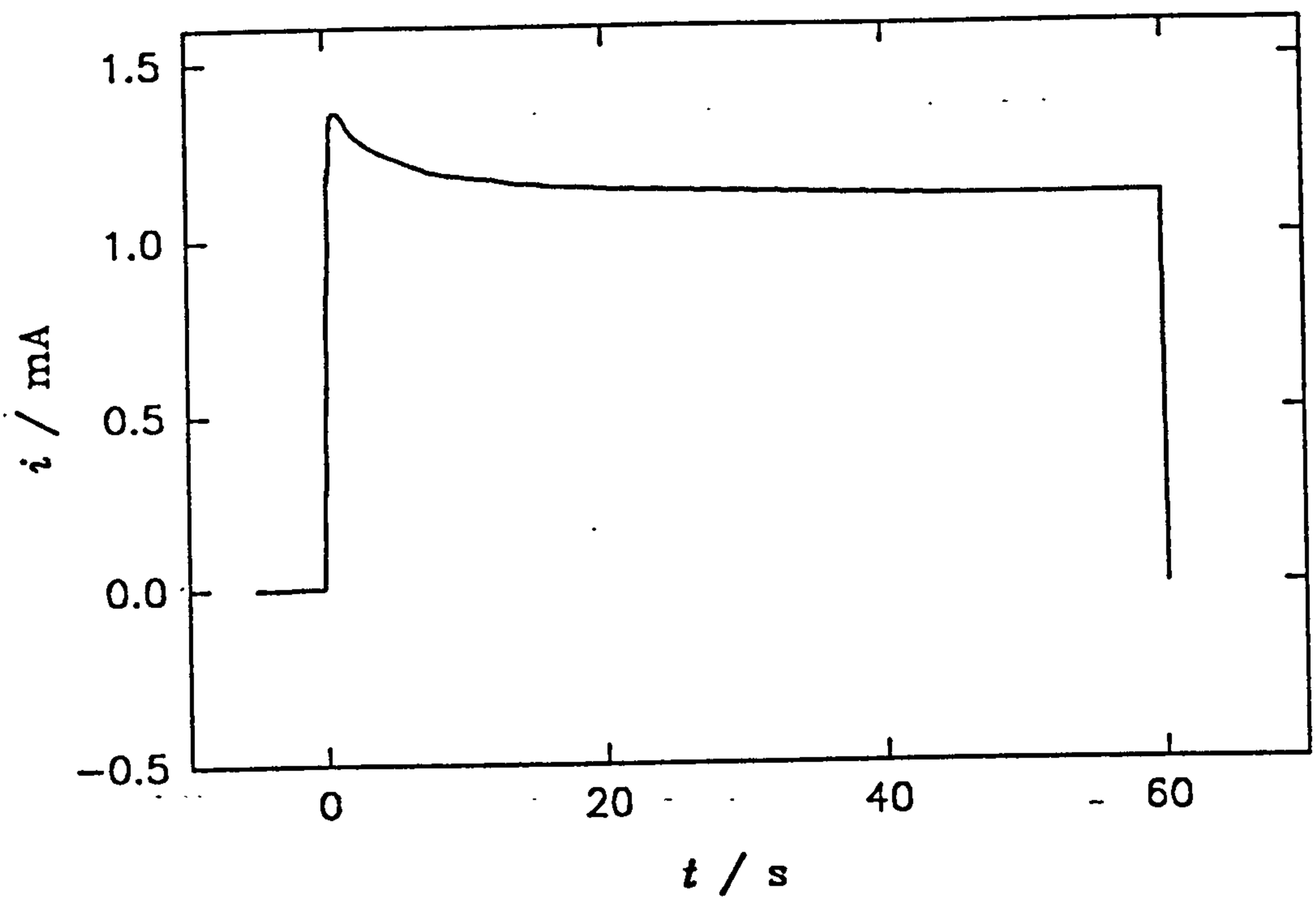

1.35 V (vs. SCE) at a polished stationary platinum disc electrode ($A = 0.385$ cm^2). An initial nucleation is observed followed by a decreasing transient similar to the diffusion limited $i - t^{-1/2}$ transients observed by Pletcher *et al.*[35], figure 3.2.

Neither polymer could be grown in McIlvaine[128] citrate/phosphate pH 7 buffered solutions of the monomer (0.1 mol dm^{-3}).

3.3 Electrochemistry of Poly(1-(2-cyanoethyl)pyrrole) and Poly(1-(2-carboxyethyl)pyrrole)

Films of Poly(1-(2-cyanoethyl)pyrrole) display very reproducible cyclic voltammetry, from fully reduced to fully oxidised, in background acetonitrile solution containing TEAT (0.1 mol dm^{-3}) between -0.3 V and 1.1 V (vs. SCE) with no apparent loss in electroactivity. The cyclic voltammograms show an initial pre-wave between 0.4 and 0.5 V (vs. SCE) and a much larger redox wave which has an $E_{pa} = 0.75$ V (r = 0.998, n = 9) and an $E_{pc} = 0.75$ V (r = 0.993, n = 9) (vs. SCE) at limiting low sweep rates, figure 3.3; this eliminates iR drop effects. The values obtained for the E_{pa} and E_{pc} are slightly higher than other reported N-substituted poly(pyrroles)[130] indicating increased disruption in the planarity of the polymer.[115] Plots of anodic peak current (i_{pa}) vs. sweep rate (υ) for a film grown for 60 s, figures 3.4 and 3.5, are linear (r = 0.999, n = 9) corresponding to immobilised redox site behaviour.

The dopancy (δ) of a long chain conducting polymer can be roughly estimated from the ratio of the charge passed in the growth transient (Q_T) to the charge passed under the cyclic voltammogram (Q_{CV}) using the trivially derived equation (3.1).

$$(Q_T/Q_{CV}) = 2/\delta + 1 \qquad (3.1)$$

Figure 3.2 Growth of poly(1-(2-carboxyethyl)pyrrole) by potentiometrically stepping from 0.0 V to 1.35 V (vs. SCE) in a solution of 1-(2-carboxyethyl)pyrrole (20 mmol dm^{-3}) in acetonitrile containing TEAT (0.1 mol dm^{-3}) at a stationary platinum electrode (A = 0.385 cm^2)

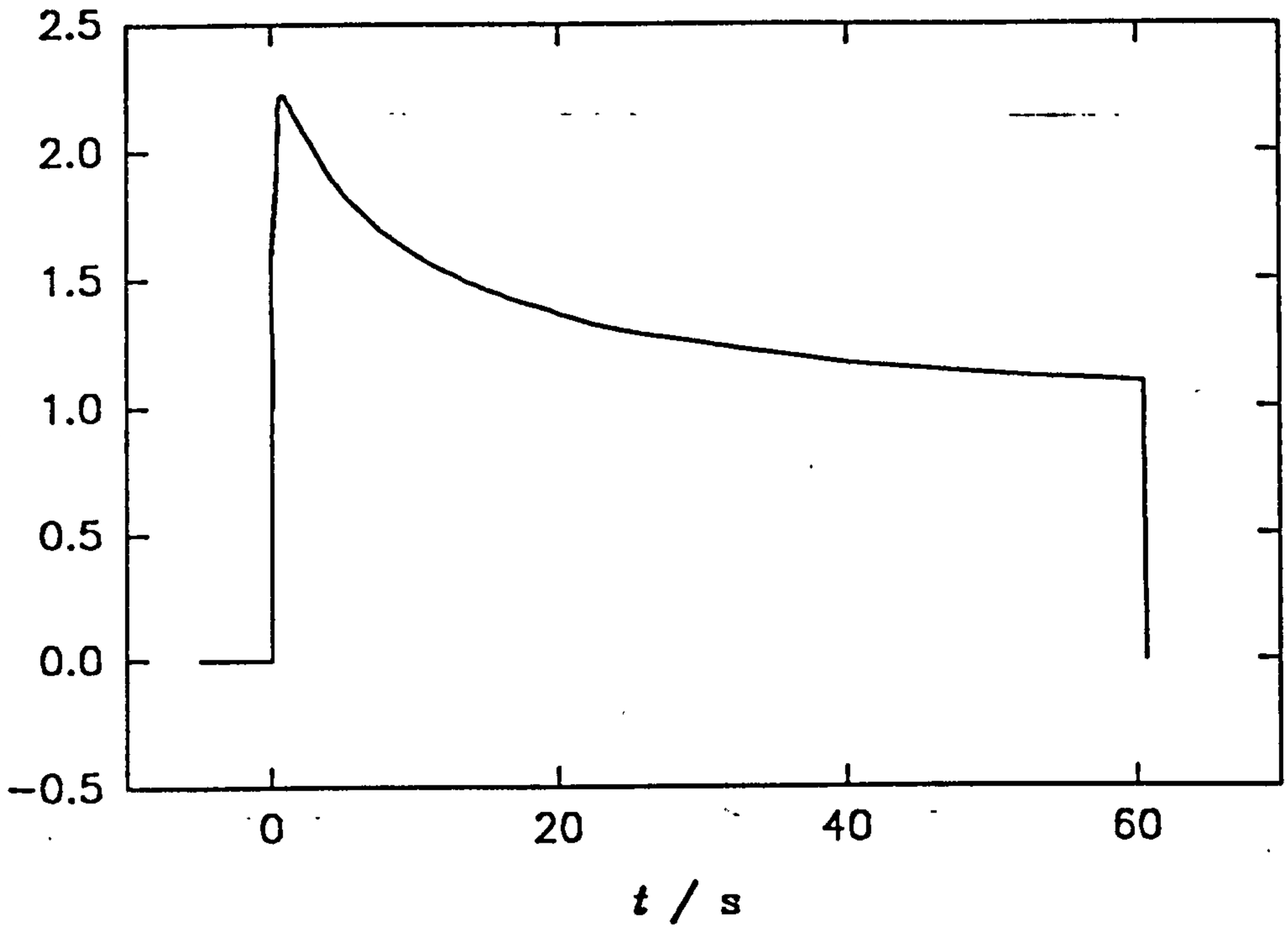

Figure 3.3 Plot of E_{pa} (○) and E_{pc} (●) V (vs. SCE) against sweep rate (υ) for a film of poly(1-(2cyanoethyl)pyrrole) (previously grown for t = 60 s at a platinum electrode (A = 0.385 cm2)) (○, r = 0.998, n = 9) (●, r = 0.993, n = 9)

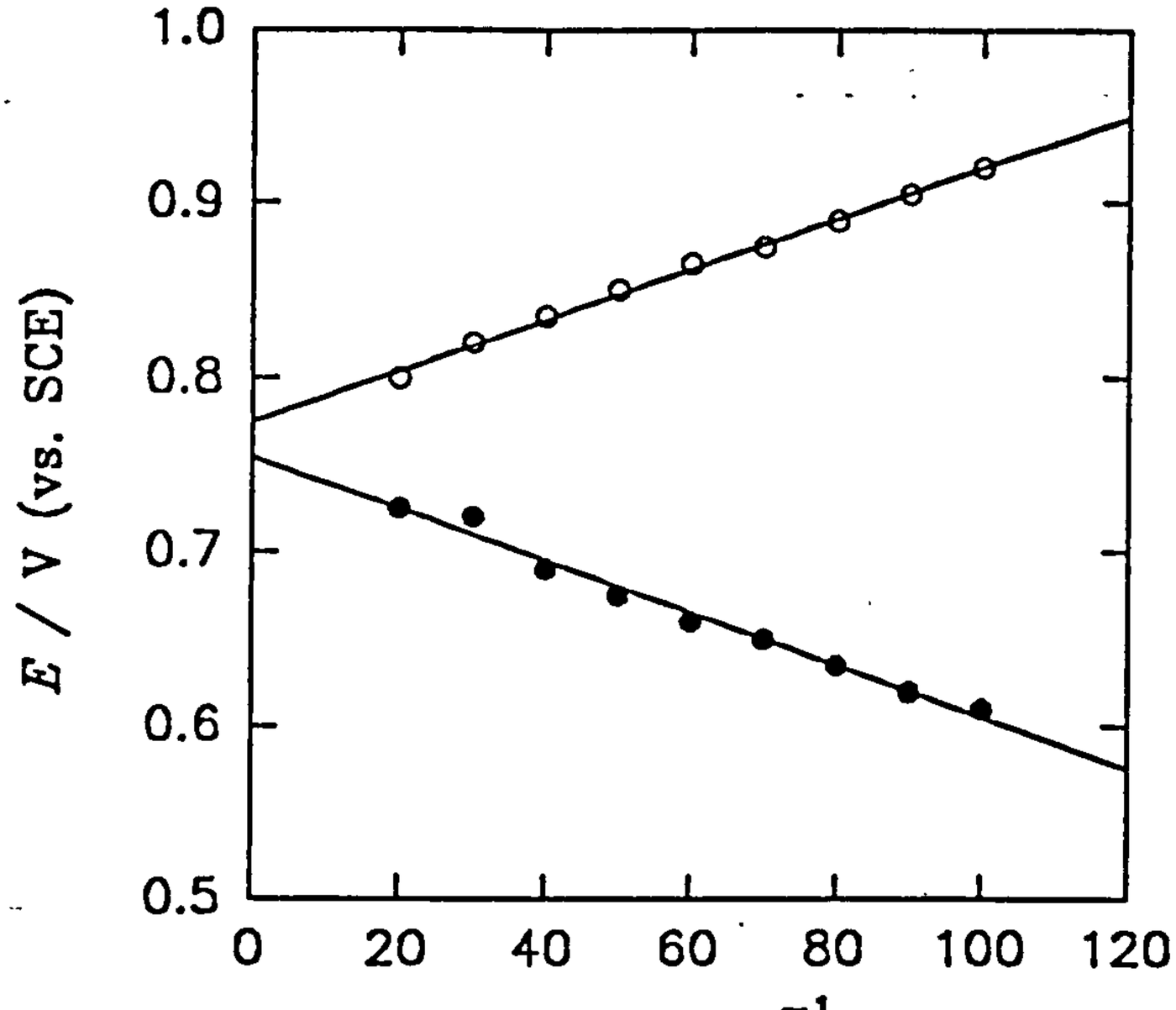

Figure 3.4 Cyclic voltammetry at 20, 50 and 100 mV s^{-1} in acetonitrile containing TEAT (0.1 mol dm^{-3}) of a poly(1-(2cyanoethyl)pyrrole) film, grown for t = 60 s, on a platinum electrode (A = 0.385 cm^2)

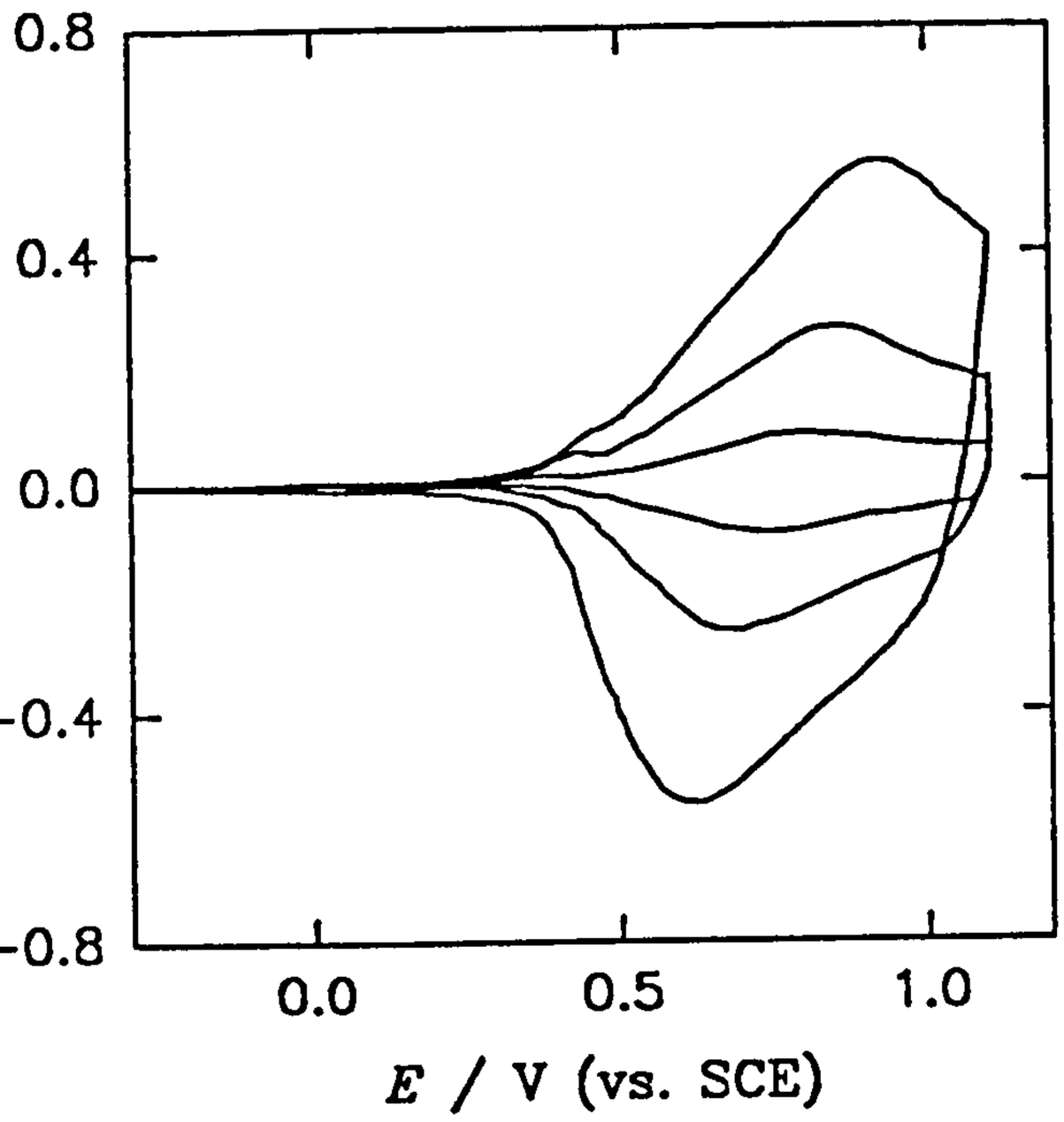

Figure 3.5 Plot of i_{pa} against sweep rate (υ) for the poly(1-(2-cyanoethyl)pyrrole) film whose cyclic voltammetry is shown in figure 3.4 ($r = 0.999$, $n = 9$)

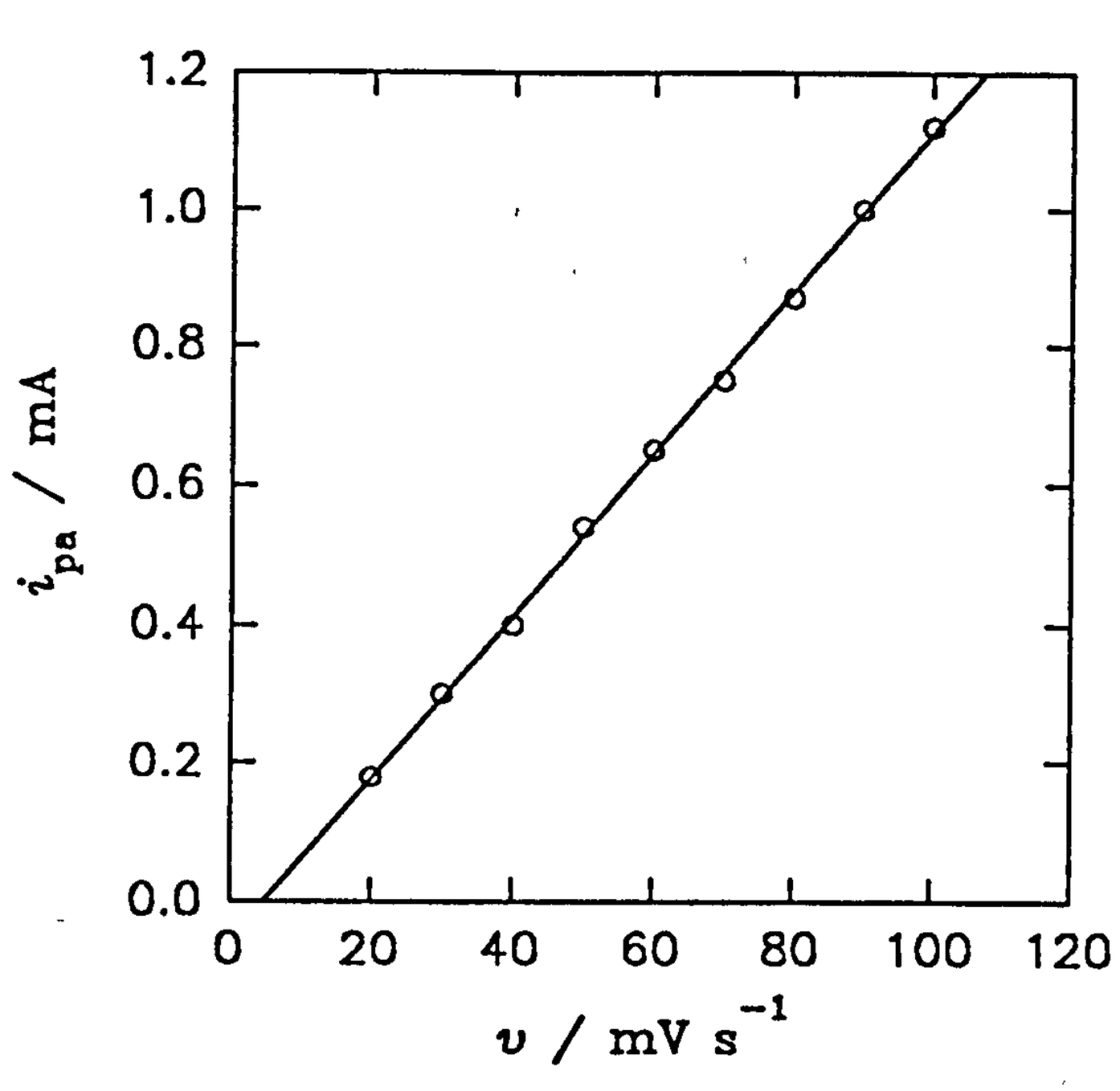

For poly(1-(2-cyanoethyl)pyrrole) the dopancy calculated from equation (3.1) was $\delta = 0.15$ which is rather low compared to poly(pyrrole). However the value is consistent with other reported N-substituted poly(pyrroles)[130]. The calculation assumes a totally faradaic efficient polymerisation and no losses during cyclic voltammetry.

Poly(1-(2-carboxyethyl)pyrrole) displays very irreproducible cyclic voltammetry in background acetonitrile solution containing TEAT (0.1 mol dm^{-3}) where Q_{CV} diminishes on successive cycles. A sweep rate analysis could not be performed and dopancy (δ) was not calculated.

Neither polymer displayed any electrochemistry in aqueous potassium nitrate solution (0.1 mol dm^{-3}) or aqueous citric acid (0.1 mol dm^{-3}) and sodium chloride (0.1 mol dm^{-3}) solution. For poly(1-(2-cyanoethyl)pyrrole) the polymer appeared to be hydrophobic and for poly(1-(2-carboxyethyl)pyrrole) it has been reported that the polymer is soluble in water.[131] The absence of aqueous electrochemistry seriously reduces the potential applications of these two polymers. FTIR studies were performed to complete the overall characterisation of the polymers.

3.4 FTIR Spectroscopic Characterisation of Poly(1-(2-cyanoethyl)pyrrole) and Poly(1-(2-carboxyethyl)pyrrole)

Reflectance FTIR spectra of poly(1-(2-cyanoethyl)pyrrole) and poly(1-(2-carboxyethyl)pyrrole) were recorded in their fully reduced and fully oxidised states. Polymer spectra were compared to spectra of the two monomers and were found to have broad bands typical of polymer species.[132] The polymers were always carefully washed in neat acetonitrile and allowed to dry before being studied.

The reflectance FTIR spectrum of fully reduced

poly(1-(2-cyanoethyl)pyrrole) held at 0 V (vs. SCE) in an acetonitrile solution containing TEAT (0.1 mol dm^{-3}), figure 3.6, displays a weak aromatic pyrrole βC-H stretch at 3120 cm^{-1} but no aromatic pyrrole αC-H stretch which is present at 3105 cm^{-1} in the monomer spectrum. Aliphatic C-H stretches are observed in both the monomer and polymer spectra between 2920 cm^{-1} and 2960 cm^{-1}. The C≡N stretch in the monomer spectrum appears as a strong band at 2253 cm^{-1}, in the polymer spectrum the same band is observed but is either attributed to free monomer trapped within the polymer or surface polymer since a broader band centred again at 2253 cm^{-1} is likely to be due to bulk polymer C≡N stretching. The remainder of the polymer spectrum, below 2000 cm^{-1}, is complex and hard to assign. However there are bands between 1360 cm^{-1} and 1505 cm^{-1} which can be assigned to aromatic ring stretches.[133] Interestingly a peak at 1700 cm^{-1} is also observed which may be due to α,β unsaturated carbonyls produced during overoxidation.[36,37] The monomer spectrum has a strong peak at 722 cm^{-1} corresponding to an aromatic pyrrole C-H out of plane stretch which is not present in the polymer spectrum indicating that this feature is due mainly to αC-H. The feature between 3300 cm^{-1} and 4000 cm^{-1} in the polymer spectrum has not been assigned but may be electronic in nature.

The reflectance FTIR spectrum of fully oxidised poly(1-(2-cyanoethyl)pyrrole) held at 1.25 V (vs. SCE) in acetonitrile solution containing TEAT (0.1 mol dm^{-3}), figure 3.7, displays marked differences from the reflectance FTIR spectrum of the fully reduced polymer, figure 3.6. Between 2500 cm^{-1} and 4000 cm^{-1} electronic transitions are observed which totally obscure the C-H stretching regions. The C≡N monomer stretch at 2253 cm^{-1} is observed again but the polymer C≡N broad band is now centred at 2100 cm^{-1} indicating a marked environment change. The aromatic ring stretching region[133] between 1360 cm^{-1} and 1505 cm^{-1} shows the largest deviations from the

Figure 3.6 The FT-IR spectrum of a fully reduced film of poly(1-(2-cyanoethyl)pyrrole) previously held at 0.0 V (vs. SCE) in acetonitrile containing TEAT (0.1 mol dm^{-3})

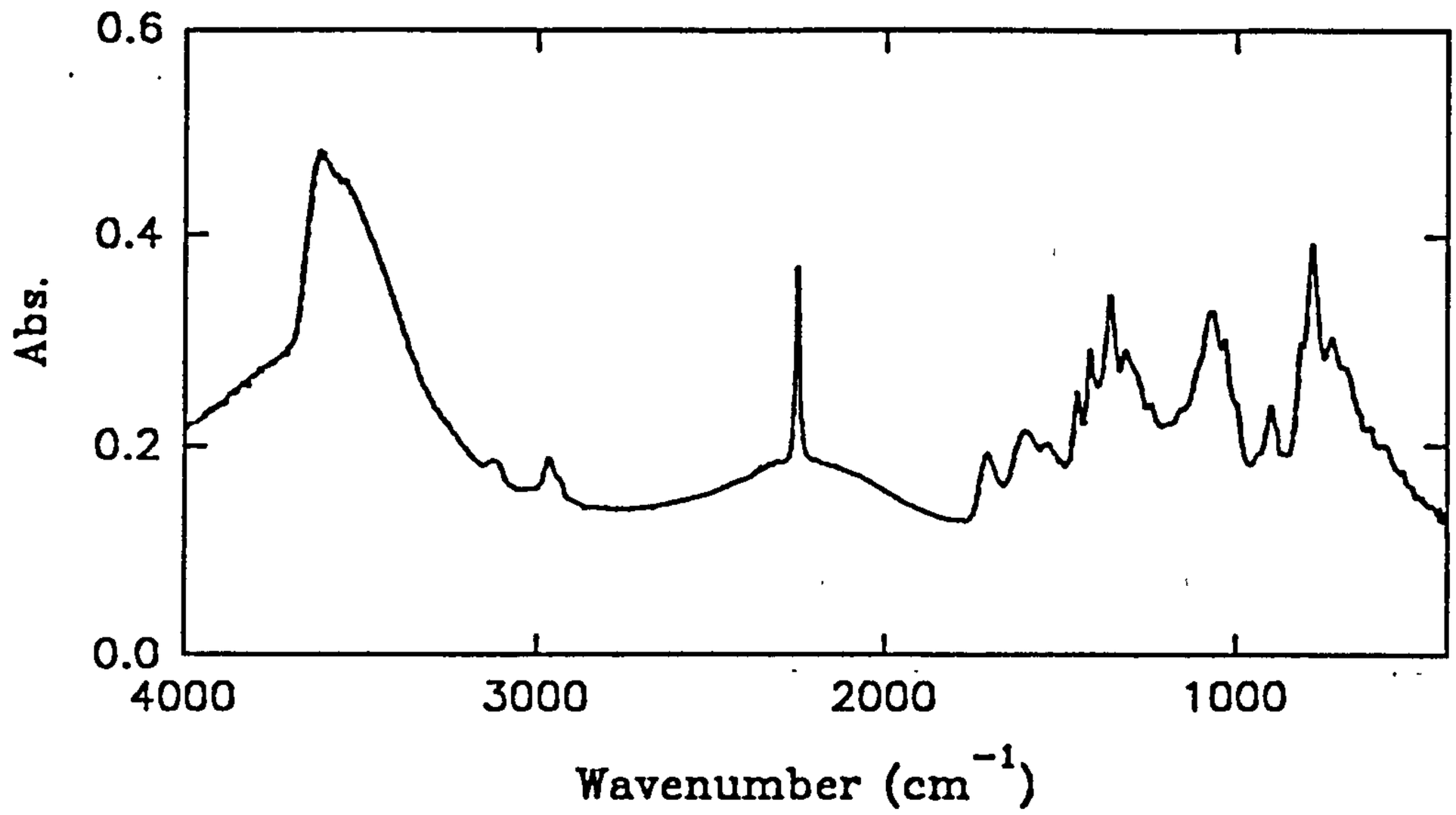

Figure 3.7 The FT-IR spectrum of a fully oxidised film of poly(1-(2-cyanoethyl)pyrrole) previously held at 1.25 V (vs. SCE) in acetonitrile containing TEAT (0.1 mol dm^{-3})

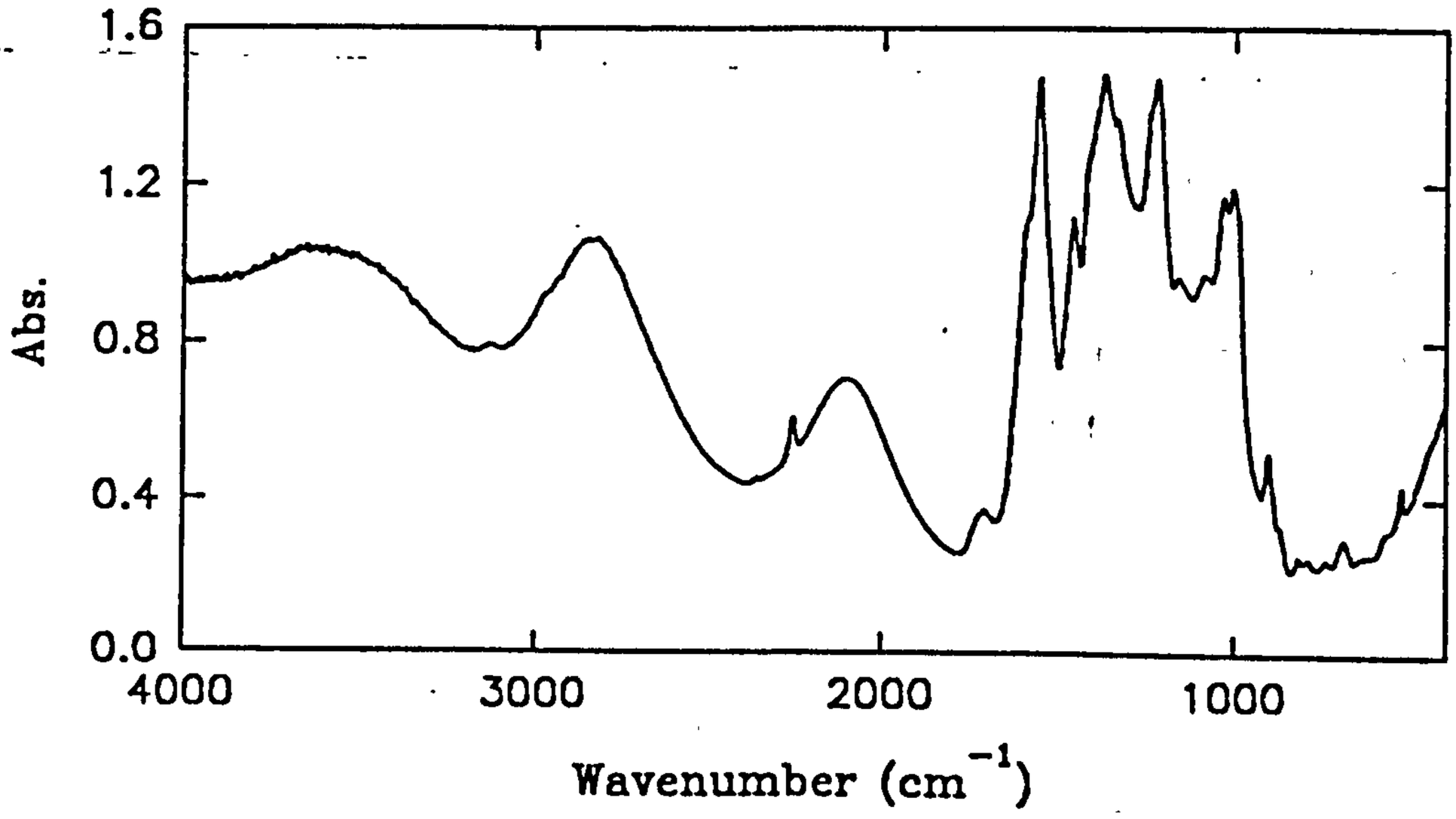

fully reduced polymer which is expected from the large structural changes incurred during oxidation of the polymer. There is evidence, in terms of increased absorption, for the incorporation of BF_4^- in the polymer at 1060 cm^{-1}; this is slightly obscured by other peaks in that region.

The reflectance FTIR spectrum of fully reduced poly(1-(2-carboxyethyl)pyrrole) held at 0.0 V (vs. SCE) in a solution of acetonitrile containing TEAT (0.1 mol dm^{-3}), figure 3.8, showed similarities with the monomer spectrum in nujol mull. The region between 2000 cm^{-1} and 4000 cm^{-1} is ill-defined due to the O-H stretch in both the monomer and polymer spectrum. The polymer and monomer spectra both have strong C=O peaks at 1703 cm^{-1} corresponding to typical dimerised carboxylic acid carbonyl stretches. Aromatic ring stretches are observed between 1350 cm^{-1} and 1550 cm^{-1} for both the monomer and polymer. The monomer spectrum displays a medium strength peak at 726 cm^{-1} corresponding to an aromatic C-H out of plane stretch; this is absent from the polymer spectrum indicating that this band is due mainly to αC-H on the pyrrole ring.

The reflectance FTIR spectrum of fully oxidised poly(1-(2-carboxyethyl)pyrrole) held at 1.35 V (vs. SCE) in acetonitrile containing TEAT (0.1 mol dm^{-3}), figure 3.9, has only minor differences compared to the fully reduced polymer spectrum, figure 3.8. The acid carbonyl peak is unchanged but the aromatic ring stretching region[133] between 1350 cm^{-1} and 1550 cm^{-1} shows small differences from the fully reduced monomer. A peak at 1060 cm^{-1} is observed which is due to the BF_4^- counter ion.

Both polymers display FTIR spectra which confirms their proposed structures and shows standard behaviour for fully reduced and fully oxidised poly(pyrroles). The functionalities associated with the two monomers have been shown to be preserved during polymerisation.

Figure 3.8 The FT-IR spectrum of a fully reduced film of poly(1-(2-carboxyethyl)pyrrole) previously held at 0.0 V (vs. SCE) in acetonitrile containing TEAT (0.1 mol dm^{-3})

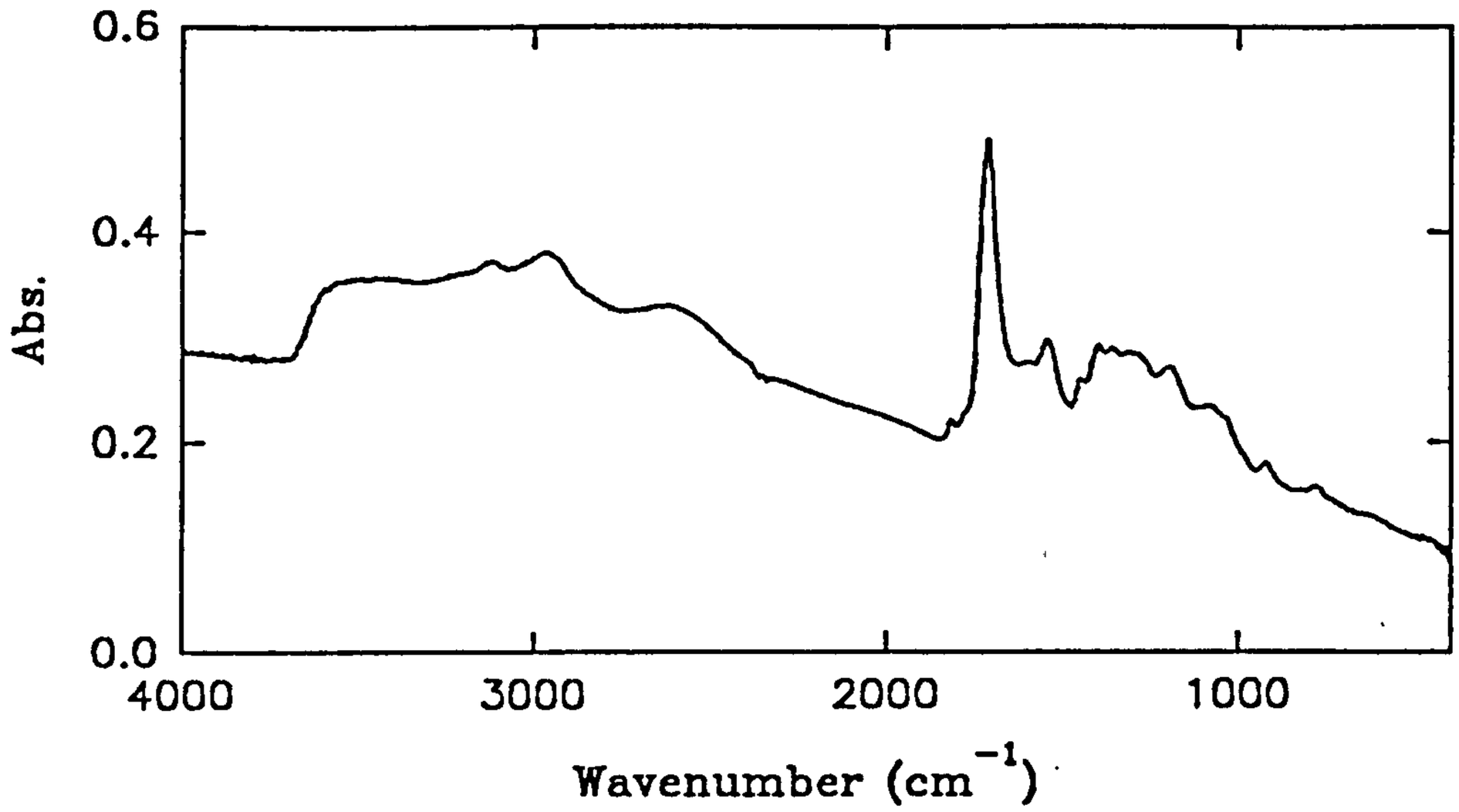

Figure 3.9 The FT-IR spectrum of an oxidised film of poly(1-(2-carboxyethyl)pyrrole) previously held at 1.35 V (vs. SCE) in acetonitrile containing TEAT (0.1 mol dm^{-3})

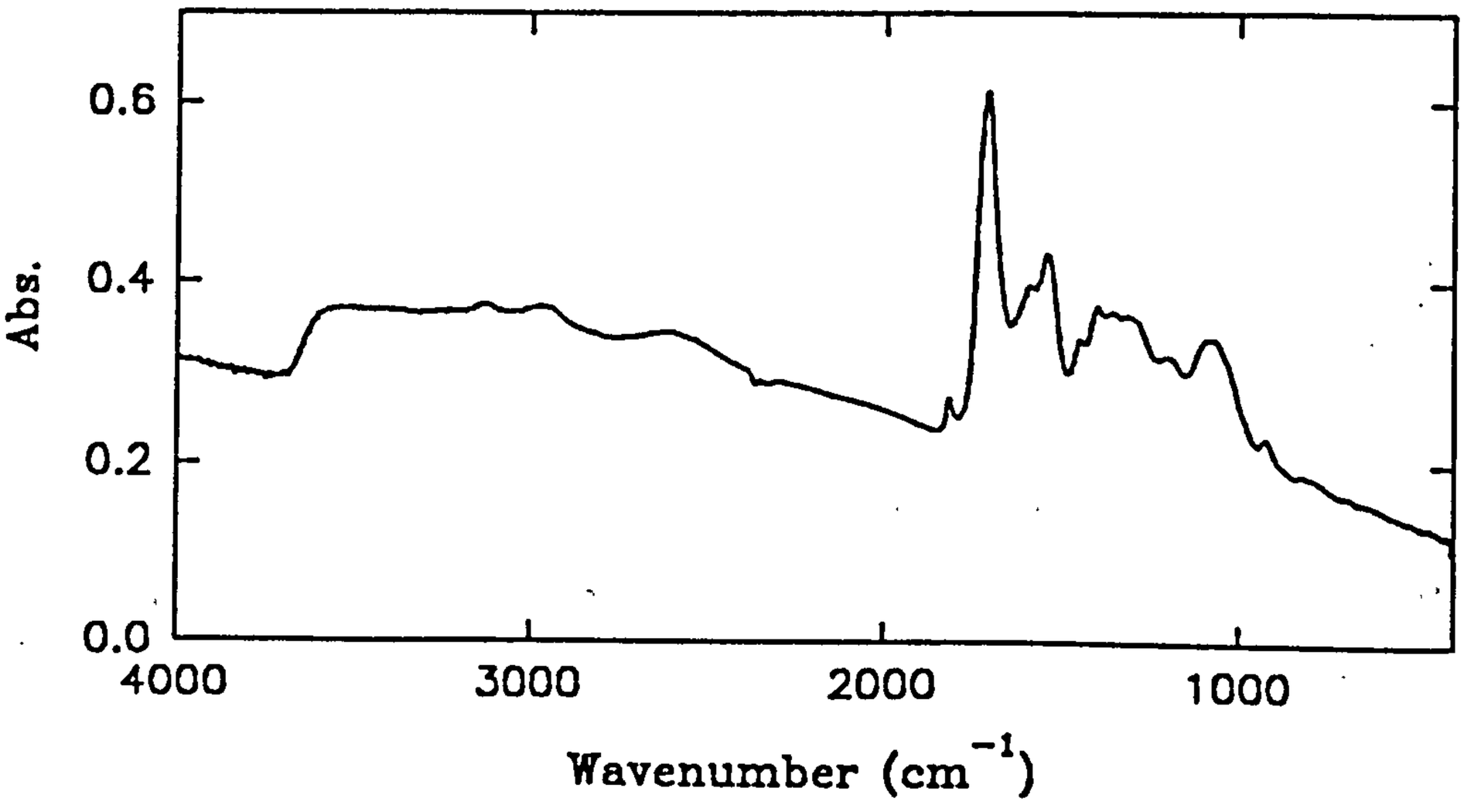

The spectrum for poly(1-(2-cyanoethyl)pyrrole) shows that the nitrile peak is more sensitive to oxidation of the polymer than the carbonyl peak in the spectrum for poly(1-(2-carboxyethyl)pyrrole). This is probably due to the ability of the carboxylic acid groups to dimerise which would tend to reduce the effect of the incorporated counter ion on the substituent.

The two polymers, poly(1-(2-cyanoethyl)pyrrole) and poly(1-(2-carboxyethyl)pyrrole), will not be discussed further since their limited aqueous electrochemistry prevents any additional studies from being made.

3.5 Growth, Electrochemistry and Characterisation of poly(15-(1-pyrrolyl)methyl[benzo-15-crown-5])

Films of poly(15-(1-pyrrolyl)methyl[benzo-15-crown-5]) (appendix 1) were grown on a polished stationary platinum disc electrode by cyclic voltammetry of a solution of 15-(1-pyrrolyl)methyl[benzo-15-crown-5] (III) (10 mmol dm^{-3}) in acetonitrile containing TEAP (0.1 mol dm^{-3}) at 50 mV s^{-1} between 0 V and 1.1 V (vs. SCE), figure 3.10. Films could also be grown under the same conditions by potentiometrically stepping from 0 V to 1.1 V (vs. SCE) but a lower quality polymer, in terms of visual appearance, is formed. Only limited experiments could be performed on this compound due to its low availability

Benzo-15-crown-5[134] is known to bind Na^+ more strongly than Li^+, K^+ or TEA^+ and when covalently bound to a conducting polymer there may be significant changes in electrochemistry in the presence of alkali metal ions due to Donnan type interactions and bulk restructuring of the polymer. Other poly(ether) modified conducting polymers have previously been studied[70,135] and shown to have differing electrochemistry in alkali metal ion electrolyte solutions but poly(15-(1-pyrrolyl)methyl[benzene-15-crown-5]) is believed to be the

Figure 3.10 The growth of poly(15-(1-pyrrolyl)methyl-[benzene-15-crown-5]) by cyclic voltammetry between 0.0 V and 1.1 V (vs. SCE) of a solution of 15-(1-pyrrolyl)methyl[benzo-15-crown-5] (III) (10 mmol dm^{-3}) in acetonitrile containing TEAP (0.1 mol dm^{-3}) at a stationary platinum electrode (A = 0.385 cm^2) (sweep rate υ = 50 mV s^{-1})

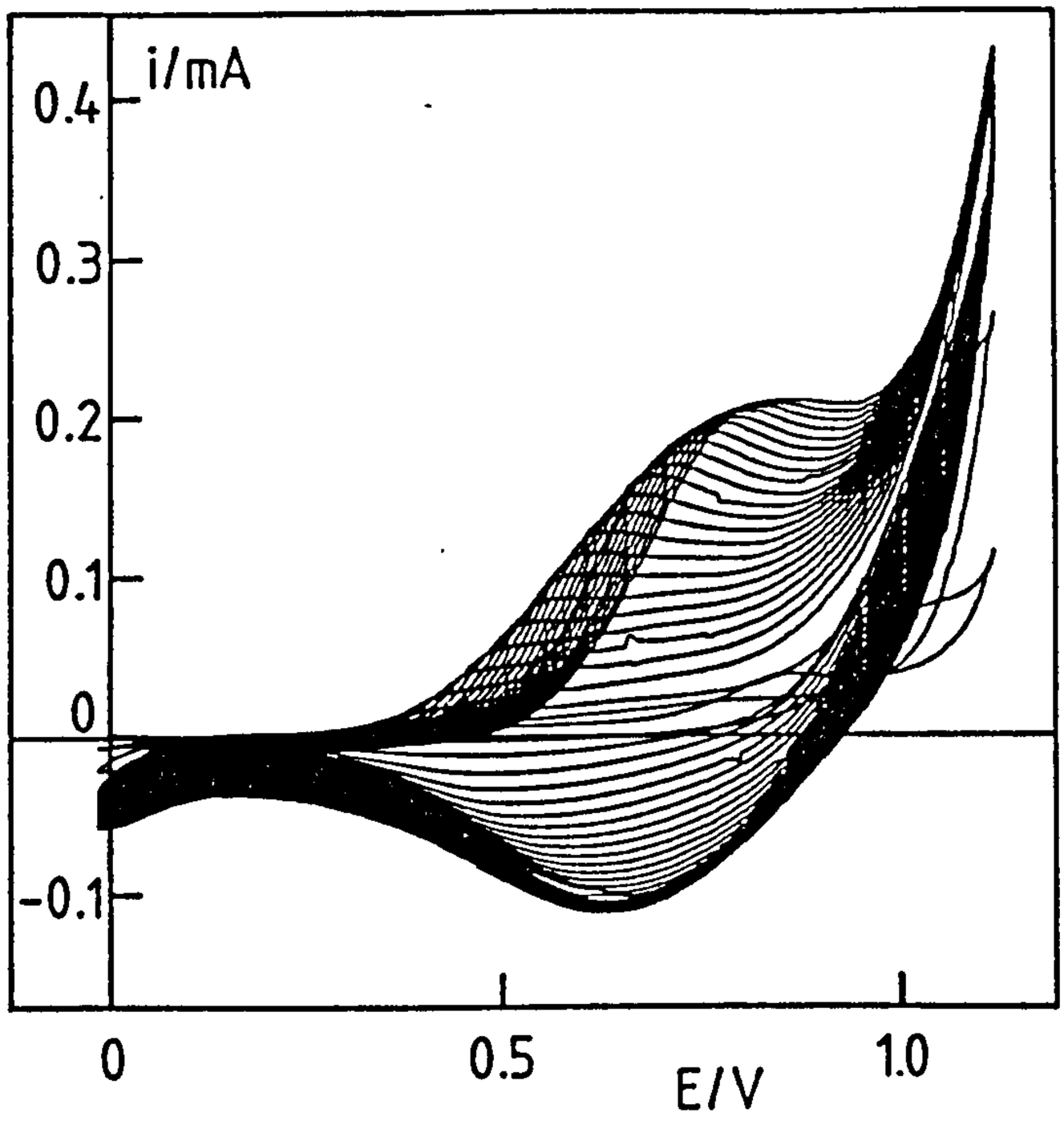

only crown ether modified conducting polymer to be studied to date other than a pseudo crown ether thiophene polymer studied by Roncali *et al.*[136]

The films formed were studied by cyclic voltammetry in acetonitrile solutions containing either TEAP (0.1 mol dm^{-3}), $LiClO_4$ (0.1 mol dm^{-3}), $NaClO_4$ (0.1 mol dm^{-3}) and, because of the low solubility of $KClO_4$, TEAP (0.1 mol dm^{-3}) saturated with $KClO_4$. Reproducible cyclic voltammograms, typical of poly(pyrrole) type conducting polymers, were obtained between 0 V and 0.9 V (vs. SCE) but the E_{pa} values (*ca.* 0.78 V (vs. SCE)) varied slightly from film to film under the same electrolyte conditions. The polymer E_{pa} peak positions in the different electrolytes were compared to ferrocene (1.0 mmol dm^{-3}) $E_{1/2}$ values in the same electrolytes at a clean polished stationary platinum disc electrode (A = 0.385 cm^2) at a sweep rate of 50 mV s^{-1}, table 3.1, to correct for changes in the liquid junction potentials between the aqueous calomel electrode and the acetonitrile background electrolyte solution. There were only small variations in the cyclic voltammetry of the polymer at 50 mV s^{-1} in terms of the shape or position of the E_{pa} in the different electrolyte solutions, figure 3.11. This suggests that the benzo-15-crown-5 macrocycle within either the fully oxidised or fully reduced polymer does not bind alkali ions including Na^+ which means that the polymer only undergoes type (i) doping (see section **1.6**) with ClO_4^-.

The electrochemical results agree with EDAX data (appendix 1) provided by Dr. L-Y. Chung which showed that no Na^+ ions were present in the film in either the fully oxidised of fully reduced form after being cycled in $NaClO_4$ (0.1 mol dm^{-3}) acetonitrile solution. The same result was also found to be true for the other ions studied. Oxidised polymers were found to have large traces of chlorine incorporated corresponding to the ClO_4^- dopant.

Figure 3.11 Cyclic voltammetry, between 0.0 V and 0.9 V (vs. SCE) (sweep rate $\upsilon = 50$ mV s^{-1}), of a film of poly(15-(1-pyrrolyl)methyl[benzo-15-crown-5] in three individual acetonitrile solutions containing 0.1 mol dm^{-3} $LiClO_4$ (···), $NaClO_4$ (– –) and TEAP (——)

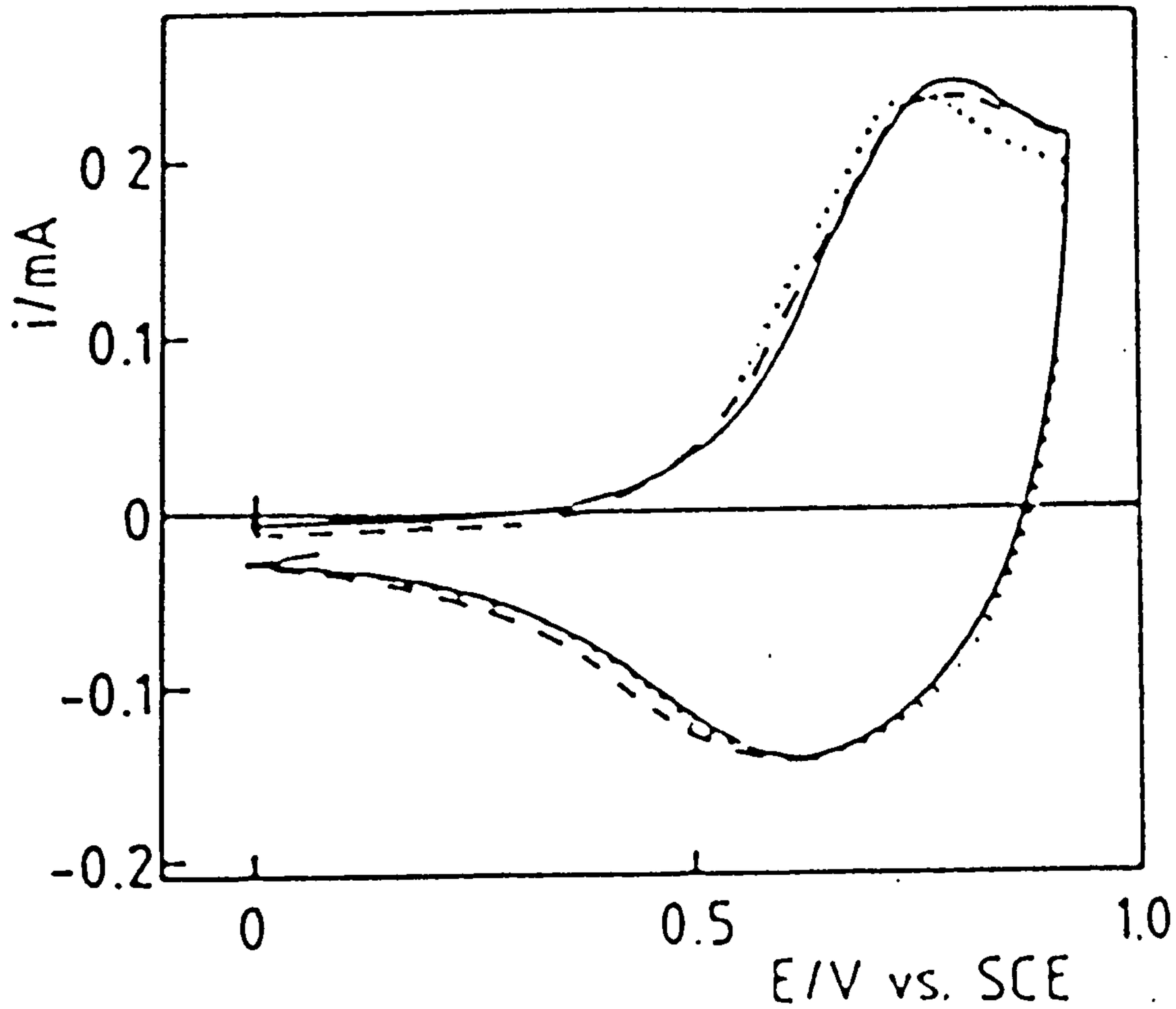

Table 3.1 Comparison of the $E_{1/2}$ of ferrocene with the E_{pa} of poly(15-(1-pyrrolyl)methyl[benzo-15-crown-5] in the various background electrolytes

Background electrolyte	$E_{1/2}$(Fc/Fc$^+$) vs. SCE/V	E_{pa}(polymer) vs. SCE/V	E_{pa} - $E_{1/2}$ (Fc/Fc$^+$)/V
TEAP	0.38	0.78	0.40
$NaClO_4$	0.30	0.78	0.48
$LiClO_4$	0.31	0.75	0.44
TEAP/$KClO_4$	0.38	0.78	0.40

These surprising results are thought to be due to the close stacking of the benzo-15-crown-5 rings which are approximately perpendicular to the plane of the polymer chain. Using a computer generated molecular model of the polymer and assuming that the monomers have a trans arrangement the centre to centre distance between the macrocycles was estimated to be 7 Å. If the crown ether groups are tilted as shown in figure 3.12 then the actual gap is further reduced. These gaps are thought to be too small for an ion solvated with acetonitrile, introducing a steric barrier to complexation.

The reflectance FTIR of fully reduced poly(15-(1-pyrrolyl)methyl[benzo-15-crown-5]) is shown in figure 3.13 and the assignments compared to the monomer are shown in table 3.2. Peaks corresponding to both pyrrole and benzo-15-crown-5 are observed in both the monomer and polymer spectrum.

3.6 Conclusion

The results obtained for the three pyrrole monomers **(I)**, **(II)** and **(III)** described in this preliminary chapter illustrate some of the difficulties commonly encountered when studying chemically modified conducting polymers. The substituted group can not only reduce the electrochemical stability of the polymer but can also have its own chemical behaviour impeded. The next chapter will discuss the study of chemically modified poly(thiophenes) and the problems associated with that class of polymer.

Figure 3.12 Simplified representation of the spacial arrangement of poly(15-(1-pyrrolyl)methyl[benzene-15-crown-5])

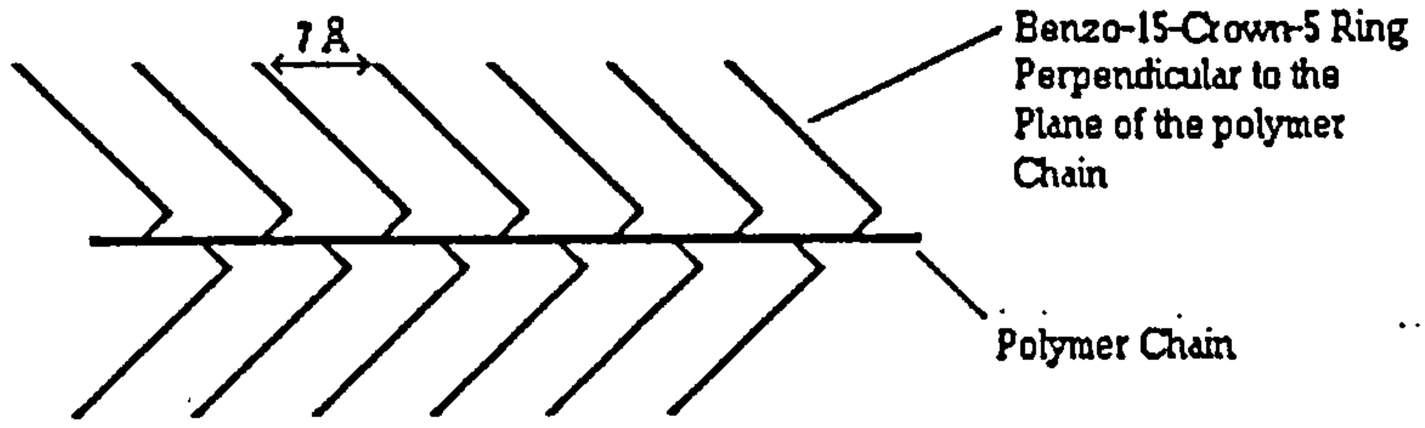

Figure 3.13 The FT-IR spectrum of a fully reduced poly(15-(1-pyrrolyl)methyl[benzene-15-crown-5]) film previously held at 0.0 V (vs. SCE) in acetonitrile solution containing TEAP (0.1 mol dm^{-3})

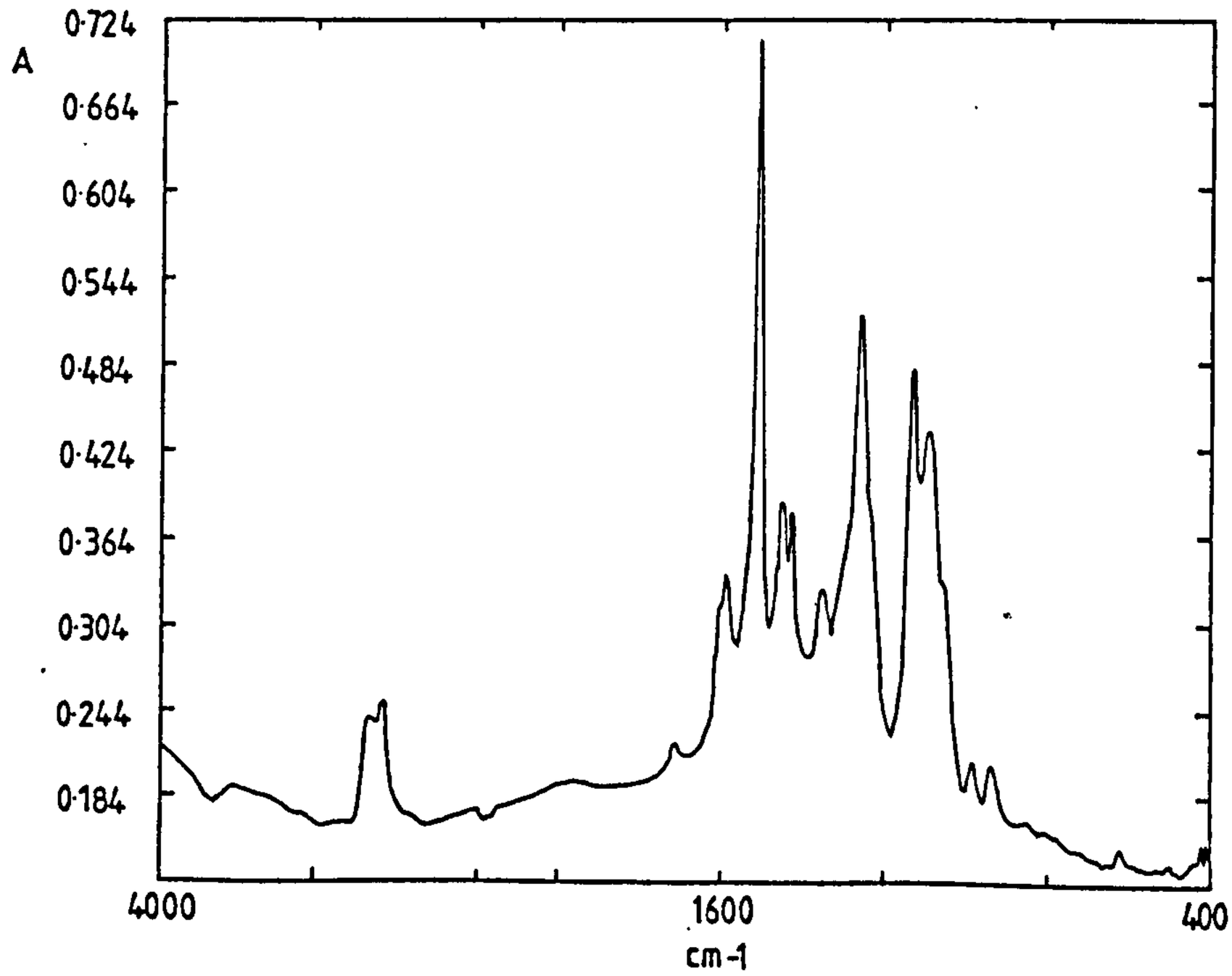

Table 3.2 Peak assignments for the FT-IR spectrum shown in figure 3.13

Wavenumber (cm^{-1}) ± 4 cm^{-1}		
Polymer	Monomer	Assignments
2871(s)	-	C-H stretches
1350-1590(ms)	1350-1590(ms)	Aromatic ring stretching
1263(s)	1263(s)	O-Aryl symetric stretch
1132(s)	1139(s)	C-O-C antisymetric stretch
1093(s)	1089(s)	Aryl-O-C antisymetric stretch

Chapter 4

Chemically Modified Poly(thiophenes)

4.1 Introduction

Poly(thiophenes) being one of the largest class of heterocyclic conducting polymer are unusual in that their electrochemistry is largely limited to nonaqueous solution[68,69] (see Chapter 1). On occasions aqueous electrochemistry of the polymers has been performed but with limited success. Since many of the eventual applications of conducting polymers including poly(thiophenes) are likely to be in aqueous media the specific conditions required to perform stable aqueous electrochemistry need to be determined. This coupled with the increasing interest in substituted poly(thiophenes)[115,137] provides a challenging research area. The effects of chemically bound carboxylic acid functionalities on the aqueous electrochemistry of poly(thiophenes) are studied in this chapter, in addition to their potential for further chemical modification both before and after polymerisation. Reflectance FTIR is performed throughout the studies to monitor any chemical changes imparted upon the various films during electrochemistry in both aqueous and nonaqueous solutions.

4.2 Summary, Growth and Electrochemistry of Poly(3-methylthiophene)

Poly(3-methylthiophene) is one of the most intensively studied conducting polymers[90] and was chosen as a general reference conducting polymer, for comparison purposes, in this thesis because of its highly reproducible electrochemistry. The particular growth conditions for poly(3-methylthiophene) applied in this thesis will be discussed briefly along with its subsequent electrochemistry. The reflectance FTIR and impedance spectroscopy will then be discussed in more detail.

Films of poly(3-methylthiophene) were grown from solutions of

3-methylthiophene (IV) (0.1 mol dm^{-3}) in acetonitrile containing TEAT (0.1 mol dm^{-3}) potentiometrically stepping from 0.0 V to 1.65 V (vs. SCE) at a polished stationary platinum disc electrode (A = 0.385 cm^2). The growth transient observed is shown in figure 4.1, and is similar to i - t transients observed by Hillman *et al.*[38] However, after the initial 5 s nucleation period the transient current increases steadily by a small constant amount instead of levelling out. This increase is largely due to the polymer growing in more than one direction, even after nucleation, and was confirmed visually when thick films were studied under a microscope. The current density passed during the growth of thin films of the polymer (t < 60 s) was found to be 2.6×10^{-3} A cm^{-2}. Polymer films could also be grown under the same solution conditions by cyclic voltammetry between 0.0 V and 1.7 V (vs. SCE) at variable sweep rates (50 to 100 mV s^{-1}). All the poly(3-methylthiophene) films discussed in this chapter were grown using the potential step method described in this paragraph.

Films of poly(3-methylthiophene) were studied by cyclic voltammetry in acetonitrile solutions containing TEAT (0.1 mol dm^{-3}) between -0.3 V and 1.1 V (vs. SCE), figure 4.2. Films cycled to potentials above 1.1 V (vs. SCE) experienced small but continual losses in Q_{CV} due to overoxidation.[36,37] There is a simple anodic peak on forward scans with a limiting E_{pa} of 0.64 V (vs. SCE) (r = 0.995, n = 5), figure 4.3, which is consistent with previously reported values. The behaviour on the reverse scan is more complex with a shoulder appearing at much lower potentials (0.0 V to 0.4 V (vs. SCE)). The i_{pa} has a linear dependence with sweep rate (r = 0.998, n = 0.998), figure 4.4, consistent with immobilised redox species. The dopancy (δ) was calculated using equation 3.1 by plotting Q_T against Q_{CV} for films of different thickness grown for 10 s, 20 s, 30 s, 40 s, 50 s and 60 s, figure 4.5, and was found to be δ = 0.18 (r = 0.999, n = 6), which is slightly lower than reported

Figure 4.1 Growth of poly(3-methylthiophene) by potential stepping from 0.0 V to 1.65 V (vs. SCE) in a solution of 3-methyl thiophene (IV) (0.1 mol dm^{-3}) in acetonitrile containing TEAT (0.1 mol dm^{-3}) at a stationary platinum electrode (A = 0.385 cm^2)

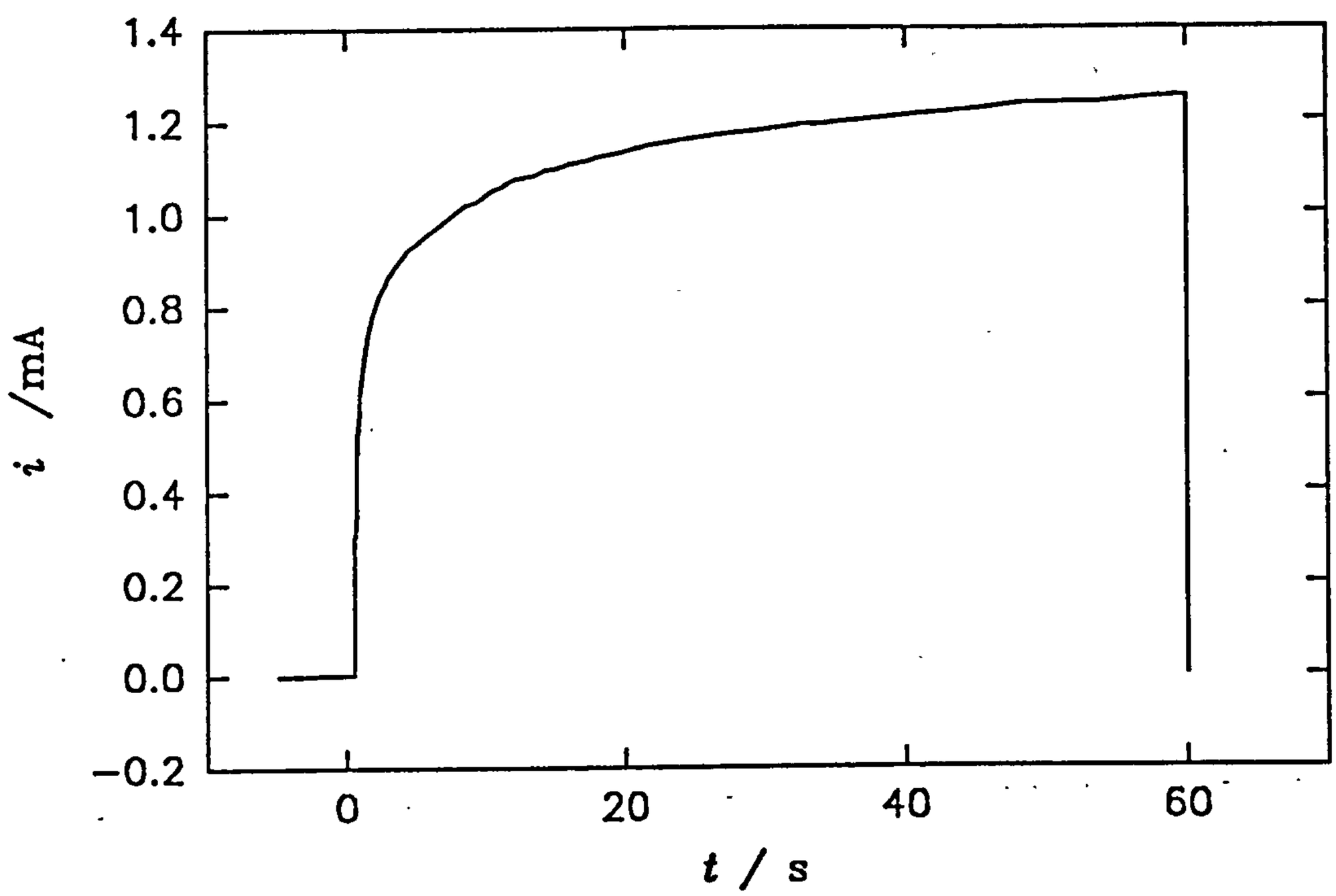

Figure 4.2 Cyclic voltammetry of poly(3-methylthiophene) in acetonitrile containing TEAT (0.1 mol dm^{-3}) between -0.3 V and 1.1 V (vs. SCE) at sweep rates of υ = 20, 40, 60, 80 and 100 mV s^{-1}

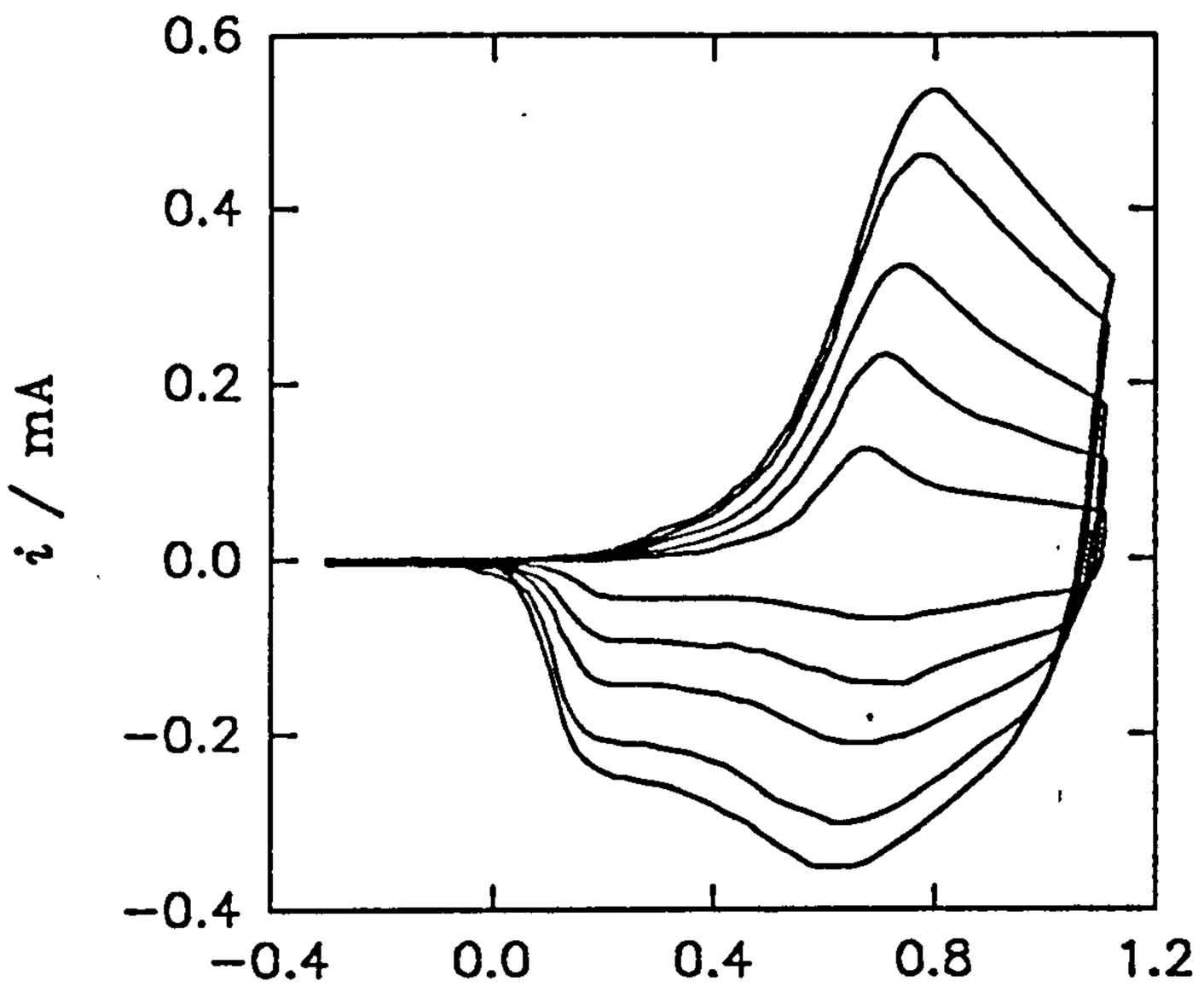

Figure 4.3 The E_{pa} vs. sweep rate (υ) graph for poly(3-methylthiophene) (r = 0.995, n = 5) plotted from the data shown in figure 4.2

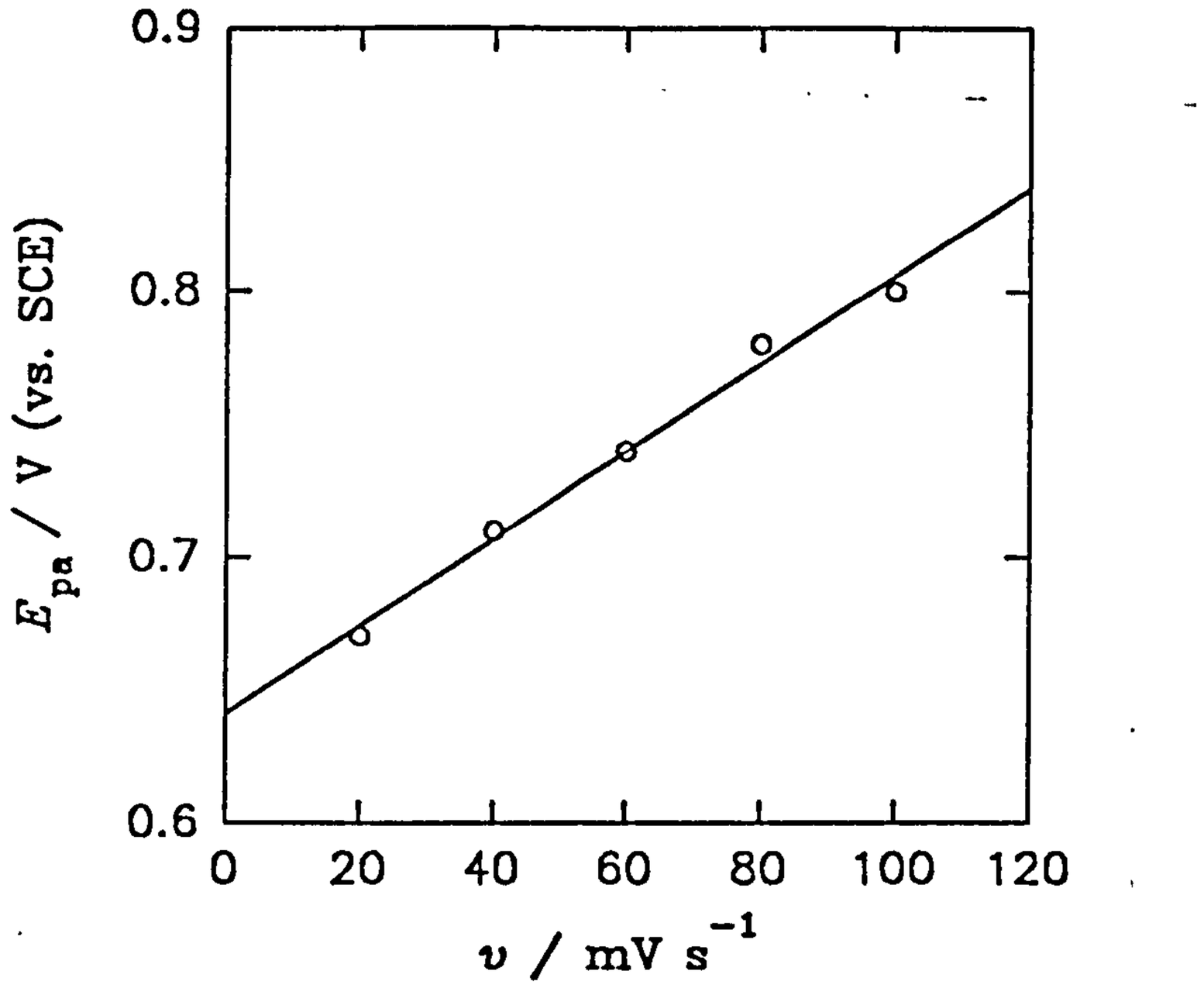

Figure 4.4 The i_{pa} vs. sweep rate (υ) graph for poly(3-methylthiophene) (r = 0.998, n = 5) plotted from the data shown in figure 4.2

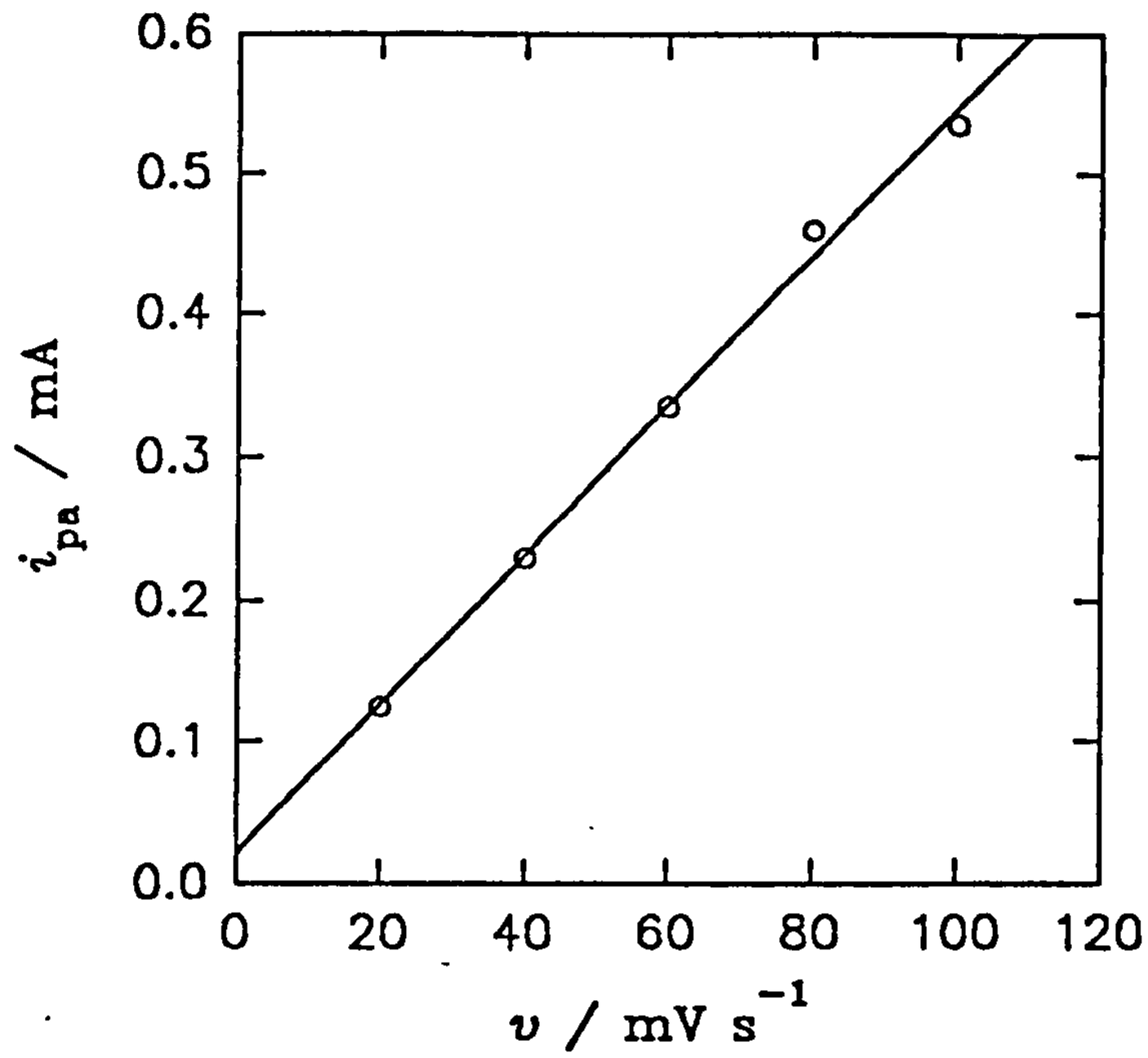

Figure 5.5 The Q_T vs. Q_{CV} plot (r = 0.999, n = 6) for films of poly(3-methylthiophene) grown for t = 10, 20, 30, 40, 50 and 60 s

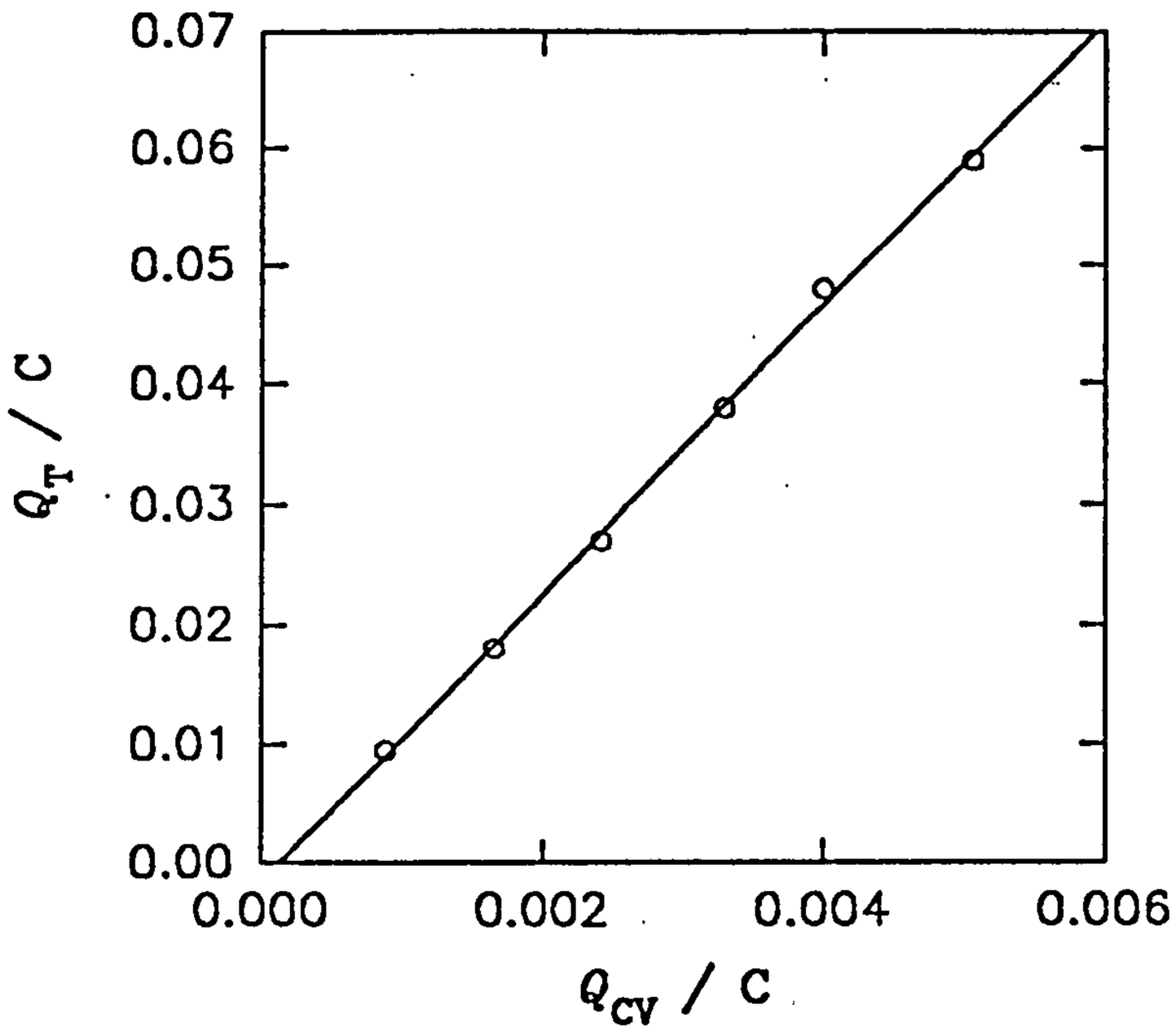

dopancy figures for thiophenes, suggesting a slightly inefficient polymerisation.

4.3 FTIR Spectroscopy of Poly(3-methylthiophene)

Obtaining good reproducible reflectance FTIR of poly(3-methylthiophene) proved to be difficult since a large degree of infra red scattering is observed in the spectrum above 2000 cm^{-1} compared to the relatively weak absorptions of the film. To obtain persistently reproducible spectra thick films were grown for 180 s. These films produced excellent FTIR spectra which could be given assignments in their fully reduced form, figure 4.6. However, in their fully oxidised form the peaks became very ill-defined. The effect observed in the spectra of the fully oxidised polymer is likely to be due to either enhanced scattering or some unusual concentration effect since ATR and transmission studies do not display this behaviour.[89,90]

The FTIR spectrum of fully reduced poly(3-methylthiophene) in figure 4.6 is compared to an FTIR spectrum of 3-methylthiophene in table 4.1.

The spectra compare well with previously reported data showing that the poly(3-methylthiophene) grown by the method described in section 4.2 is consistent with other films studied in the literature and possesses few defects, since the only aromatic C-H peaks observed correspond to those for C-H in the β-position.[89,90]

4.4 AC Impedance Spectroscopy of Poly(3-methylthiophene)

AC impedance measurements were performed on poly(3-methylthiophene) films grown for 30 s. Measurements were always taken in background electrolyte solutions of TEAT (0.1 mol dm^{-3}) in acetonitrile on films stabilised for 300 s at several selected potentials.

Figure 4.6 The reflectance FT-IR spectrum of a film of fully reduced poly(3-methylthiophene) grown for t = 180 s

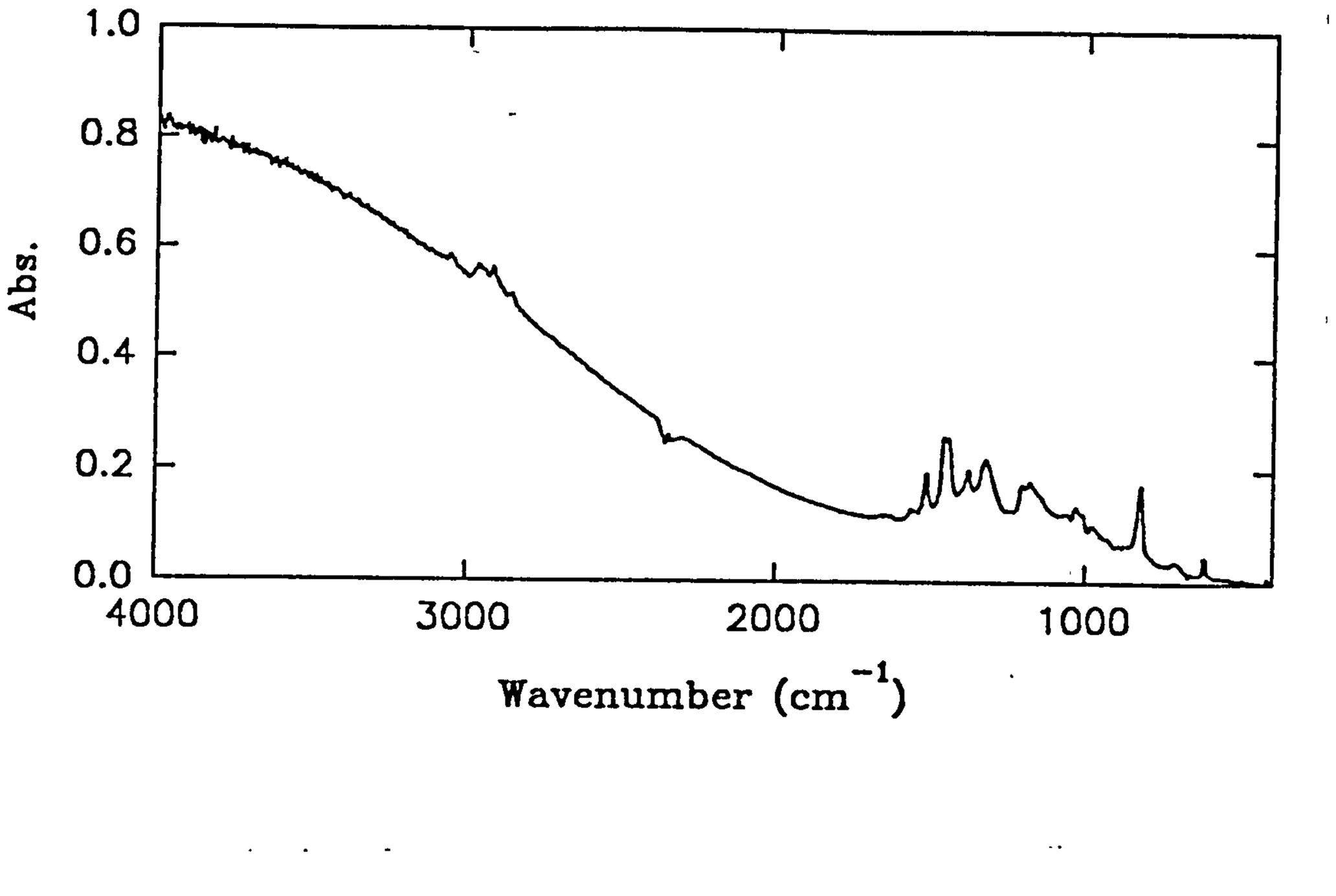

Table 4.1 The peak assignments for the reflectance FT-IR spectrum of poly(3-methylthiophene) shown in figure 4.6

Wavenumber (cm^{-1}) ± 4 cm^{-1}		
3-methylthiophene	Fully Reduced P3MT	Assignment
3100(w)	-	αC-H stretch
3055(w)	3055(w)	βC-H stretch
2800-3000(ms)	2800-3000(ms)	C-H methyl stretches
1360-1590(s)	1360-1590(s)	Aromatic ring stretches
-	1321(s)	C-C ring stretches
853(s)	-	αC-H o.p. bend
817(vs)	817(vs)	βC-H o.p. bend

The amplitude of the modulation was 10 mV (RMS) and a frequency range of between 50 mHz and approximately 500 Hz was used. The potentials studied were -0.3 V (vs. SCE) and then upwards from 0.5 V to 1.1 V (vs. SCE) in steps of 0.1 V and then downward from 1.0 V to 0.2 V (vs. SCE) in steps of 0.1V.

The Nyquist plot for poly(3-methylthiophene) held at -0.3 V (vs. SCE) shows very complex behaviour in figure 4.7 consistent with previously described data for fully reduced films.[53] At the other potentials studied the behaviour corresponded to a simple resistance and capacitance acting in series.[107] The Nyquist plot recorded at 0.6 V (vs. SCE) during the upward steps is shown in figure 4.8. The resistance (*ca.* 40 Ω) recorded at high frequency as the intercept on the real axis of the Nyquist plot is constant for all potentials measured and is due solely to the uncompensated resistance of the solution. This resistance is also present at a bare platinum electrode (A = 0.385 cm^2) studied under the same conditions. The Nyquist plots were analysed using equation 4.1 for a resistance and capacitance in series by plotting the imaginary component (Z'') against frequency.

$$Z = R - \frac{i}{\omega C} \qquad (4.1)$$

Z - Impedance

R - Resistance

ω - $f/2\pi$ (f - Frequency)

C - Capacitance

The data recorded at 0.6 V (vs. SCE) during the anodic potential steps shown in figure 4.8 when analysed gives the plot shown in figure 4.9. The capacitances calculated in this way for the entire

Figure 4.7 The Nyquist plot for a poly(3-methylthiophene) film (previously grown for t = 30 s at a platinum electrode (A = 0.385 cm^2)) held at -0.3 V (vs. SCE) in acetonitrile containing TEAT (0.1 mol dm^{-3}) (frequency range - 50 mHz to 500 Hz, amplitude - 10 mV (RMS))

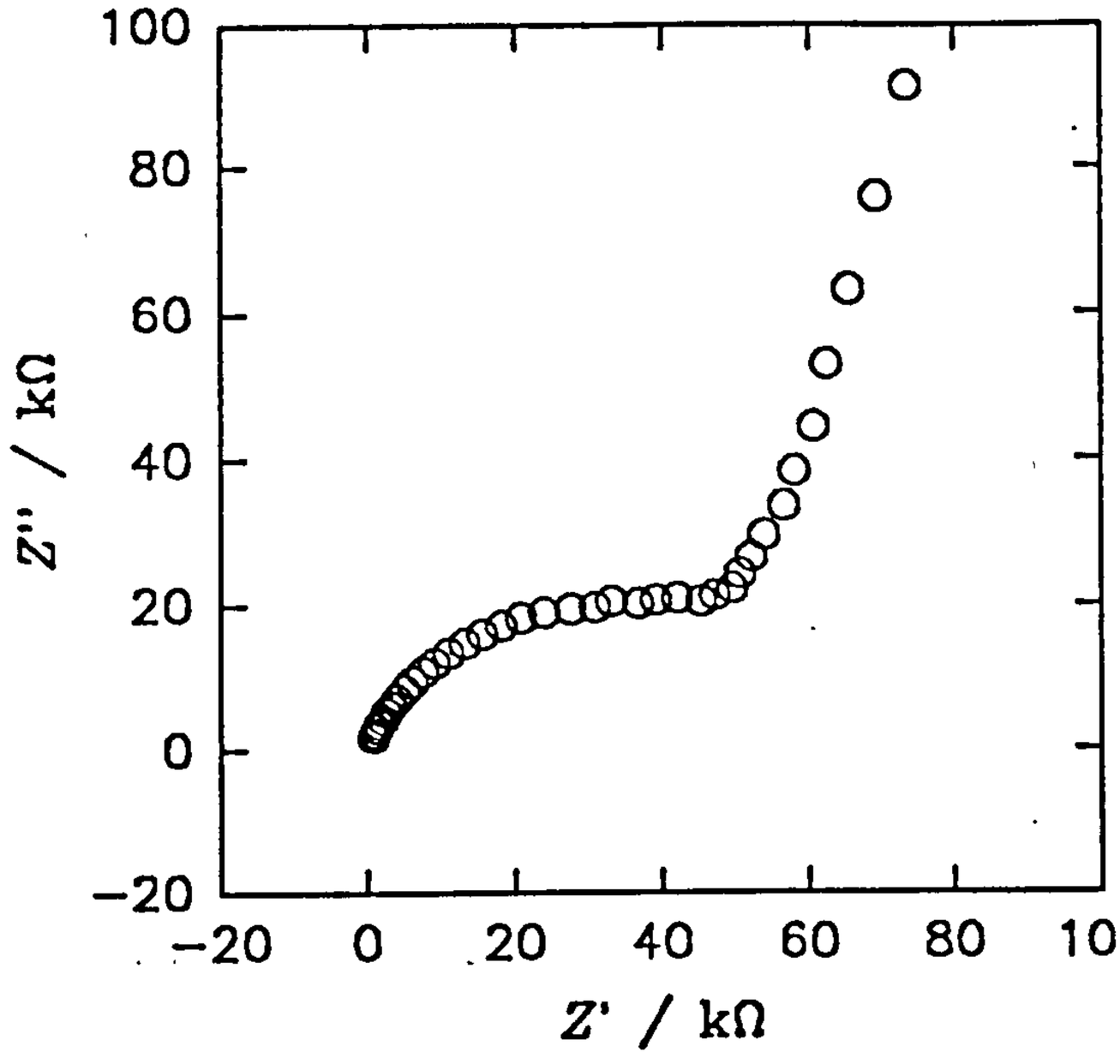

Figure 4.8 The Nyquist plot for poly(3-methylthiophene) grown for t = 30 s at a platinum electrode (A = 0.385 cm^2) and held at 0.6 V (vs. SCE) in acetonitrile containing TEAT (0.1 mol dm^{-3}) (frequency range - 50 mHz to 500 Hz, amplitude - 10 mV (RMS))

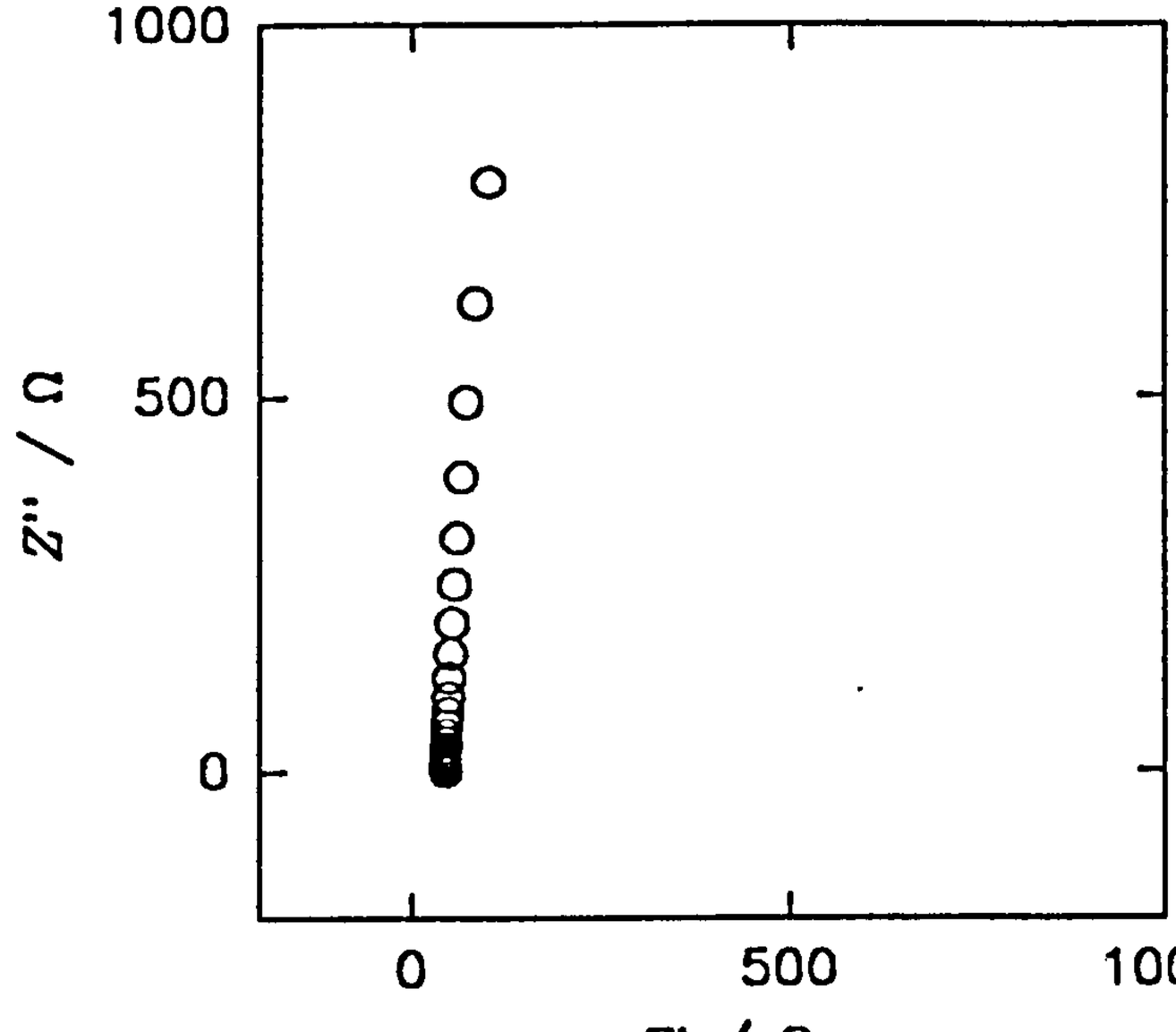

Figure 4.9 Interpretation of the data shown in figure 4.8 using equation 4.1 (r = 0.999)

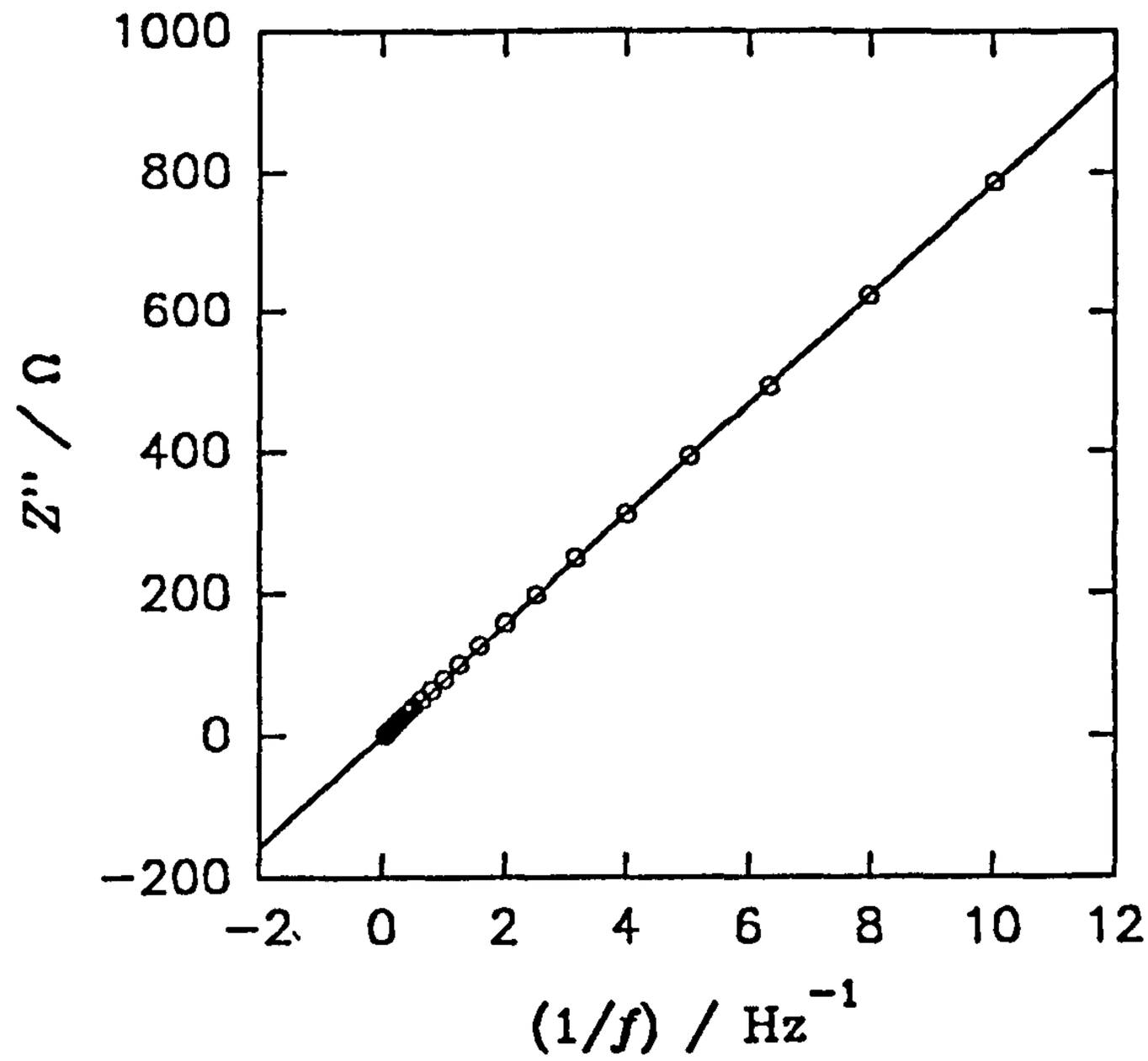

potential data set are shown in figure 4.10.

The magnitude of the capacitances measured are particularly large and are probably the result of charging between the individual chains of the polymer and the background electrolyte solution.[109] The volume of a film of poly(3-methylthiophene) grown for 30 s is estimated to be $V_{TOT} = 1.3 \times 10^{-12}$ m^3 from a monomer volume of $V_{MON} = 1.77 \times 10^{-29}$ m^3 estimated from dimensions calculated by molecular modelling. The area of the polymer is estimated by comparing the capacitance of the polymer at a particular potential with an estimate of the capacitance of a typical metal under the same solution conditions (approximately 0.05 mF cm^{-2}). The maximum capacitance of the polymer at 0.9 V (vs. SCE), figure 4.10, is 8.0 mF cm^{-2}. So for an electrode with a geometric area $A = 3.85 \times 10^{-5}$ m^2 the effective area of poly(3-methylthiophene) at 0.9 V (vs. SCE) is $A_{EFF} = 6.2 \times 10^{-3}$ m^2. In order to investigate the scale at which the capacitance acts within the polymer, the entire volume of the polymer is considered to be bounded in the form of a cylinder. For the polymer to have these estimated values for V_{TOT} and A_{EFF} the radius of the proposed cylinder would be $r_{CYL} = 1.0 \times 10^{-10}$ m or 1 Å, which is at molecular dimensions, supporting the suggestion that the capacitances measured are due to charging at the polymer chain level.

Marked hysteresis is observed in figure 4.10 indicating that there is significant structural change during the oxidation and reduction of the polymer. The hysteresis observed during the cathodic potential steps coincides with the large shoulder observed at low potentials (0.0 V to 0.4 V (vs. SCE)) in the cyclic voltammetry of the cathodic wave, indicating that this effect is not due to slow kinetics within the film, but rather to thermodynamic effects. It is worth noting however, that hysteresis occurs throughout the whole potential range but is more marked in the low potential region.

Figure 4.10 Overall capacitance data set calculated using equation 4.1 from Nyquist data, similar to figure 4.8, obtained after anodic and cathodic potential steps upon poly(3-methylthiophene) grown for t = 30 s (the order of the steps is shown by the arrows)

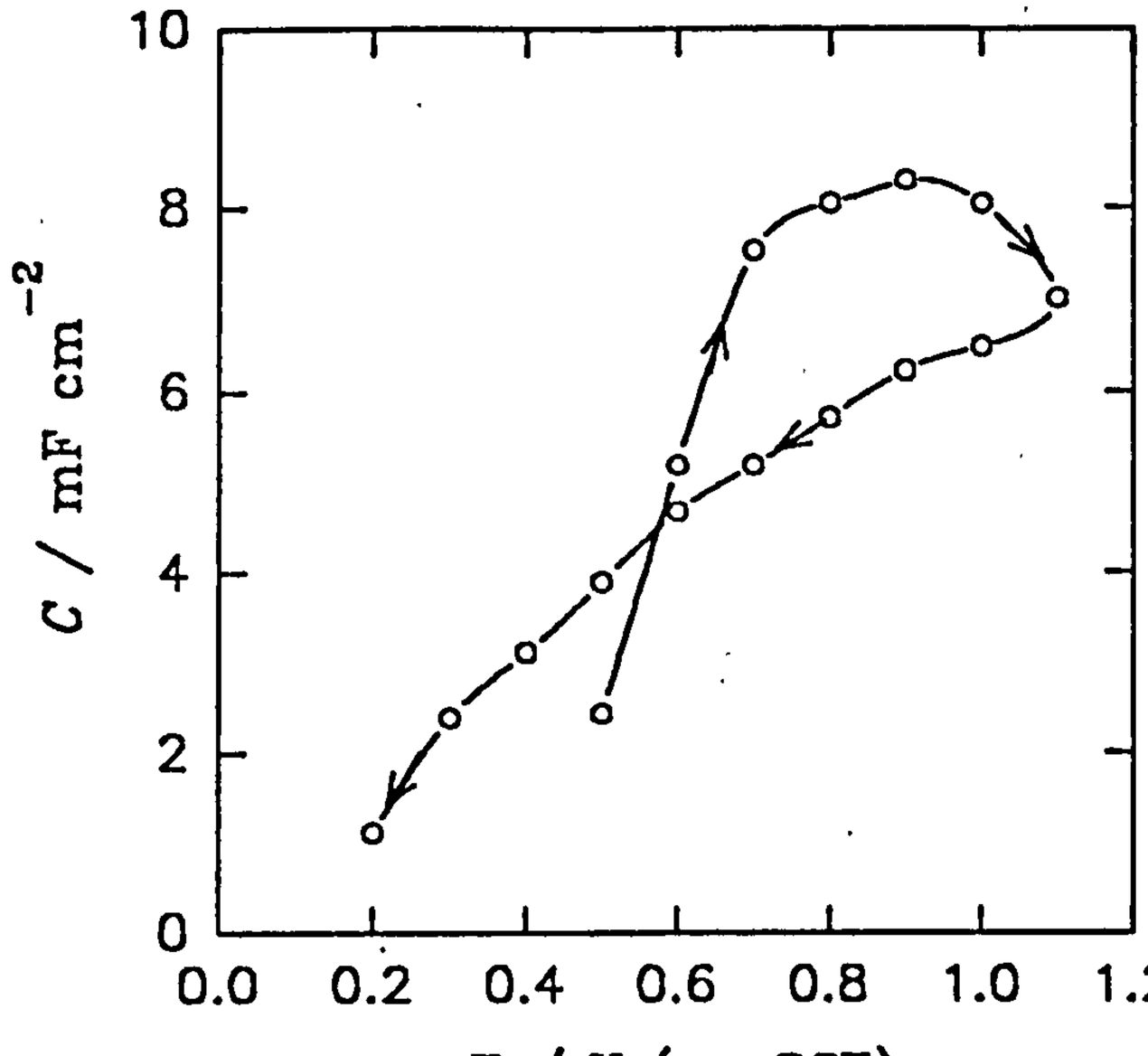

The hysteresis effect was further studied by applying an ac potential of 5 mV at 330 Hz to a poly(3-methylthiophene) film, grown for 30 s, during cyclic voltammetry in a background electrolyte solution of TEAT (0.1 mol dm^{-3}) in acetonitrile. The in-phase component of the ac current was then compared with the applied ac potential using the lock-in amplifier equipment described in Chapter 2. The RMS amplitude or the in phase ac current was then plotted as a function of potential. A typical in phase ac cyclic voltammogram is shown in figure 4.11 where the hysteresis is clearly visible in the reverse cathodic sweep.

At sweep rates below 10 mV s^{-1} the ac cyclic voltammograms remain consistent under the same sweep conditions and do not vary. The lower potential limit was always maintained at -0.27 V (vs. SCE). No hysteresis is observed for upper potential limits of less than 0.3 V (vs. SCE) and no further increase in the hysteresis is observed when the upper sweep limit is greater than 0.8 V (vs. SCE). When ac cyclic voltammograms with upper potential limits, between 0.3 V and 0.8 V (vs. SCE), are studied the size of the hysteresis loop increases steadily with potential but also increases slightly if the potential is held at the particular upper potential limit for a short finite period, this could not be measured accurately but is approximately 5 s. The in-phase current saturates at the higher potential side of the ac cyclic voltammogram and this corresponds to a resistance of 60 Ω which is due to the solution resistance indicating that the polymer becomes very conducting at these potentials.

Similar results reported by Ofer and Wrighton[138] on poly(3-methylthiophene) in SO_2 solutions at -40 °C only attribute the hysteresis effect to cyclic voltammetry, kinetic effects, which is clearly not the case.

Figure 4.11 A typical ac cyclic voltammogram between -0.3 V and 1.1 V (vs. SCE) of a poly(3-methylthiophene) film (previously grown for t = 30 s at a platinum electrode (A = 0.385 cm^2)) (amplitude = 5 mV (RMS), f = 330 Hz, sweep rate υ = 10 mV s^{-1})

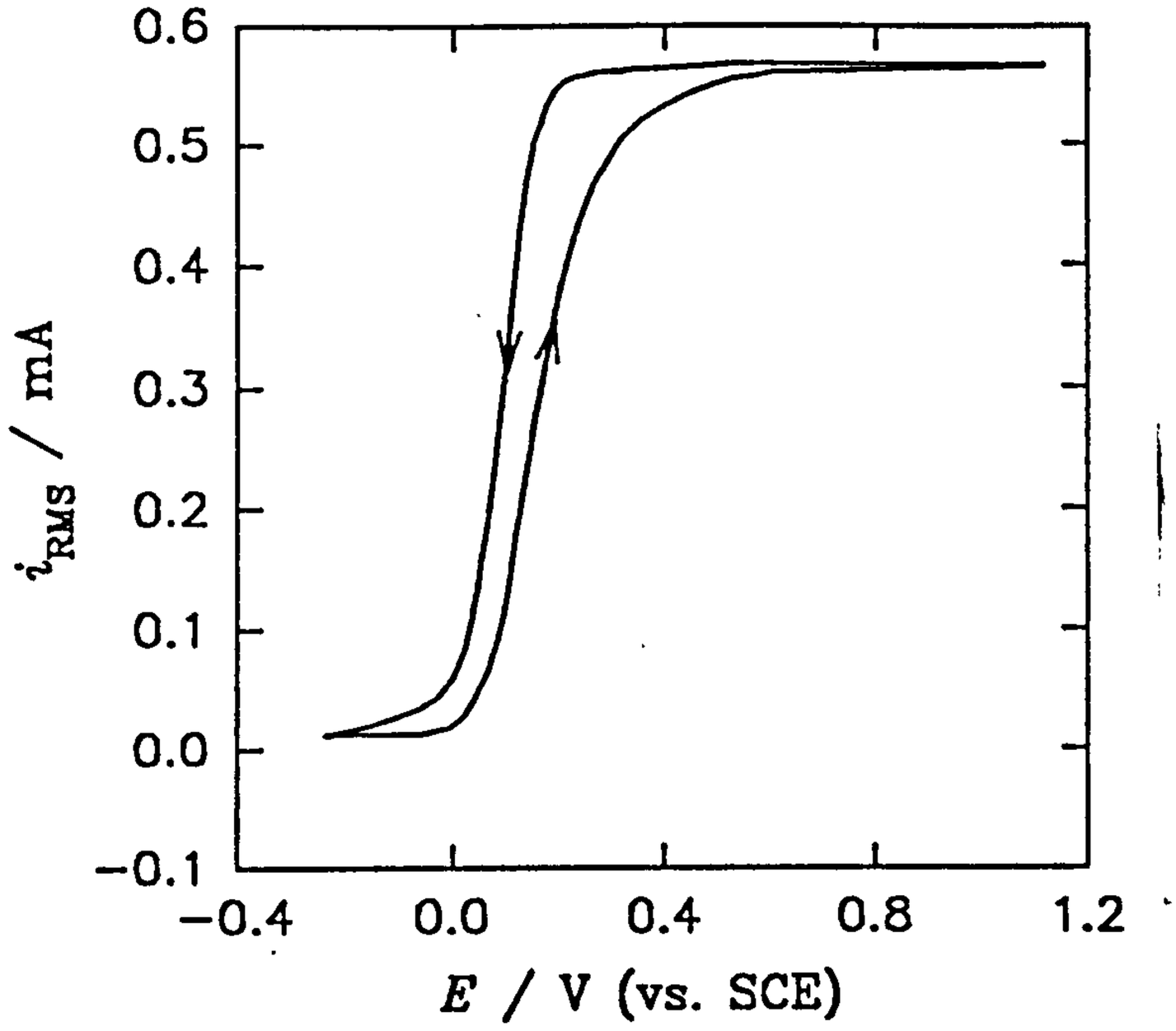

Unfortunately the data does not reveal the cause of the effect but displays its extent. Quartz crystal microbalance (QCM) studies performed by Hillman *et al.*[113,114] on poly(bithiophene) under similar conditions, but using solely cyclic voltammetry, correlate quite well with these results. The exact cause of the hysteresis is still debatable and is probably due to some extreme thermodynamic or quasi-thermodynamic effects occurring during the oxidation of the film to polarons or bipolarons. These results raise an important point about the description of the oxidation state of conducting polymer films. It is not sufficient to quote the potential at which a film is held in a background electrolyte as a standard, the history of the film needs to be taken into account, since films of the same type can be held at the same potential but have completely different dopancies.

Impedance spectroscopy was performed on poly(3-methylthiophene) films grown for 5, 10, 30, 45 and 60 s. Again an ac potential modulation of 10 mV (RMS) was applied to the films which were held at 0.8 V (vs. SCE) and allowed to settle for 300 s in a TEAT (0.1 mol dm^{-3}) acetonitrile solution. Impedance measurements were taken between 50 mHz and approximately 500 Hz and were analysed in the manner previously described to obtain capacitance data. Figure 4.12, shows the capacitances obtained plotted against Q_{CV} which gives a excellent linear relationship with a gradient of 1.16 F C^{-1} ($r = 0.998$, $n = 5$) as would be expected confirming that the capacitances measured are proportional to the amount of material present and not any bulk effects.

4.5 Growth and Electrochemistry of Poly(3-thiopheneacetic acid) and its Associated Esters

Poly(3-thiopheneacetic acid) was first grown by Albery *et al.*[139,140,141] in a series of experiments which showed that under very carefully controlled conditions the polymer could be deposited by two dimensional layer-by-layer nucleation and growth during

Figure 4.12 Capacitance of poly(3-methylthiophene) films (previously grown for t = 5, 10, 30, 45 and 60 s at a platinum electrode (A = 0.385 cm^2)) held at 0.8 V (vs. SCE) plotted against Q_T (r = 0.998, n = 5)

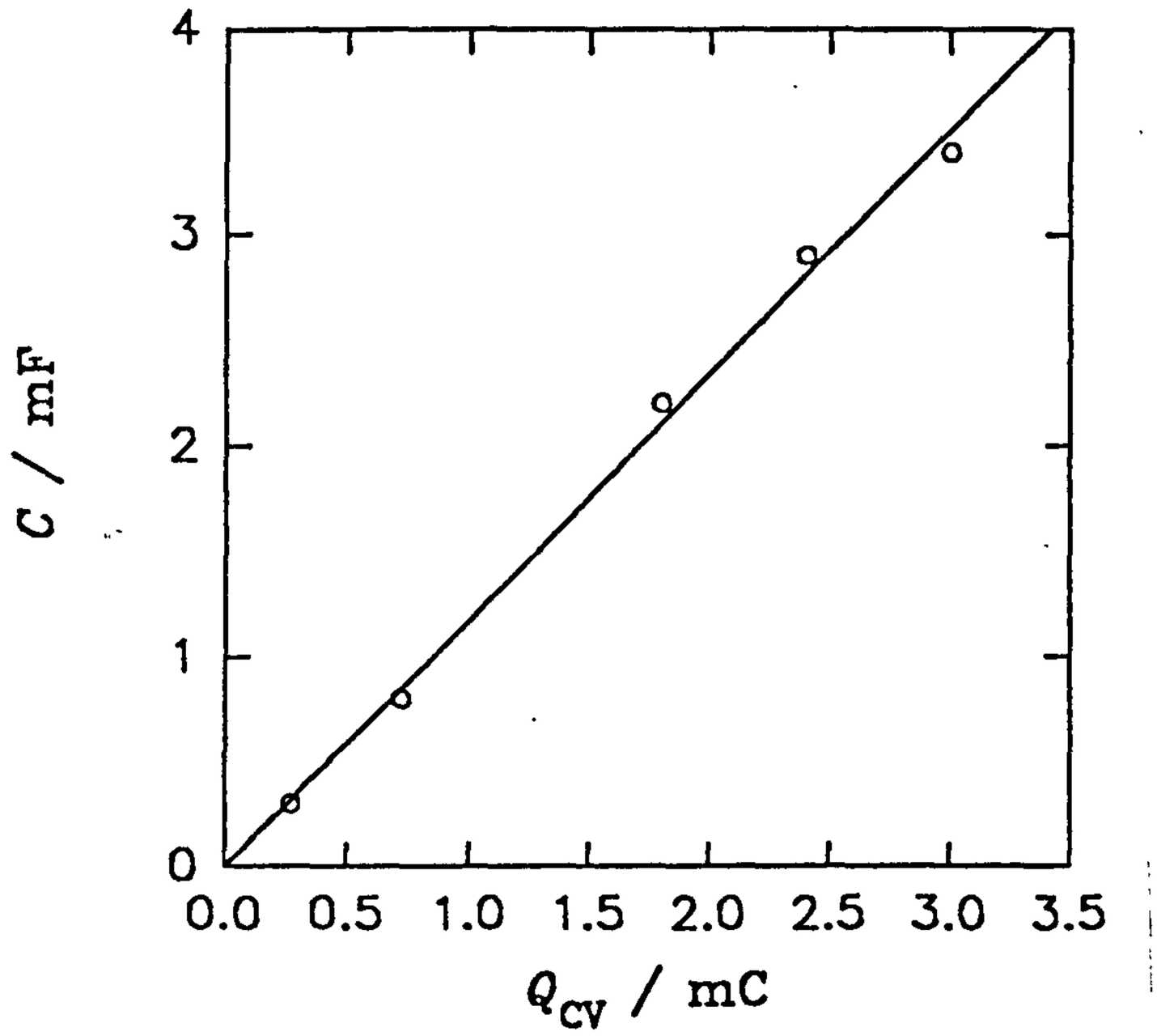

chronoamperometry. Initial experiments on the polymer grown by cyclic voltammetry showed that its electrochemistry was unstable and resulted in eventual passivation in acetonitrile solutions. No information on the electrochemical stability of the two dimensional layer-by-layer polymer was reported. For convenience poly(3-thiopheneacetic acid) was grown using cyclic voltammetry in the manner described below and was studied in both acetonitrile, aqueous and methanol solutions to determine the nature of its electrochemical behaviour.

Films of poly(3-thiopheneacetic acid) were grown from solutions of 3-thiopheneacetic acid (V) (1.0 mol dm^{-3}) in acetonitrile containing TEAT (0.1 mol dm^{-3}) by cyclic voltammetry between 0.0 V and 1.8 V (vs. SCE) at a polished stationary platinum disc electrode (A = 0.385 cm^2). Films were grown in four sweeps at 100 mV s^{-1} and then held at 0.0 V (vs. SCE) figure 4.13. Marked nucleation loops[35] were observed during each cycle and the success of the growth depended heavily upon the purity of the solution, with older solutions producing poor quality films.[139] Cyclic voltammetry in solutions of acetonitrile containing TEAT (0.1 mol dm^{-3}) was recorded between 0.0 V and 1.4 V (vs. SCE) but resulted in passivation after several scans. Cyclic voltammetric data recorded immediately after growth gave a roughly linear correlation between the sweep rate and i_{pa}, figure 4.14 (r = 0.999, n = 4) with the E_{pa} estimated to be between 1.1 V and 1.2 V (vs. SCE). The E_{pa} of monomeric 3-thiopheneacetic acid (V) (1.0 mmol dm^{-3}) in acetonitrile containing TEAT (0.1 mol dm^{-3}) was found to be 1.99 V (vs. SCE) at 100 mV s^{-1} and that of 3-methylthiophene (IV) (1.0 mmol dm^{-3}) under the same conditions was found to be 1.96 V (vs. SCE). Since the oxidation potential of 3-methylthiophene (IV) under these conditions is reported to be E_{ox}(IV) = 1.35 V (vs. SCE)[115] then the oxidation potential of 3-thiopheneacetic acid is estimated to be E_{ox}(V) $\simeq$ 1.4 V (vs. SCE). Comparing the E_{ox}(V) of the monomer to the limiting E_{pa} of the polymer

Figure 4.13 The growth of poly(3-thiopheneacetic acid) by cyclic voltammetry between 0.0 V and 1.8 V (vs. SCE) at a platinum electrode (A = 0.385 cm^2) in a solution of 3-thiopheneacetic acid (V) (1.0 mol dm^{-3}) in acetonitrile containing TEAT (0.1 mol dm^{-3}) (sweep rate υ = 100 mV s^{-1})

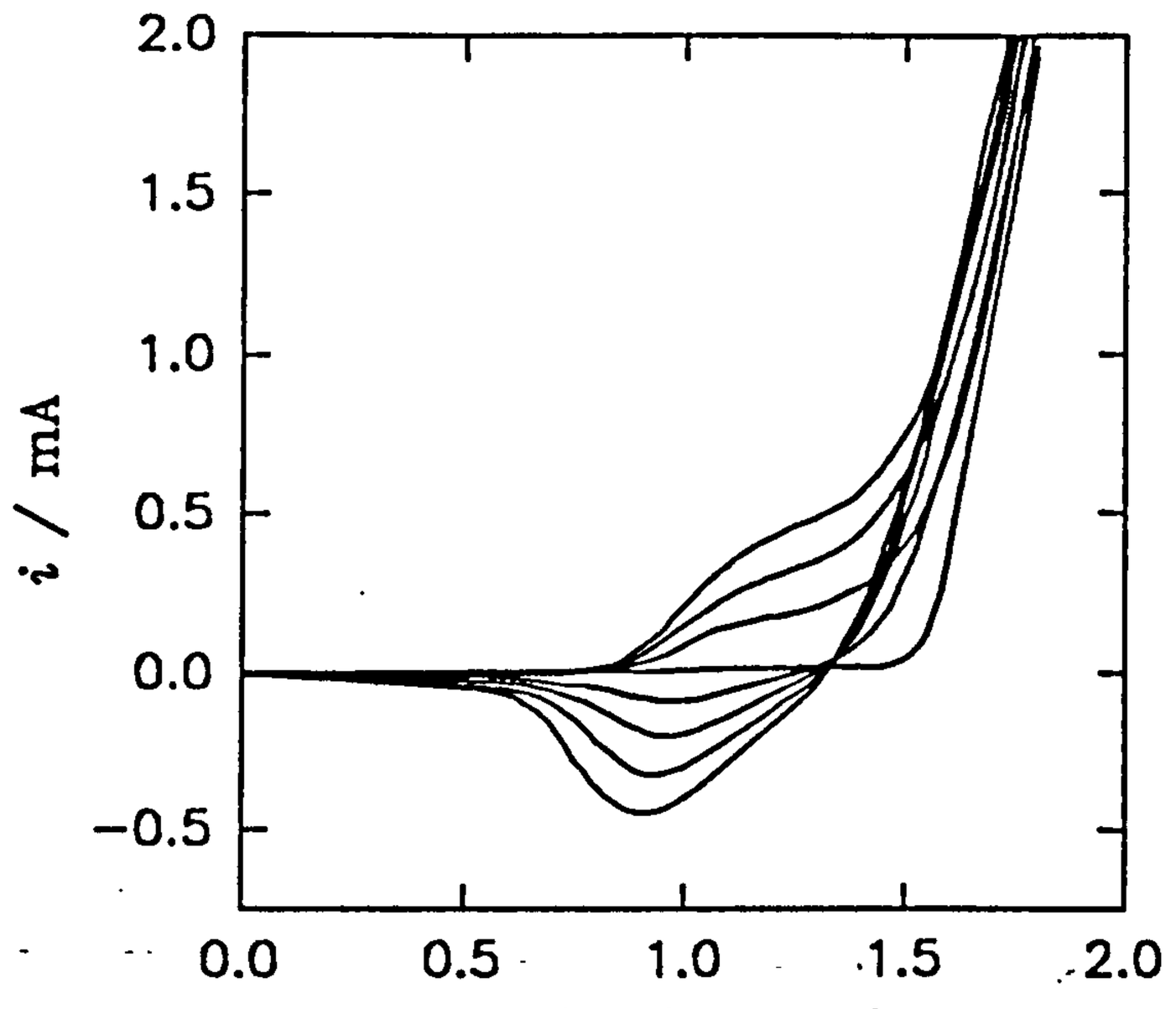

Figure 4.14 The i_{pa} vs. sweep rate (υ) plot for the cyclic voltammetry of poly(3-thiopheneacetic acid) in acetonitrile containing TEAT (0.1 mol dm^{-3}) (υ = 10, 20, 50 and 100 mV s^{-1}) (r = 0.999, n = 4)

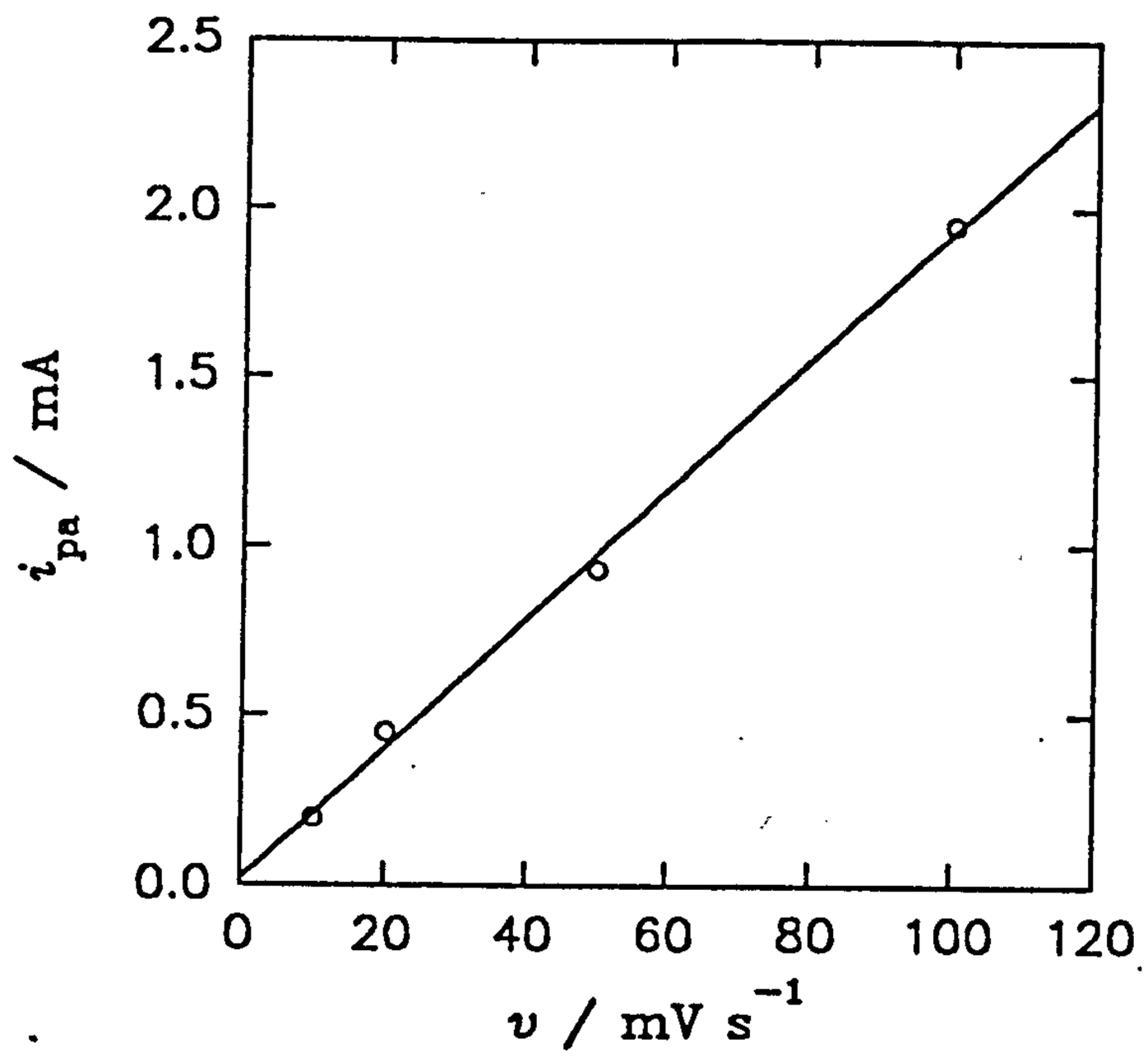

Figure 4.15 Comparison of 3-thiopheneacetic acid (V) and poly(3-thiopheneacetic acid) oxidation potential with previously reported data[115] for other thiophenes

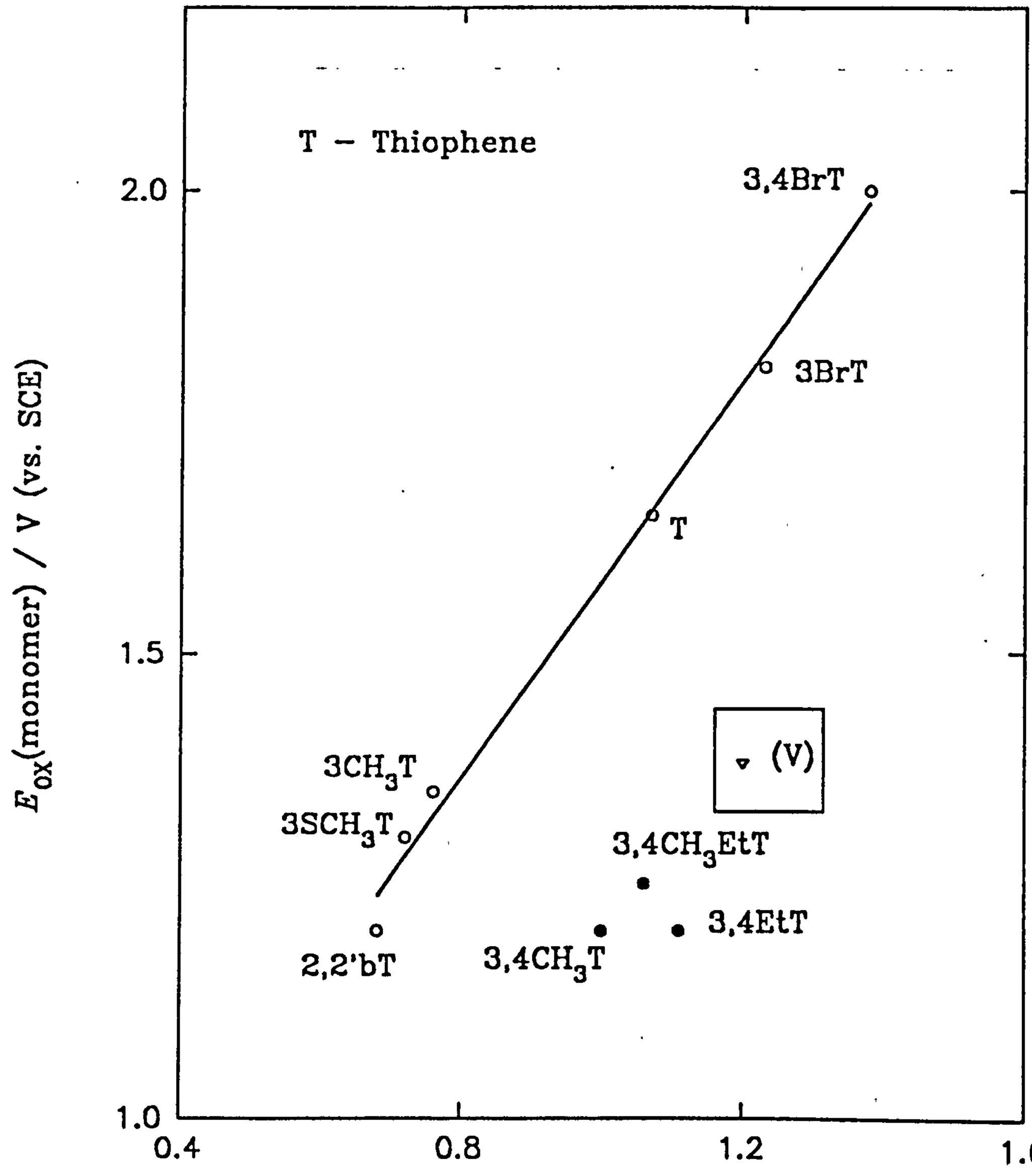

with previously reported data[115], figure 4.15, on substituted thiophenes, suggests that there are large steric effects acting within the polymer which increase the E_{pa} for the polymers by a greater amount than would be expected solely from the electron withdrawing effect on the substituent. The estimated E_{ox}(V) of monomeric 3-thiopheneacetic acid is, as described earlier, similar in value to the E_{ox}(IV) of thiophene itself suggesting that the acetic acid group has little effect on the ring. The polymer, in its fully reduced state, was found to be soluble in aqueous NaOH (1.0 mol dm^{-3}) to give a red/orange solution with a λ_{max} = 456 nm, this is lower than the value of 480 nm observed for poly(3-methylthiophene) films[115] and suggests a lower degree of conjugation.

Films of poly(methyl(3-thiopheneacetate)), poly(ethyl(3-thiopheneacetate)), poly(n-propyl(3-thiopheneacetate)) and poly(n-butyl(3-thiopheneacetate)) were grown from acetonitrile solutions of the monomers methyl(3-thiopheneacetate) (VI), ethyl(3-thiopheneacetate) (VII), n-propyl(3-thiopheneacetate) (VIII) and n-butyl(3-thiopheneacetate) (IX) (0.1 mol dm^{-3}) containing TEAT (0.1 mol dm^{-3}) by cyclic voltammetry between 0.0 V and 1.7 V (vs. SCE) at a polished stationary platinum disc electrode (A = 0.385 cm^2). The growth of poly(methyl(3-thiopheneacetate)) at 100 mV s^{-1} is shown in figure 4.16. The other polymers give growth cyclic voltammograms which are very similar to the methyl ester.

The cyclic voltammetry of poly(methyl(3-thiopheneacetate)) is very stable in acetonitrile solutions of TEAT (0.1 mol dm^{-3}), figure 4.17, giving a linear i_{pa} vs. sweep rate (υ) plot (r = 0.999, n = 5), figure 4.18. The plots for limiting E_{pa} and E_{pc} for poly(methyl(3-thiopheneacetate)) are shown in figure 4.19 and give the values of E_{pa} = 1.16 V (r = 0.998, n = 5) (vs. SCE) and E_{pc} = 1.11 V (r = 0.994, n = 5) (vs. SCE), which are as high as the corresponding poly(3-thiopheneacetic acid) values,

Figure 4.16 The growth of poly(methyl(3-thiopheneacetate)) by cyclic voltammetry between 0.0 V and 1.7 V (vs. SCE) at a platinum electrode (A = 0.385 cm^2) in a solution of methyl(3-thiopheneacetate) (VI) (0.1 mol dm^{-3}) in acetonitrile containing TEAT (0.1 mol dm^{-3}) (sweep rate υ = 100 mV s^{-1})

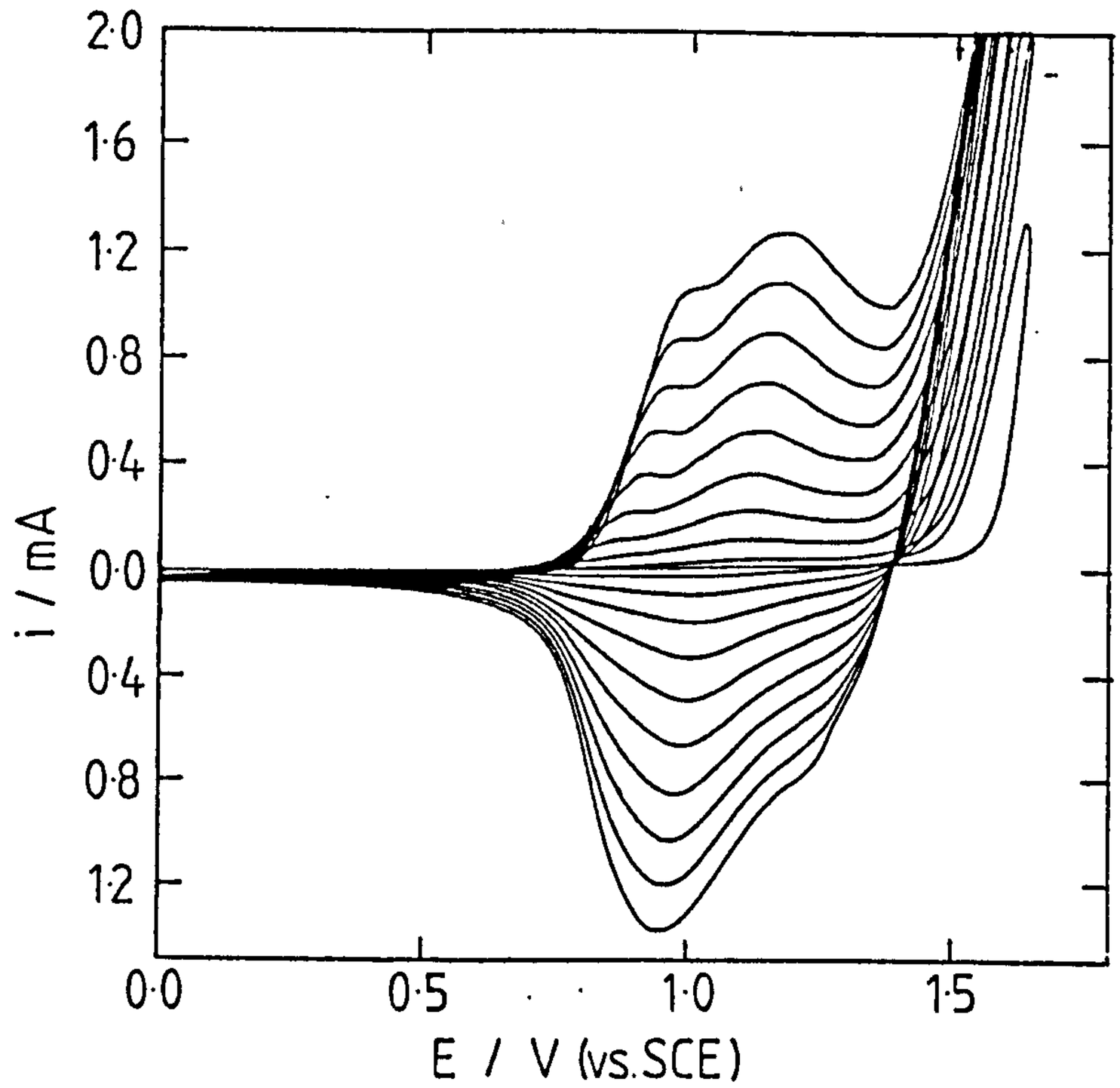

Figure 4.17 The cyclic voltammetry between 0.0 V and 1.4 V (vs. SCE) of poly(methyl(3-thiopheneacetate) in acetonitrile containing TEAT (0.1 mol dm^{-3}) at sweep rates υ = 20, 40, 60, 80 and 100 mV s^{-1}

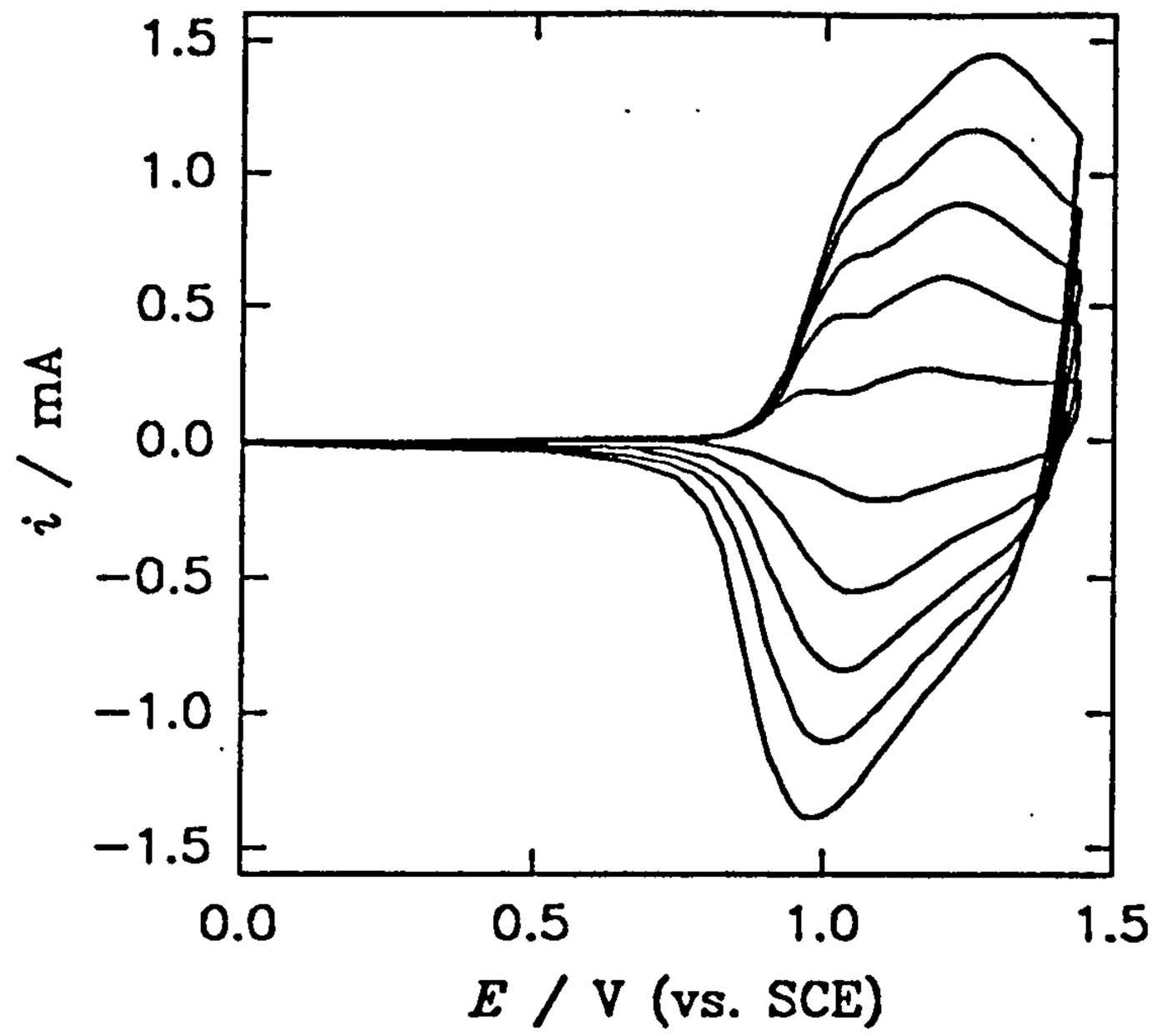

Figure 4.18 The plot of i_{pa} vs. sweep rate (υ) taken from the data presented in figure 4.17 (r = 0.999, n = 5)

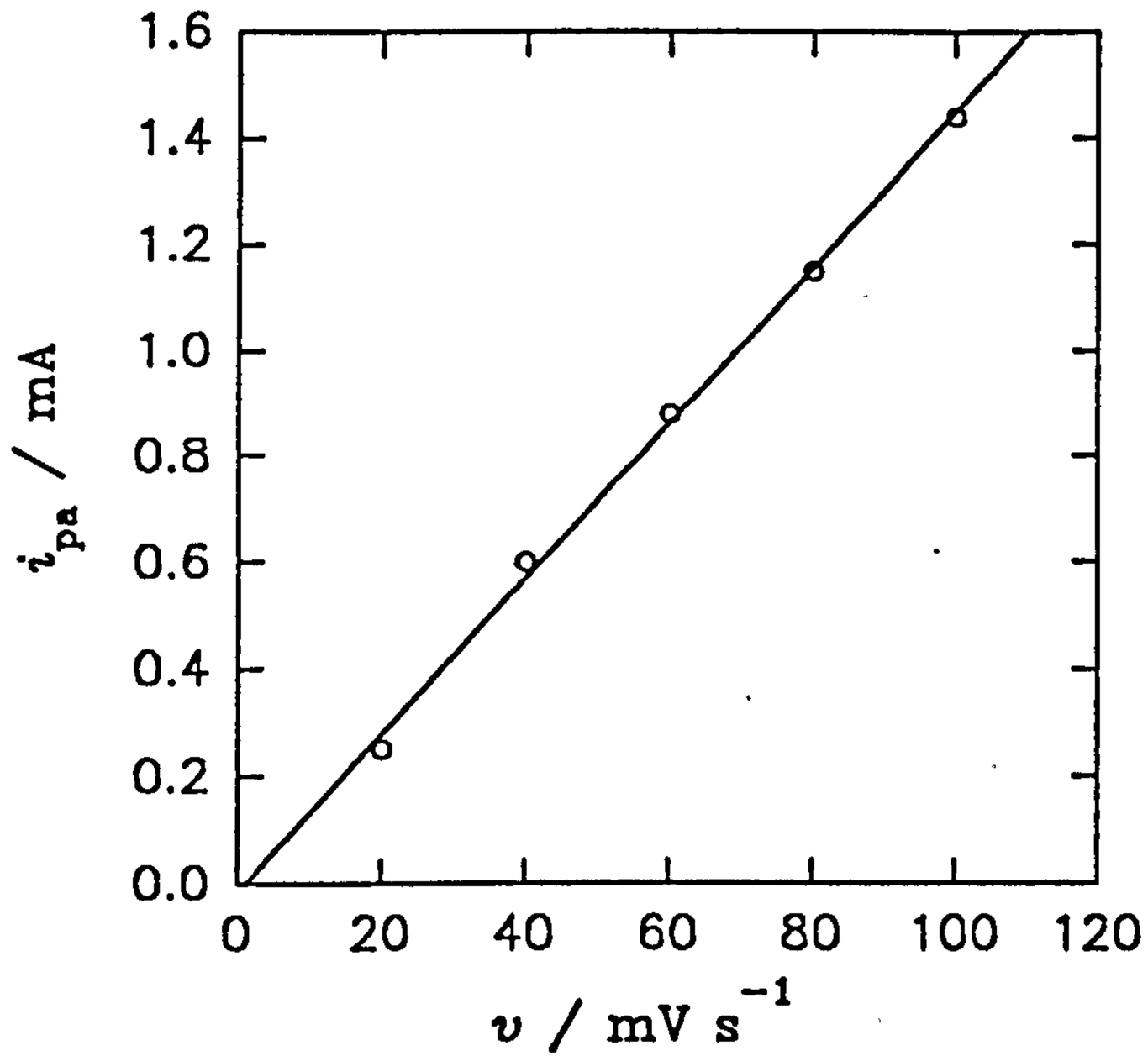

Figure 4.19 The plot of E_{pa} (○) and E_{pc} (●) vs. sweep rate (υ) taken from the data presented in figure 4.17 (○, r = 0.998, n = 5) (●, r = 0.994, n = 5)

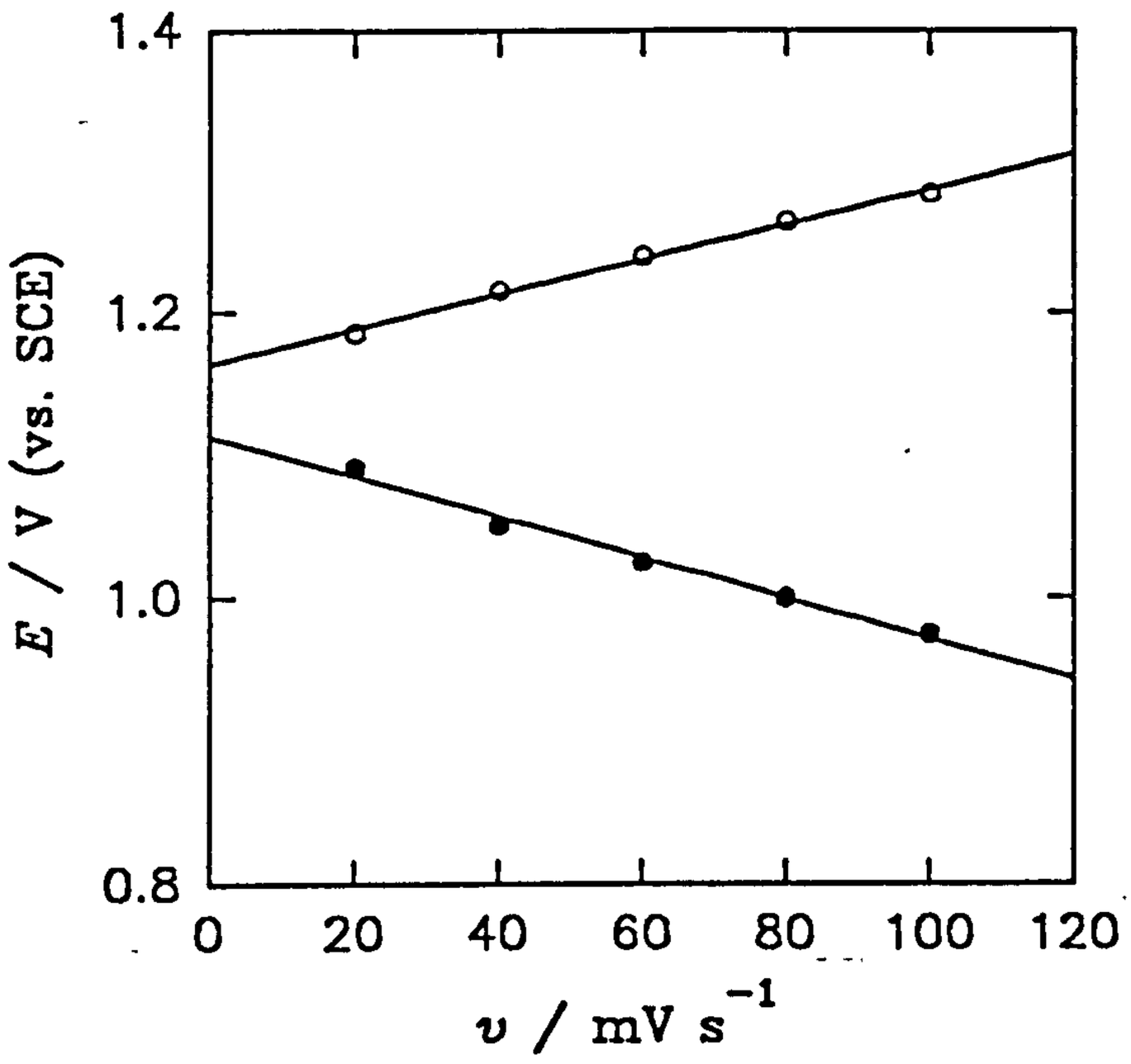

suggesting low planarity of the monomers within the polymer.[115] The other polymers have very similar electrochemistry to the methyl ester and have the following sweep rate (υ) limiting E_{pa} and E_{pc} values; poly(ethyl(3-thiopheneacetate)) E_{pa} = 1.17 V and E_{pc} = 1.04 V (vs. SCE), poly(n-propyl(3-thiopheneacetate)) E_{pa} = 1.15 V and E_{pc} = 1.01 V (vs. SCE), poly(n-butyl(3-thiopheneacetate)) E_{pa} = 1.15 V and E_{pc} = 0.96 V (vs. SCE). The films formed are of high quality except for the n-butyl polymer and are red in their fully reduced form and blue in their fully oxidised form.

Films could also be grown by potential stepping in acetonitrile solutions of the monomer at concentrations of as little as 15 mmol dm^{-3} but the best quality films were obtained by using the method described above.

4.6 Characterisation by FTIR Poly(3-thiopheneacetic acid) and Associated Ester Polymers

The FTIR spectrum of fully reduced poly(3-thiopheneacetic acid) grown in the manner described above is shown in figure 4.20. Bands above 2000 cm^{-1} are obscured by scattering and the intensity of the O-H stretch. A very strong carbonyl band is recorded at 1702 cm^{-1} corresponding to the dimerised acid group in the polymer. Medium strength bands are observed between 1300 cm^{-1} and 1590 cm^{-1} corresponding to aromatic and ring-ring stretches. The βC-H out of plane bend is observed as a weak band at 835 cm^{-1} which is higher than the corresponding βC-H out of plane stretch for poly(3-methylthiophene) (Table 4.1). There does not appear to be any significant αC-H out of plane bending in the spectrum indicating that there are few α-β or β-β defects in the polymer even when grown at relatively high potentials. This may be due to the steric directing effects of the attached acetic acid groups.

Figure 4.20 The reflectance FT-IR spectrum of fully reduced poly(3-thiopheneacetic acid)

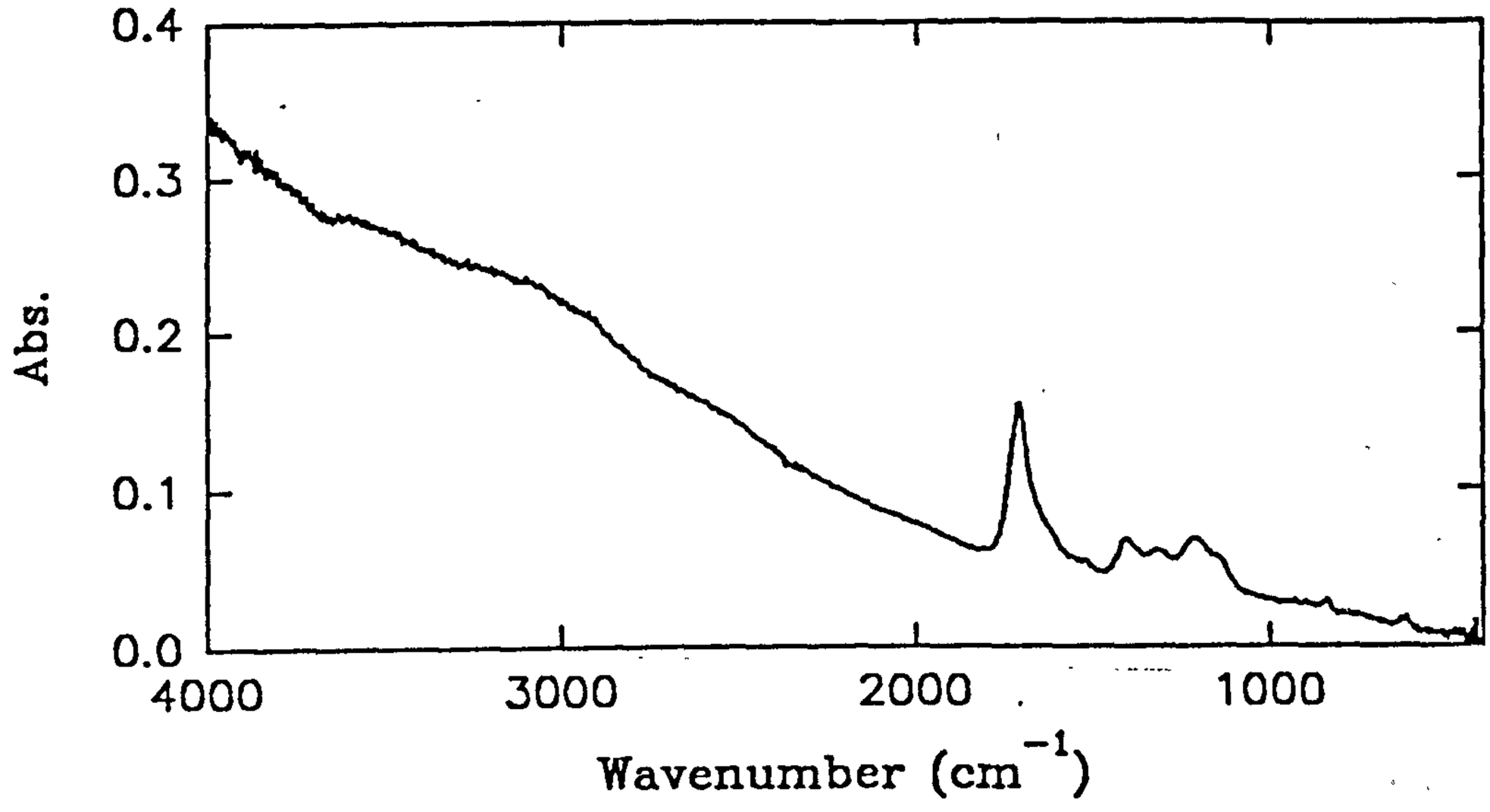

The reflectance FTIR spectrum of fully reduced poly(methyl(3-thiopheneacetate)) is shown in figure 4.21 and is very similar to the spectra of the other three ester polymers with a few exceptions. The spectra of the other ester polymers show increasing aliphatic C-H stretches between 2800 cm^{-1} and 3000 cm^{-1} as the aliphatic chain increases. Very little aliphatic C-H stretching is observed in the poly(methyl(3-thiopheneacetate)) spectrum, figure 4.21. The poly(methyl(3-thiopheneacetate)) spectrum, figure 4.21, has a medium band at 1440 cm^{-1} corresponding to a symmetric CH_3 deformation which is not observed in the other spectra. All the ester polymer spectra have carbonyl peaks corresponding to ester groups, which are compared to the carbonyl peak in the spectrum of poly(3-thiopheneacetic acid) in table 4.2, and a peak at 1150 cm^{-1} corresponding to an acetate C-C(=O)-O symmetric stretch (see Chapter 2 for reference). It is evident that there are also weaker underlying bands between 1300 cm^{-1} and 1500 cm^{-1} corresponding to aromatic ring stretching and ring-ring stretching. The βC-H out of plane bending in all the spectra occurred as a weak band at 835 cm^{-1} with no visible αC-H out of plane bending

The spectra described above quite clearly demonstrate the presence of the relevant functional groups within the polymer structure. The slight difference in position of the carbonyl peaks shown in table 4.2 from monomer to polymer is quite common and occurs in other types of polymers due to steric packing effects.[132]

4.7 Aqueous Electrochemistry of Poly(3-thiopheneacetic acid)

Based on work reported by Sunde *et al.*[68,69] degassed aqueous potassium nitrate (0.1 mol dm^{-3}) was chosen as the standard electrolyte to be used in the aqueous electrochemical studies of poly(3-thiopheneacetic acid) and its related compounds. The cyclic voltammetry between 0.0 V and 0.9 V (vs. SCE) at 20 mV s^{-1} for

Figure 4.21 The reflectance FT-IR spectrum of fully reduced poly(methyl(3-thiopheneacetate))

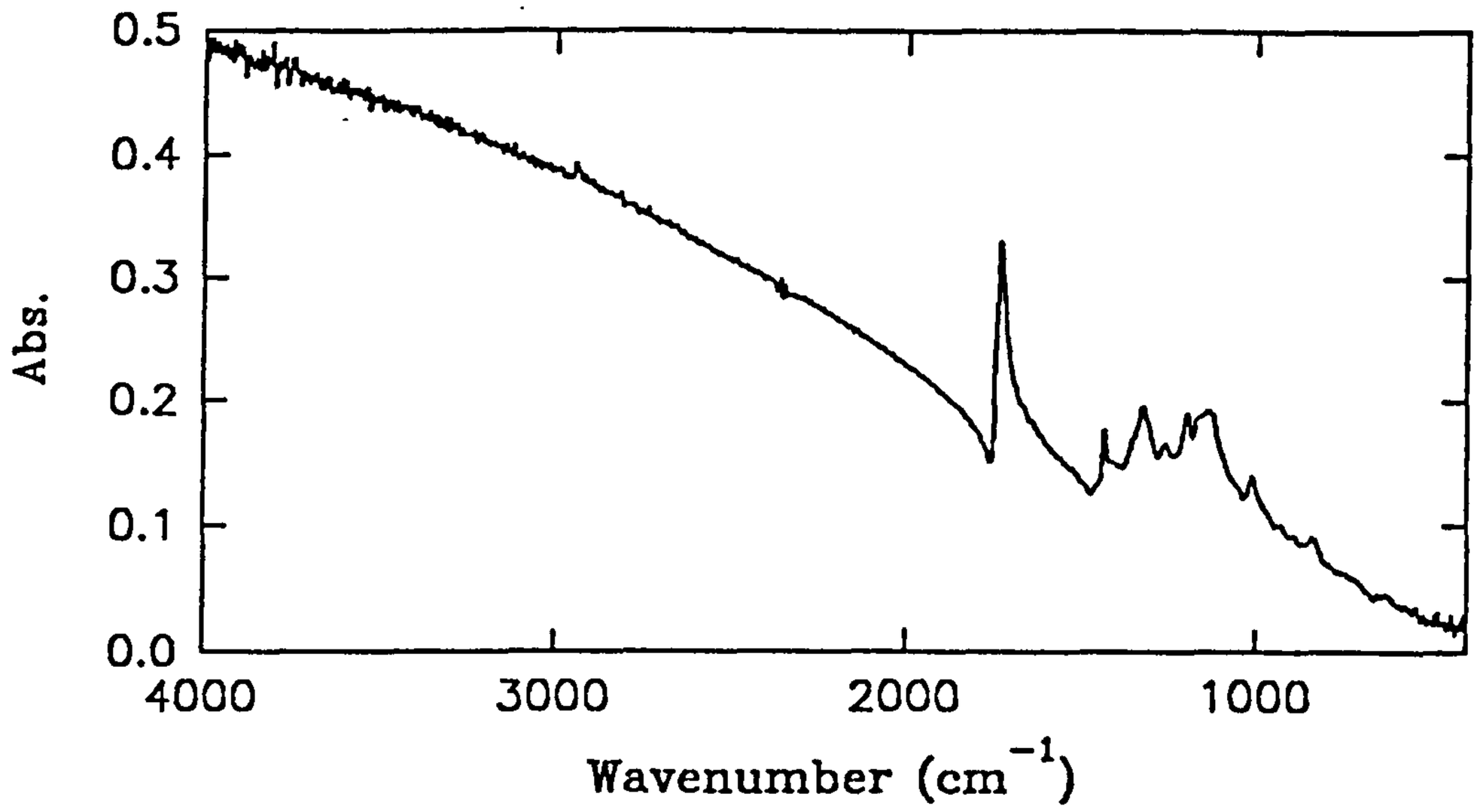

Table 4.2 Comparison of the position of the carbonyl stretches in the reflectance FT-IR spectra of poly(3-thiopheneacetic acid) and its esters

Functional Group	Peak Position (cm^{-1}) ± 4 cm^{-1}	
	Monomer	Polymer
-COOH	1709	1702
-COOMe	1741	1739
-COOEt	1735	1732
-COO^{n}Pr	1735	1730
-COO^{n}Bu	1736	1734

poly(3-methylthiophene), grown for 30 s, in degassed aqueous potassium nitrate (0.1 mol dm^{-3}) solution was consistent with the previously reported results[69] with initial losses in Q_{CV} followed by a stable trace.

When a film of poly(3-thiopheneacetic acid), grown in the manner previously described for four cycles, is placed in degassed aqueous potassium nitrate (0.1 mol dm^{-3}) and is studied by cyclic voltammetry between 0 V and 1.4 V (vs. SCE) at 10 mV s^{-1} the initial cycle passes a very large Q_{CV} and subsequent cycles show passivated behaviour figure 4.22. The ratio of the initial Q_{CV}(aqueous) to Q_{CV}(acetonitrile) is approximately 9:1 which is a very large change and must be due to an extraordinary overoxidation process.

The reflectance FTIR of poly(3-thiopheneacetic acid) before and after cyclic voltammetry in degassed aqueous potassium nitrate (0.1 mol dm^{-3}) solution is shown in figure 4.23. It is evident that a large band has appeared in the carbonyl region at a lower wave number than the acetic acid stretch. This band is likely to be due to the formation of the α,β-unsaturated ketone group within the polymer chain, figure 4.24, formed by the nucleophilic attack of water upon the polymer during oxidation. From the sizes of Q_{CV}(aqueous) and Q_{CV}(acetonitrile) and assuming a dopancy of (δ = 0.25) it can be estimated that almost every monomer has been converted to the α,β-unsaturated ketone form during the initial cycle. This result is very unusual and was investigated further.

Poly(methyl(3-thiopheneacetate)) was studied in degassed aqueous solution to provide a comparison to poly(3-thiopheneacetic acid) since both have similar E_{pa} values in acetonitrile solutions. The film of poly(methyl(3-thiopheneacetate)) whose cyclic voltammetry is shown in figure 4.17, was studied by cyclic voltammetry between 0.0 V and 1.2 V (vs. SCE) in degassed aqueous potassium nitrate (0.1 mol dm^{-3}) solution. Again passivation was observed upon the second cycle,

Figure 4.22 The passivation of poly(3-thiopheneacetic acid) during cyclic voltammetry between 0.0 V and 1.4 V (vs. SCE) in degassed aqueous potassium nitrate (0.1 mol dm^{-3}) solution (sweep rate υ = 10 mV s^{-1})

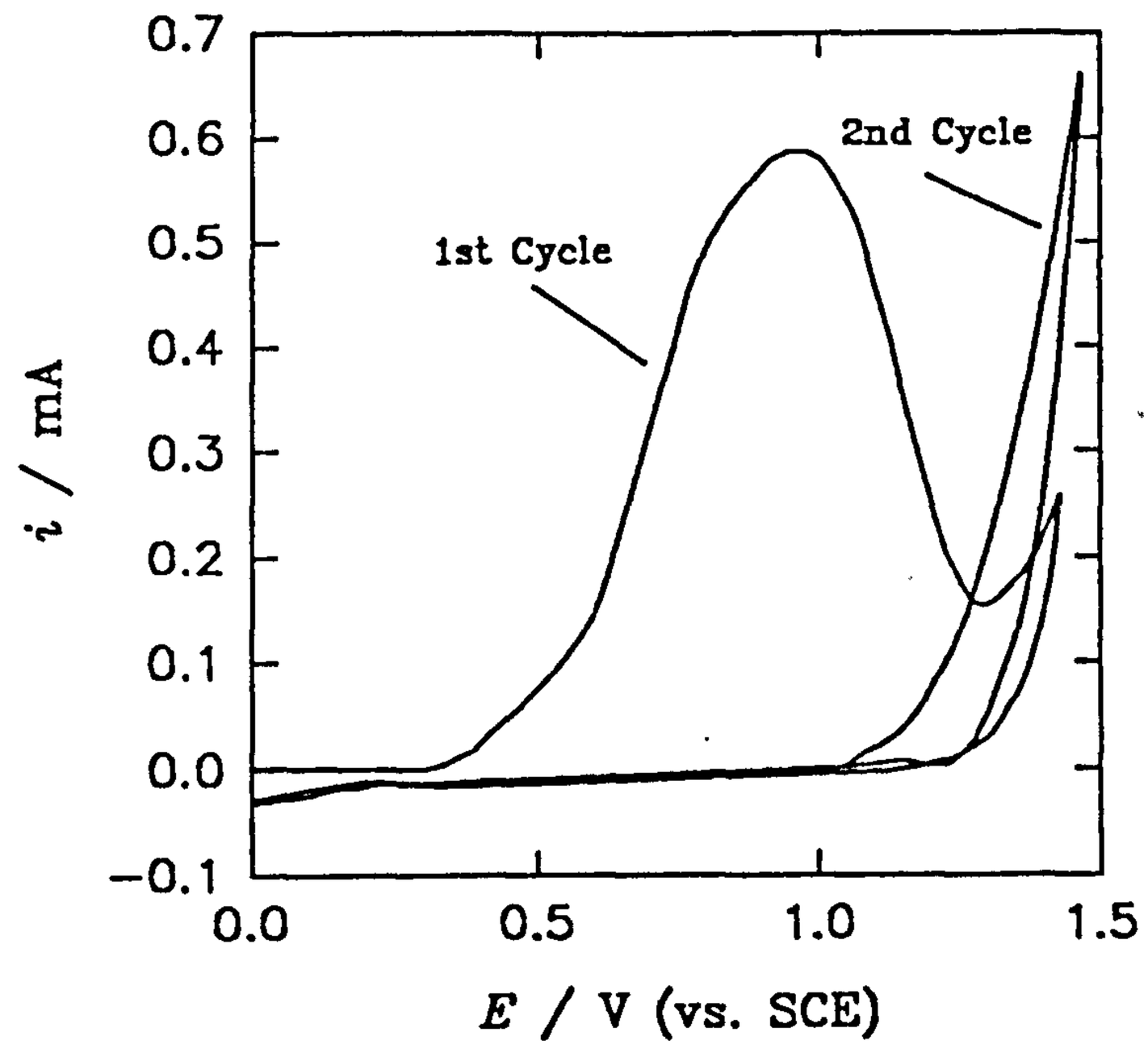

Figure 4.23 The reflectance FT-IR of poly(3-thiopheneacetic acid) before and after the passivation shown in figure 4.22

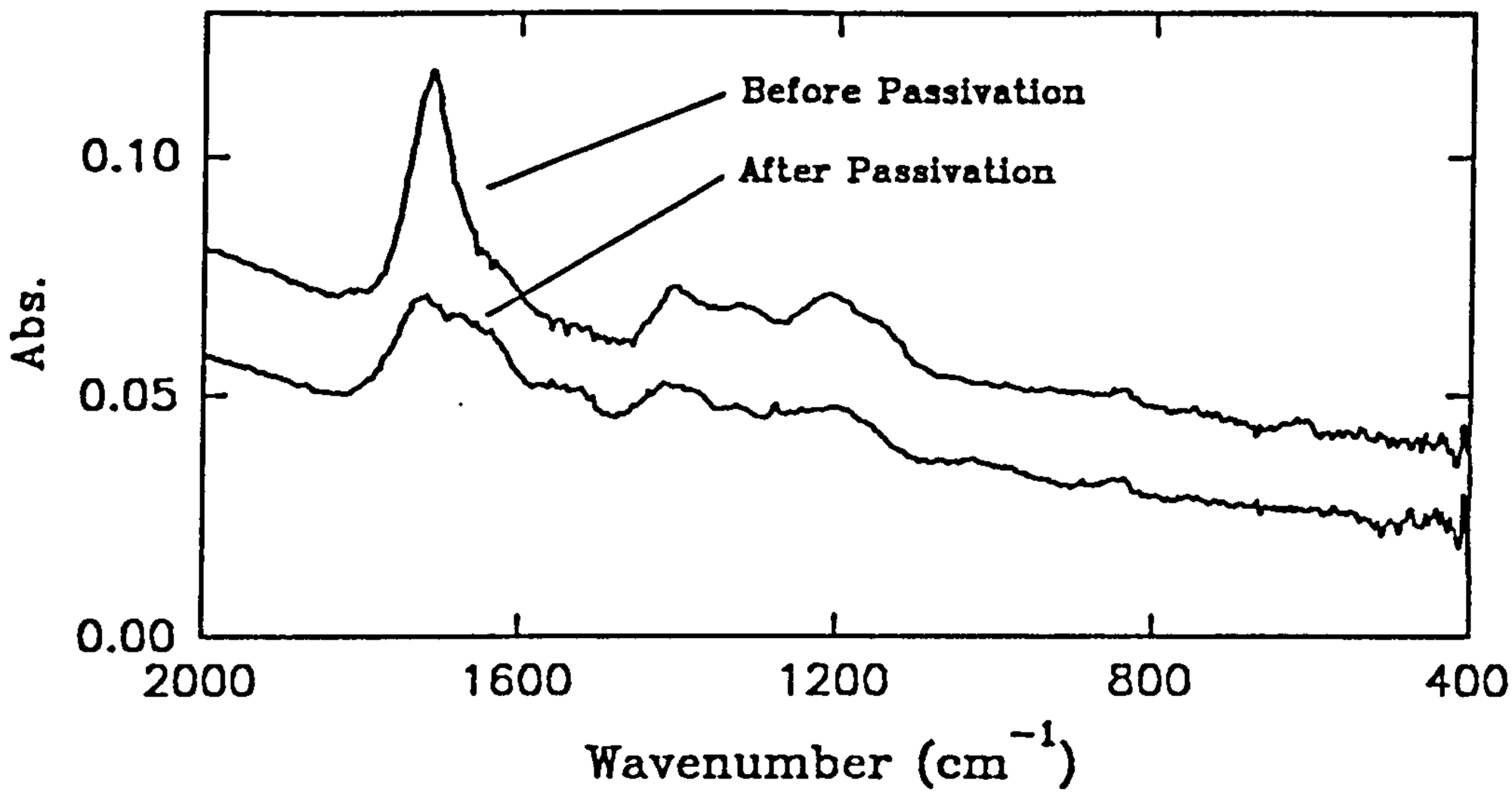

Figure 4.24 The suggested structure of the polymer after the passivation shown in figure 4.22

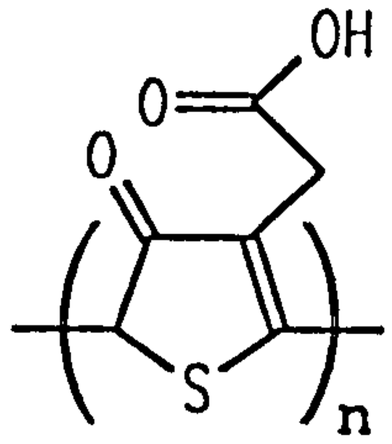

figure 4.25 however the Q_{CV}(aqueous) to Q_{CV}(acetonitrile) ratio was approximately 1:1 suggesting that the acetic acid group in poly(3-thiopheneacetic acid) may be responsible for the extraordinarily large Q_{CV}(aqueous) observed. The reflectance FTIR of the poly(methyl(3-thiopheneacetate)) film before and after cycling in aqueous solution is shown in figure 4.26 clearly showing a medium strength α,β-unsaturated ketone peak at 1650 cm^{-1} and a weak peak at 838 cm^{-1} which overlays the βC-H out of plane bend.

To further investigate the electrochemistry of poly(3-thiopheneacetic acid) electrolyte solutions of TEAT (0.1 mol dm^{-3}) in methanol were utilised. Methanol has similar properties to acetonitrile but is more nucleophilic which prevents polymer growth but not polymer electrochemistry. A film of poly(3-methylthiophene) grown for 60 s was studied by cyclic voltammetry in a degassed solution of TEAT (0.1 mol dm^{-3}) in methanol between -0.3 V and 1.0 V (vs. SCE) at 100 mV s^{-1}, figure 4.27. The electrochemistry observed in figure 4.27 is stable and consistent with the electrochemistry in acetonitrile except for differences in liquid junction potentials, at the reference electrode, which tend to shift the electrochemistry in methanol to lower potentials by *ca.* 0.1 V. There are no changes in the reflectance FTIR spectra of the polymer before and after cyclic voltammetry in methanol and the electrochemistry in acetonitrile remains unchanged, which gives conclusive evidence that methanol does not attack poly(3-methylthiophene) during oxidation and reduction.

A film of poly(3-thiopheneacetic acid), grown in the manner previously described for four cycles, was studied by cyclic voltammetry between 0.0 V and 1.6 V (vs. SCE) at 20 mV s^{-1} in a degassed solution of TEAT (0.1 mol dm^{-3}) in methanol. Again passivation was observed after the first cycle and the Q_{CV}(methanol) to Q_{CV}(acetonitrile) ratio was approximately 9:1. Inspection of the reflectance FTIR spectra of the film

Figure 4.25 The passivation of poly(methyl(3-thiopheneacetate) during cyclic voltammetry between 0.0 V and 1.2 V (vs. SCE) in degassed aqueous potassium nitrate (0.1 mol dm^{-3}) solution (sweep rate υ = 10 mV s^{-1})

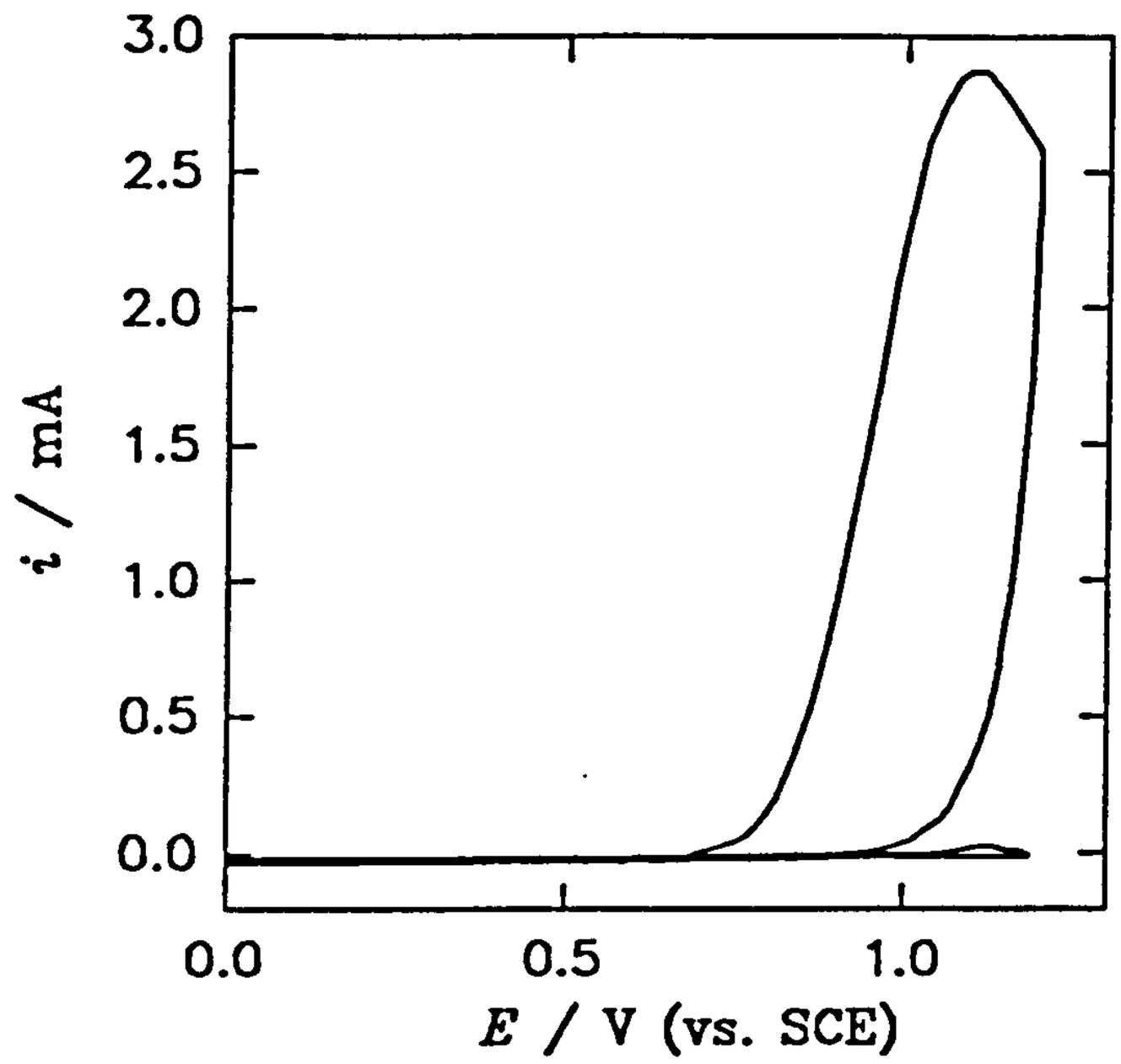

Figure 4.26 The reflectance FT-IR of poly(methyl(3-thiopheneacetate) before and after the passivation shown in figure 4.25

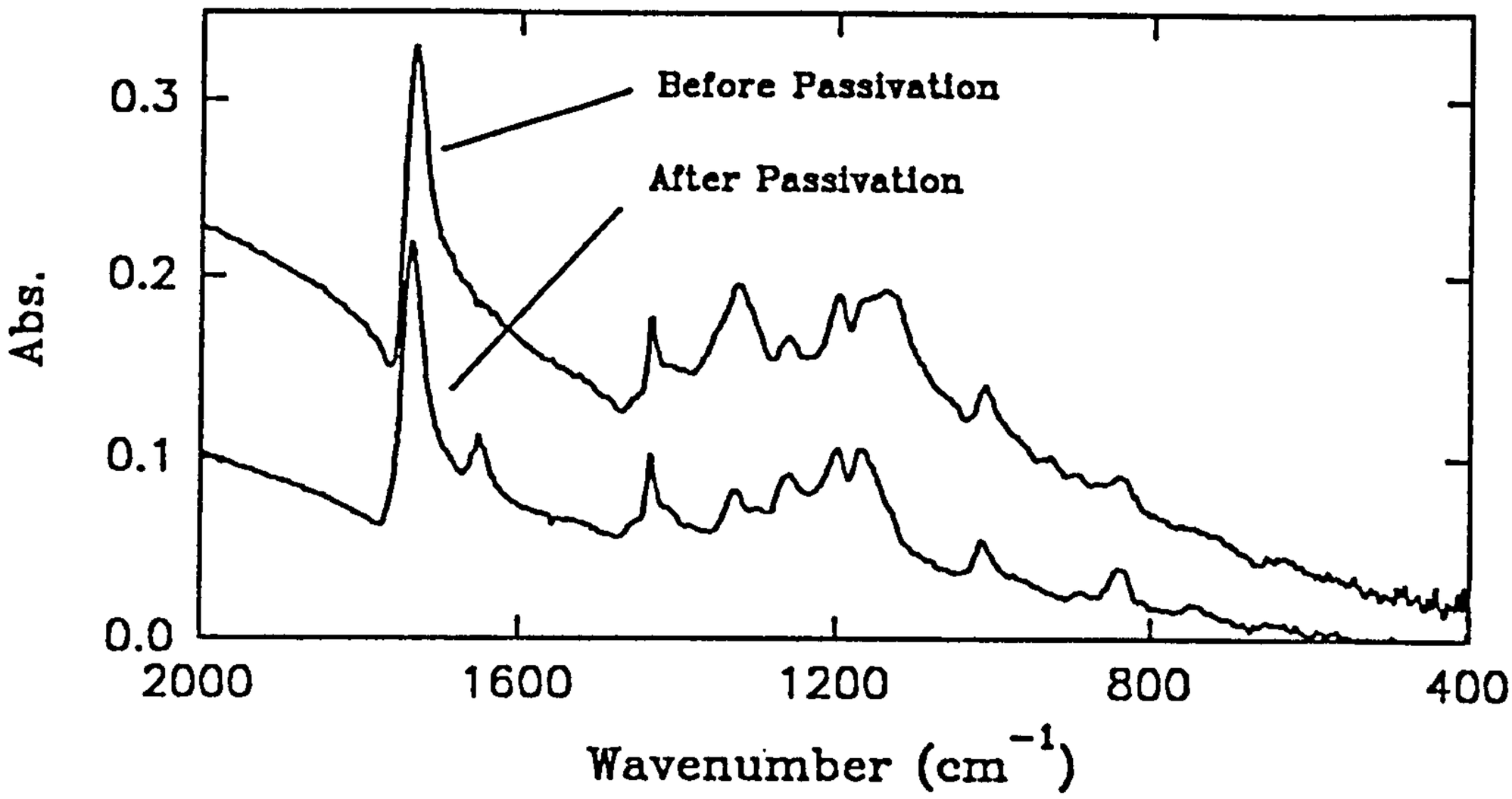

Figure 4.27 The cyclic voltammetry between -0.3 V and 1.0 V (vs. SCE) of poly(3-methylthiophene) (grown for t = 60 s) in methanol containing TEAT (0.1 mol dm^{-3}) (sweep rate υ = 100 mV s^{-1})

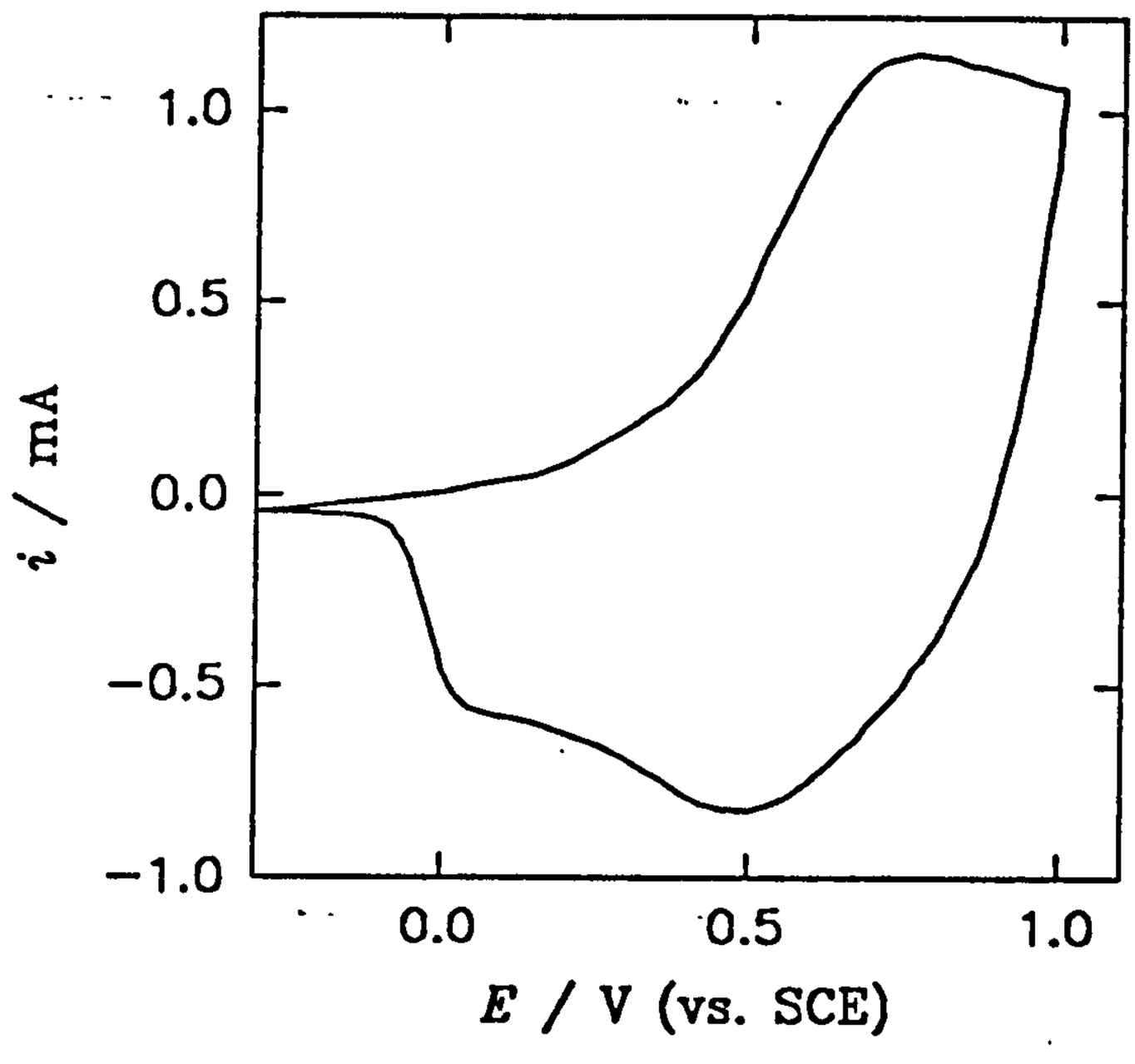

before and after cyclic voltammetry in the methanol electrolyte revealed that the carboxylic acid functionality had been totally replaced by a methyl ester functionality, figure 4.28 with a C=O stretch at 1734 cm^{-1} and a CH_3 symmetric deformation band at 1440 cm^{-1}. It therefore appears that in this case the passivation process has driven the esterification of the polymer, this is unusual since esterification usually requires conditions such as low pH and prolonged heating (see Chapter 2).

It is thought that this behaviour can be explained by poly(3-thiopheneacetic acid) reversibly forming five membered lactone rings, at the vacant β-position, which can then undergo nucleophilic attack to leave O-H groups on the vacant position. Tautomerisation would then occur to give an α,β-unsaturated ketone. The whole process is described schematically, for a two monomer bipolaron, in figure 4.29. This would explain why poly(3-thiopheneacetic acid) is both passivated and esterified in methanol solutions and why poly(methyl(3-thiopheneacetate)) has stable electrochemistry in acetonitrile solutions while having a similar E_{pa}. The large Q_{CV}(aqueous) for poly(3-thiopheneacetic acid) can be explained by the formation of the lactones which would effectively discharge the film without immediately destroying its conjugated backbone allowing further oxidation to take place. Each lactone ring requires two electrons for formation which for a dopancy of (δ = 0.25) would predict a Q_{CV}(aqueous) to Q_{CV}(acetonitrile) ratio to be 9:1 *i.e.* for a four monomer segment, within the polymer, the removal of eight electrons is required for lactone formation and one is required for doping. In acetonitrile the formation of lactones is not as favourable because of the necessity to eject protons, explaining why passivation of the film occurs over more cycles.

Figure 4.28 The reflectance FT-IR of poly(3-thiopheneacetic acid) before and after passivation in methanol

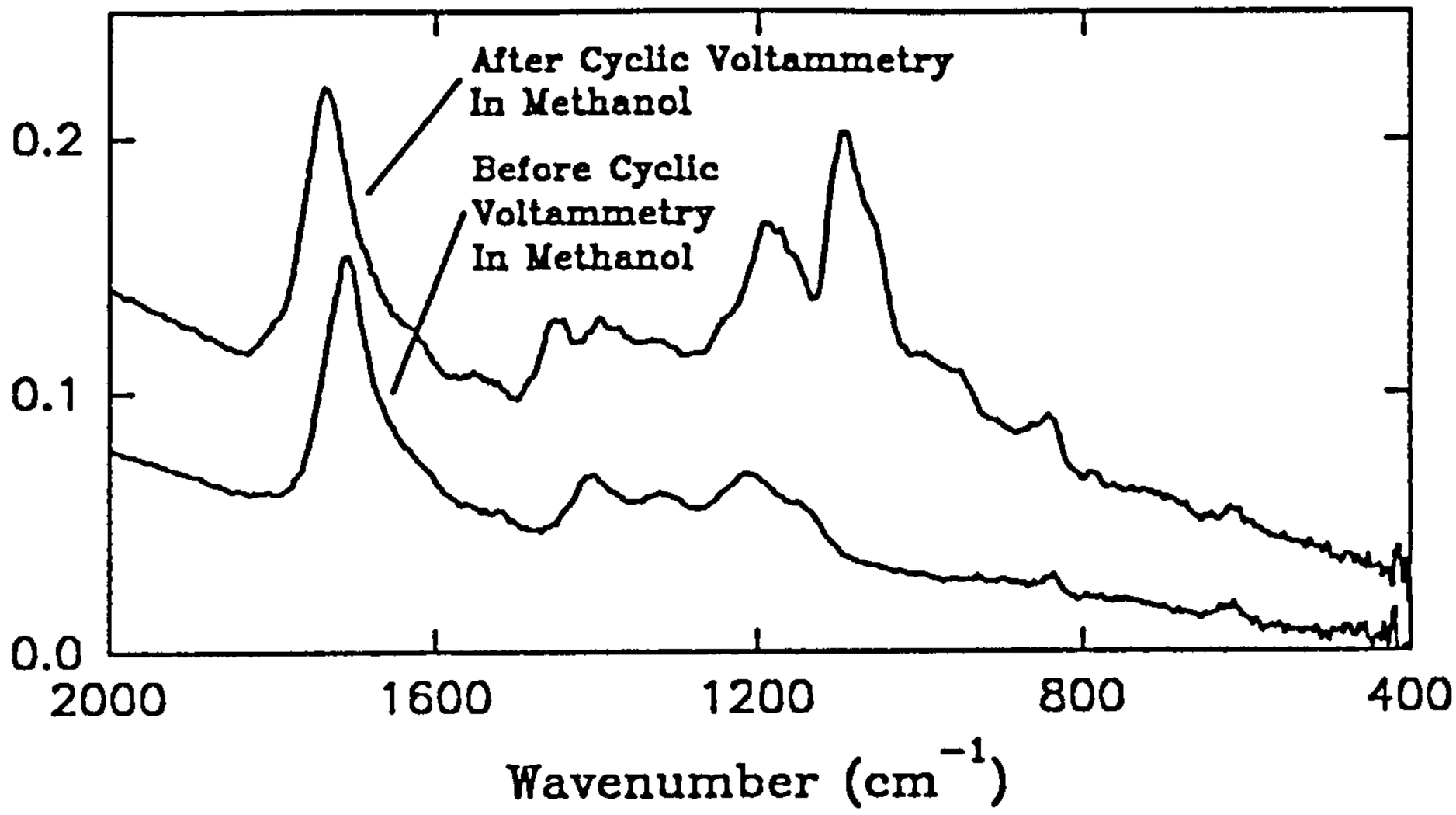

Figure 4.29 Schematic representation of the passivation of poly(3-thiopheneacetic acid) in various solvents using a two monomer bipolaron model

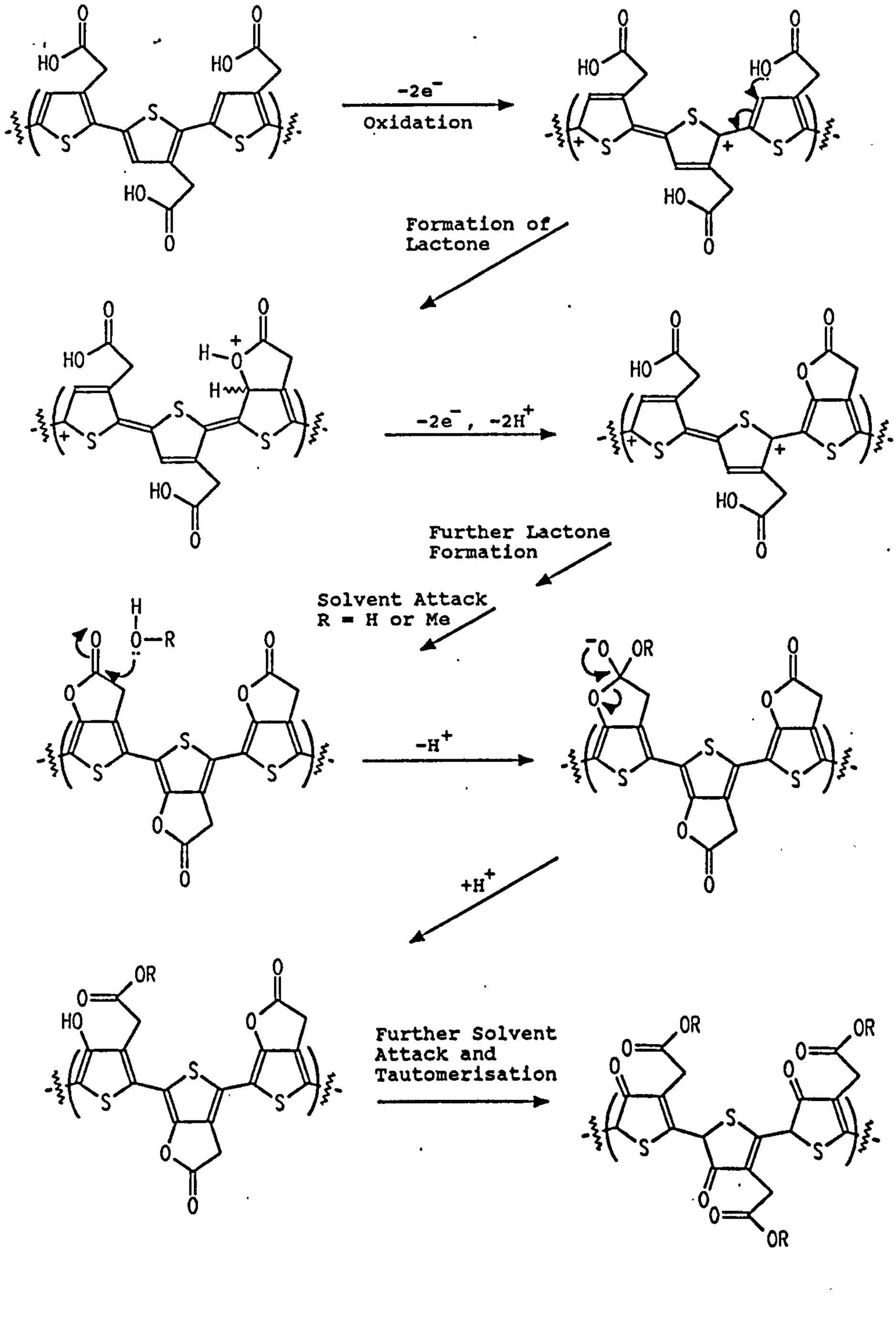

4.8 The Copolymerisation of 3-Thiopheneacetic Acid and 3-Methylthiophene

The copolymerisation of 3-thiopheneacetic (V) acid with 3-methylthiophene (IV) was studied to stabilise the electrochemistry of the polymer in acetonitrile solutions. The copolymerisation of 3-thiophenecarboxylic acid and thiophene has previously been studied[140] but 3-methlythiophene is a better monomer to use in order to reduce the E_{pa} of the resulting copolymer.

Copolymerisation experiments were performed on solutions of 3-thiopheneacetic acid (V) with concentrations between 50 mmol dm^{-3} and 1.0 mol dm^{-3} in solutions of TEAT (0.1 mol dm^{-3}) in acetonitrile. All the solutions contained 3-methylthiophene (IV) (50 mmol dm^{-3}) and were studied by potentiometrically stepping from 0 V to 1.7 V (vs. SCE) for 30 s at a polished stationary platinum disc electrode (A = 0.385 cm^2). The films formed were then studied by cyclic voltammetry and by reflectance FTIR. It proved to be impossible to estimate the monomer incorporation in the polymers by reflectance FTIR due to the lack of comparison peaks and micro-analysis was regarded as too inaccurate to derive any meaningful data so no monomer-monomer percentage incorporations were calculated. The reflectance FTIR results did however reveal the presence of 3-thiopheneacetic acid in the polymers. Lower concentrations of 3-methylthiophene in the copolymerisation mixture were studied but the quality of films was found to be unacceptable.

Polymers grown from concentrations of 3-thiopheneacetic acid below 0.1 mol dm^{-3} do not contain any appreciable amounts of 3-thiopheneacetic acid monomer when studied by reflectance FTIR. The electrochemistry and appearance of these polymers is very similar to the poly(3-methylthiophene) films studied earlier. Polymers grown from concentrations of 3-thiopheneacetic acid greater than 0.2 mol dm^{-3}

contain appreciable amounts of 3-thiopheneacetic acid monomer as evidenced by reflectance FTIR and the electrochemistry has behaviour which is intermediate between that of poly(3-methylthiophene) and poly(3-thiopheneacetic acid). The films appeared to be slightly different to poly(3-methylthiophene) being red/orange in their fully reduced state and blue in their fully oxidised state. The reflectance FTIR of copolymer films grown for 30 s in the manner described above from solutions containing 3-thiopheneacetic acid (V), with concentrations of 0.1, 0.2 and 0.6 mol dm^{-3}, are shown in figure 4.30.

Copolymer films grown in the manner described above from solutions with concentrations of 0.6 mol dm^{-3} 3-thiopheneacetic acid (V) show similar growth transients to poly(3-methylthiophene) and have stable cyclic voltammetry between -0.3 and 1.3 V (vs. SCE), figure 4.31. The i_{pa} vs. sweep rate (υ) plot has a linear correlation shown in figure 4.32 and the limiting values for the peak potentials are E_{pa} = 1.03 V (vs. SCE) (r = 0.983, n = 9) and E_{pc} = 0.95 V (vs. SCE)(r = 0.990, n = 9), figure 4.33. The effect of introducing the 3-methylthiophene groups has had a marked effect on the E_{pa} of the acetic acid polymer. However when the aqueous electrochemistry was studied passivation was again observed with a Q_{CV}(aqueous) to Q_{CV}(acetonitrile) ratio of approximately 9:1 confirming that there is a high percentage of 3-thiopheneacetic acid in the polymer. When films of this type of copolymer were fully oxidised in acetonitrile and then placed into degassed aqueous potassium nitrate (0.1 mol dm^{-3}) solution the film immediately turned from blue to red/orange indicating complete discharge. This process could only be performed a limited number of times on the same film before the film became totally inactive supporting the lactone formation theory. Reflectance FTIR data taken of the copolymer film before and after aqueous passivation revealed similar changes to those previously observed for poly(3-thiopheneacetic acid) described earlier.

Figure 4.30 The reflectance FT-IR of copolymer films grown from solutions of 3-thiopheneacetic acid (V) with the concentrations of 0.1, 0.2 and 0.6 mol dm^{-3} and 3-methylthiophene (IV) (50 mmol dm^{-3}) in acetonitrile containing TEAT (0.1 mol dm^{-3}) by potential stepping from 0.0 V to 1.7 V (vs. SCE) at a platinum electrode (A = 0.385 cm^2) for t = 30 s

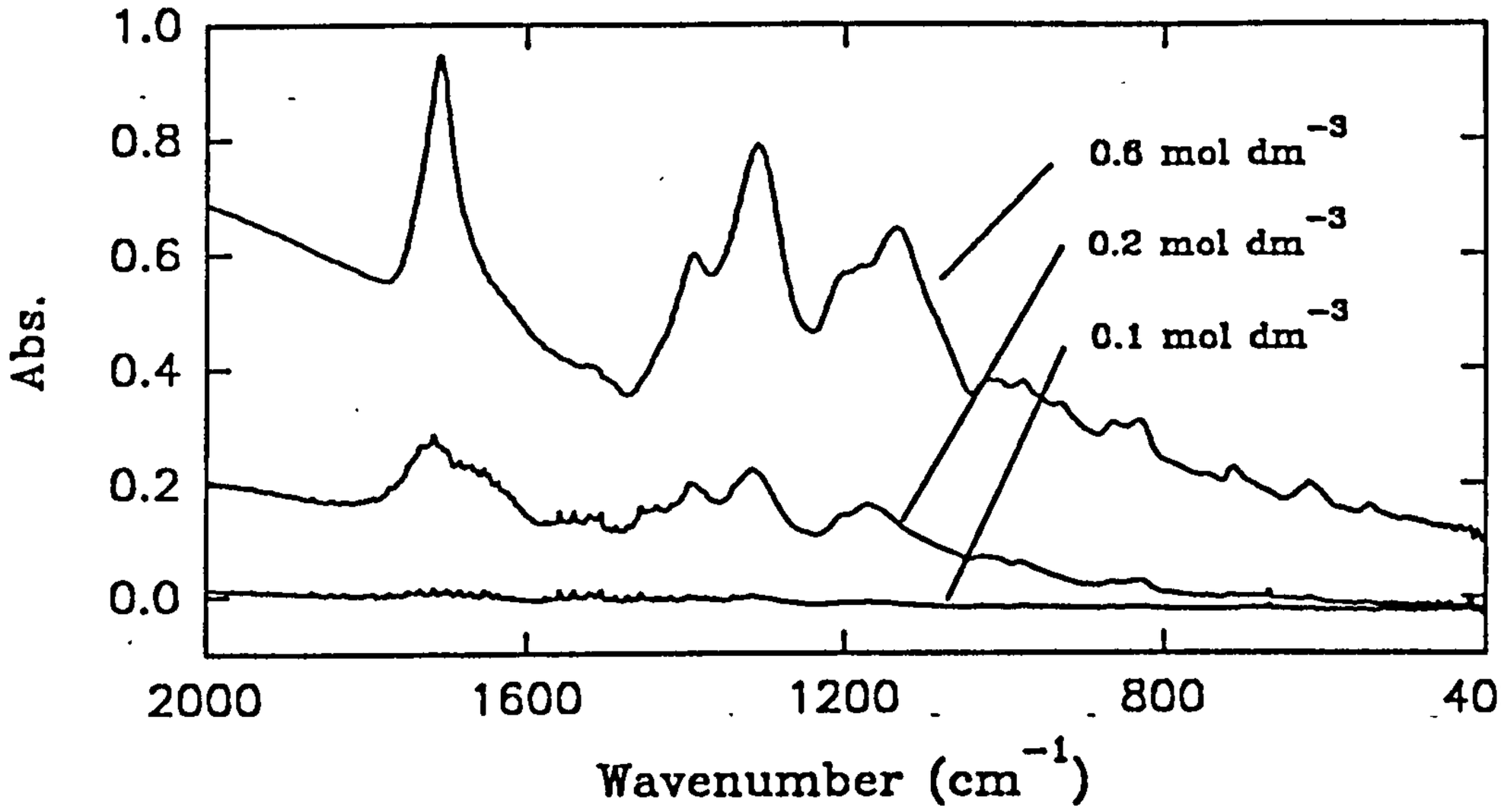

Figure 4.31 The cyclic voltammetry between 0.3 V and 1.3 V (vs. SCE) in acetonitrile containing TEAT (0.1 mol dm^{-3}) at sweep rates of υ = 20, 30, 40, 50, 60, 70, 80, 90 and 100 mV s^{-1} of the copolymer initially grown from a solution containing 3-thiopheneacetic acid (0.6 mol dm^{-3}) (see figure 4.30)

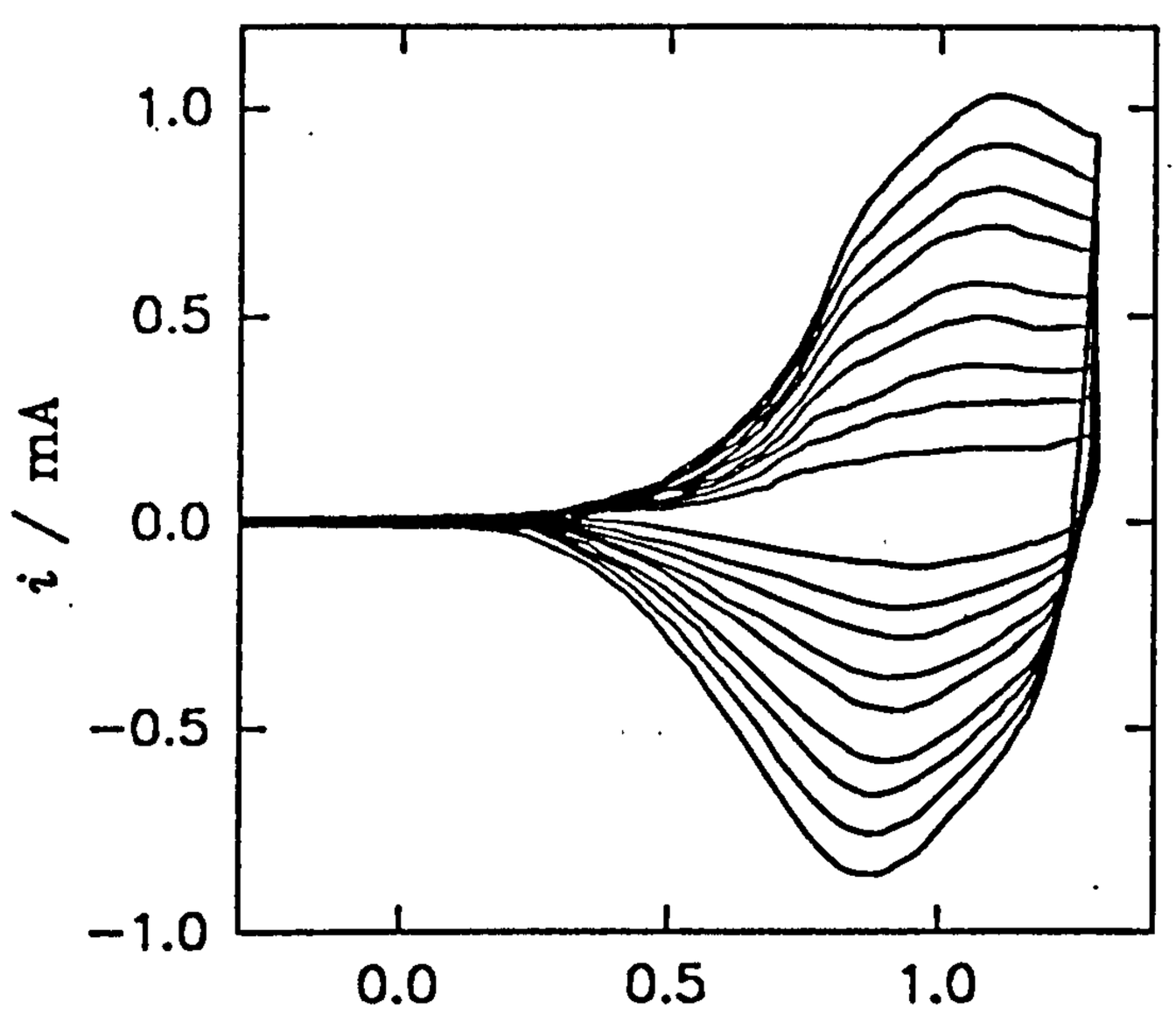

Figure 4.32 The i_{pa} vs. sweep rate (υ) plotted from the data shown in figure 4.31 (r = 0.998, n = 9)

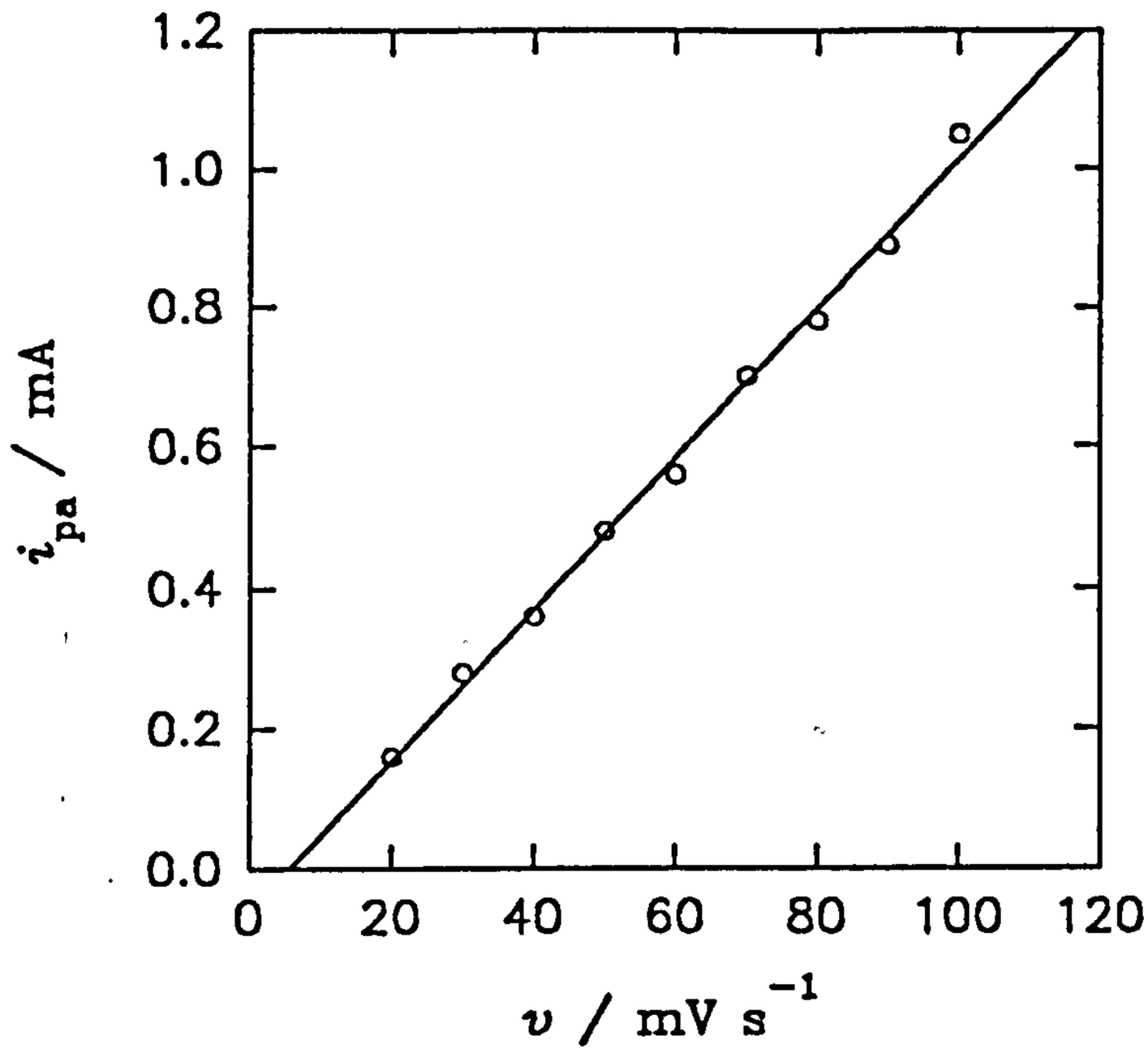

Figure 4.33 The plot of E_{pa} (○) and E_{pc} (●) vs. sweep rate (υ) taken from the data presented in figure 4.31 (○, r = 0.983, n = 9) (●, r = 0.990, n = 9)

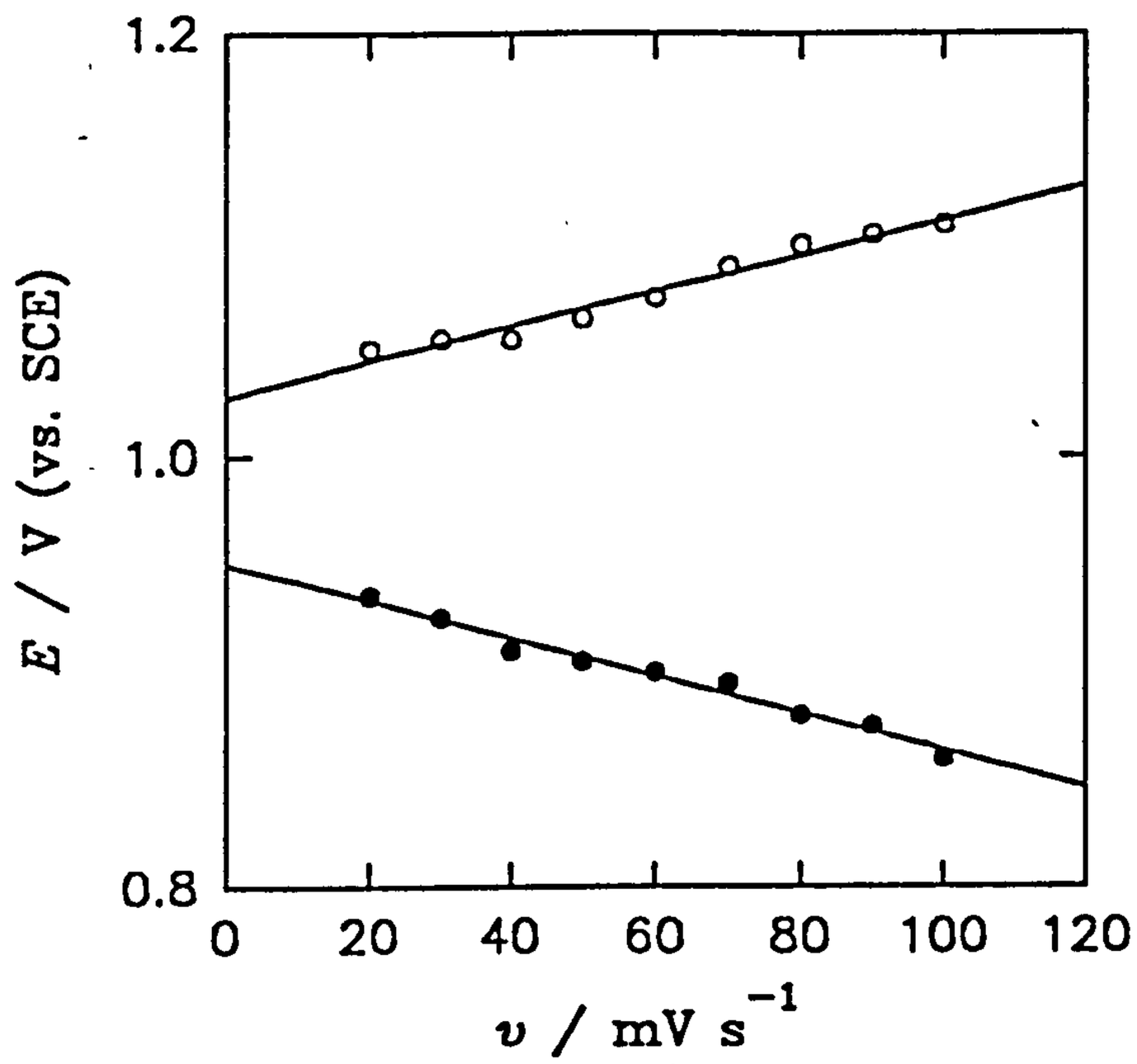

It is quite clear that thiophene polymers based on 3-thiopheneacetic acid have serious instability problems under aqueous conditions which leads to passivation when oxidation is attempted. It has been found that this behaviour is due to both the high oxidation potentials of the polymers and the attached acetic acid group.

4.9 Other Chemically Modified Poly(thiophenes)

Films of the substituted thiophene monomer (X) could not be grown from solutions of the monomer (X) (0.5 mol dm^{-3}) in acetonitrile containing TEAT (0.1 mol dm^{-3}) by either potentiometrically stepping or cyclic voltammetry at a polished stationary platinum disc electrode. However thin low quality films could be obtained if 3-methylthiophene (0.05 mol dm^{-3}) was added to the growth solution before cyclic voltammetry between 0.0 V and 1.7 V (vs. SCE) at 100 mV s^{-1} was performed.

The cyclic voltammetry of the films in acetonitrile containing TEAT (0.1 mol dm^{-3}) between 0.0 V and 1.3 V (vs. SCE) is very ill-defined but stable and the reflectance FTIR spectra of the fully reduced polymer showed the presence of appreciable amounts of monomer (X) with carbonyl peaks at 1739 cm^{-1} corresponding to the ester group and at 1645 cm^{-1} corresponding to the amide group. In addition peaks between 2800 cm^{-1} and 3000 cm^{-1} corresponding to aliphatic C-H stretches and at 3400 cm^{-1} corresponding to N-H stretches were also observed.

Again there was no aqueous electrochemistry recorded and deprotection by de-esterification of the attached peptide group on the polymer could not be achieved.

Films of poly(3-thiopheneacetic acid), grown in the manner described previously for four cycles on vacuum dried aqua regia treated

platinum flags (1 cm × 1 cm), were treated with the carbodiimide coupling agent 2-ethoxy-1-ethoxycarbonyl-1,2-dihydroquinoline (EEDQ),[82] valine(hydrochloride) and triethylamine in dichloromethane overnight, figure 4.34. Upon inspection by reflectance FTIR, after washing in neat dichloromethane and a saturated aqueous solution of sodium hydrogen carbonate, the film was found to be modified by a peptide linkage with carbonyl peaks at 1739 cm^{-1} and 1646 cm^{-1} corresponding to an ester and peptide carbonyl stretch respectively.

This shows that films grown from the 3-thiopheneacetic acid monomer (V) can subsequently be modified by further substitution. The obvious advantage being that modified conducting polymeric systems could be produced without direct polymerisation through a bulky monomer. Other peptide modifications of 3-thiopheneacetic acid have been performed but not directly on the polymer.[137]

Only electrochemically inactive films of 3-thiophenemethanol (XI) could be grown in acetonitrile solutions containing TEAT (0.1 mol dm^{-3}). A variety of monomer concentrations are studied but in all cases a passive green/brown film was formed. Figure 4.35 shows the first two cycles during the cyclic voltammetry of a 3-thiophenemethanol (XI) (0.1 mol dm^{-3}) solution between 0.0 V and 2.55 V (vs. SCE), at 100 mV s^{-1}, at a polished stationary platinum disc electrode (A = 0.385 cm^2). Polymerisation could also not be achieved if the acetonitrile solutions were protonated by means of $Zn(BF_4)_2.xH_2O$, in order to reduce the nucleophilicity of the monomer.[78] The films formed partially blocked the platinum electrode since the electrochemistry of ferrocene solutions in acetonitrile containing TEAT (0.1 mol dm^{-3}) was inhibited at these modified electrodes. It is thought that the methanol group on the monomer prevents the formation of a conducting polymer by acting as a nucleophile and attacking the α-position of the oxidised

Figure 4.34 The carbodiimide reaction for the chemical modification of poly(3-thiopheneacetic acid) using valine(methyl ester) and EEDQ

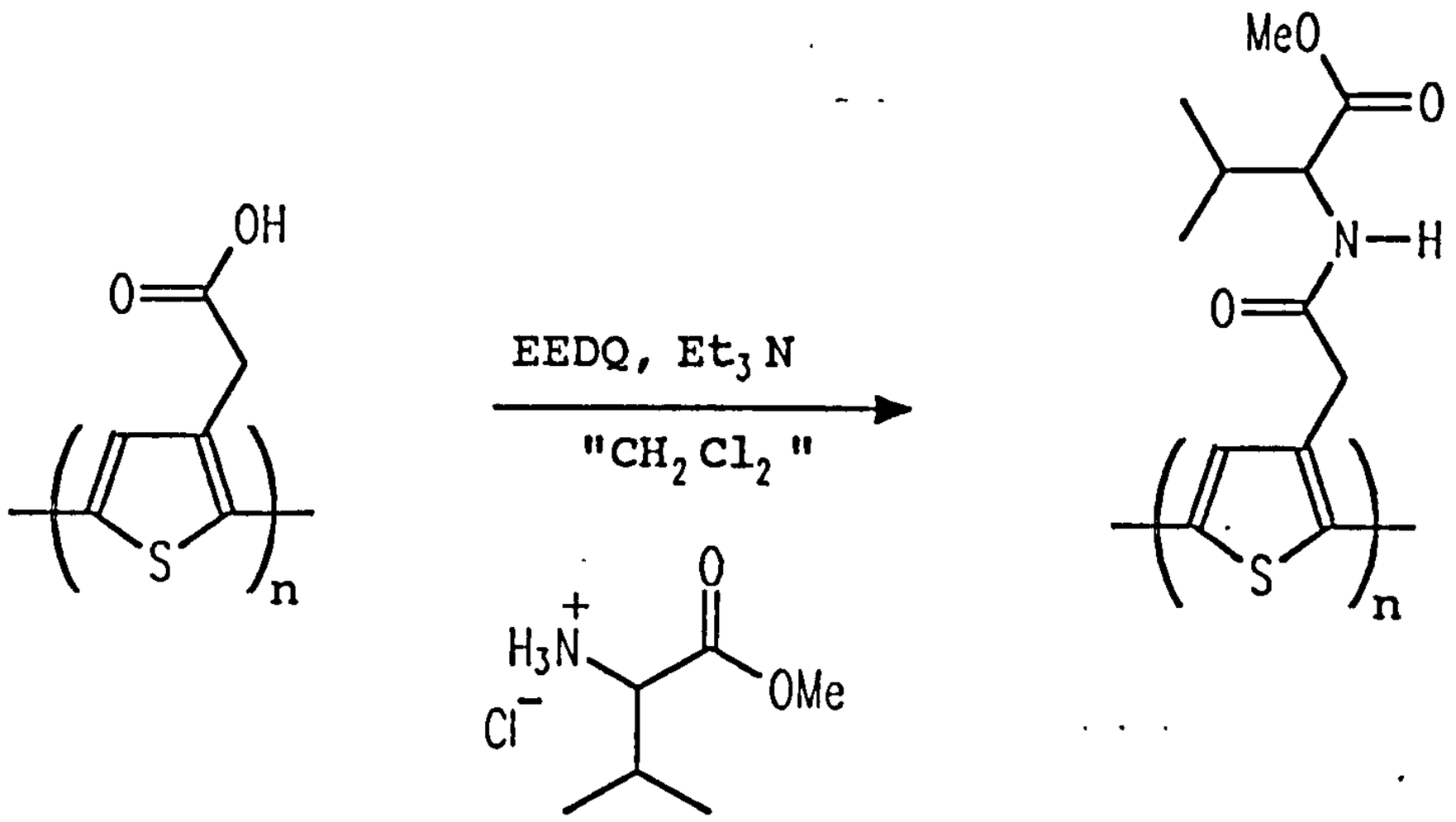

Figure 4.35 The cyclic voltammetry between 0.0 V and 2.55 V (vs. SCE) of a solution of 3-thiophenemethanol (XI) (0.1 mol dm^{-3}) in acetonitrile containing TEAT (0.1 mol dm^{-3}) at a platinum electrode (A = 0.385 cm^2) (sweep rate υ = 100 mV s^{-1})

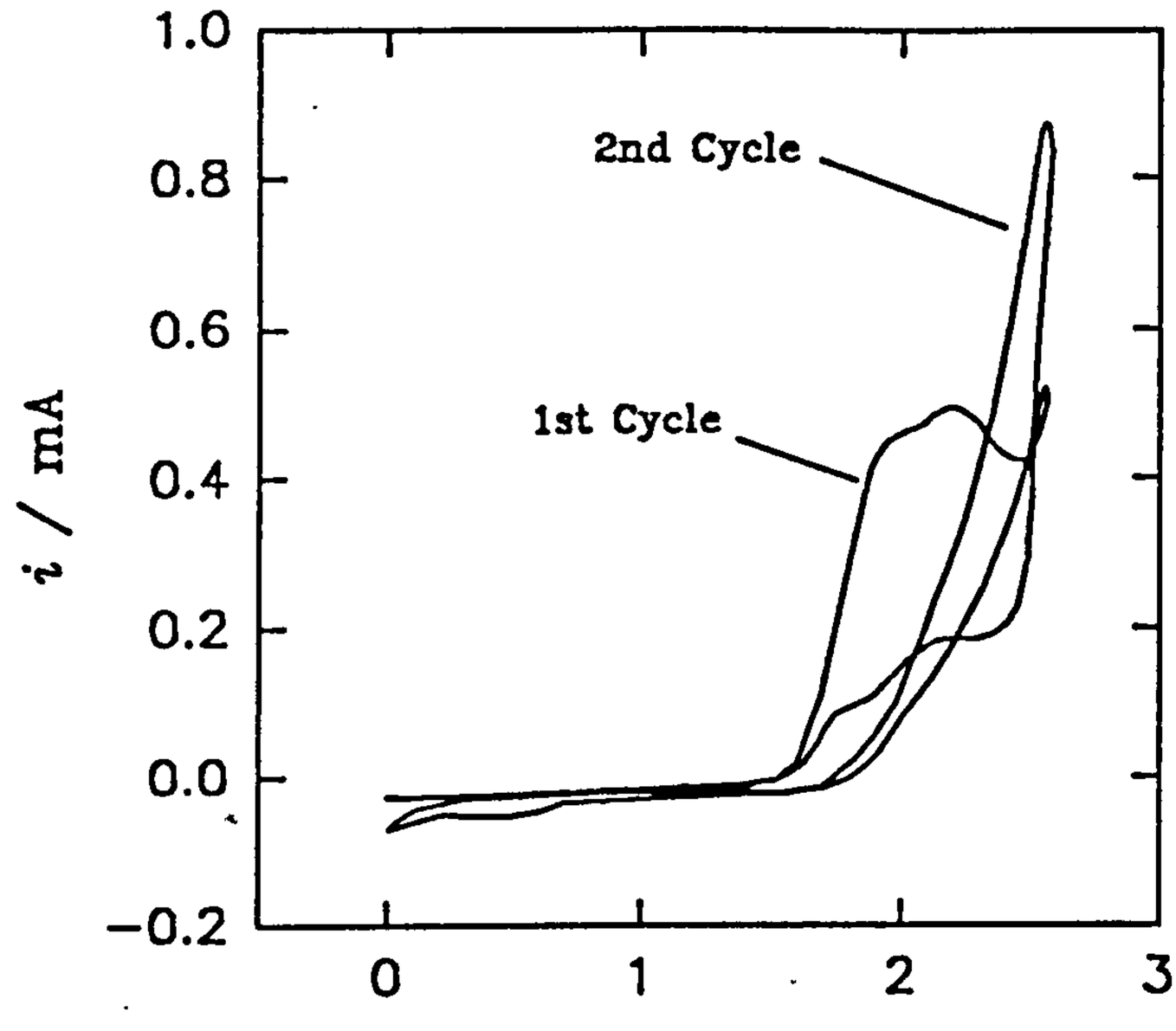

Figure 4.36 The proposed structure of poly(3-thiophenemethanol)

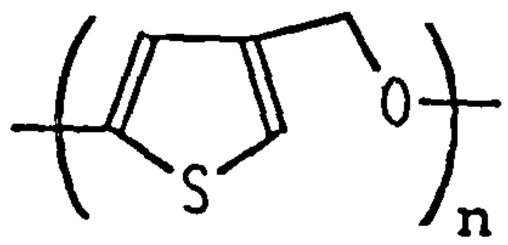

monomers forming a film which is reminiscent of poly(phenol),[141] figure 4.36.

4.10 Conclusions

It has been shown that poly(3-methylthiophene) has very complex electrochemistry which cannot be explained as a simple reversible oxidation and reduction. When more complex poly(thiophenes) were studied they were found to have major electrochemical instability problems, particularly in the case of poly(3-thiopheneacetic acid) which was not even stable in acetonitrile solutions. These stability problems were found to be related to the oxidation potentials of the polymers (in terms of E_{pa}) and, in the case of poly(3-thiopheneacetic acid), the action of the β-substituent. It was also evident that when large substituents were present on the thiophene ring, in the case of thiophene monomer (X), the polymerisation process was inhibited by steric effects. The 3-thiophenemethanol monomer could not form a conducting polymer due to the substituent's nucleophilicity.

It is evident that the high oxidation potentials associated with both thiophenes and poly(thiophenes) presents problems in their electrochemical study, making them more susceptible to nucleophilic attack than, for example, pyrroles. Most practical applications of these monomers are likely to be in aqueous solutions and the work described above illustrates how difficult it is to encourage poly(thiophenes) to exhibit simple non-destructive electrochemistry under these conditions. The aqueous electrochemistry of poly(thiophenes) with various useful substituents is not however a distant and impossible goal but can only be achieved by the very careful design of the monomers required and a complete understanding of the electrochemical problems associated with these monomers.

Chapter 5

Poly(indole) and Poly(5-carboxyindole)

5.1 Introduction

The poly(indoles)[27,119,120,121,144,145] remain a very infrequently studied class of heterocyclic conducting polymer, largely because they suffer from the general inability to form stable and reproducible high quality conducting polymer films. The growth and properties, in acetonitrile solutions, of an electrochemically reproducible and stable poly(indole) film are reported in this chapter. The particular conditions for the electrochemical growth of poly(5-carboxyindole) in acetonitrile solutions have previously been reported[121] (appendix 2) but the unusual growth system is studied further in order to obtain a fuller electrochemical characterisation. Upon introduction to buffered aqueous solutions poly(5-carboxyindole) displays marked variation in its electrochemistry at different pH values[121] (appendix 2) which is discussed and characterised. In addition an in-depth study of the properties of electrochemically stable films of poly(5-carboxyindole) in buffered aqueous solutions is reported using the techniques of reflectance FTIR spectroscopy, UV/vis spectroscopy and impedance spectroscopy. The results reported in this chapter represent a significant advance in the understanding of the poly(indole) type conducting polymer system and open up the possibilities for further investigations into this interesting class of polymer.

5.2 Electrochemical Growth of Poly(indole) and Poly(5-carboxyindole)

The growth and electrochemistry of poly(indole) has previously been described in a number of reports[27,119,120,121,144,145] but has always failed to display stable electrochemistry and the films were found to be of very low quality resulting in easy detachment from electrodes.[145] It was found

that in order to obtain high quality films of poly(indole) the purity of the indole in the acetonitrile growth solution had to be exceptionally high. To obtain the required high purity indole needs to be sublimed under reduced pressure and then stored under nitrogen in the absence of light at below 0 °C. Indole which is not treated in this way discolours very easily and produces polymers upon electrochemical polymerisation with inferior properties in terms of quality of film, electrochemical stability and electrochemical reproducibility. The impurities are most likely to be in the form of N-N coupled dimers which are formed quite easily under mild conditions.[129]

Films of poly(indole) were grown from solutions of purified indole (5 mmol dm^{-3}) in acetonitrile solutions of TEAT (0.1 mol dm^{-3}) by potentiometrically stepping from 0 V to 1.4 V (vs. SCE) at a polished stationary platinum disc electrode (A = 0.385 cm^2) for between 10 s and 60 s. The transient shown in figure 5.1 is similar to the diffusion limited $i - t^{-1/2}$ transients observed by Pletcher *et al.*[35] but without any observable nucleation process. Films grown for longer than 60 s proved to be unstable electrochemically and peeled easily off the electrodes, however films grown for under 60 s were of very good quality and adhered strongly to the electrode. All the poly(indole) films described in this chapter were grown in this manner.

Figure 5.2 shows the cyclic voltammetry of a poly(indole) film grown for 60 s, between -0.3 V and 1.1 V (vs. SCE) at various sweep rates in an acetonitrile solution containing TEAT (0.1 mol dm^{-3}). The cyclic voltammetry is very stable but losses in Q_{CV} are recorded if the upper potential sweep limit is raised to potentials of above 1.0 V (vs. SCE). The plot of i_{pa} vs. sweep rate (υ), figure 5.3, is linear (r = 0.999, n = 9), consistent with an immobilised redox species. The limiting E_{pa} and E_{pc} values from figure 5.4 are calculated to be $E_{pa} \simeq 0.90$ V (vs. SCE) (r = 0.982, n = 9) and the $E_{pc} \simeq 0.66$ V (vs. SCE)

Figure 5.1 The growth of poly(indole) by potential stepping from 0.0 V to 1.4 V (vs. SCE) in a solution of indole (XII) (5 mmol dm^{-3}) in acetonitrile containing TEAT (0.1 mol dm^{-3}) at a platinum electrode (A = 0.385 cm^2)

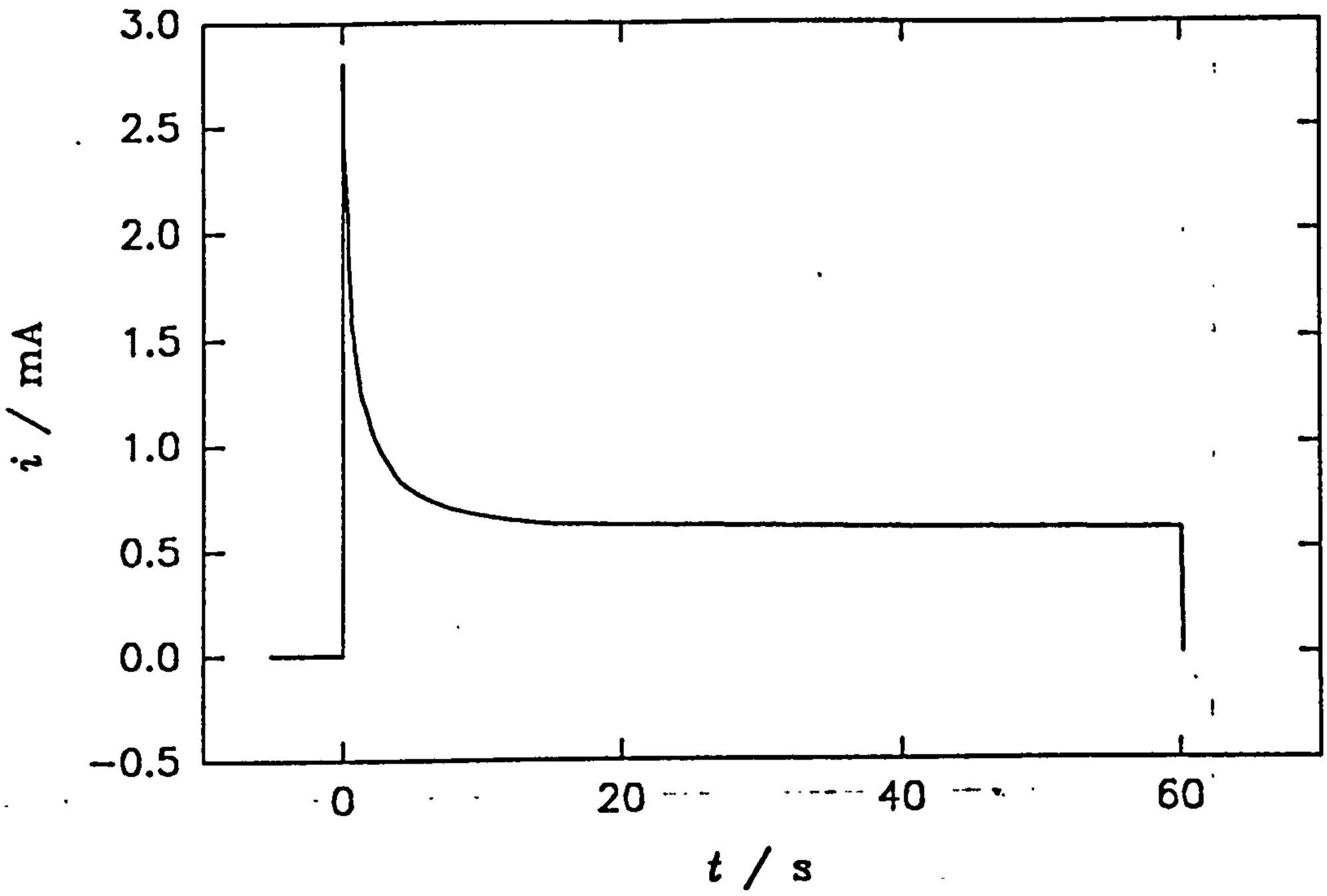

Figure 5.2 The cyclic voltammetry between -0.3 V and 1.1 V (vs. SCE) of a poly(indole) film (grown for t = 60 s) in acetonitrile containing TEAT (0.1 mol dm^{-3}) at sweep rates of υ = 20, 30, 40, 50, 60, 70, 80, 90 and 100 mV s^{-1}

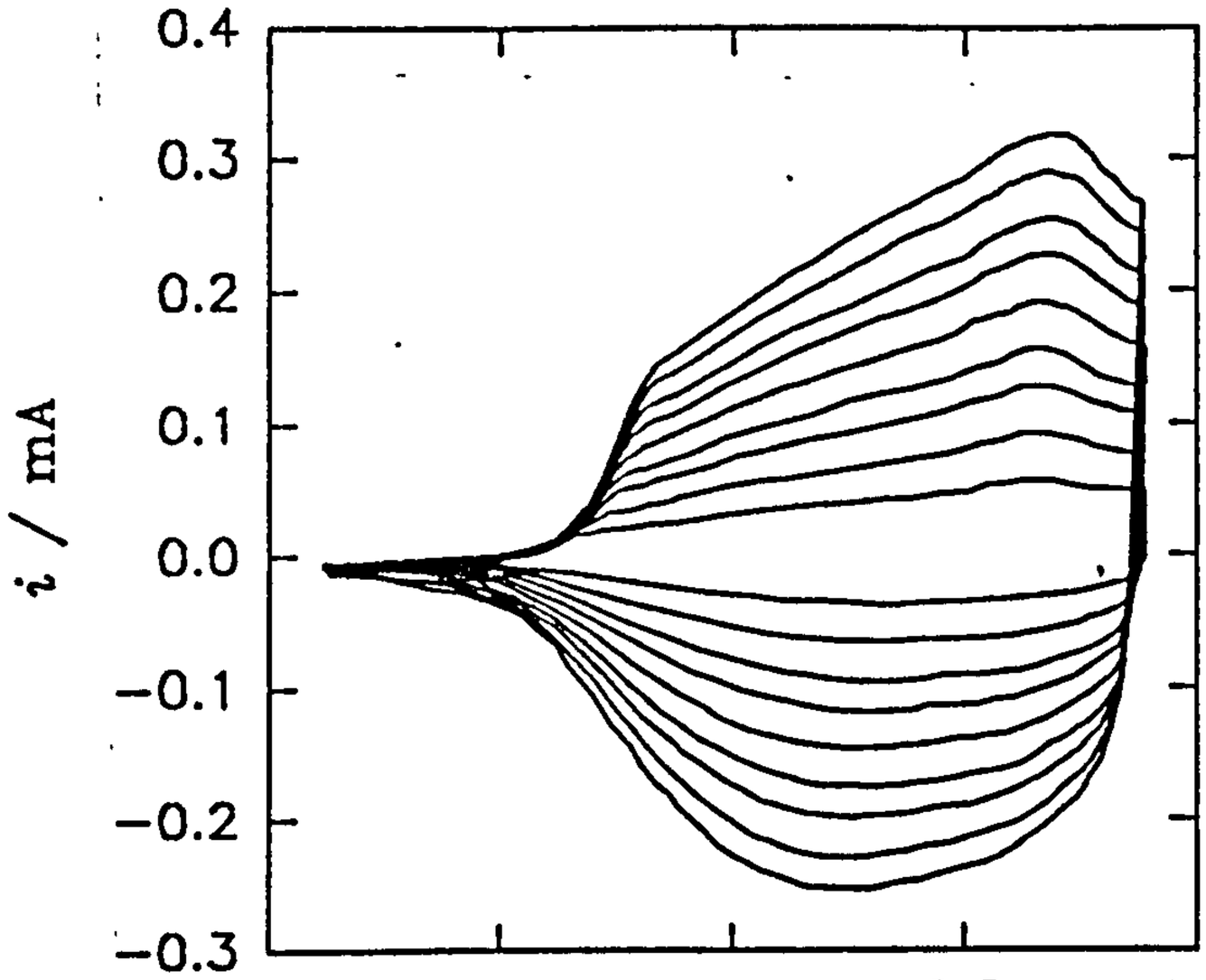

Figure 5.3 The i_{pa} vs. sweep rate (υ) plotted from the data presented in figure 5.2 (r = 0.999, n = 9)

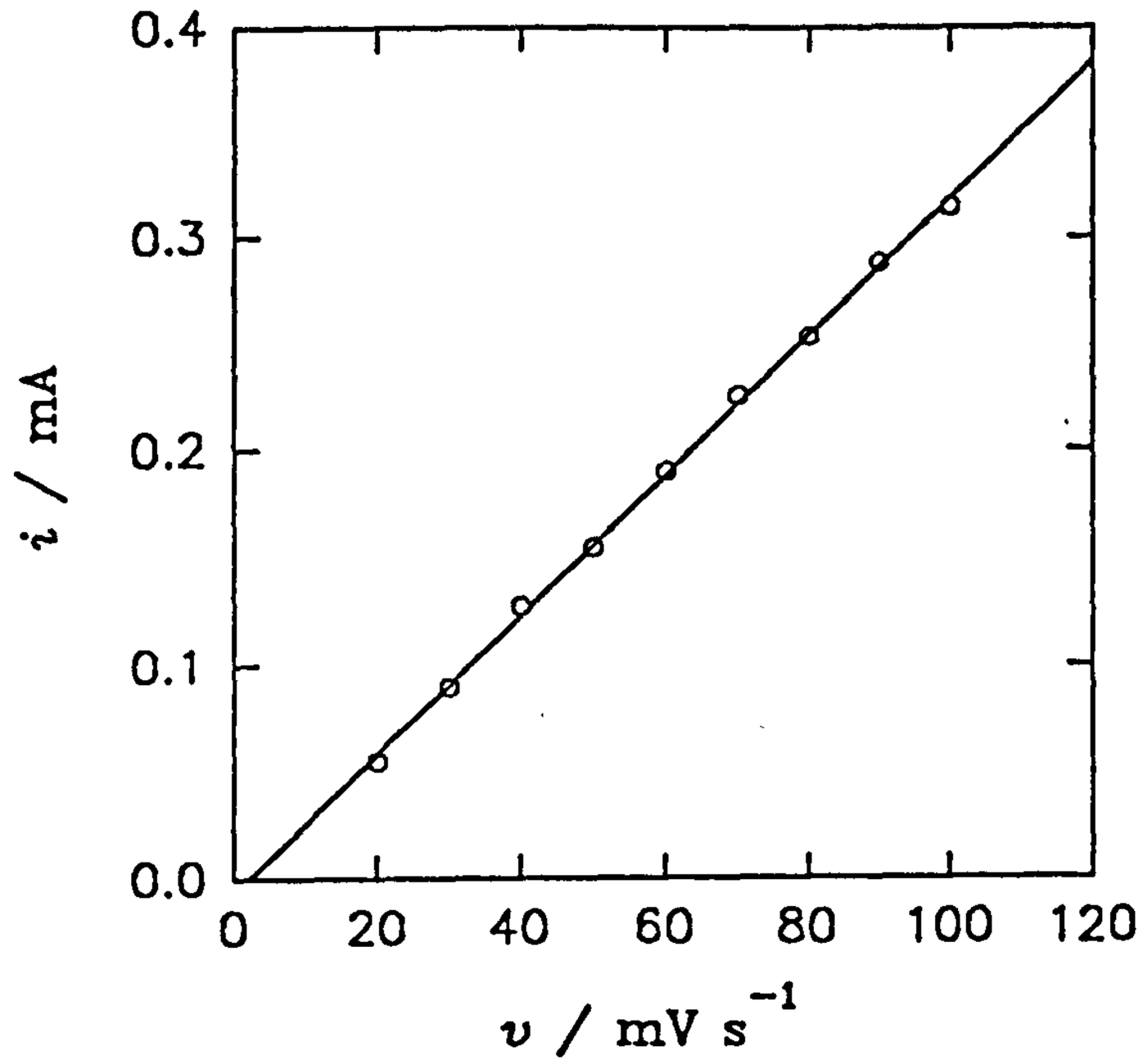

Figure 5.4 The E_{pa} (○) and E_{pc} (●) vs. sweep rate (υ) plotted from the data presented in figure 5.2 (○, r = 0.982, n = 9) (●, r = 0.977, n = 9)

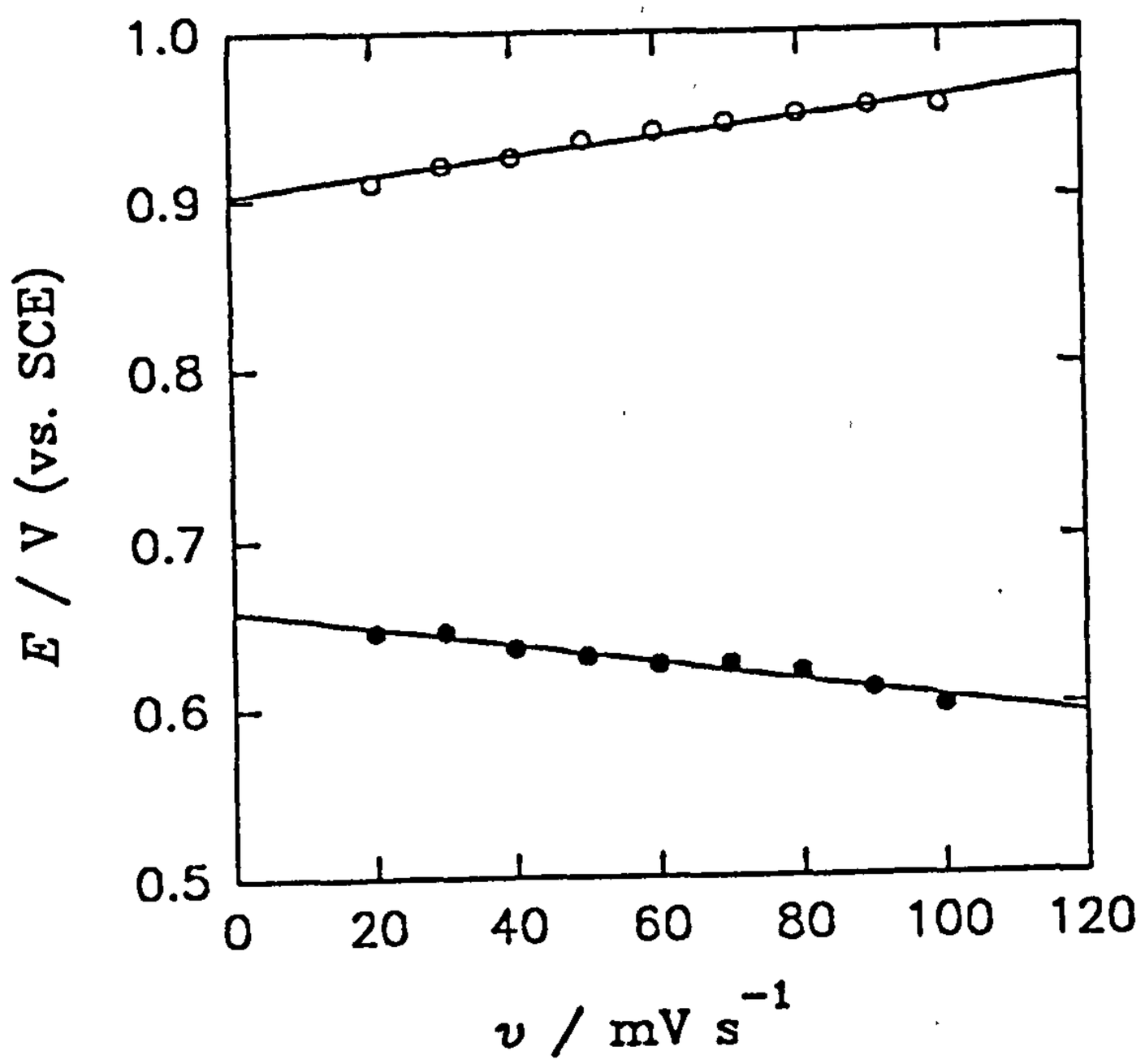

($r = 0.977$, $n = 9$). The dopancy was estimated to be $\delta \simeq 0.2$ which is consistent with previously reported values.[145]

The growth of poly(5-carboxyindole) films has previously been described[121] (appendix 2) but a summary of the standard growth method is given below. This growth method is utilised for all the poly(5-carboxyindole) films described in this chapter unless otherwise stated.

Films of poly(5-carboxyindole) were grown from solutions of 5-carboxyindole (5 mmol dm^{-3}) in acetonitrile containing TEAT (0.1 mol dm^{-3}) by potentiometrically stepping from 0.0 V to 1.4 V (vs. SCE) at a polished rotating ($W = 4$ Hz) platinum disc electrode ($A = 0.385$ cm^2). A linear i - t transient is observed after 20 s, figure 5.5, similar to the electron transfer limiting process proposed by Hillman *et al.*[38] However, this occurs at a rotating disc electrode suggesting in fact that the process is actually diffusion limited. The deposition rate of 3.08 mA cm^{-2} is calculated from equation 3.1 using Q_T data from growth transients of 15, 30, 45 and 60 s, figure 5.6. The calculation of the value of the dopancy (δ) will be discussed in the aqueous electrochemistry section **5.4** due to the film's increased electrochemical stability in aqueous solutions, but is quoted here as $\delta = 0.49$ to facilitate further discussion of the electrochemical growth in this section.

Rotating disc electrode (RDE) and rotating ring disc electrode (RRDE) studies have only been performed during the polymerisation of common polymers in a limited number of cases. It has been found that when rotating the electrode during electrochemical polymerisation of standard conducting polymers, for example pyrrole and thiophene, growth becomes inhibited presumably due to enhanced mass transport of oligomers from the electrode.[146]

Figure 5.5 The growth of poly(5-carboxyindole) by potential stepping from 0.0 V to 1.4 V (vs. SCE) in a solution of 5-carboxyindole (XIII) (5 mmol dm^{-3}) in acetonitrile containing TEAT (0.1 mol dm^{-3}) at a rotating (W = 4 Hz) platinum electrode (A = 0.385 cm^2)

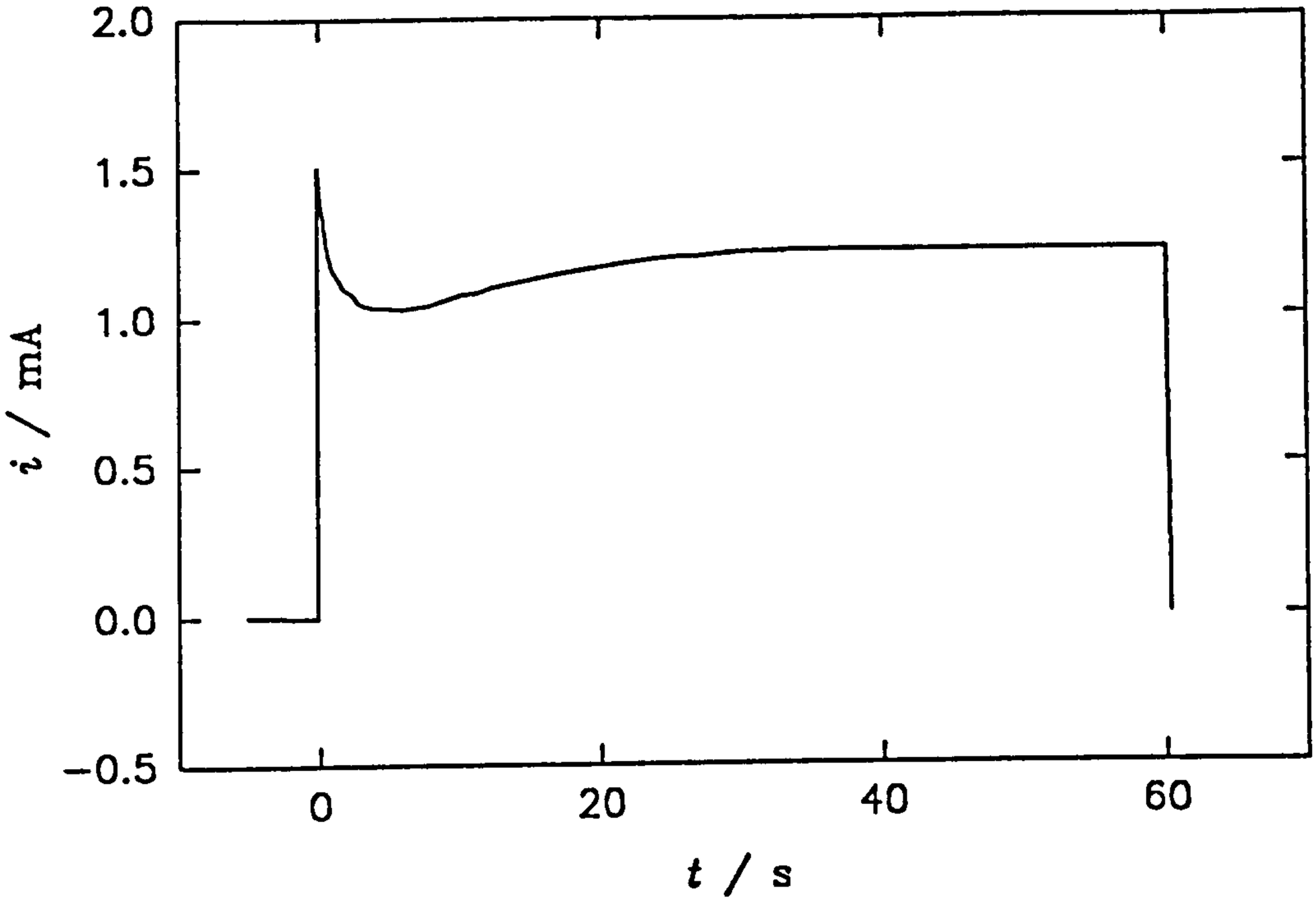

Figure 5.6 The Q_T vs. t plot for poly(5-carboxyindole) growth transients of t = 15, 30, 45 and 60 s

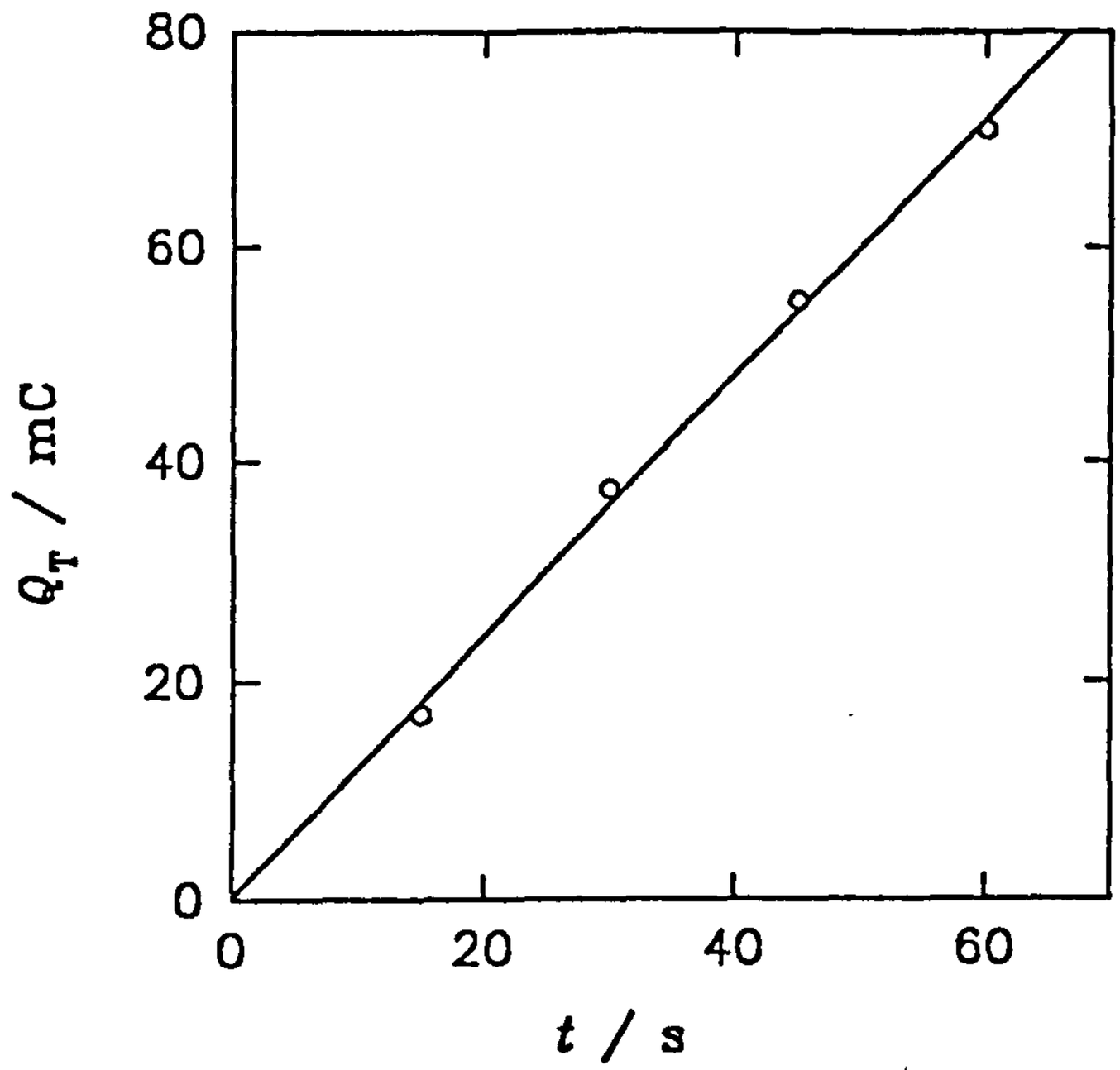

Poly(5-carboxyindole) requires electrode rotation to sustain growth[121] (appendix 2) and is hence an excellent polymer to study by these techniques.

The potential dependence of the growth of poly(5-carboxyindole) was studied at a polished platinum rotating disc electrode (A = 0.385 cm^2) at 4 Hz by potentiometrically stepping from 0.0 V (vs. SCE) to various potentials between 1.0 V and 1.6 V (vs. SCE) in a solution of 5-carboxyindole (5 mmol dm^{-3}) in acetonitrile containing TEAT (0.1 mol dm^{-3}) and measuring the current density after 60 s, figures 5.7 and 5.8. The increase in current density observed between 1.0 V and 1.4 V (vs. SCE) with potential can be interpreted in terms of a sigmoidal increase which begins to plateau at 1.3 V (vs. SCE) followed by a similar reduction in current when the potential is increased to values greater than 1.4 V (vs. SCE). The decrease in current density at higher potentials may be due to increased passivation and/or side reactions or an increase in the resistivity of the film (section 5.8).

The rotation speed dependencies of the growth of poly(5-carboxyindole) were studied by potentiometrically stepping solutions of 5-carboxyindole of varying concentrations from 0.0 V (vs. SCE) to 1.125 V and 1.4 V (vs. SCE) at a polished rotating platinum disc electrode (A = 0.385 cm^2). Three solutions of 5-carboxyindole (5 mmol dm^{-3}, 7 mmol dm^{-3} and 10 mmol dm^{-3}) in acetonitrile containing TEAT (0.1 mol dm^{-3}) were studied. Figure 5.9 shows the transients observed for the potentiometric steps to 1.4 V (vs. SCE) in the solution of 5-carboxyindole (5 mmol dm^{-3}) at different rotation speeds.

Curved Levich[107,122] plots are obtained for each of the three concentrations studied when the current (i), after 60 s, is plotted against the square root of the rotation speed ($W^{1/2}$) using the data recorded at the

Figure 5.7 The potential dependence of the growth of poly(5-carboxyindole) shown for transients of t = 60 s at growth potentials of 1.0, 1.1, 1.4, 1.5 and 1.6 V (vs. SCE) (all the other growth conditions are summarised in figure 5.5)

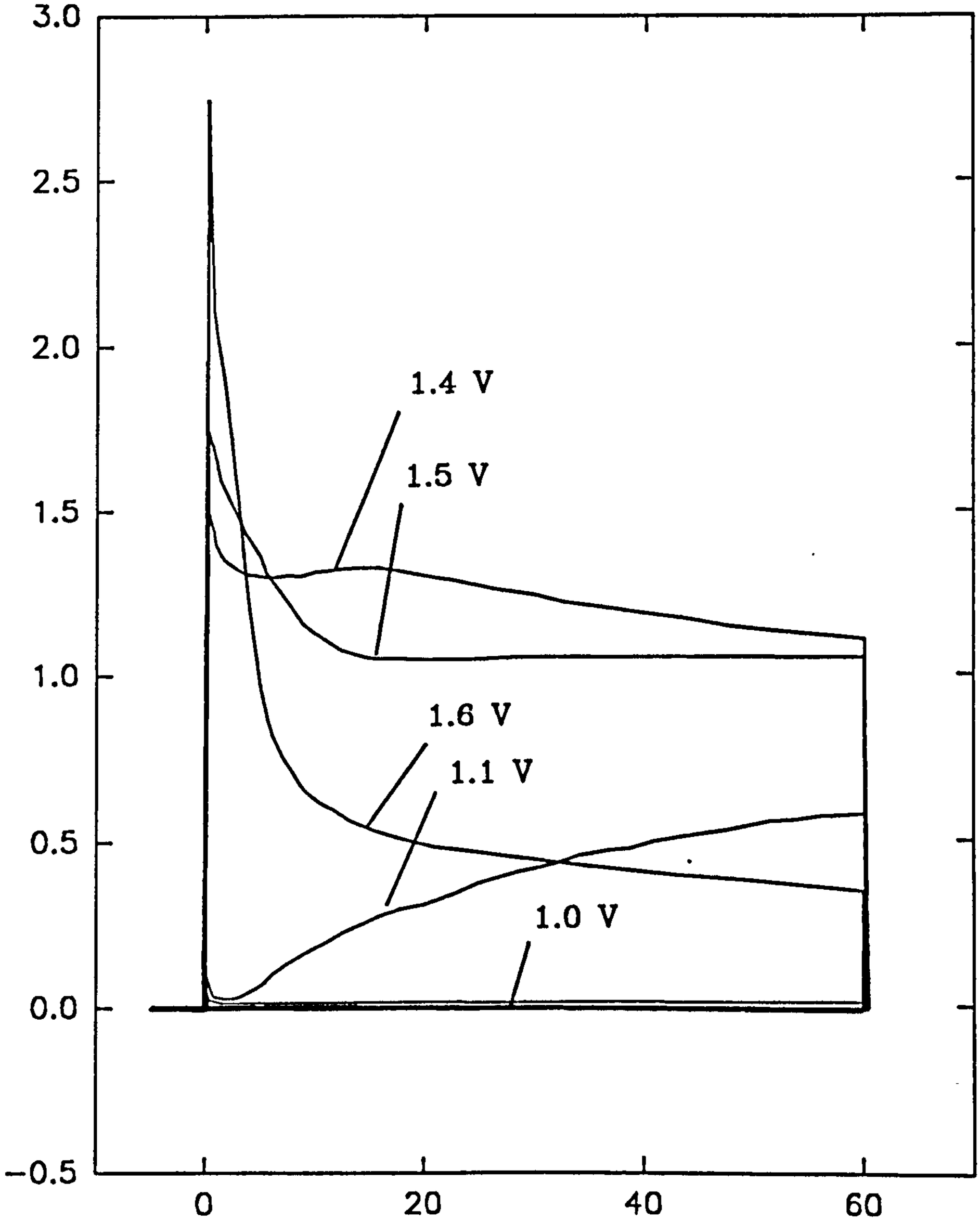

Figure 5.8 The overall data set for the potential dependence of the growth of poly(5-carboxyindole) with $i_{(t = 60\ s)}$ plotted against potential (vs. SCE)

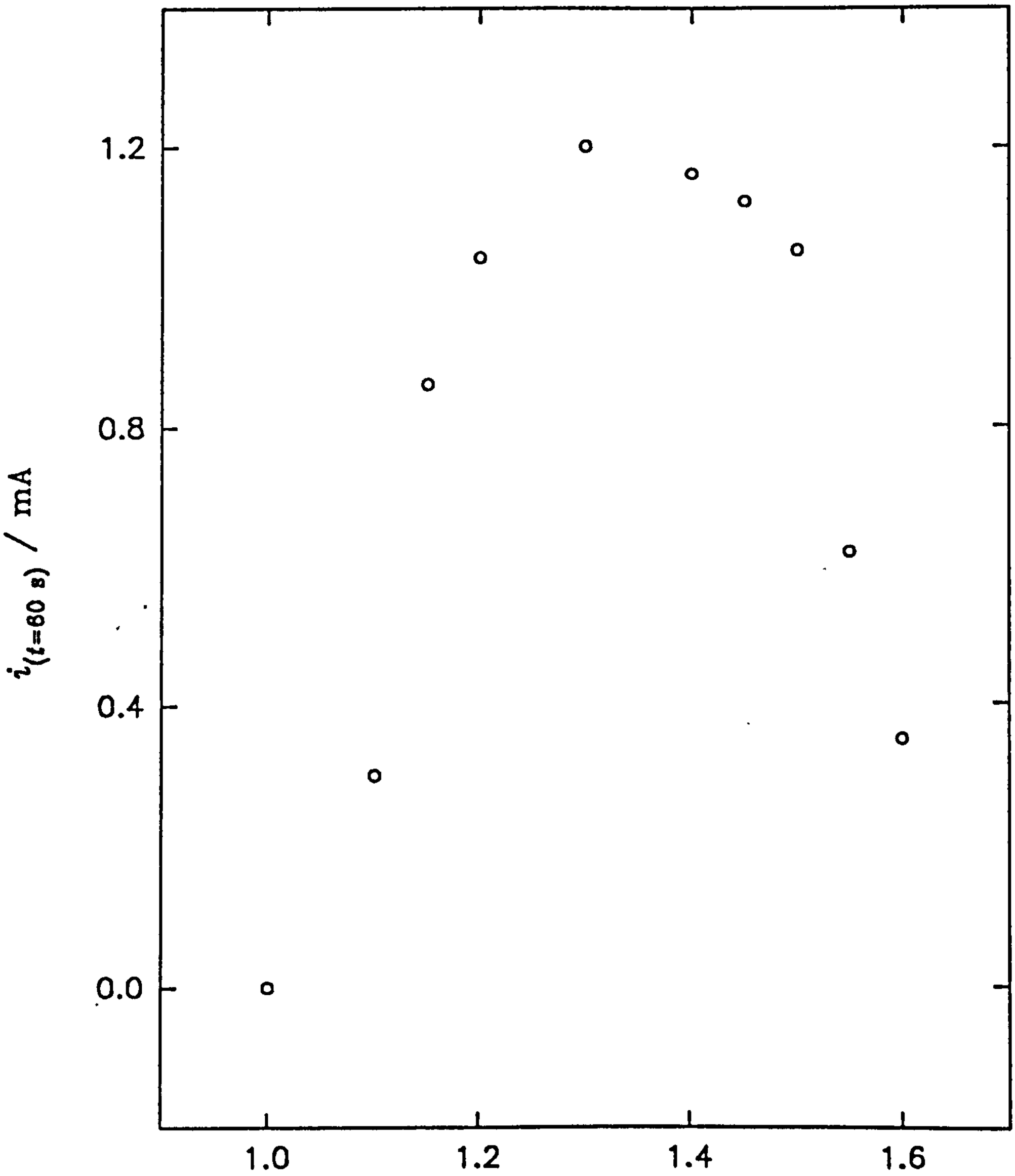

Figure 5.9 The growth of poly(5-carboxyindole) by potential stepping from 0.0 V to 1.4 V (vs. SCE) for t = 60 s in a solution of 5-carboxyindole (XIII) (5 mmol dm^{-3}) in acetonitrile containing TEAT (0.1 mol dm^{-3}) at a rotating platinum electrode (A = 0.385 cm^2) where W = 1, 4, 9, 16 and 25 Hz

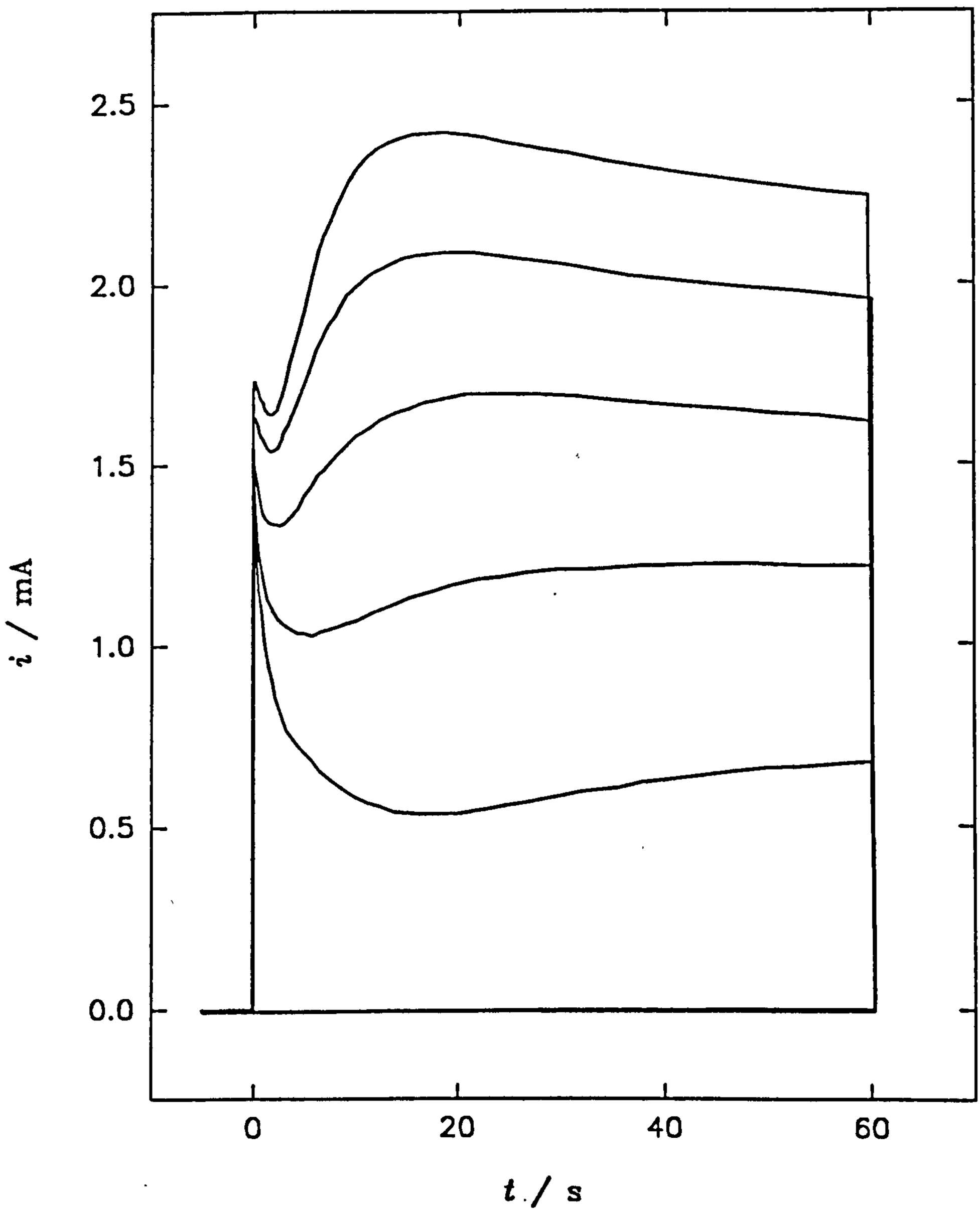

Figure 5.10 The Levich[107,122] plots of $i_{(t\ =\ 60\ s)}$ vs. $W^{1/2}$ for the growth of poly(5-carboxyindole) by potentiometricallyy stepping from 0.0 V to 1.125 V (vs. SCE) at a rotating platinum electrode (A = 0.385 cm^2, W = 1, 4, 9, 16 and 25 Hz) in a solution of 5-carboxyindole (5 mmol dm^{-3}) in acetonitrile containing TEAT (0.1 mol dm^{-3})

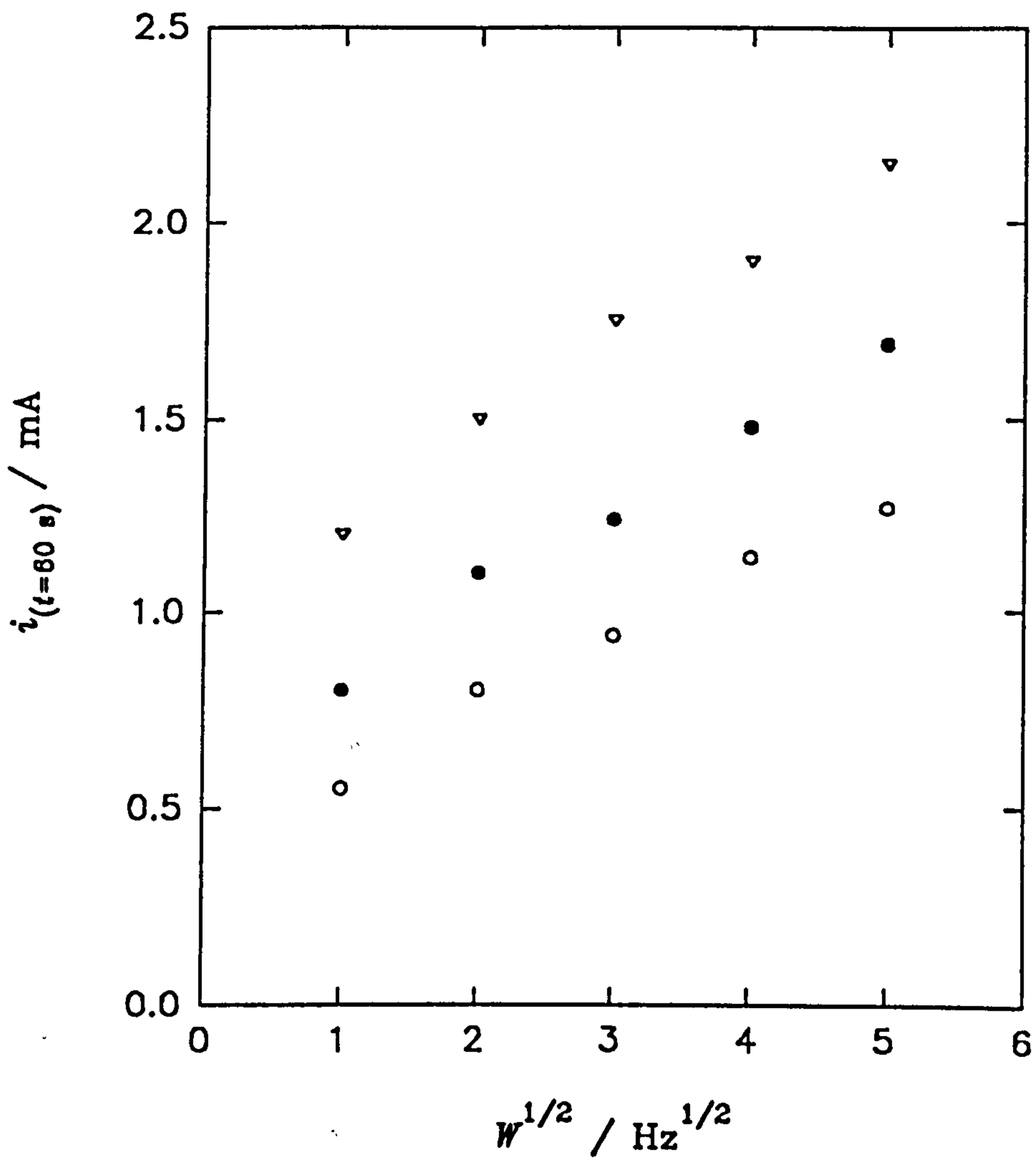

Figure 5.11 The Levich[107,122] plots of $i_{(t\ =\ 60\ s)}$ vs. $W^{1/2}$ for the growth of poly(5-carboxyindole) by potentioimetrically stepping from 0.0 V to 1.4 V (vs. SCE) at a rotating platinum electrode (A = 0.385 cm^2, W = 1, 4, 9, 16 and 25 Hz) in a solution of 5-carboxyindole (5 mmol dm^{-3}) in acetonitrile containing TEAT (0.1 mol dm^{-3})

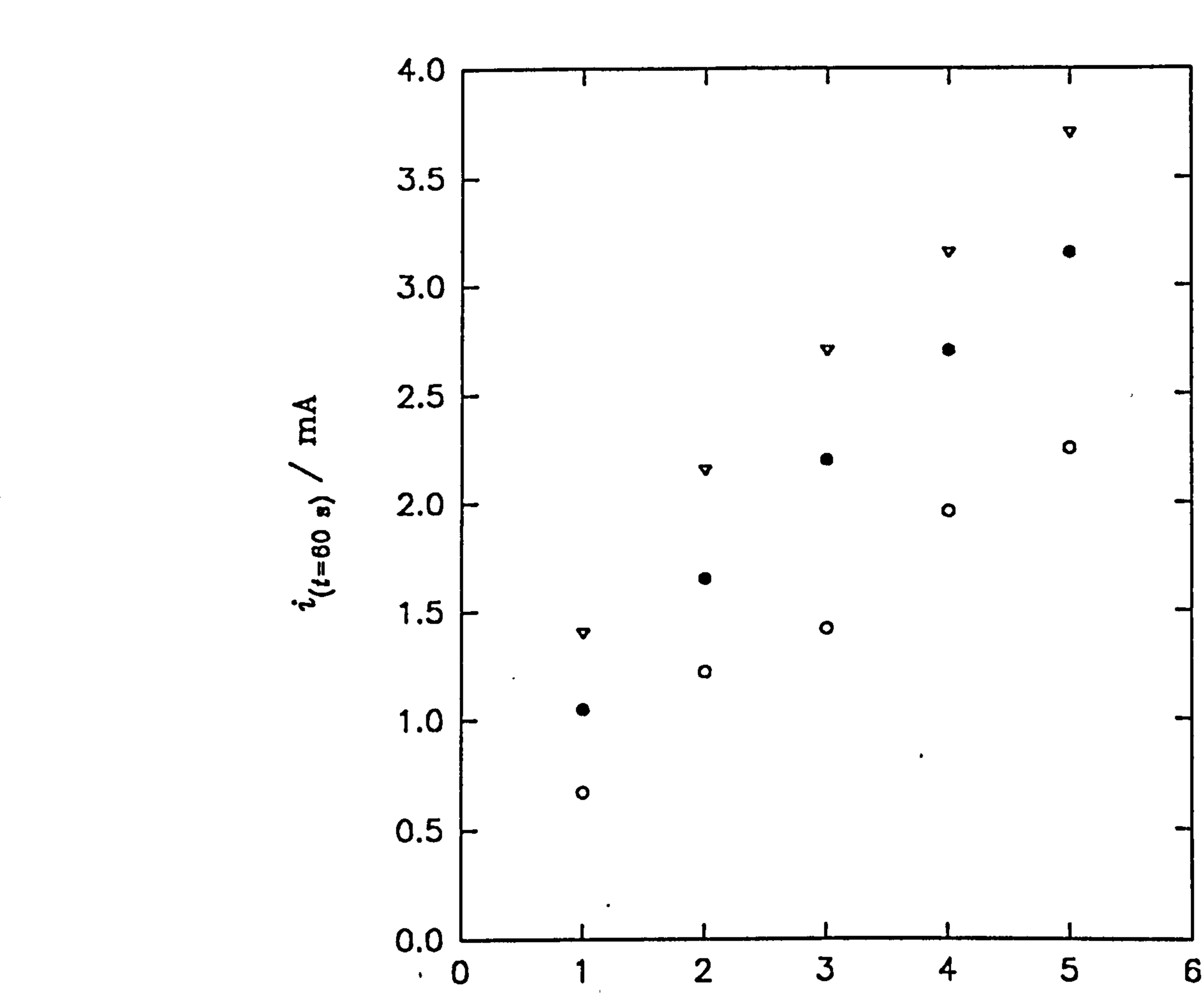

two potentials studied, figure 5.10 and 5.11.

When the data for the different concentrations is converted into Koutecky-Levich[107,122] plots by plotting $(i)^{-1}$ against $(W)^{-1/2}$, figures 5.12 and 5.13, curved plots are again observed that appear to converge to the same intercept on the y axis suggesting that the polymerisation reaction is zero order with respect to the concentration of poly(5-carboxyindole) at infinite rotation speed. The position of the intercept does however depend upon the potential. This agrees with the results taken solely at 4 Hz, figure 5.8. The currents observed for the transients are compared to those predicted from the Levich equation,[107,122] this is assuming a diffusion coefficient for 5-carboxyindole in acetonitrile of $D_o = 5.0 \times 10^{-6}$ cm^2 s^{-1} and a viscosity of acetonitrile $\nu = 3.45 \times 10^{-3}$ g cm^{-1} s^{-1}, the density being d = 0.786 g cm^{-3}. This predicts a current of i_{cal} = 1.0 mA at W = 4 Hz from the Levich equation[107,122] assuming that two electrons are required per monomer unit for polymerisation and that the dopancy δ = 0.49 so that the estimated value for n = 2.49. The actual current observed is i_{obs} = 1.1 mA which is in excellent agreement with i_{cal} and suggests a diffusion limited process at 4 Hz.

Limited studies using a rotating ring disc electrode (RRDE) have also been performed to study the growth of conducting polymers[147,148] by detecting protons formed during electrochemical polymerisation. Ring disc experiments were performed at a polished platinum rotating ring disc electrode (RRDE, r_1 = 0.201 cm, r_2 = 0.210 and r_3 = 0.227 cm) in a degassed solution of 5-carboxyindole (5 mmol dm^{-3}) in acetonitrile containing TEAT (0.1 mol dm^{-3}) by potentiometrically stepping the disc from 0.0 V to 1.4 V (vs. SCE) initially at 4 Hz.

Figure 5.12 The Koutecky-Levich[107,122] plots of $i_{(t\ =\ 60\ s)}^{-1}$ vs. $W^{-1/2}$ for the growth of poly(5-carboxyindole) by potentiometricallyy stepping from 0.0 V to 1.125 V (vs. SCE) at a rotating platinum electrode (A = 0.385 cm^2, W = 1, 4, 9, 16 and 25 Hz) in a solution of 5-carboxyindole (XIII) (5 mmol dm^{-3}) in acetonitrile containing TEAT (0.1 mol dm^{-3})

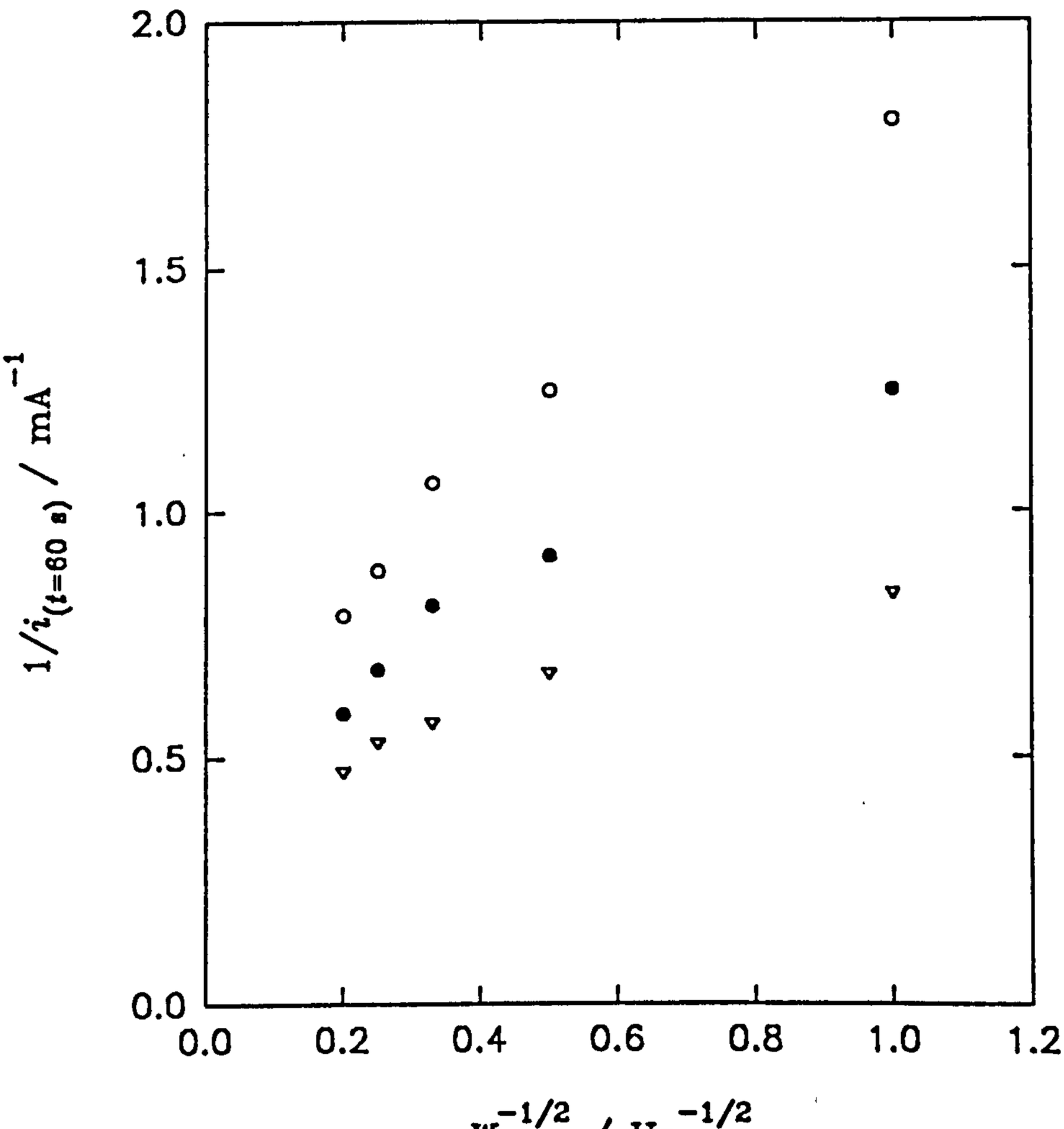

Figure 5.13 The Koutecky-Levich[107,122] plots of $i_{(t\,=\,60\ s)}^{-1}$ vs. $W^{1/2}$ for the growth of poly(5-carboxyindole) by potentiometrically stepping from 0.0 V to 1.4 V (vs. SCE) at a rotating platinum electrode (A = 0.385 cm^2, W = 1, 4, 9, 16 and 25 Hz) in a solution of 5-carboxyindole (XIII) (5 mmol dm^{-3}) in acetonitrile containing TEAT (0.1 mol dm^{-3})

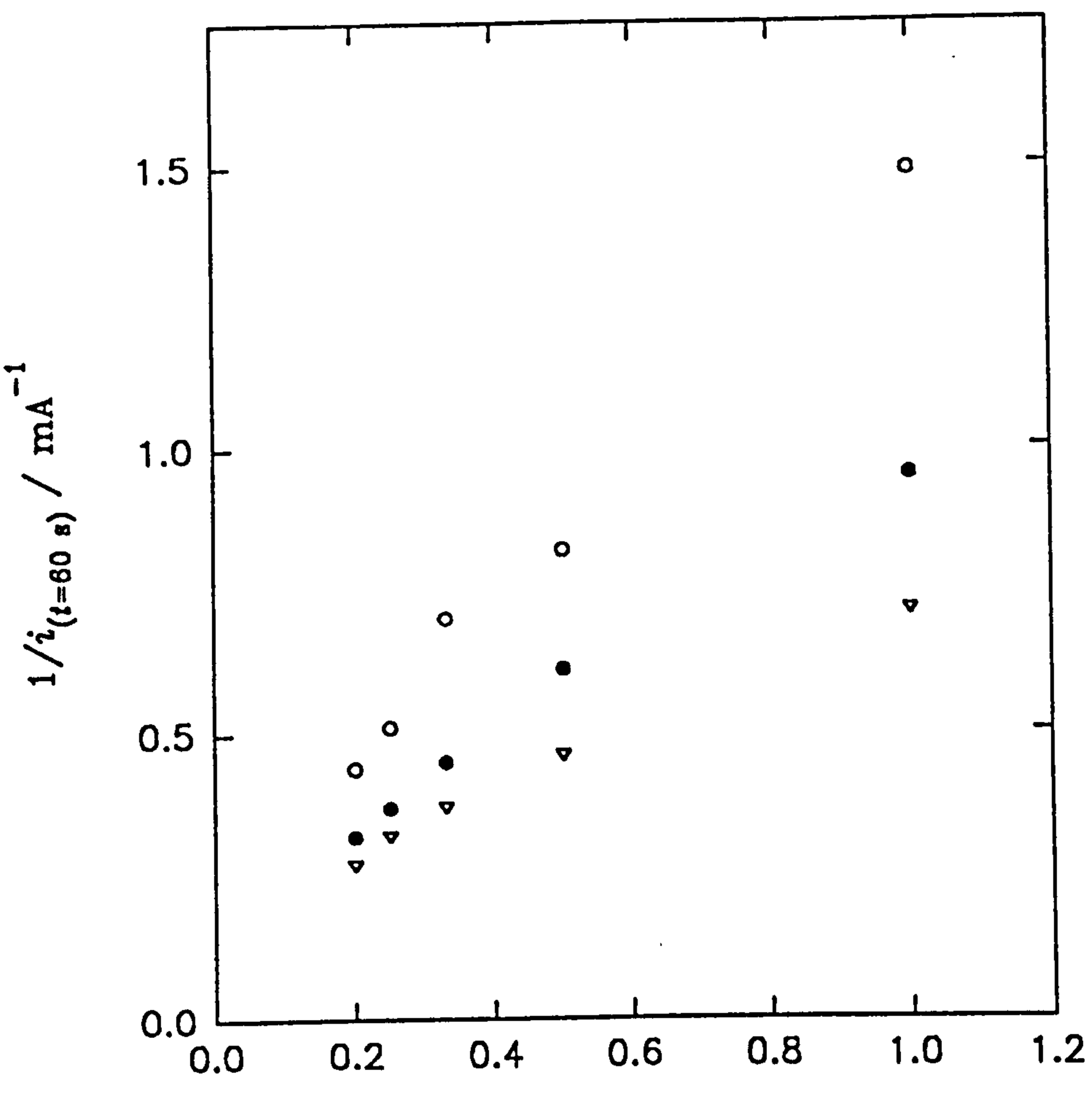

The ring was held at potentials between -1.0 V and 1.0 V (vs. SCE) but the only species detected were protons. This suggests that the electrochemical polymerisation was very efficient since no soluble oligomers were detected.

For a very efficient electrochemical polymerisation at a disc potential of 1.4 V (vs. SCE) and a dopancy of δ = 0.49, the amount of charge consumed during the polymerisation other than the dopancy charge is estimated to be 80 % of the total charge passed. This estimate is based upon the assumption that the polymer chains are sufficiently long so that the end groups are negligible and that there are no other non-faradaic processes occurring. At a ring potential of -0.8 V (vs. SCE) the current observed due to the protons formed during polymerisation is found to plateau so readings were taken at this point, this is in agreement with previously reported data.[147] For a potentiometric step at the disc electrode of 1.4 V (vs. SCE) the corrected ring current ($-i_R/N_o$) at -0.8 V (vs. SCE) for a rotation speed of 4 Hz, figure 5.14, was found to be consistently 40 % of the total transient current. This was also found to be true at higher rotation rates (W) and is exactly half of the value expected. The reproducibility of the results and the fact that ($-i_R/N_o$) does not decay at a faster rate than i_D eliminates fouling of the ring electrode as being responsible for the observed results.

There could be a number of explanations for this. The polymer could in fact be essentially dimeric which would predict a ($-i_R/N_o$) of 40 % of (i_D). However, this is unlikely for two reasons. Firstly, such dimers would be soluble in certain organic solvents whereas in fact the films are largely insoluble in all organic solvents.[121] Secondly, there is strong reflectance FTIR evidence (section 5.3) that a polymer bonded at the 1 and 3 positions of the 5-carboxyindole monomer is in fact the product of the electrochemical polymerisation. Alternatively 50 % of the protons, *i.e.* one per monomer unit polymerised, may be adsorbed in the growing

Figure 5.14 The i_D and i_R/N_0 recorded during the polymerisation of poly(5-carboxyindole) at the disc of a platinum ring disc electrode (r_1 = 0.201 cm, r_2 = 0.210 cm and r_3 = 0.227 cm) by potentiometrically stepping from 0.0 V to 1.4 V (vs. SCE) in a solution of 5-carboxyindole (XIII) (5 mmol dm^{-3}) in acetonitrile containing TEAT (0.1 mol dm^{-3}) W = 4 Hz

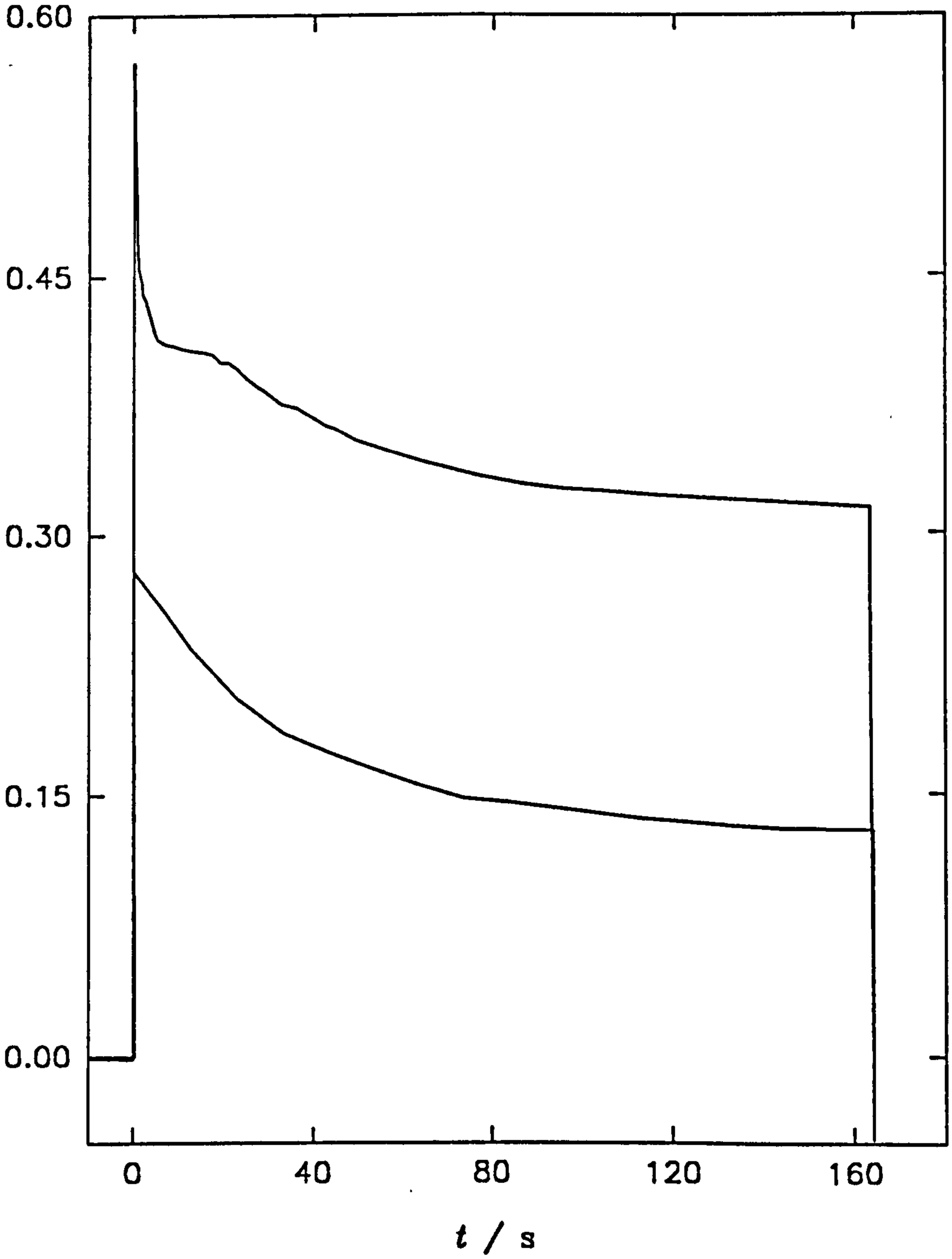

Figure 5.15 Graphical representation of the absorption of 50 % of the protons formed during polymerisation

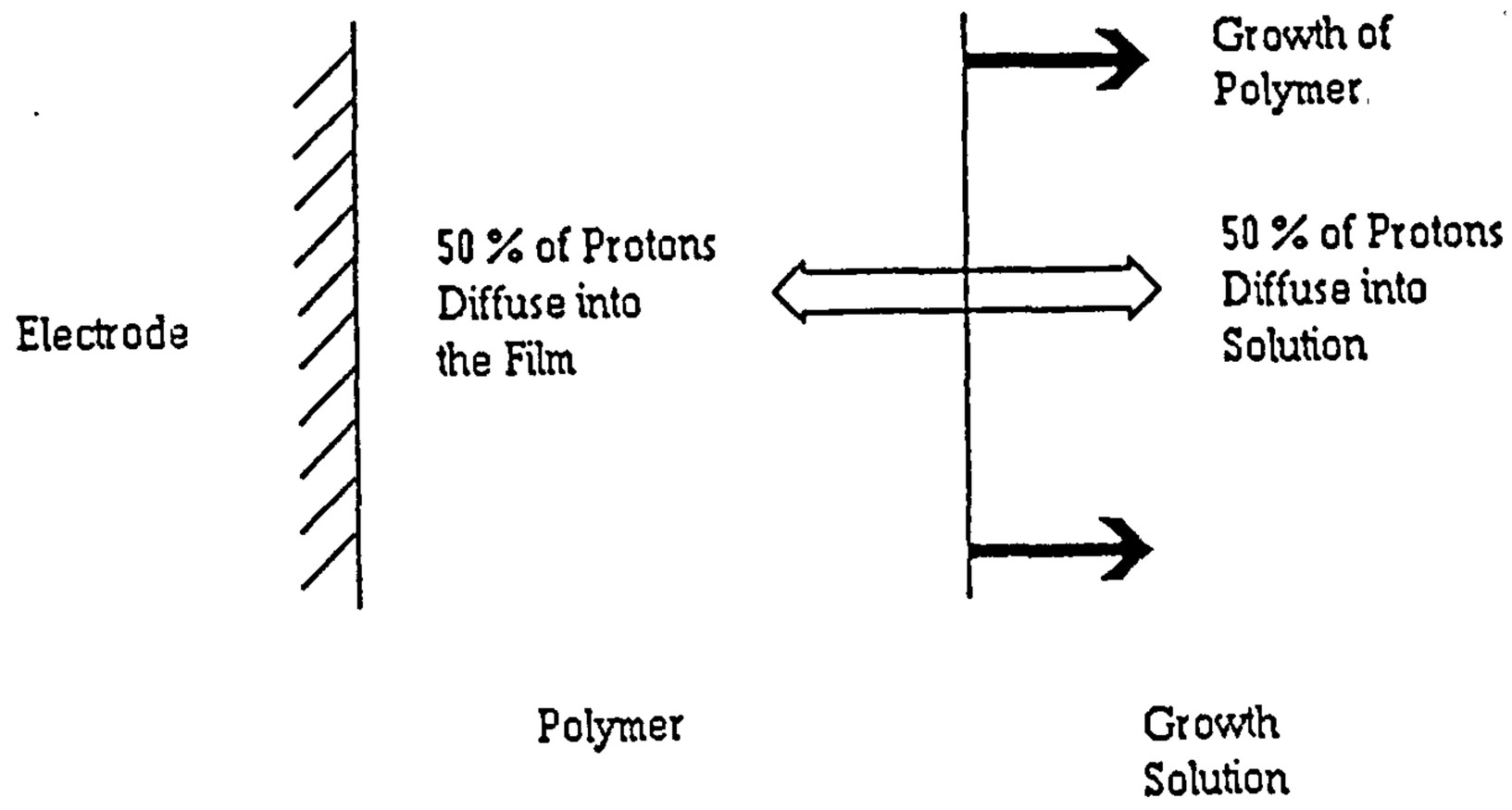

polymer film, figure 5.15, which is a larger value than other reported adsorptions.[148] But this would not be surprising considering the chemical nature of the film with possible protonation sites at both the nitrogen and carboxylic acid groups. Unfortunately no adsorbed protons have been detected in the electrochemistry of the film or by detecting their counter ions by reflectance FTIR; however, this does not disprove their existence. The 40 % ($-i_R/N_o$) to (i_D) value may also be due to smaller adsorption effects coupled with shorter polymer chains, but it is most likely that the number of protons predicted from charging theory has been halved in some way.

The growth conditions for poly(5-carboxyindole) have been further investigated but it is clear that a very complicated electrochemical polymerisation process is taking place which needs further in depth study to be fully characterised. What has been established is that at low rotation rates (W) the electrochemical polymerisation is diffusion limited and that at high rotation rates the reaction is zero order with respect to the concentration of the monomer. This suggests that the polymerisation proceeds via a surface bound site which would also explain why the polymerisation appears to be extremely efficient in faradaic terms and why no oligomers are observed during the ring disc experiments. Further supporting data could be obtained by performing *in situ* FTIR spectroscopy, UV/vis spectroscopy and quartz crystal microbalance (QCM) studies during the growth of the polymer. Clearly the rotation of the electrode would present problems with some of these techniques but constant stirring of the solution can be utilised to mimic the hydrodynamic effects of rotation.

The chemical characterisation and aqueous electrochemistry of poly(5-carboxyindole) will now be discussed in detail.

5.3 Structural Characterisation of Poly(indole) and Poly(5-carboxyindole) by Reflectance FTIR

The reflectance FTIR spectra of fully reduced and fully oxidised poly(indole) films grown for 60 s, are shown in figure 5.16, and table 5.1 gives their assignments. There are however a few features that are worth discussing further. As previously reported[119,120] the N-H stretching peak at 3400 cm^{-1} is very much diminished in the polymer spectra compared to the monomer spectra suggesting that the nitrogen position is one of the polymer bonding positions. In addition a weak C-H out of plane bending is also observed at 747 cm^{-1} corresponding a 1,2-disubstituted six membered benzene[87] ring suggesting that polymer bonding does not occur at the 4, 5, 6 and 7 positions of the molecule. It is also worth noting that the spectra of the fully oxidised and fully reduced poly(indole) vary only slightly and the presence of BF_4^- is only just detected at 1060 cm^{-1}.

The reflectance FTIR spectrum of a fully reduced poly(5-carboxyindole) film grown for 30 s and held at -0.3 V (vs. SCE) in acetonitrile solution containing TEAT (0.1 mol dm^{-3}), is shown in figure 5.17 (between 400 cm^{-1} and 4000 cm^{-1}) and in more detail in figure 5.18 (between 400 cm^{-1} and 2000 cm^{-1}). No spectra were recorded for fully oxidised poly(5-carboxyindole) because of its instability in acetonitrile solutions.

The assignments for the spectra are given in table 5.2, and show that the carboxylic acid functionality remains intact after polymerisation. One major feature in the spectra, figures 5.17 and 5.18, is the presence of C-H out of plane bending at 746 cm^{-1} and 822 cm^{-1} corresponding to a 1,2,4-trisubstituted benzene.[87] This indicates that, as with poly(indole), the six membered ring remains intact after polymerisation. In addition the peak at 767 cm^{-1} corresponds to C-H out of plane bending in the five

Figure 5.16 The reflectance FT-IR spectrum of a fully reduced poly(indole) film previously held at -0.3 V (vs. SCE) and fully oxidised poly(indole) film previously held at 1.1 V (vs. SCE) in acetonitrile solution containing TEAT (0.1 mol dm^{-3})

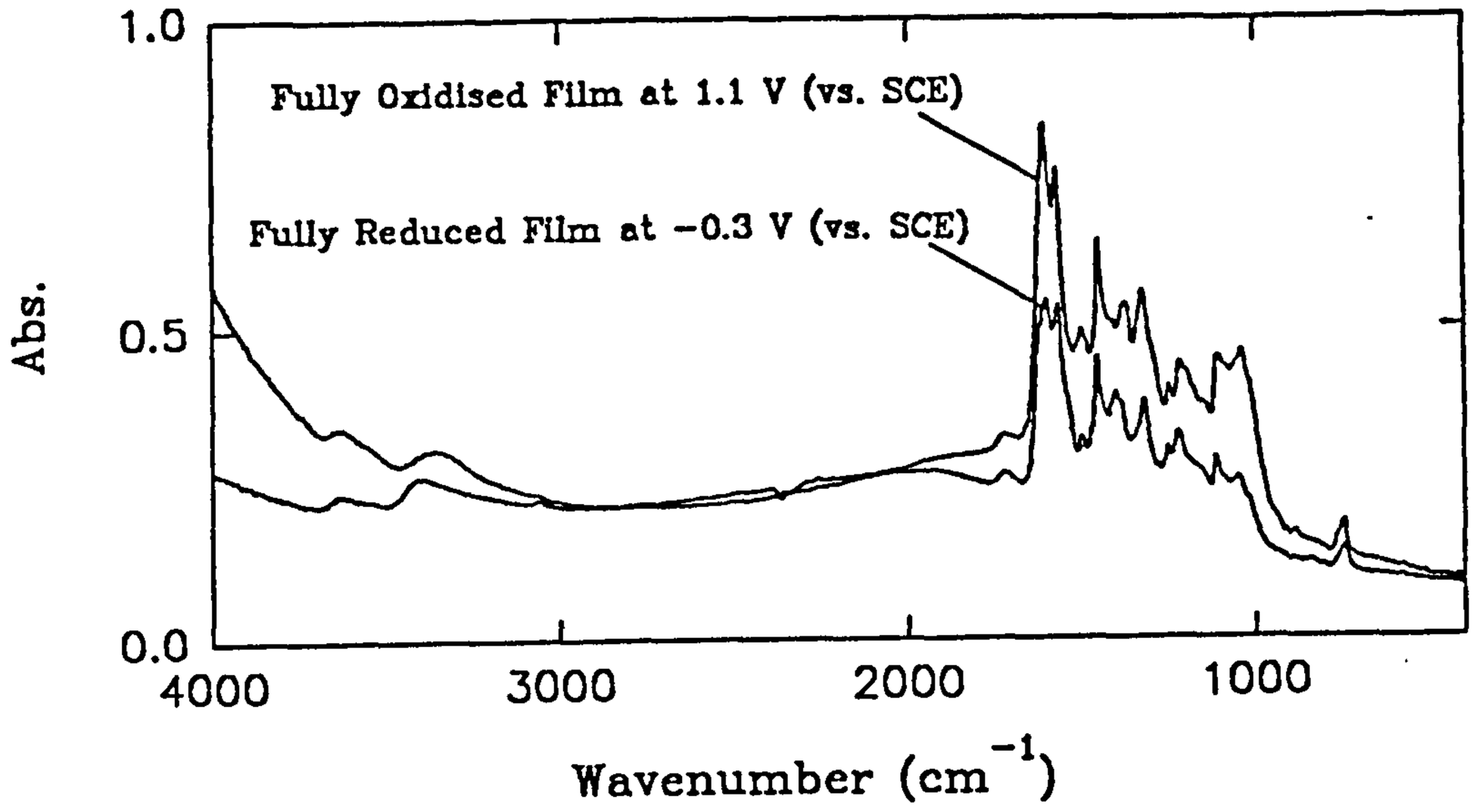

Table 5.1 The assignments for the reflectance FT-IR spectrum of poly(indole) shown in figure 5.16

Wavenumber (cm^{-1}) $\pm$ 4 cm^{-1}	Assignment
1500-1650(vs)	C-C aromatic ring stretches typical of indoles
1465(s)	C-N aromatic ring stretch (?)
747(vw)	C-H o. p. bend of six membered indole ring

Figure 5.17 The reflectance FT-IR spectrum of fully reduced poly(5-carboxyindole) between 400 and 4000 cm^{-1}

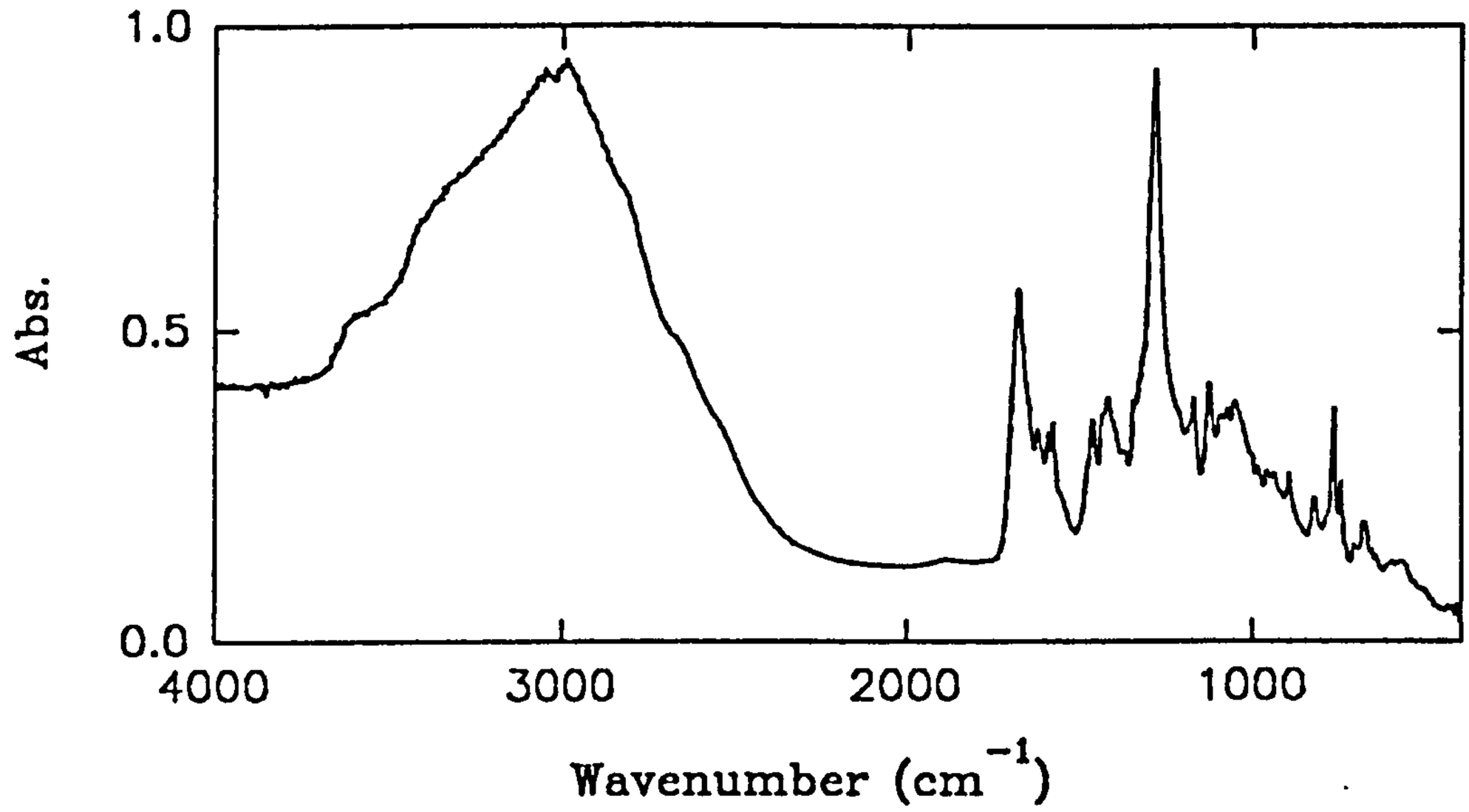

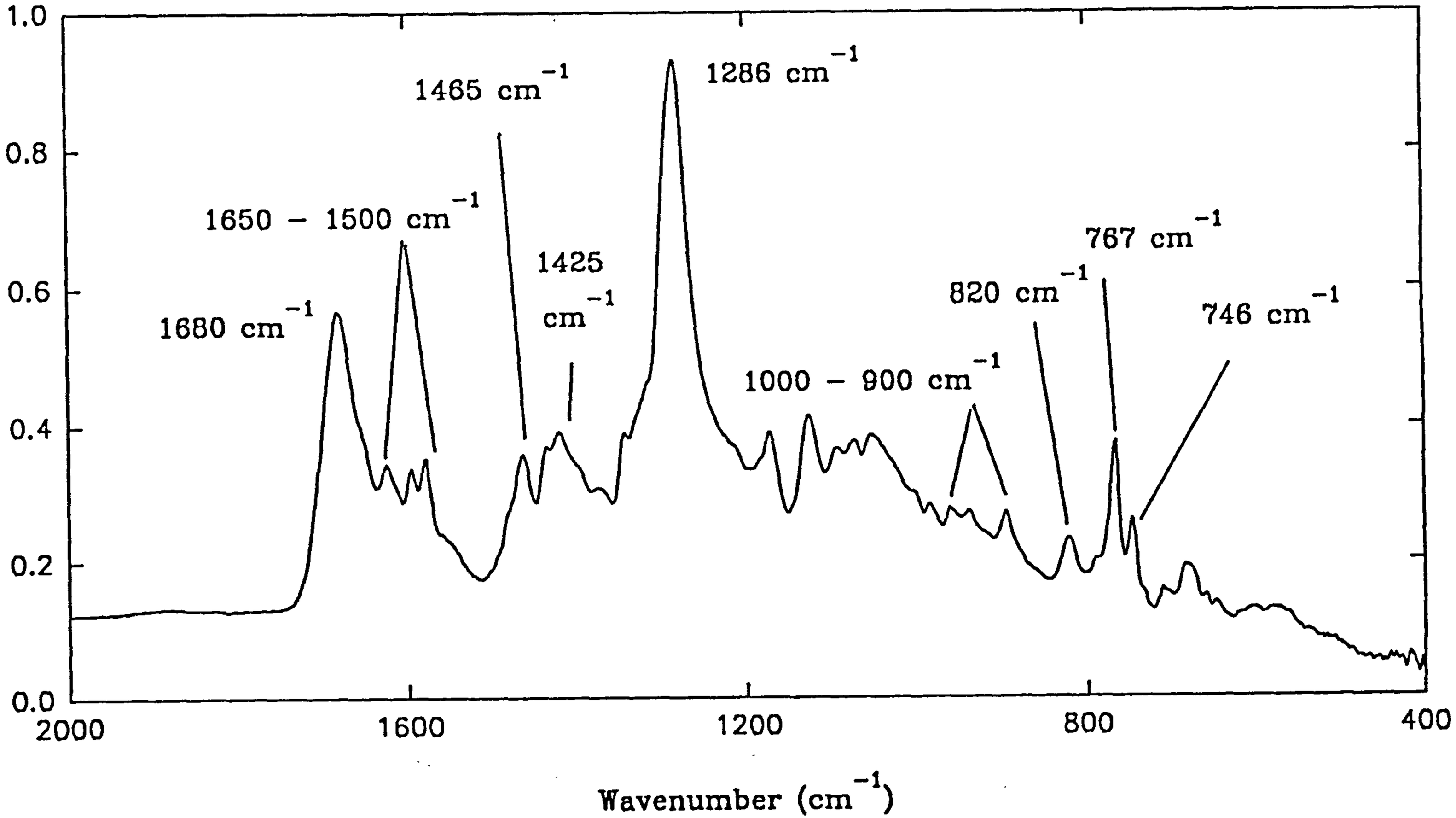

Figure 5.18 The reflectance FT-IR spectrum of fully reduced poly(5-carboxyindole) in more detail between 400 and 2000 cm^{-1}

Table 5.2 The assignments for the reflectance FT-IR spectra of poly(5-carboxyindole) shown in figures 5.17 and 5.18

Wavenumber (cm^{-1}) ± 4 cm^{-1}	Assignment
2500-3750(vs)	O-H carboxylic acid stretch
1680(vs)	carbonyl stretch of carboxylic acid dimer
1500-1650(m)	C-C aromatic ring stretches typical of indoles
1465(m)	C-N aromatic ring stretch (?)
1425(m)	carboxylic acid OH bend
1286(vs)	C-O carboxylic acid stretch
900-1000(w)	aromatic C-H i. p. bends
820(w)	C-H o. p. bend, typical of 1,2,4 tri-substituted benzene ring
767(m)	C-H o. p. bend, typical of five membered ring
746(w)	C-H o. p. bend, typical of 1,2,4 tri-substituted benzene ring

membered ring of the indole monomer suggesting that either the 2 or the 3 C-H position remains intact and is not involved in polymer coupling. No N-H stretching is observed in the spectra, figure 5.17, suggesting again that this is one of the bonding positions.

The reflectance FTIR spectra of poly(indole) figure 5.16 and poly(5-carboxyindole) figure 5.18 show some similarities other than the substitution related bands, but because of the weak nature of the poly(indole) reflectance FTIR spectrum, figure 5.16, the definition of the C-H out of plane bending region is low and hence poly(5-carboxyindole) is the most favoured polymer upon which to perform further studies. Labelling compounds with deuterium enables IR bands involving hydrogen to be identified by inducing a $1/\sqrt{2}$ shift in wavenumber from the original undeuterated compound. For these reasons, and the fact that indole easily degrades under the deuteration conditions, 5-carboxyindole was deuterated at the 3-position (see Chapter 2) and the FTIR of the undeuterated and deuterated monomers, in nujol mull, were compared in figure 5.19.

The C-H out of plane bending region between 700 cm^{-1} and 900 cm^{-1} will be discussed thoroughly since this region is directly comparable to the reflectance FTIR spectra of the polymers. The spectra did however show shifts upon deuteration for 5-carboxyindole in other regions, the most notable being the N-H stretch at 3400 cm^{-1} which shifted to 2490 cm^{-1} with the presence of N-D and also the broad O-H band was shifted to lower frequencies upon the formation of O-D bonds. In addition other smaller shifts were recorded for bands which did not involve the bonding of deuterium directly but are affected by hydrogen bonding.

The FTIR spectrum of deuterated 5-carboxyindole shows a significant reduction in the peak at 752 cm^{-1} from the undeuterated

Figure 5.19 The FT-IR spectra of 5-carboxyindole (XIII) and deuterated 5-carboxyindole in nujol mull between 600 and 1000 cm^{-1}

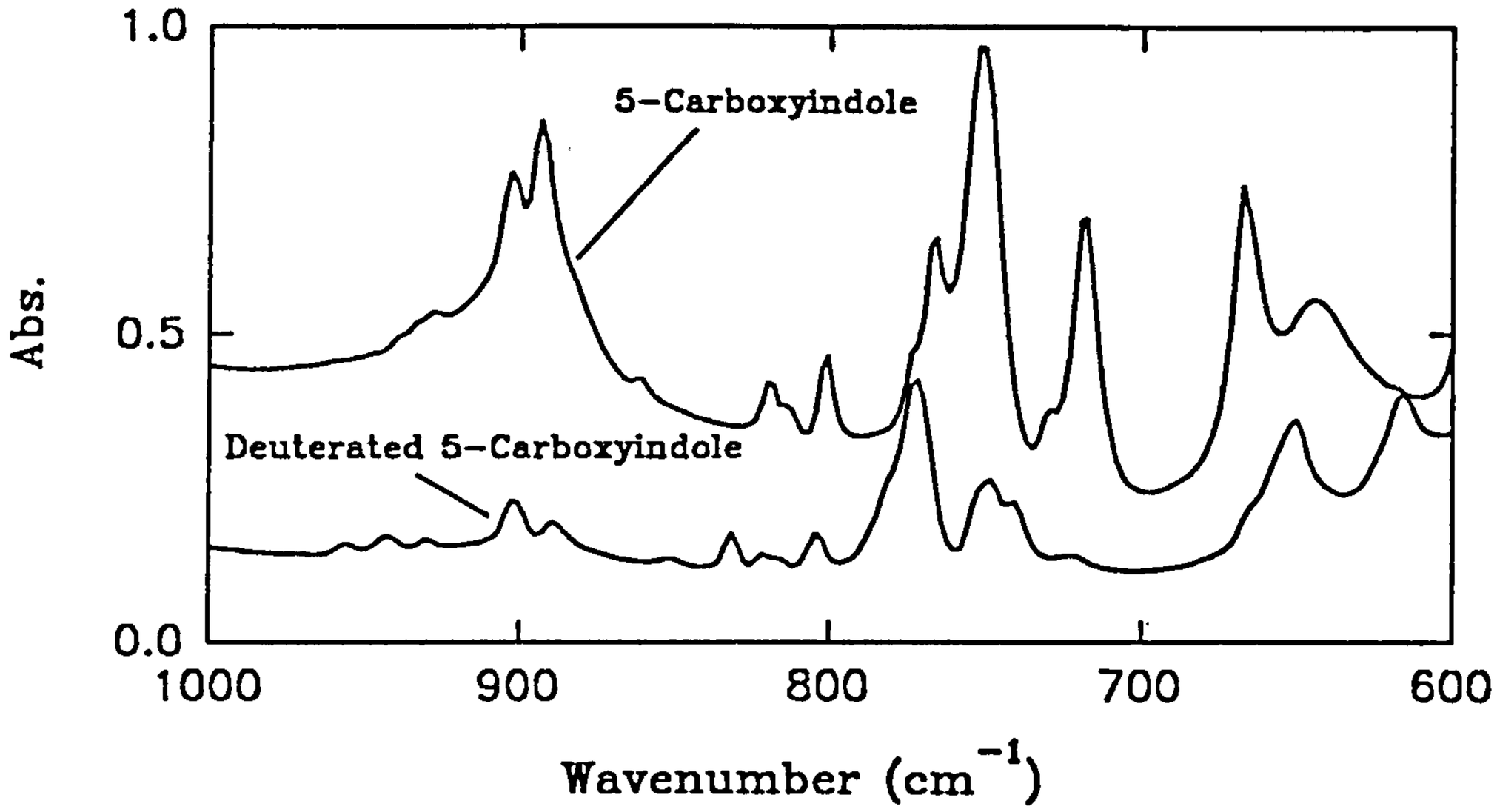

5-carboxyindole FTIR spectrum. This peak is assigned to the C-H out of plane bend of the 3-position of the 5-carboxyindole monomer which is completely removed upon deuteration. The underlying peak observed at 747 cm^{-1} in the deuterated spectrum is assigned to the C-H out of plane bend for a 1,2,4-trisubstituted benzene. The peak at 770 cm^{-1} in the deuterated 5-carboxyindole, figure 5.19, spectrum and at 767 cm^{-1} in the undeuterated 5-carboxyindole spectrum, figure 5.19, is assigned to the C-H out of plane bend at the 2-position of the 5-carboxyindole monomer. The peak at 718 cm^{-1} in the undeuterated 5-carboxyindole spectrum may be due to the N-H out of plane bend, this peak is not present in the FTIR spectrum of deuterated 5-carboxyindole and is consistent with the fact that this position is also mainly deuterated. The C-H out of plane bending peak at 822 cm^{-1} is present in both the spectra which is consistent with its assignment as a 1,2,4-trisubstituted benzene band.

Finally the reflectance FTIR spectra of poly(5-carboxyindole) films, grown for 30 s, from both the deuterated and undeuterated 5-carboxyindole monomers is shown in figure 5.20 and 5.21.

The spectra in figure 5.21 are identical, except in the O-H stretching region, and show no difference between each other suggesting that there is no deuterium present on the five membered ring in either of the polymers. What is even more remarkable is the similarity between the reflectance FTIR spectra in figure 5.21 and the FTIR spectrum of the deuterated monomer, figure 5.19, in the region between 700 cm^{-1} and 900 cm^{-1}. None of the spectra have the strong band at 750 cm^{-1} or the band at 718 cm^{-1} but display all the other previously assigned bands.

The overwhelming conclusion from the data described above is that poly(5-carboxyindole) is bonded at the 1-position and the 3-position of the 5-carboxyindole monomer, figure 5.22, since it has been shown conclusively that in the polymer spectra the six membered ring remains

Figure 5.20 The reflectance FT-IR spectra of fully reduced poly(5-carboxyindole) grown from deuterated and undeuterated 5-carboxyindole (XIII)

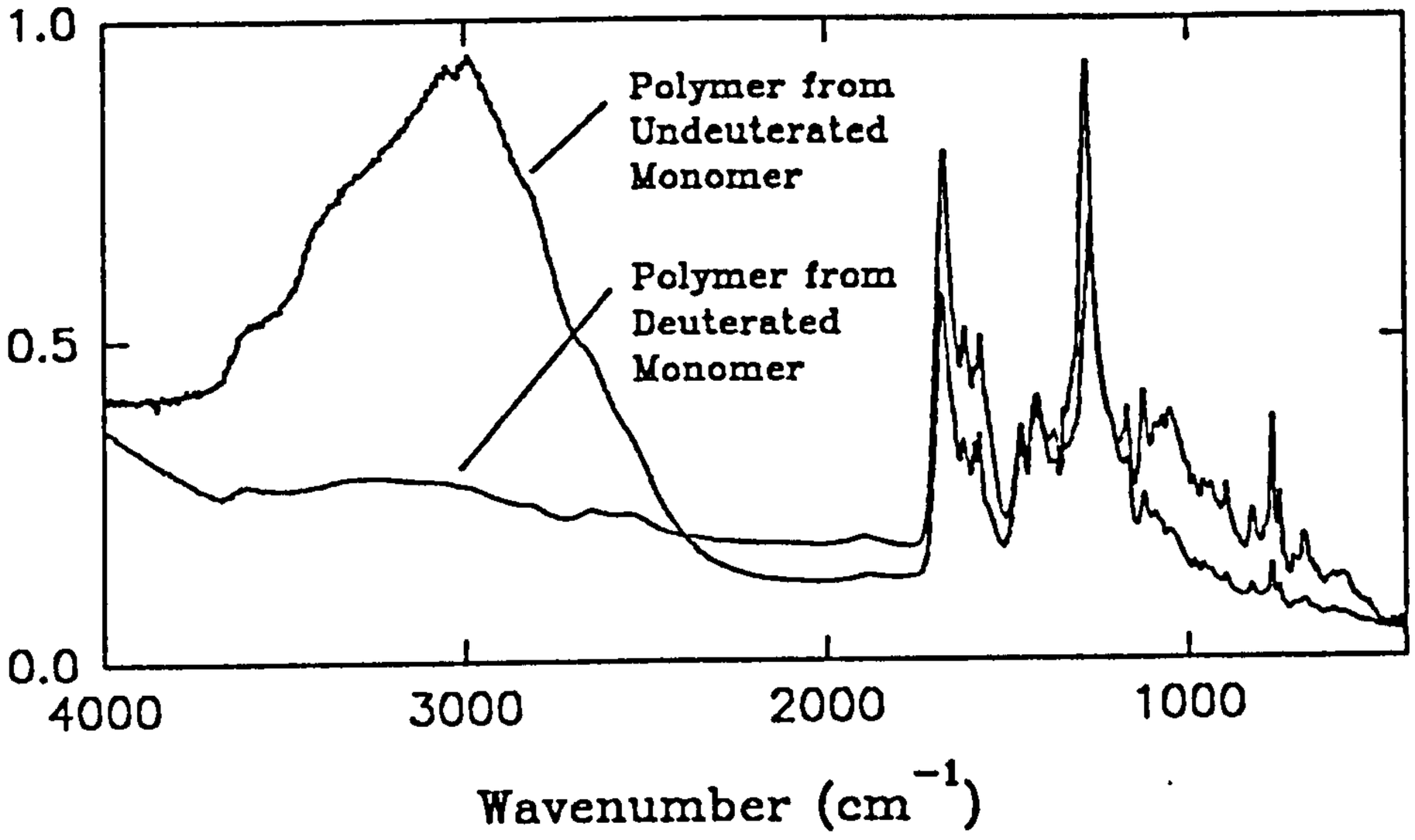

Figure 5.21 The reflectance FT-IR spectra of fully reduced poly(5-carboxyindole) grown from deuterated and undeuterated 5-carboxyindole (XIII) between 600 and 1000 cm^{-1} with the deuterated sample scaled in absorbance by a factor of two to give a better comparison

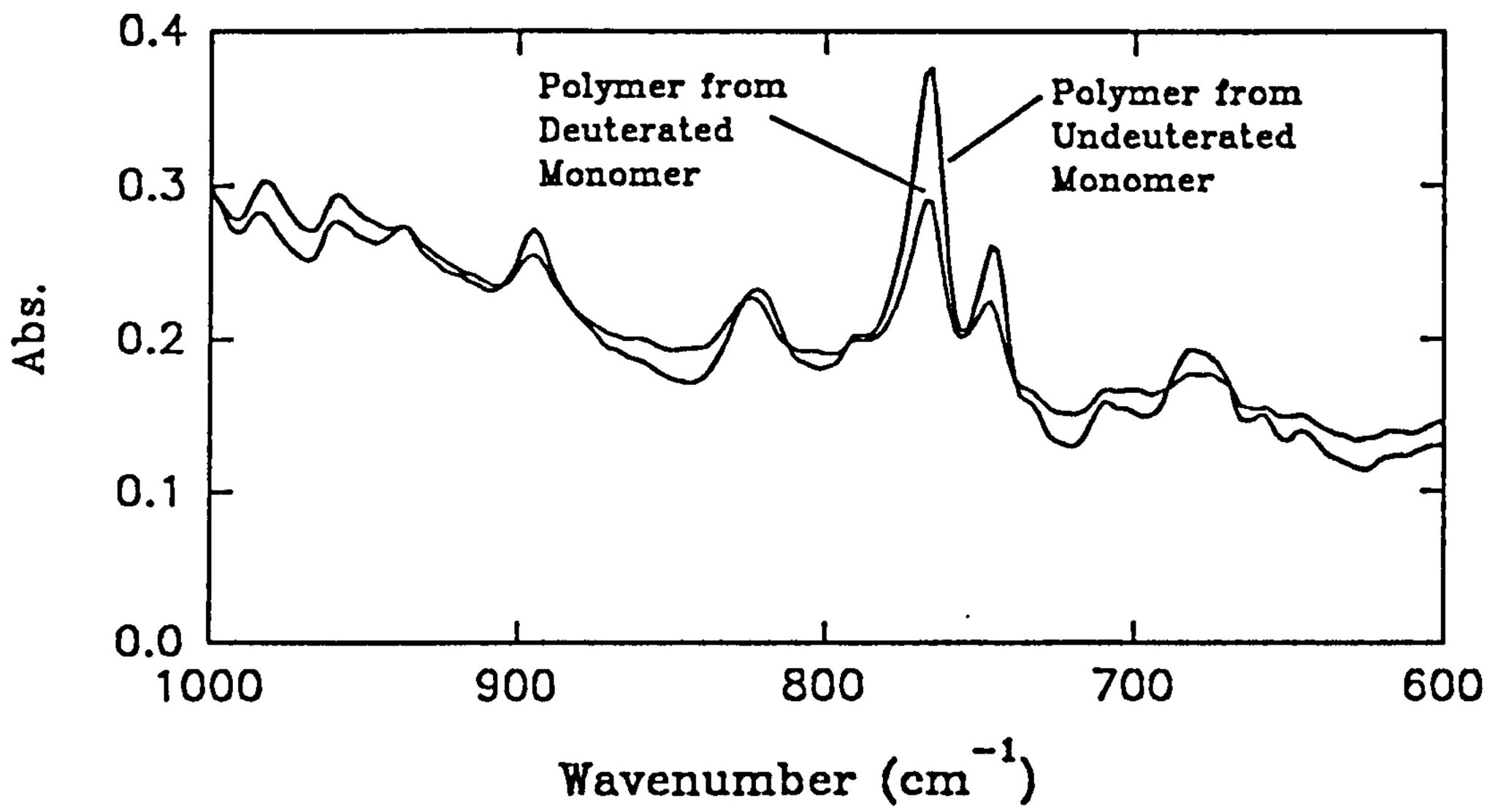

unchanged and that the N-H stretch, and the C-H out of plane bend corresponding to the 3-position are not present. This experimental evidence compliments the predictions based on calculated spin density for the bonding positions of poly(indole) made by Waltman *et al.*[144]

The structure of the polymer suggested in figure 5.22 and by other research workers[27,144] has been found by molecular modelling to be incapable of attaining a completely planar form when the contributions from π-bonding are taken into account. The most energetically favourable conformation by molecular modelling, taking into account the conjugation energy as well as the bonding energy and steric interactions is the trans form of the polymer, figure 5.23.

Even in the trans conformation planarity would be impossible to achieve. Figure 5.24 shows a dimer of 5-carboxyindole indicating the clear steric barrier created by the hydrogen atoms in the 2 and 7 positions on the monomers. The dihedral angle between the two essentially planar monomers was calculated to be approximately 35°.

This has consequences for the type of electrical conduction mechanism predicted for this polymer which is likely to be via a charge hopping mechanism.

5.4 Aqueous Electrochemistry of Poly(5-carboxyindole)

The aqueous electrochemistry of poly(5-carboxyindole) has previously been discussed, but only in a very brief manner.[121] The following section describes the study of this polymer in aqueous solutions and explains its very interesting pH behaviour in some detail. The transition from acetonitrile electrochemistry to aqueous electrochemistry has previously been described but a brief summary is given in order to provide a full explanation of this polymer's properties.

Figure 5.22 The suggested chemical structure for poly(5-carboxyindole)[27,144]

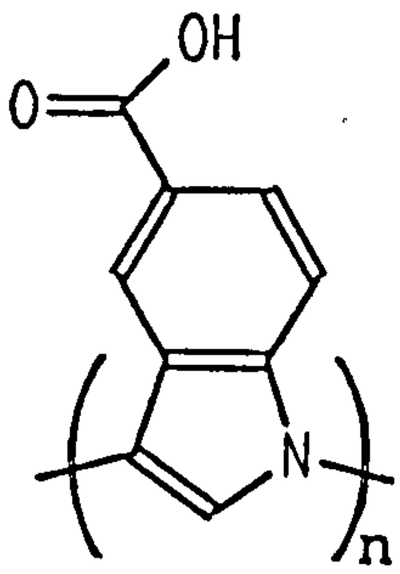

Figure 5.23 The trans conformation of poly(5-carboxyindole)

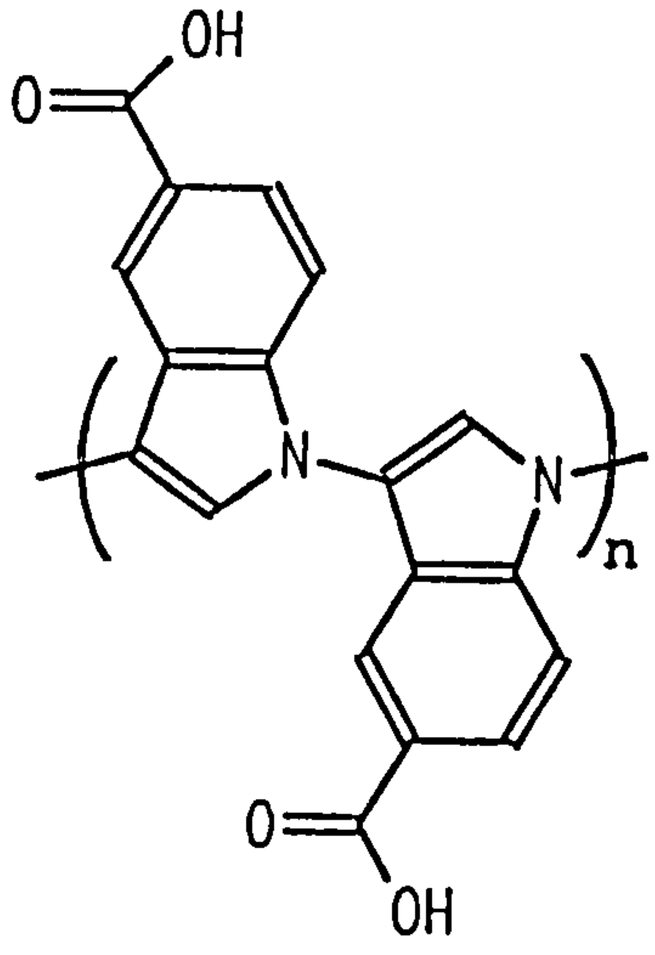

Figure 5.24 Molecular model of a 5-carboxyindole dimer clearly showing the steric interactions between the hydrogens at the 2 and 7 positions of the monomers

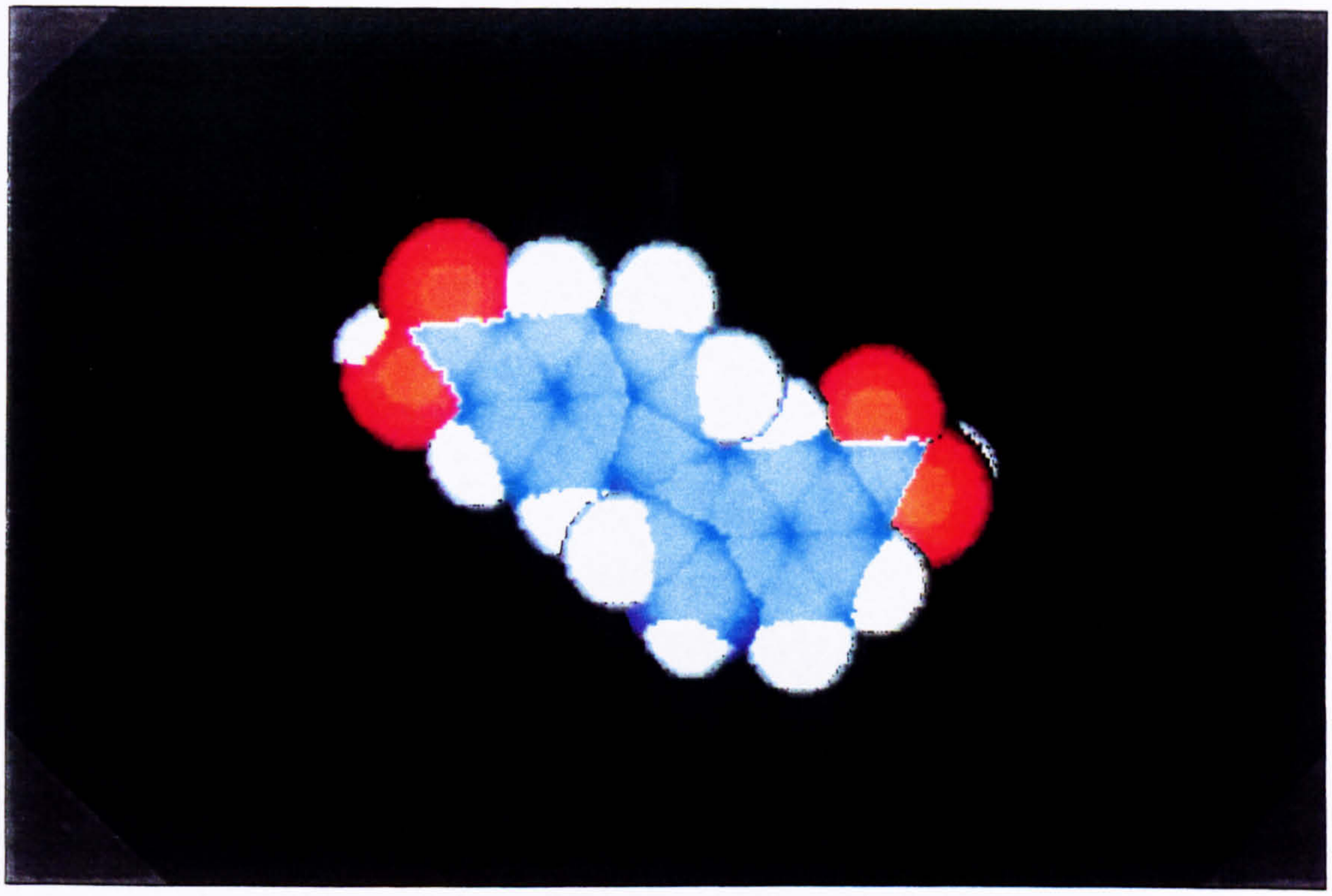

In order to perform electrochemistry upon films of poly(5-carboxyindole) in aqueous solutions the polymer had to be successively washed in serially diluted mixtures of acetonitrile and Whatman RO water with the ratios of 4:1, 3:2, 2:3 and 1:4 followed by a final wash in neat Whatman RO water. The polymers could then be introduced to strongly acidic solutions or aqueous buffered McIlvaine solutions, between pH 0 and pH 7. At pH's above 7 the polymer immediately dissolved without any electrochemistry being performed. Without the initial serial dilution washing procedure, after growth in acetonitrile, the polymers immediately cracked upon contact with aqueous solutions. This is attributed to the swelling or contraction of the polymer in the different solvent occurring at an unmanageable rate. This cracking occurs when the polymer is placed at any potential and cannot be prevented when the polymer is fully oxidised.[121]

All aqueous electrochemistry, unless otherwise stated, was performed in strongly acidic solutions or McIlvain buffer containing sodium chloride (0.1 mol dm^{-3}) to provide a high ionic strength. The cyclic voltammetry at 20 mV s^{-1} of poly(5-carboxyindole) films, grown for 30 s, at pH 2.00, 3.25 and 5.00 is shown in figure 5.25.

It is quite clear from figure 5.25 that the polymer undergoes two oxidation processes, the first being very broad over a wide potential region and the second having well defined oxidation and reduction peaks that vary in position with pH. The two oxidation processes appear to overlap in the cyclic voltammetry, figure 5.25, which makes it difficult to determine whether the charge passed during each redox process is equal, but intuitively it can be estimated that the both processes pass the same amount of charge.

Since the cyclic voltammetry of poly(5-carboxyindole) is much better defined in aqueous solutions than acetonitrile solutions dopancy studies

Figure 5.25 The cyclic voltammetry of poly(5-carboxyindole) (previously grown for 30 s at a platinum electrode (A = 0.385 cm^2)) in pH 2.00, 3.25 and 5.00 McIlvaine buffers (Sweep rate υ = 20 mV s^{-1})

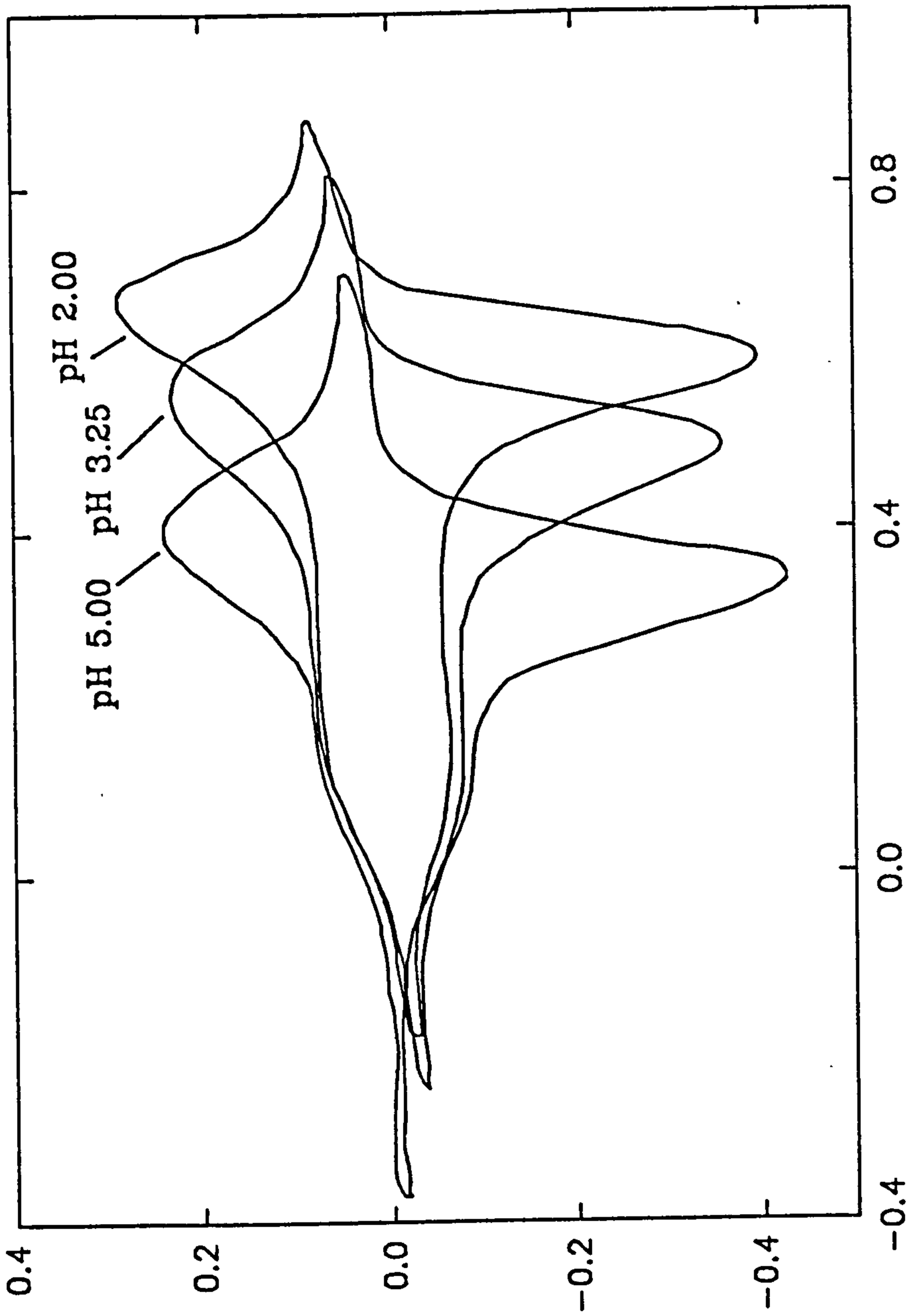

were performed using acetonitrile growth transients and aqueous solution cyclic voltammograms. Films of poly(5-carboxyindole) were grown for 15, 30, 45 and 60 s and introduced to aqueous conditions. The films grown for 15 s and 45 s were studied in pH 2 buffer solution and the films grown for 30 s and 60 s were studied in pH 5 buffer solution. It was found that slight losses in Q_{CV} were recorded during the first few potential cycles of the polymer so each polymer was studied for one cycle only, immediately after growth. Each polymer was studied by holding at a fully oxidising potential until no current was recorded followed by cathodically sweeping at 10 mV s^{-1} to fully reducing potentials and recording the Q_{CV}. Applying equation 3.1 gives a dopancy of $\delta = 0.49$, figure 5.26 ($r = 0.977$, $n = 4$), which is a very large number, compared to most conducting polymers, and suggests one charge for every two monomer units for the fully oxidised polymer or, since it is clear that two oxidation processes are taking place, two charges in every four monomer units for the fully oxidised polymer.

The pH dependency of the second wave was studied by measuring the mid peak potentials of poly(5-carboxyindole) films, grown for 30 s, during cyclic voltammetry at 20 mV s^{-1} in degassed aqueous solutions between pH 0.5 and pH 6. The potential limits of the cyclic voltammetry depended mainly upon the pH of the particular solution used at the time since varying pH has an effect upon both cathodic and anodic solvent limits. Fortunately full electrochemistry was recorded at all the pH values studied. For solutions between pH 2 and pH 6 McIlvaine buffers were utilised and hydrochloric acid solutions were used between pH 0.5 and pH 1.75. The overall data set is plotted in figure 5.27 showing that the mid-peak potential pH dependence is not linear. Towards pH 0.5 and pH 6.0 the gradient of the line becomes 120 mV per pH unit corresponding to an electrochemical process involving the transfer of two protons and one electron. In the central pH region between pH 2 and pH 4.5 the gradient of the line is much less than 120 mV per pH unit

Figure 5.26 The plot of Q_T vs. Q_{CV} for films of poly(5-carboxyindole) grown for t = 15, 30, 45 and 60 s at a platinum electrode (A = 0.385 cm^2) and studied by cyclic voltammetry under aqueous conditions (r = 0.977, n = 4)

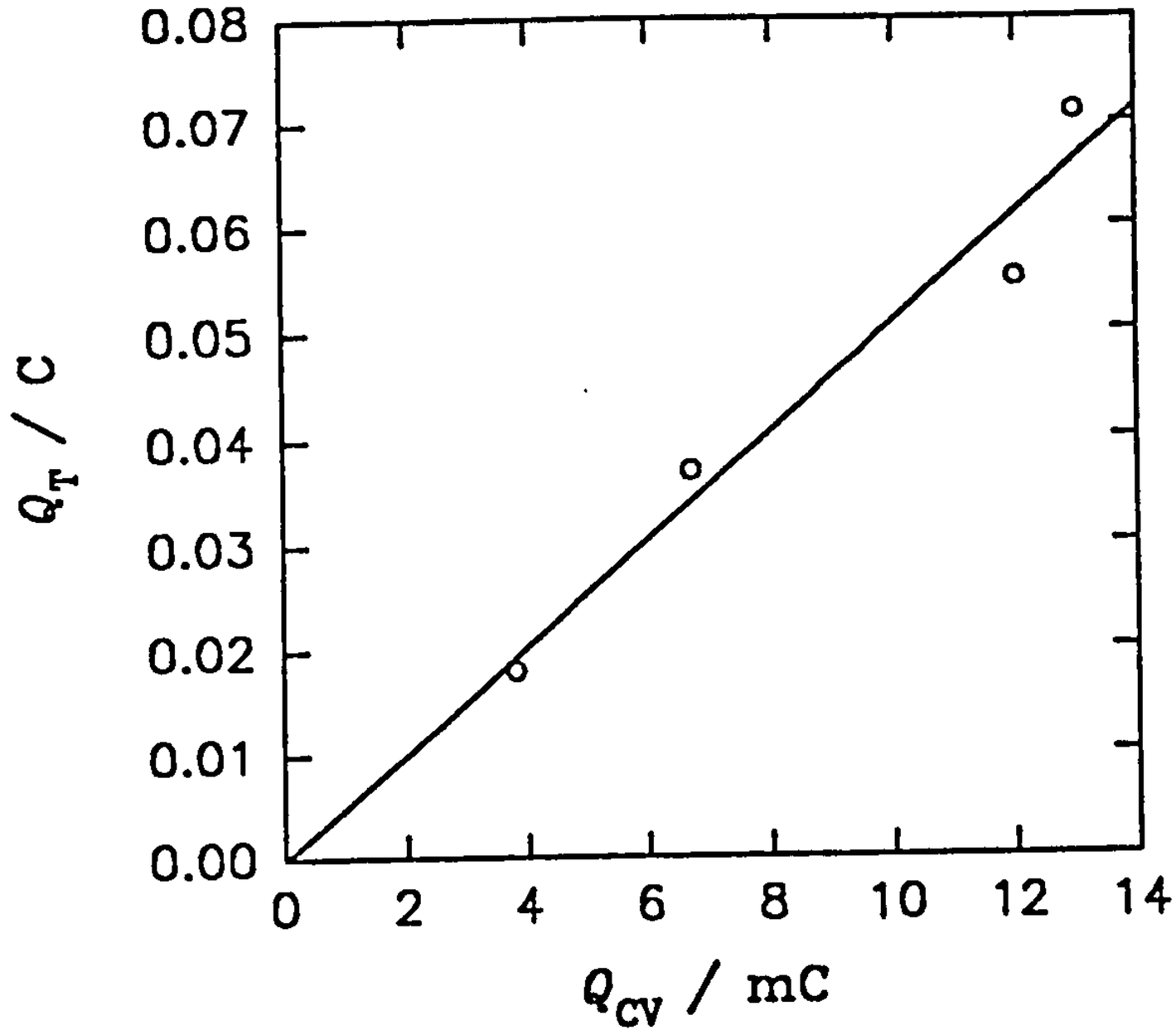

Figure 5.27 The plot of $E_{1/2}$ vs. pH recorded for the second oxidation process of poly(5-carboxyindole) during cyclic voltammetry at a sweep rate of υ = 20 mV s^{-1} for films grown for t = 30 s

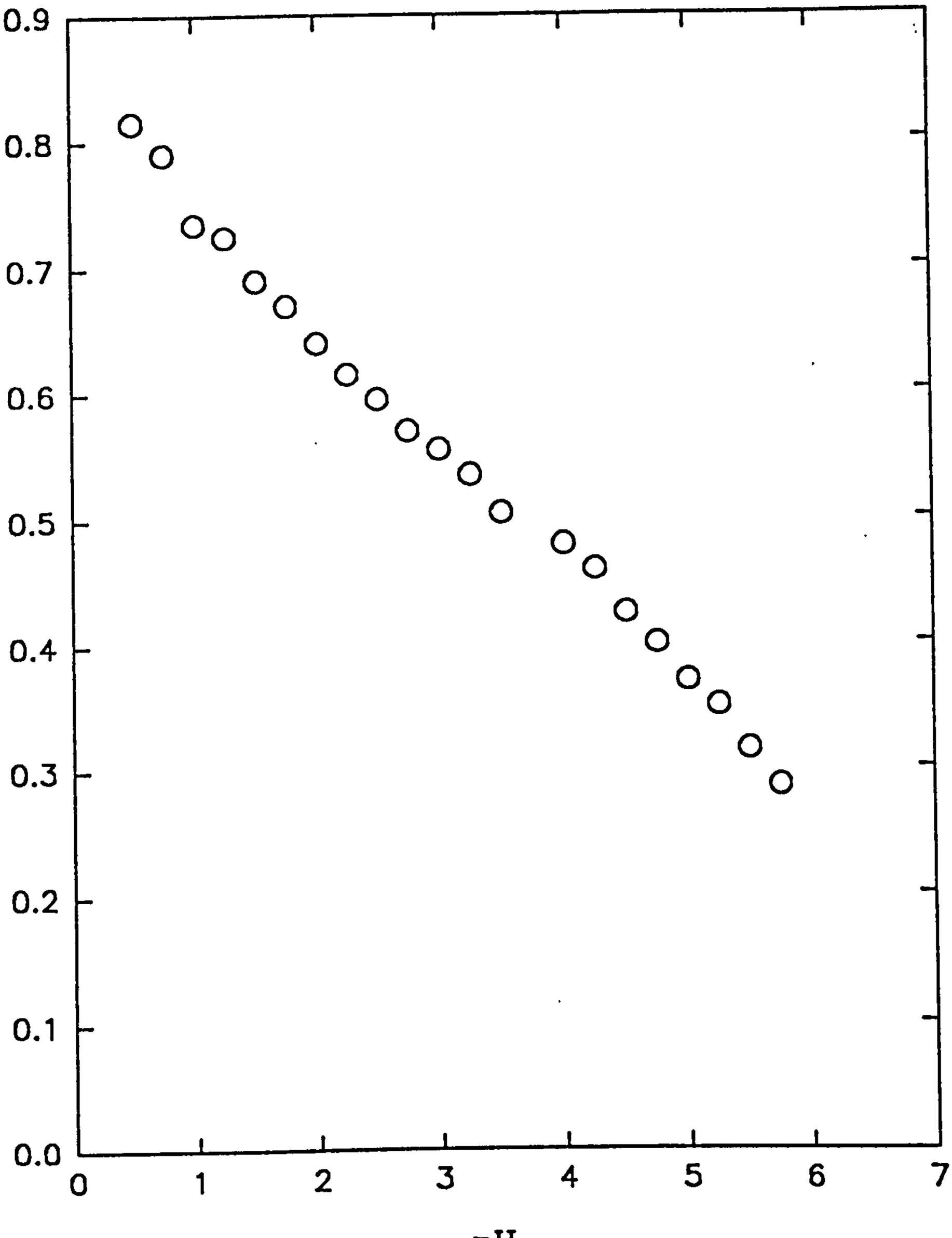

and hence corresponds to less protons transferred during oxidation or reduction.

The results have been interpreted in equation scheme 5.1 by taking into account the pK_a's of the partially oxidised and fully oxidised polymer and curve fitting to equation (5.1.8).

Equation Scheme 5.1

We assume that the redox reaction can be represented by,

$$X + ne^- + mH^+ \rightarrow YH_m^{(m-n)+} \qquad (5.1.1)$$

K_X and K_Y are equilibrium constants for X and Y,

$$XH_\alpha^{\alpha+} \rightleftharpoons X + \alpha H^+ \qquad (5.1.2)$$

$$K_X = \frac{[X][H^+]^\alpha}{[XH_\alpha^{\alpha+}]} \qquad (5.1.3)$$

$$\text{and } YH_{(\beta+m)}^{(m-n+\beta)+} \rightleftharpoons YH_m^{(m-n)} + \beta H^+ \qquad (5.1.4)$$

$$K_Y = \frac{[YH_m^{(m-n)}][H^+]^\beta}{[YH_{(\beta+m)}^{(m-n+\beta)+}]} \qquad (5.1.5)$$

Applying the Nernst Equation,

$$E^{\circ\prime} = E^\circ + \frac{RT}{nF} \ln\left\{\frac{[X][H^+]^m}{[YH_m^{(m-n)+}]}\right\} \qquad (5.1.6)$$

$$E^{\circ\prime} = E^\circ + \frac{RT}{nF} \ln\left\{\frac{[H^+]^m(1 + K_Y^{-1}[H^+]^\beta)}{(1 + K_X^{-1}[H^+]^\alpha)}\right\} \qquad (5.1.7)$$

Substitute n = 1, m = 2 and $\alpha = \beta = 1$,

$$E^{\circ\prime} = E^{\circ} + \frac{RT}{F} \ln \left\{ \frac{[H]^2 (1 + K_Y^{-1}[H^+])}{(1 + K_X^{-1}[H^+])} \right\} \qquad (5.1.8)$$

$pK_X = 4.1$ and $pK_Y = 2.5$ (pK_a(monomer) = 5.55).[121]

The results show that the pK_a of the fully oxidised polymer is $pK_X = 4.1$ and the pK_a of the partially reduced polymer is $pK_Y = 2.5$. Figure 5.28 shows the schematic representation of the polymer at different potentials (vs. SCE) and pH values. A tetrameric charging unit is used to describe the charged states of the polymer assuming the calculated dopancy ($\delta = 0.49$) for the fully oxidised polymer. For convenience the partially oxidised polymer has been drawn as a radical site but there is no direct evidence for this and the state may be as simple as a bipolaron.[47,48,49] Unfortunately the first oxidation process cannot easily be defined so no information on the pK_a of the fully reduced poly(5-carboxyindole) can be obtained electrochemically. The fully reduced and fully oxidised poly(5-carboxyindole) are labelled as electronically insulating and the partially oxidised poly(5-carboxyindole) is labelled as an electronic conductor. This will be explained and justified in section 5.8.

With regards to the second oxidation process it seems unusual that the redox behaviour obeys the simple nernstian analysis so well, equation scheme 5.1, since it would be predicted that the activity effects within the film would distort the behaviour significantly. It is suggested that this near perfect behaviour occurs because the partially oxidised and/or fully oxidised polymer is charge compensated, in the pH range studied.

The polymer in its fully reduced state at low pH is assumed to be fully protonated. For this reason the partially oxidised polymer tetramer

Figure 5.28 The schematic representation of poly(5-carboxyindole) redox chemistry at different pH values and potentials (vs. SCE)

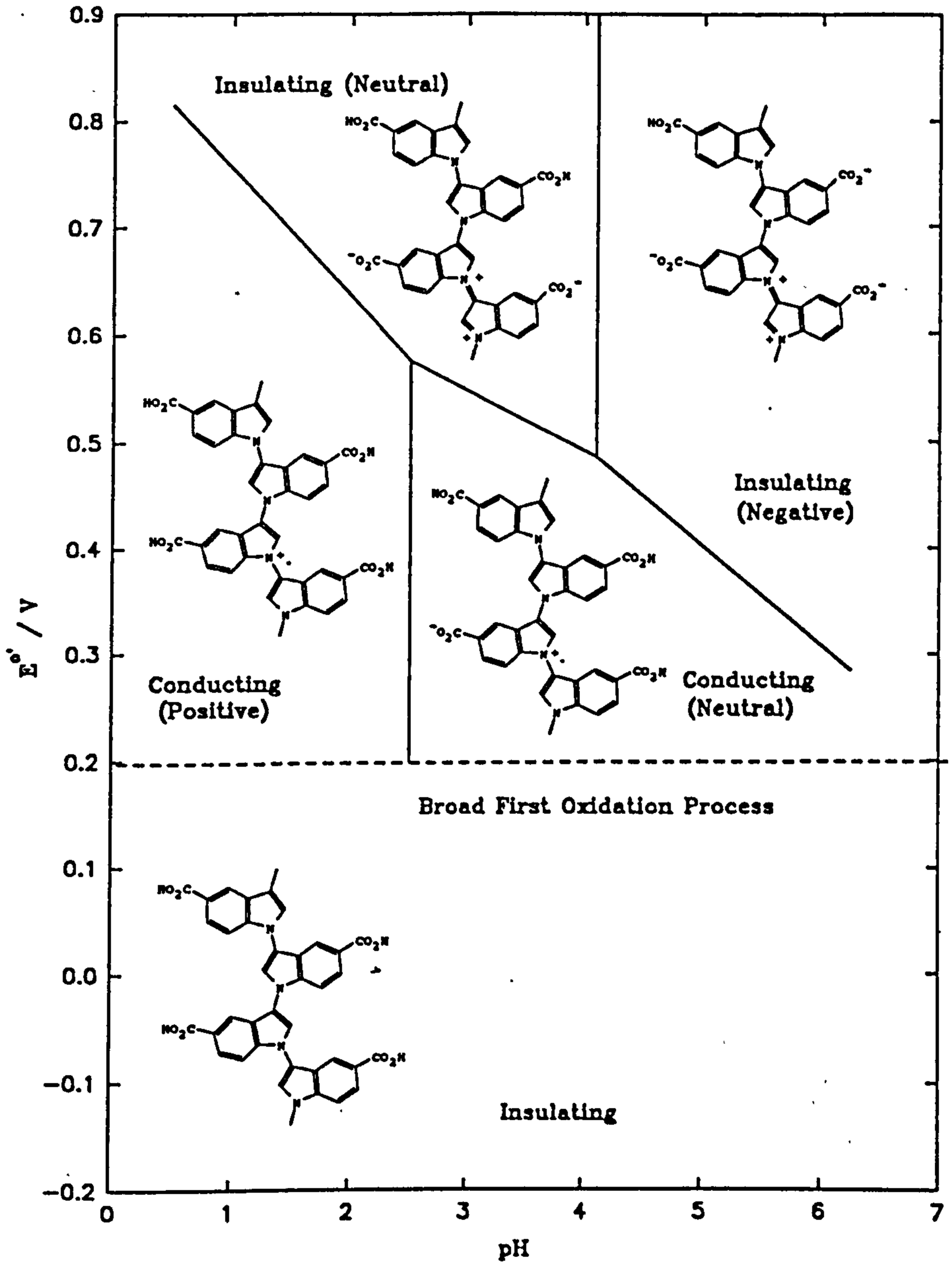

unit below pH 2.5 is also assumed to be fully protonated and has been assigned a positive charge and the fully oxidised polymer tetramer unit above pH 4.1 has been assigned a negative charge in figure 5.28. This means that below pH 2.5 the partially oxidised positive poly(5-carboxyindole) is oxidised by the removal of two protons and one electron per tetramer unit to give neutrally charged fully oxidised poly(5-carboxyindole). Between pH 2.5 and 4.1 the partially oxidised neutrally charged poly(5-carboxyindole) is oxidised by the removal of one proton and one electron per tetramer unit to give neutrally charged fully oxidised poly(5-carboxyindole). Above pH 4.1 the partially oxidised neutrally charged poly(5-carboxyindole) is oxidised by the removal of two protons and one electron per tetramer unit to give negatively charged fully oxidised poly(5-carboxyindole).

To confirm the assigned charges on the poly(5-carboxyindole) tetrameric units in the various different oxidation states at different pH values a film of poly(5-carboxyindole), grown for 60 s, was initially held at 0.4 V (vs. SCE) in degassed aqueous pH 1.0 solution containing only perchloric acid until no current was recorded, before a reflectance FTIR spectrum was recorded of the partially oxidised polymer. The polymer was then placed in the same pH 1.0 solution and held at 0.96 V (vs. SCE) until no current was detected before a second reflectance FTIR spectrum was recorded of the fully oxidised polymer. Both reflectance FTIR spectra are compared in figure 5.29 the main difference being a very strong peak in the spectra of the partially oxidised poly(5-carboxyindole) at 1100 cm^{-1}, corresponding to large amounts of ClO_4^-, which is not present in the spectra of the fully oxidised poly(5-carboxyindole). This result is consistent with the assumption that the partially oxidised poly(5-carboxyindole) is positively charged in pH 1.0 solution.

Figure 5.29 The reflectance FT-IR spectra of poly(5-carboxyindole) (previously grown for t = 60 s) before being held at 0.4 V and 0.96 V (vs. SCE) in degassed aqueous pH 1.0 perchloric acid solution

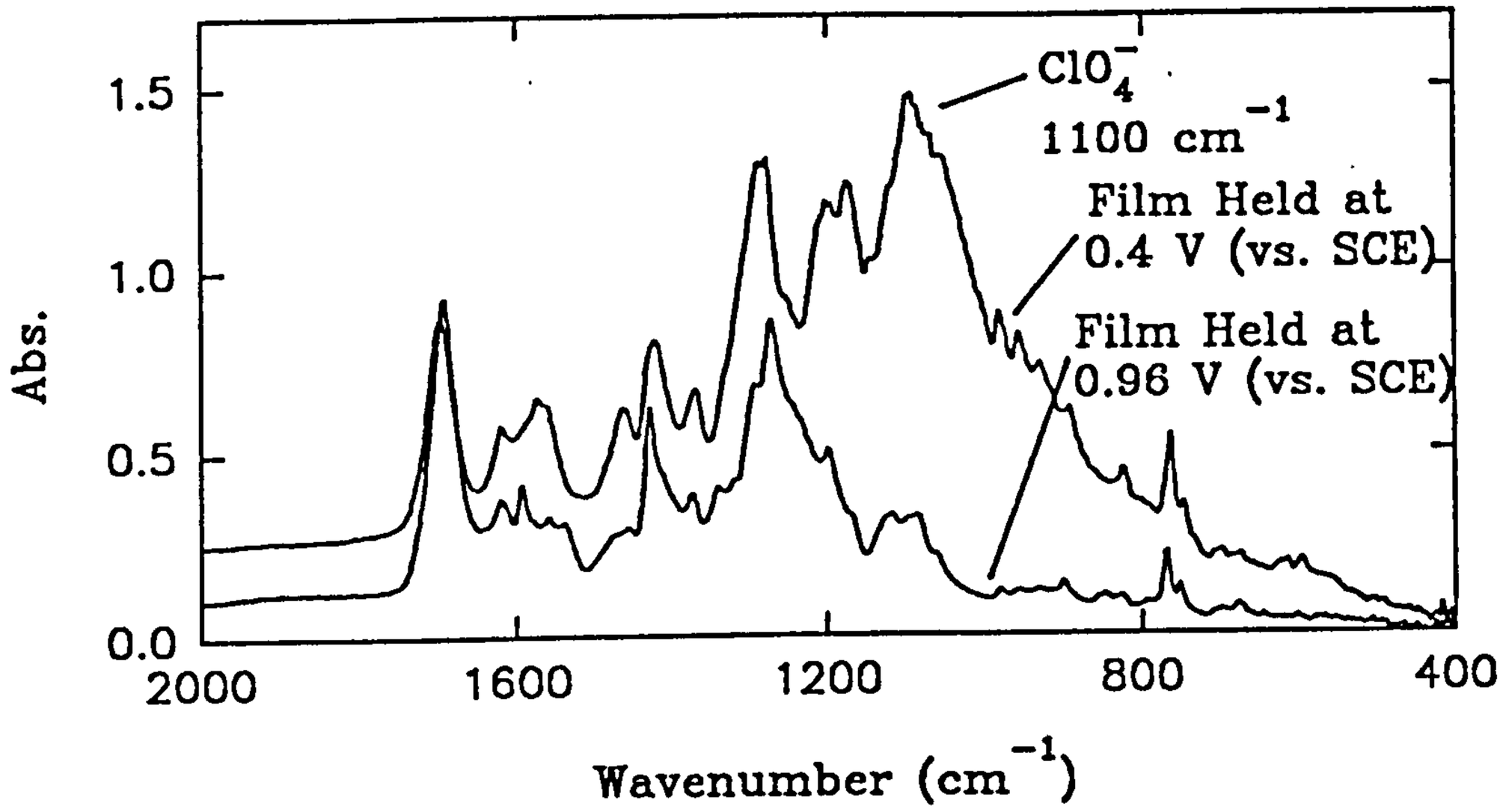

Figure 5.30 The reflectance FT-IR spectra of poly(5-carboxyindole) (previously grown for t = 60 s) before being held at 0.4 V and 0.85 V (vs. SCE) in degassed aqueous pH 3.25 perchloric acid solution

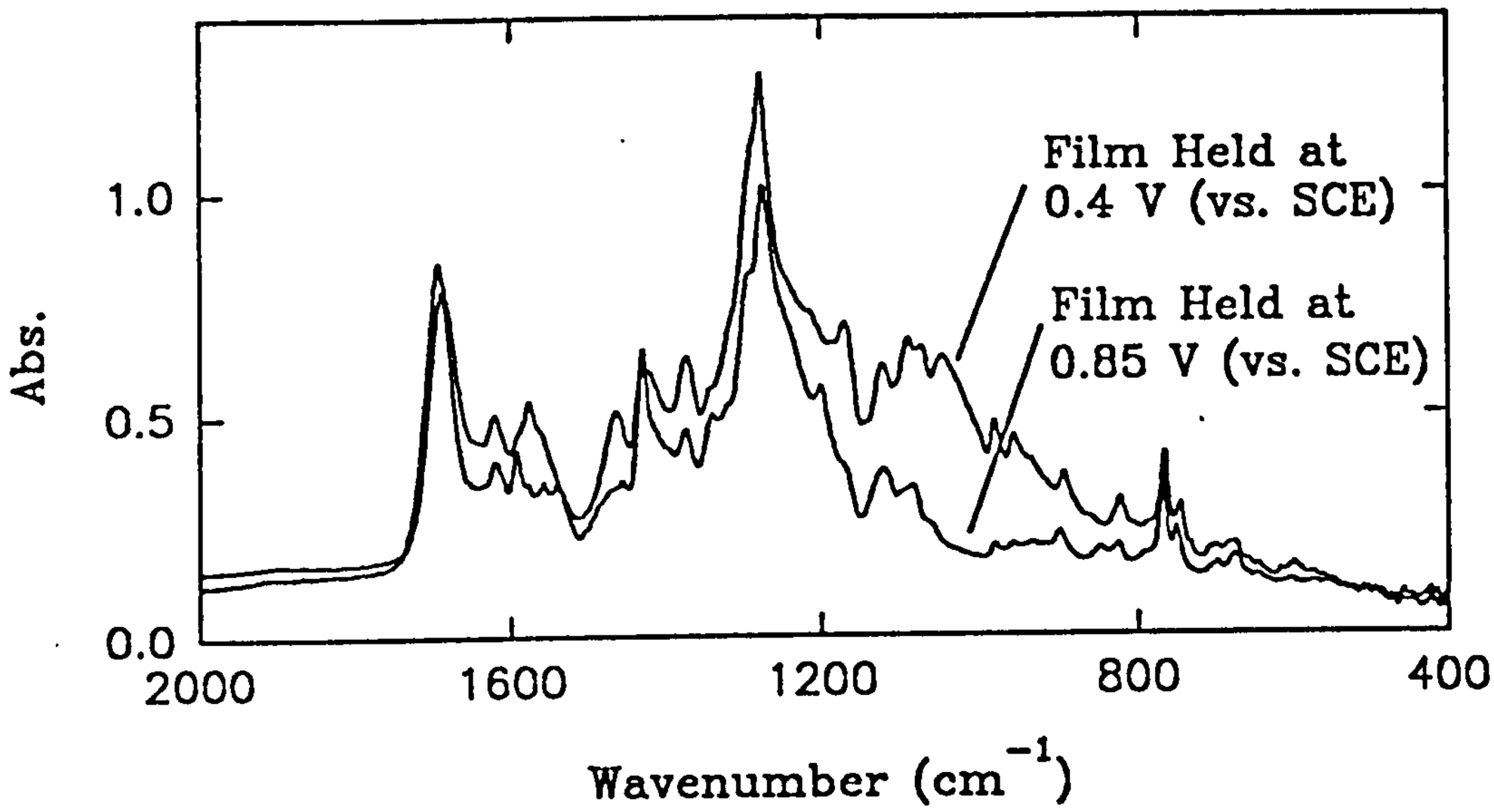

A film of poly(5-carboxyindole), grown for 60 s, was then placed in a degassed aqueous pH 3.25 solution containing only perchloric acid and held at 0.4 V (vs. SCE) until no current was recorded before a reflectance FTIR was recorded. The same film was then held at 0.85 V (vs. SCE) in the same pH 3.25 solution until no current was observed before a second reflectance FTIR was recorded. The two reflectance FTIR spectra are compared in figure 5.30 and show no discernable differences. There is no peak corresponding to perchlorate in either of the spectra. This result is also consistent with the assumption that partially oxidised and fully oxidised poly(5-carboxyindole) films have a neutral charge at pH 3.25. Unfortunately it is not possible to detect positively charged counter ions in the same way that perchlorate was detected by FTIR, due to the low availability of strongly IR active cations. This means that studies in the pH region above pH 4.5 were difficult to perform. The charge of poly(5-carboxyindole), in its partially oxidised and fully oxidised state, in this pH region, still therefore remain unconfirmed.

Further study of figure 5.30 shows great similarities between the spectra of the polymer FTIR spectra taken directly from the acetonitrile growth solutions, figure 5.18. This confirms that there are no major chemical differences between poly(5-carboxyindole) grown in acetonitrile and poly(5-carboxyindole) which is introduced into aqueous conditions. Only slight differences in the reflectance FTIR spectra of the partially oxidised and fully oxidised poly(5-carboxyindole) are observed between 1500 cm^{-1} and 1600 cm^{-1} in the C-C aromatic stretching region and at 1465 cm-1 where the peak diminishes upon oxidation and is probably due to the disruption of the aromatic C-N bond. The position of the carboxylic acid C=O has moved only slightly to a value of 1690 cm^{-1} probably due to a slight change in the strength of the hydrogen bonding within the film.

Figure 5.30 The reflectance FT-IR spectra of poly(5-carboxyindole) (previously grown for t = 60 s) before being held at 0.4 V and 0.85 V (vs. SCE) in degassed aqueous pH 3.25 perchloric acid solution

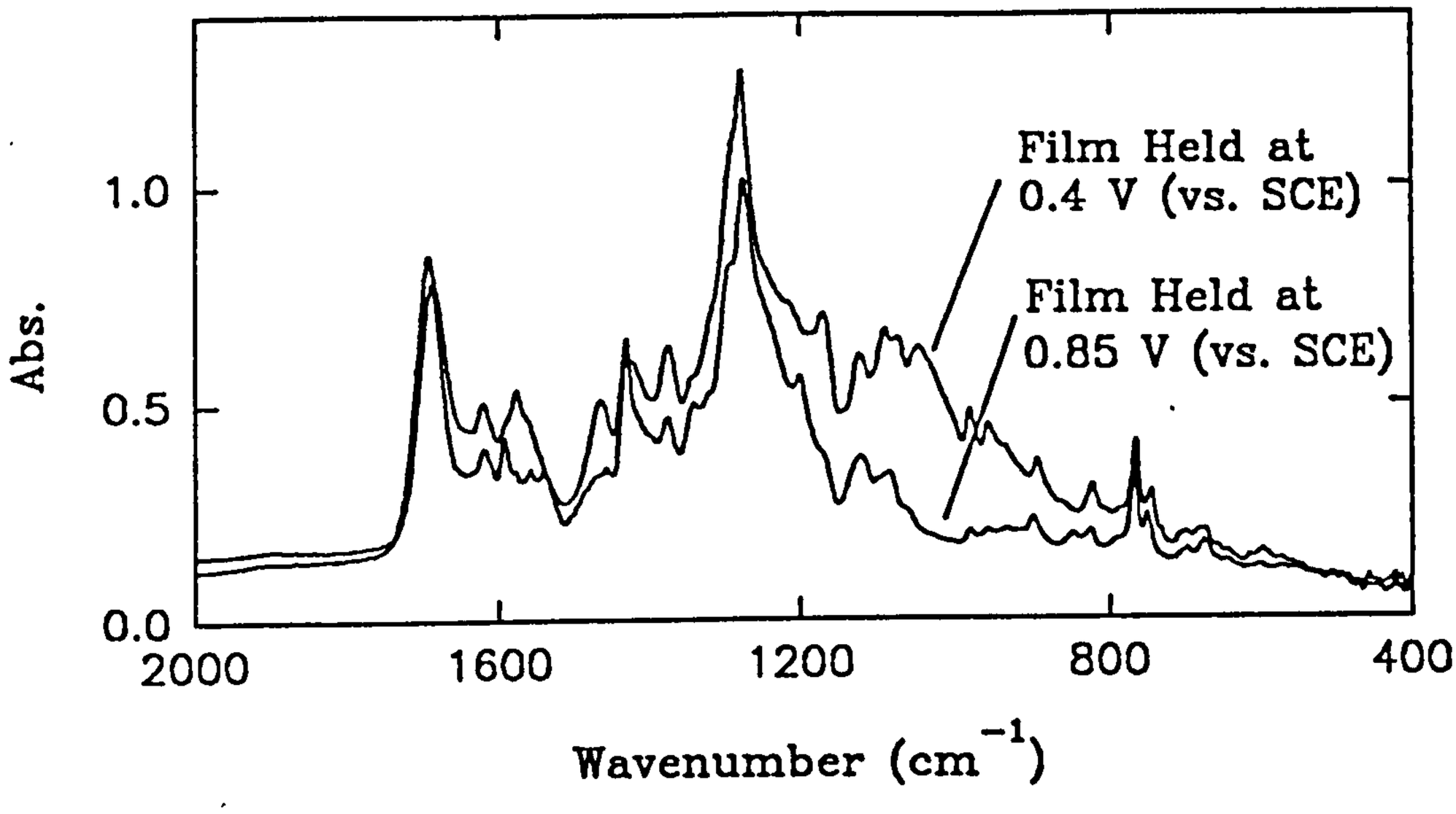

PAGE NUMBERING AS ORIGINAL

Figure 5.31 The current (i) due to oxygen plotted against fixed potentials (vs. SCE) measured at a clean platinum electrode (A = 0.385 cm^2) (○) and at a platinum electrode (A = 0.385 cm^2) with deposited poly(5-carboxyindole) (○) (previously grown for t = 30 s) in aqueous pH 3.25 buffered solution

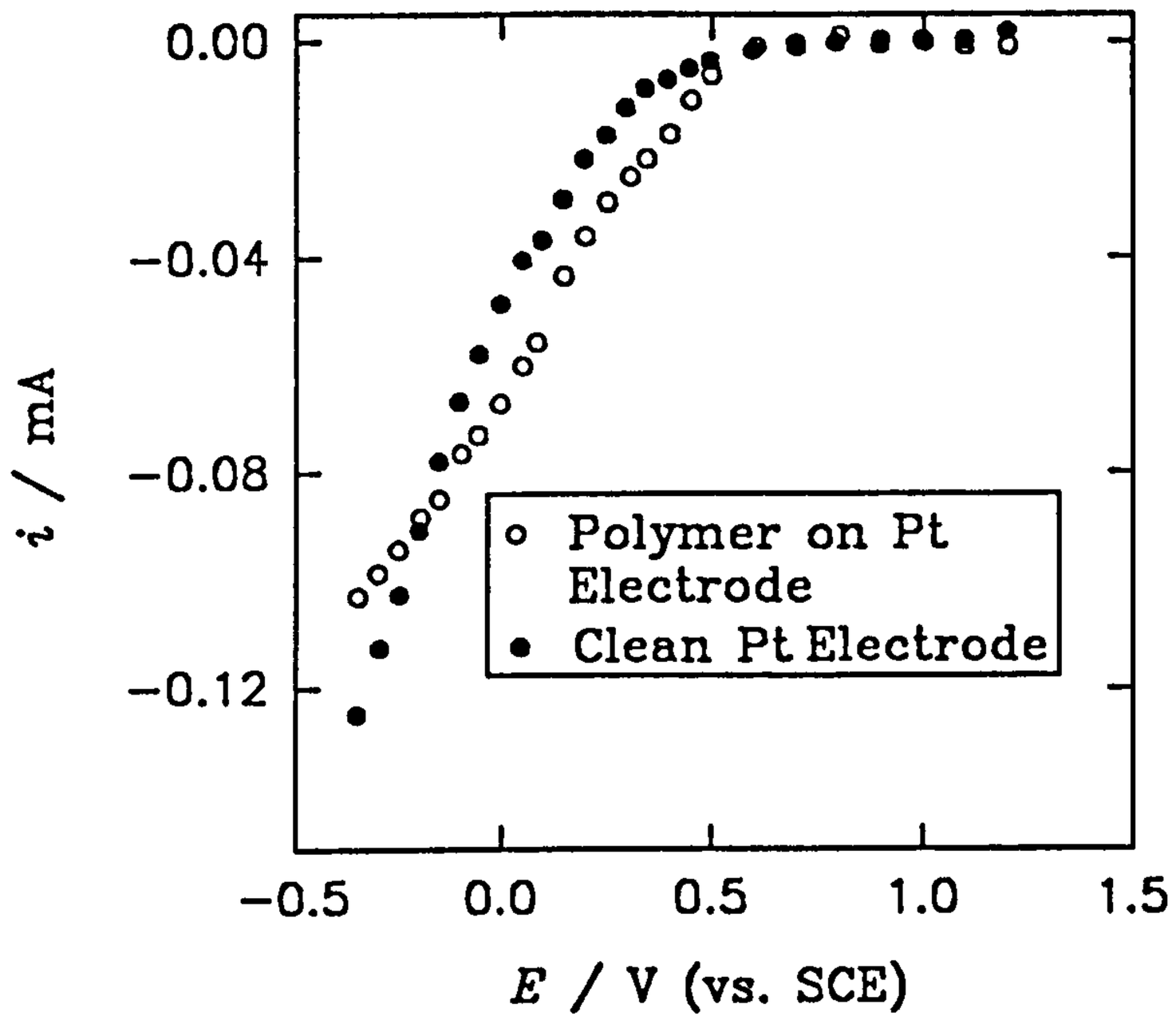

Figure 5.32 The cyclic voltammetry of a poly(5-carboxyindole) film, previously grown for t = 30 s on a platinum electrode (A = 0.385 cm^2), in aqueous pH 3.25 buffer solution (sweep rate υ = 10 mV s^{-1}) with oxygen present

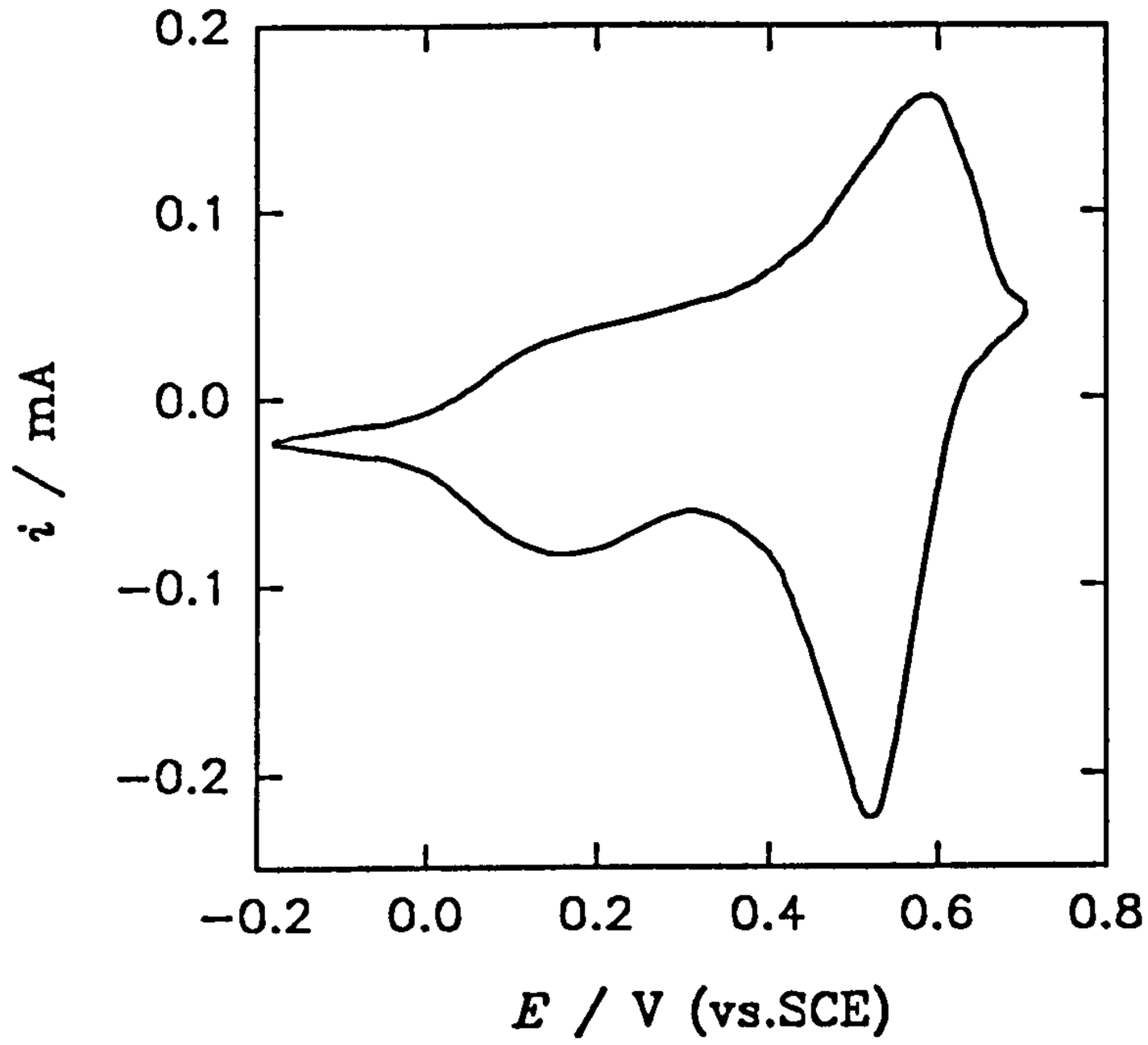

Figure 5.33 The cyclic voltammetry of a poly(5-carboxyindole) film (previously grown for t = 30 s on a glassy carbon electrode (A = 0.323 cm^2)) in aqueous pH 3.25 buffer solution (sweep rate υ = 10 mV s^{-1}) with oxygen present

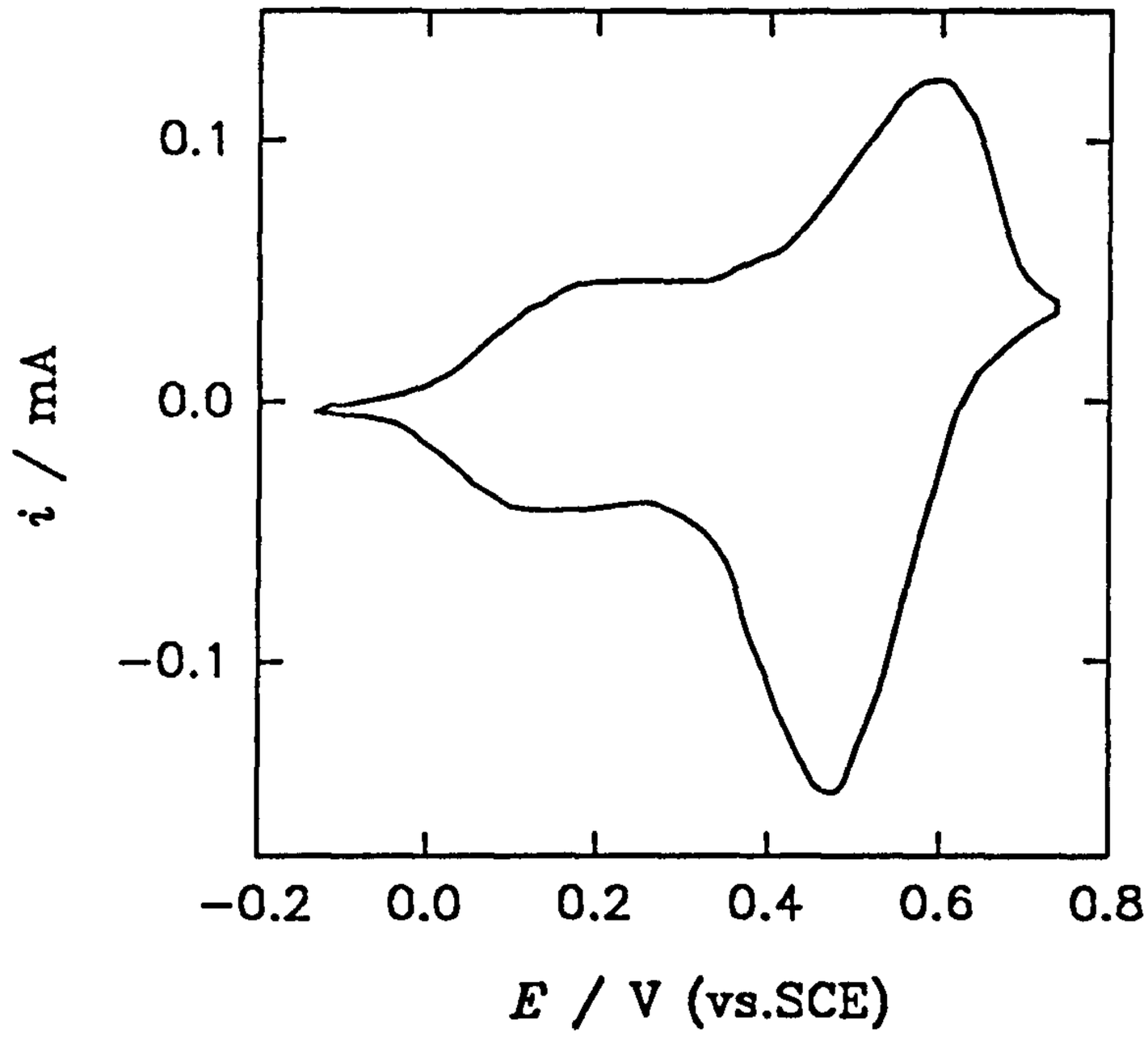

Figure 5.34 Schematic representation of the oxidation of poly(5-carboxyindole) by oxygen in solution at a platinum electrode

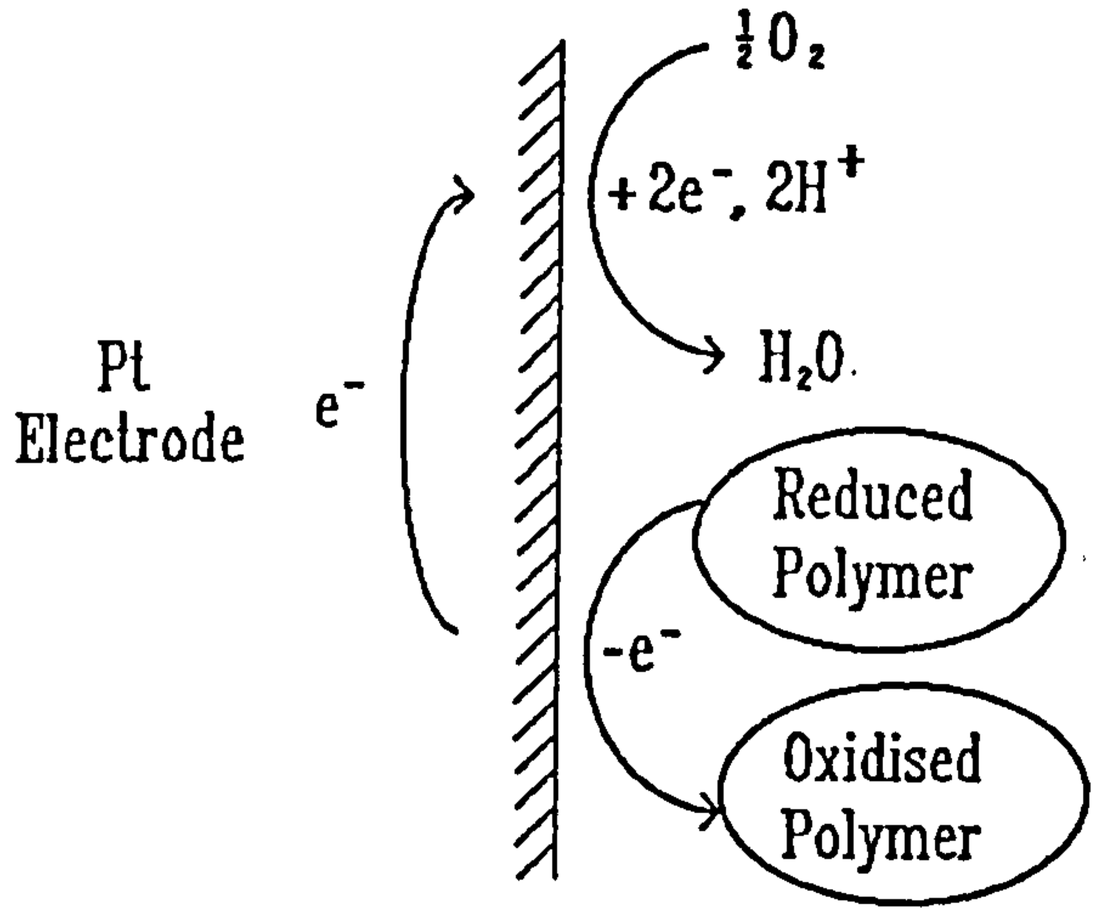

This means that poly(5-carboxyindole) is not directly oxidised by oxygen in solutions. This result has the same consequence that films deposited upon platinum will be more readily oxidised by oxygen than those deposited upon glassy carbon even out of electrolyte solutions.

5.6 UV/visible Spectroscopy of Poly(5-carboxyindole) in Aqueous Solutions

UV/visible spectroscopy was performed on poly(5-carboxyindole) films to measure the relative concentrations of redox species over a range of potentials in order to determine the nature of the redox processes taking place during oxidation and reduction. The colours observed during cyclic voltammetry in pH 3.25 McIlvaine buffer solution are labelled in figure 5.35, as fully reduced species {A}, partially oxidised species {B} and fully oxidised species {C}.

To study the UV/visible spectra of poly(5-carboxyindole), films were grown in the standard acetonitrile growth solution upon ITO plates (9×50 mm^2) but in a strongly stirred solution instead of rotating the electrode at 4 Hz. Films were typically grown along approximately 40 mm of the ITO plate with 10 mm remaining bare to maintain a dry contact. The length of each individual film was measured separately if charge density studies were required. The films were then treated in exactly the same way as in other studies.

A film of poly(5-carboxyindole), grown for 40 s, was held at potentials between -0.1 V and 0.9 V (vs. SCE) at separated intervals of 0.1 V in an aqueous pH 2.00 degassed McIlvaine buffer solution until the background current decayed to zero. UV/visible spectra were then recorded between 320 nm and 820 nm using the UV/visible electrochemical cell set up described in chapter 2. The entire data set is displayed in figure 5.36.

Figure 5.35 The colours of poly(5-carboxyindole) (previously grown for t = 60 s on a platinum electrode (A = 0.385 cm^2)) in its three oxidation states labelled on a cyclic voltammogram of a film in degassed aqueous pH 3.25 buffer (sweep rate υ = 10 mV s^{-1})

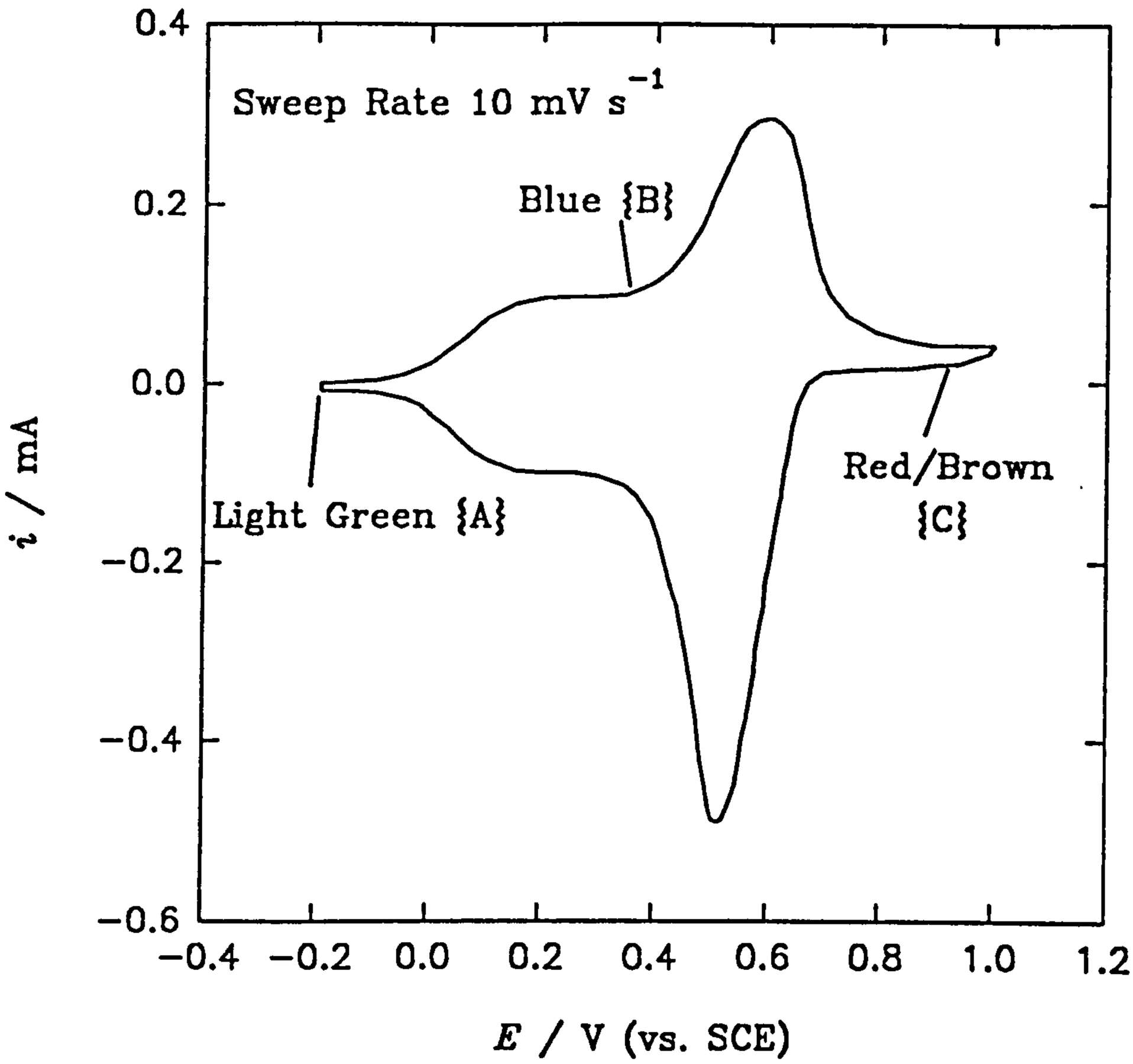

Figure 5.36 The UV/vis spectra of a poly(5-carboxyindole) film (previously grown for t = 40 s on an ITO electrode) recorded in aqueous pH 2.00 buffer at stationary potentials between -0.1 V and 0.9 V (vs. SCE) at intervals of 0.1 V

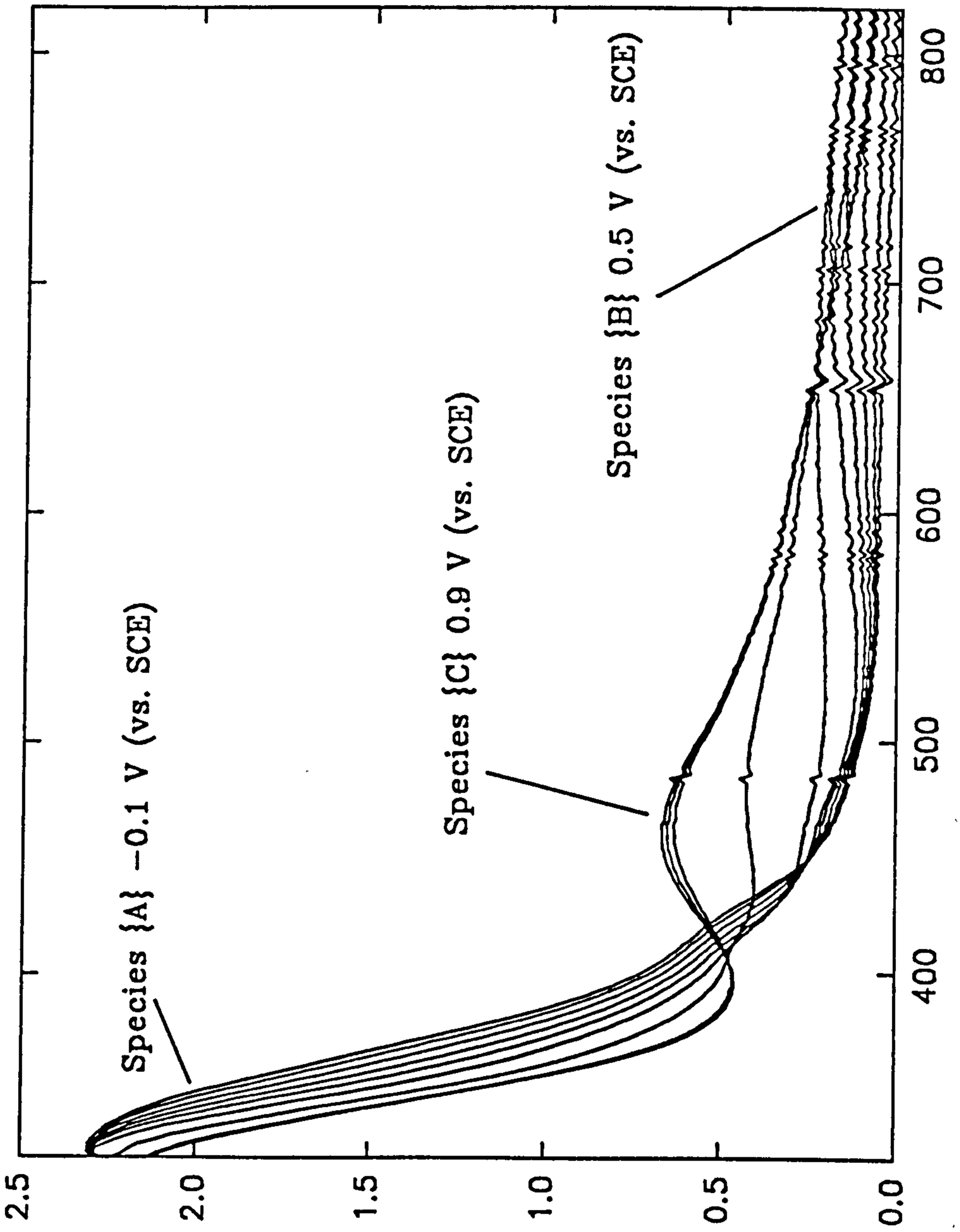

The largest absorption observed in the spectra is obscured by the 320 nm cutoff of the ITO plates. This absorption appears to decrease slightly as poly(5-carboxyindole) is oxidised but still remains very strong when the polymer is fully oxidised and is therefore a common feature of all the species present ({A}, {B} and {C}). There are no other discernable peaks in the UV/visible spectra of fully reduced poly(5-carboxyindole) species {A}. Partially oxidised poly(5-carboxyindole) species {B} has a very broad visible peak centred at $\lambda_{max}^{\{B\}}$ = 722 nm with an isosbestic point at $\lambda_i^{\{A\}-\{B\}}$ = 448 nm. Species {B} still maintains a very strong absorption in the ultra violet region of the spectrum near the ITO cut off. The peak due to the partially oxidised poly(5-carboxyindole) species {B} diminishes as the species is depleted and the polymer becomes fully oxidised to species {C}. The fully oxidised poly(5-carboxyindole) species {C} absorb strongly at a peak centred at $\lambda_{max}^{\{C\}}$ = 458 nm forming two isosbestic points at $\lambda_{i,1}^{\{B\}-\{C\}}$ = 660 nm and $\lambda_{i,2}^{\{B\}-\{C\}}$ = 408 nm with the partially oxidised species {B}. Again as mentioned earlier species {C} maintains an additional very strong absorbance in the ultraviolet region of the spectrum beyond the ITO cut off point.

The potential dependence of the relative concentrations of species {A}, {B} and {C} in poly(5-carboxyindole) in McIlvaine pH 2.00 buffer shown in figure 5.37 were deconvoluted by factor analysis of the data shown in figure 5.36. The initial results suggest that species {A} undergoes an initially slow depletion mirrored by a similarly slow increase in the concentration of species {B} with potential. Species {A} then rapidly undergoes depletion, over a range of approximately 0.3 V, to zero concentration, to give a maximum concentration of species {B} at higher potentials when species {C} begins its formation. Beyond this point the concentrations of species {B} and {C} vary with potential in a nernstian manner with an estimated $E^{\circ\prime}$ = 0.64 V (vs. SCE) which correlates to that predicted from figure 5.28. The calculated nernstian concentration profile

Figure 5.37 The relative concentrations of species {A} (○), {B} (●) and {C} (▽) at different potentials deconvoluted by factor analysis of the data shown in figure 5.36

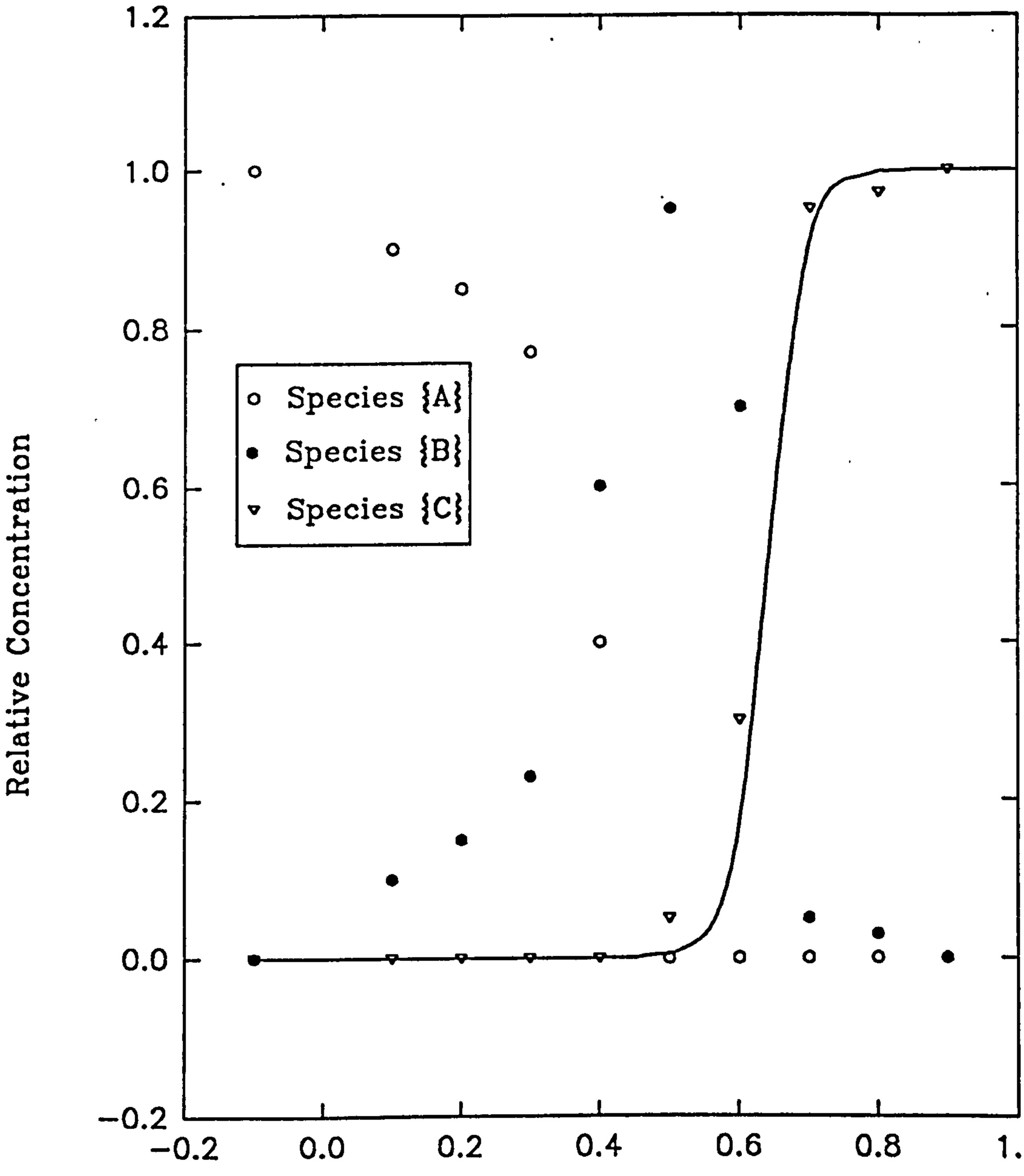

for species {C} is also shown in figure 5.37, assuming $E^{\circ\prime}$ = 0.64 V (vs. SCE), for comparison with the data.

The first redox process for the oxidation of species {A} to {B} was further studied using films of poly(5-carboxyindole), grown for 40 s, in degassed aqueous pH buffer solutions ranging from pH 0 to pH 4.25. The absorbances recorded, up to a maximum absorbance, over a range of stationary potentials in aqueous degassed perchloric acid solutions containing sodium chloride (0.1 mol dm^{-3}) at pH 0.05, 0.38, 0.75, 1.50 and 2.00 are shown in figure 5.38. The maximum absorption recorded increases with decreasing pH and occurs at higher potentials. However there do not appear to be any other major deviations with pH and the onset of oxidation from species {A} to {B} occurs at the same potential at all pH values. From these results it would appear that species {B} has an increasing extinction coefficient with decreasing pH since when the film consists of species {B} only, the absorbance at $\lambda_{max}^{\{B\}}$ = 722 nm decreases with increasing pH.

One other striking feature of the data shown in figure 5.38 is the linearity in the increase of the absorbance at $\lambda_{max}^{\{B\}}$ = 722 nm with potential over a wide potential range (0.25 to 0.4 V) . This suggests that after the initial onset of formation of species {A} to species {B}, between -0.1 V and 0.2 V (vs. SCE), the formation of species {B} becomes linearly dependent upon potential. Attempts to interpret the results shown in figure 5.37 in terms of the Nernst equation failed since unrealistically small values for n were obtained. It has been suggested by Evans *et al.*[149] that this behaviour may be due to the thermodynamic effect of dopant ions entering the polymer and enforcing swelling against cross links such as hydrogen bonds. Such a model invokes an additional mechanical term in the Nernst equation which depends upon the bulk modulus (K_B) of the polymer shown in equation (5.2).

Figure 5.38 The UV/vis absorbance ($\lambda_{max}^{\{B\}}$ = 722 nm) recorded up to a maximum against potential (vs. SCE) plot for a film of poly(5-carboxyindole) (previously grown for t = 40 s on an ITO electrode) in degassed aqueous pH 0.05, 0.38, 0.75, 1.50 and 2.00 buffer solutions

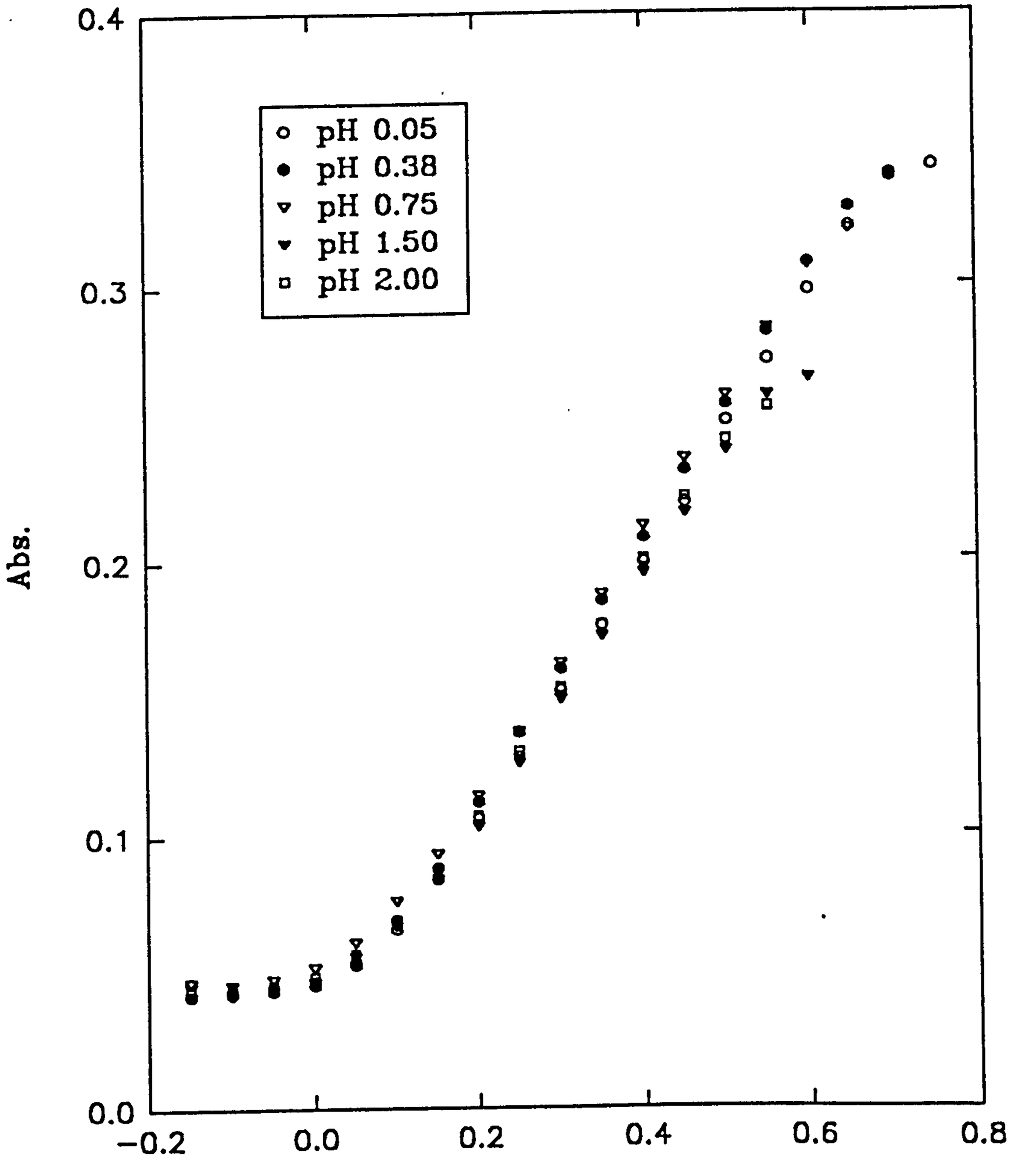

$$E = E^{\circ\prime} + \frac{RT}{nF} \ln \left\{ \frac{f}{f - 1} \right\} + \frac{n\nu_A c K_B (f - 0.5)}{10^4 F z^2} \qquad (5.2)$$

f - fraction of oxidised species.

ν_A- molar volume of monomer.

c - concentration of redox sites within the polymer.

Roncali *et al.*[150] performed experiments upon poly(thiophene) assuming a value for $K_B = 1.8 \times 10^{10}$ dyn cm^{-2} to interpret UV/vis data in terms of equation (5.2) with good agreement. It is likely that the first oxidation process of poly(5-carboxyindole) behaves in a similar manner since hydrogen bonding needs to be interrupted to accommodate counter ions in the structure of the polymer.

Recently Levi *et al.*[151] have developed a theory based upon Donnan exclusion to explain both the elongated oxidation process and the dynamic hysteresis observed during cyclic voltammetry. This theory suggests that there are potential distributions across the electrode/polymer and polymer/solution interfaces caused by the Donnan exclusion of ions in the film. Evans *et al.*[149] neglected Donnan effects and concentrated upon mechanical effects suggesting that at high ionic strength Donnan exclusion becomes negligible.

The second oxidation process from species {B} to {C} was further studied using a poly(5-carboxyindole) film grown for 40 s in acetonitrile before being introduced to a degassed aqueous solution of perchloric acid at pH 0 containing sodium chloride (0.1 mol dm^{-3}). The film was held at stationary potentials between -0.15 V and 1.1 V (vs. SCE) until the background current decayed to zero before absorption measurements were

taken at $\lambda_{max}^{\{C\}}$ = 458 nm, figure 5.39.

The absorbance vs. potential curve obtained, figure 5.39, showed behaviour consistent to that expected for an immobilised redox couple obeying the Nernst equation. The absorbance data was normalised with the absorbance at 1.1 V (vs. SCE) given the value of A_{max} = 1 and the absorbance at 0.65 V (vs. SCE) given the value A_{min} = 0. The normalised absorbance (A_{norm}) at each potential is applied to equation 5.3, derived from the Nernst equation.

$$E = E^{\circ\prime} + \frac{RT}{nF} \ln\left\{ \frac{A_{norm}}{1 - A_{norm}} \right\} \qquad (5.3)$$

The overall data set interpreted by equation 5.3 is not entirely linear due to slight deviations in the first few points. These deviations are largely due to small interferences from other bands in the UV/visible spectra which become insignificant at higher A_{norm}, these interference bands arise from species {B} since no deconvolution is performed. If the first four data points in the Nernst plot are neglected then a more linear plot is observed, figure 5.40, with an intercept at 0.87 mV (vs. SCE) corresponding to the mid-peak potential predicted from figure 5.28 for the polymer in pH 0.0 solutions. A gradient of 25.9 mV (r = 0.994, n = 9) is also recorded corresponding to a value of n = 1, indicating that the redox process is indeed nernstian.

The behaviour observed is reversible and repeatable at other values of pH however the kinetics of oxidation and reduction appear to be very slow when the polymer becomes fully oxidised to species {C} probably due to the resistance of the film. This explains why the second redox process looks slightly distorted in its cyclic voltammetry with a large peak

Figure 5.39 The UV/vis absorbance ($\lambda_{max}^{\{C\}}$ = 458 nm) against potential (vs. SCE) for a film of poly(5-carboxyindole) (previously grown for t = 40 s on an ITO electrode) in degassed aqueous pH 0.0 perchloric acid solution

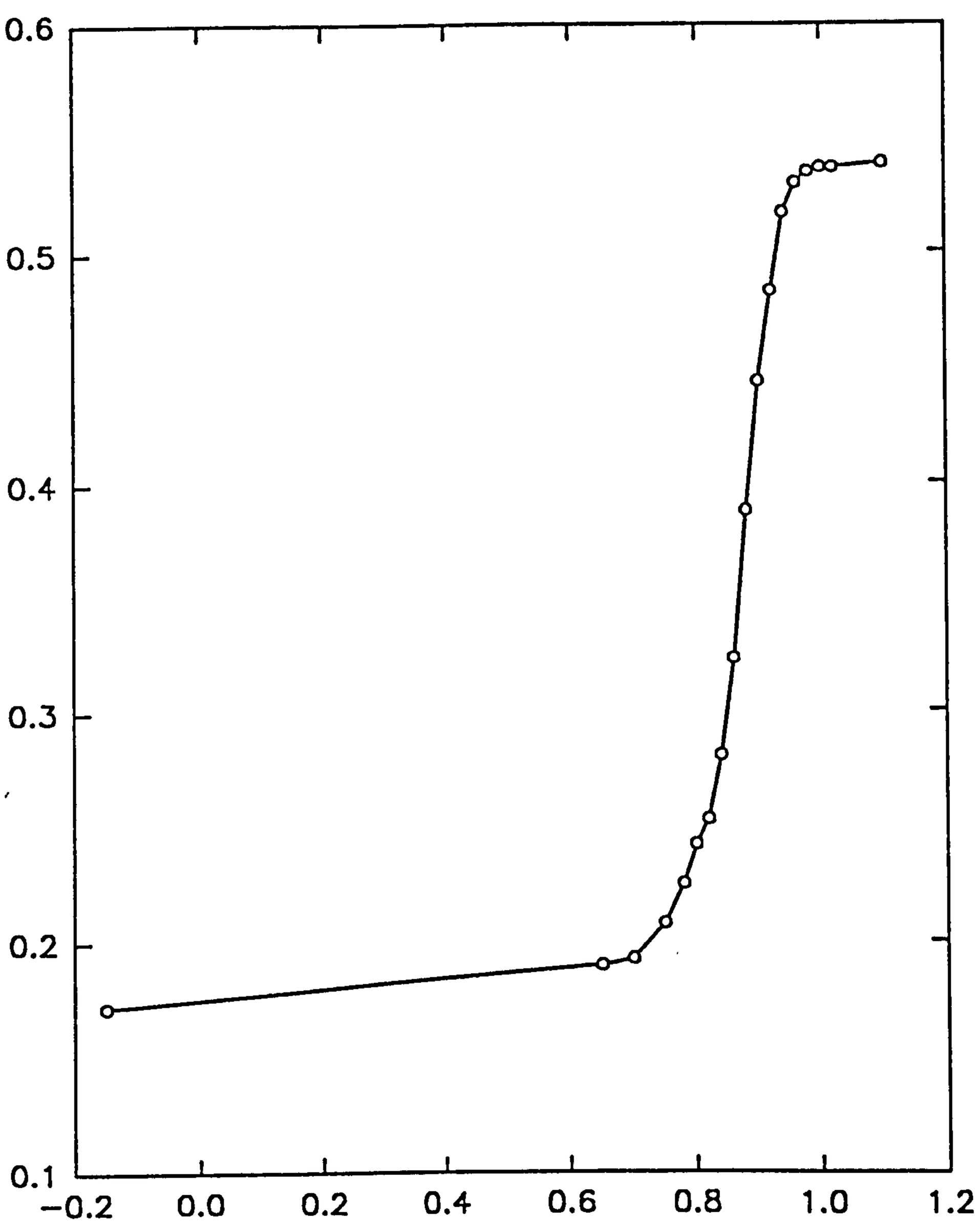

Figure 5.40 Nernst plot for the normalised data shown in figure 5.39 using equation 5.3 and neglecting the first four points ($r = 0.994$, $n = 9$)

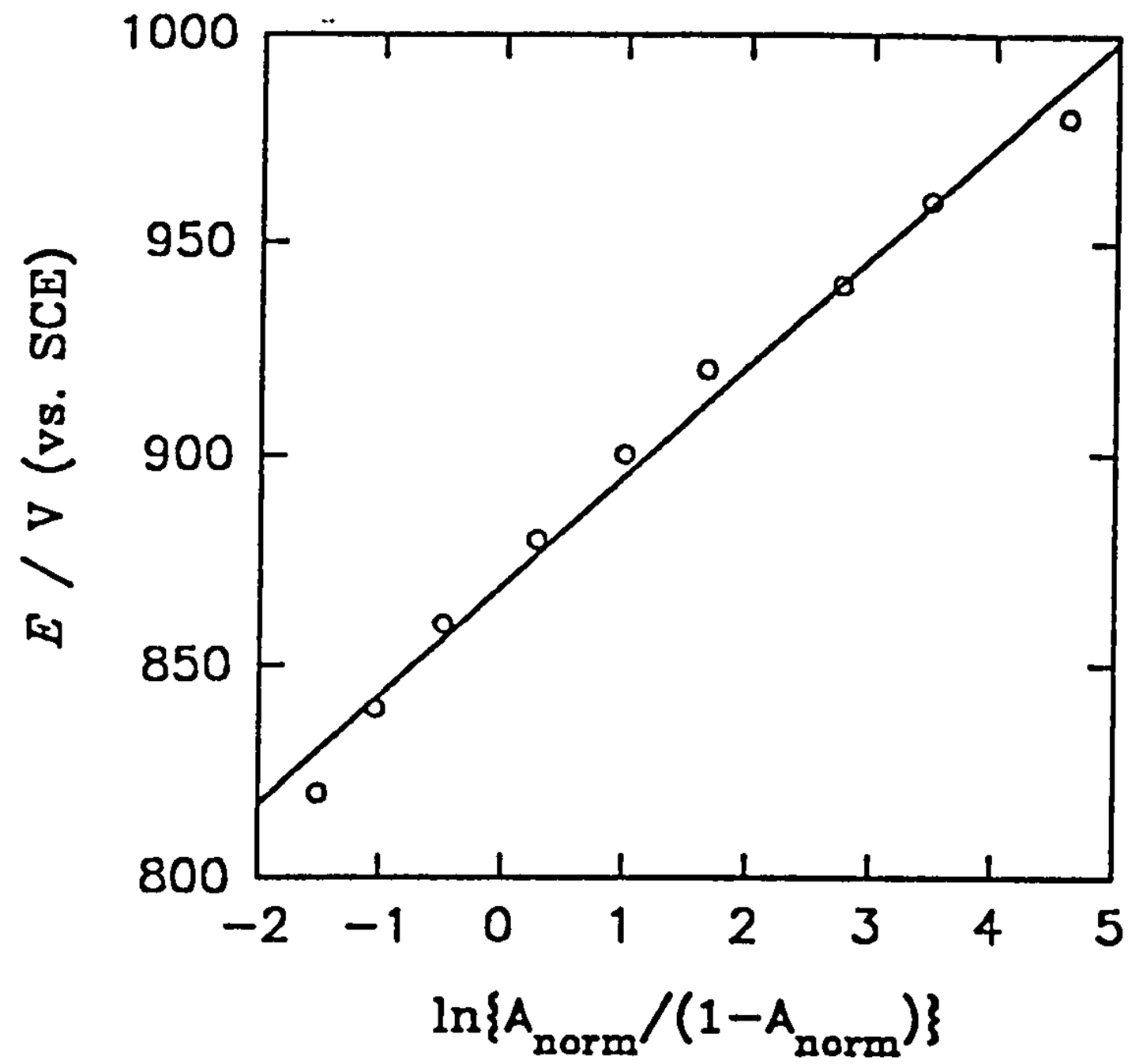

separation and hence does not appear to behave like a standard immobilised electrochemically reversible redox couple.

The extinction coefficient of species {C} remains constant at all pH values since no deviations in the UV/vis spectra of species {C} was recorded using the same film in different pH solutions. The extinction coefficient for species {C} was calculated by studying films of poly(5-carboxyindole) grown for 30 s, 40s and 50s in degassed aqueous pH 3.25 McIlvaine buffer held at 0.9 V (vs. SCE) until the background current decayed to zero. A linear plot was observed, figure 5.41 ($r = 0.999$, $n = 4$), giving an extinction coefficient of $\varepsilon_{\lambda_{max}}^{\{C\}}$ (458 nm) = 3.77×10^6 mol^{-1} cm^2 which is consistent with extinction coefficients recorded for other conducting polymers.[106]

It would be interesting to consider what would happen if the pH were lowered significantly to move $E^{\circ\prime}$ to even higher potentials. The most likely result would be the further deprotonation of the film.

The effect on the concentration of each of the three species during potential stepping from fully reduced potentials to fully oxidised potentials and *vice versa* was briefly studied in degassed aqueous pH 2.00 McIlvaine buffer using a poly(5-carboxyindole) film grown for 40 s. The visible absorptions at both $\lambda_{max}^{\{C\}}$ = 458 nm and $\lambda_{max}^{\{B\}}$ = 722 nm were monitored with time during a potential step. The experimental system used suffered from *iR* drop (see chapter 2) making it impossible to perform a quantitative kinetic study but some interesting results were nevertheless observed which could be interpreted qualitatively. Deconvolution was not performed since only bulk concentration effects are discussed, there are contributions to the absorbance from all three species at the two wavelengths studied but the contribution from species {A} is small at both wavelengths.

Figure 5.41 Plot of absorbance ($\lambda_{max}^{\{C\}}$ = 458 nm) vs. charge density (ρ) (calculated from Q_{CV}) for films of poly(5-carboxyindole) grown on ITO electrodes for t = 30, 40 and 50 s (r = 0.999, n = 4)

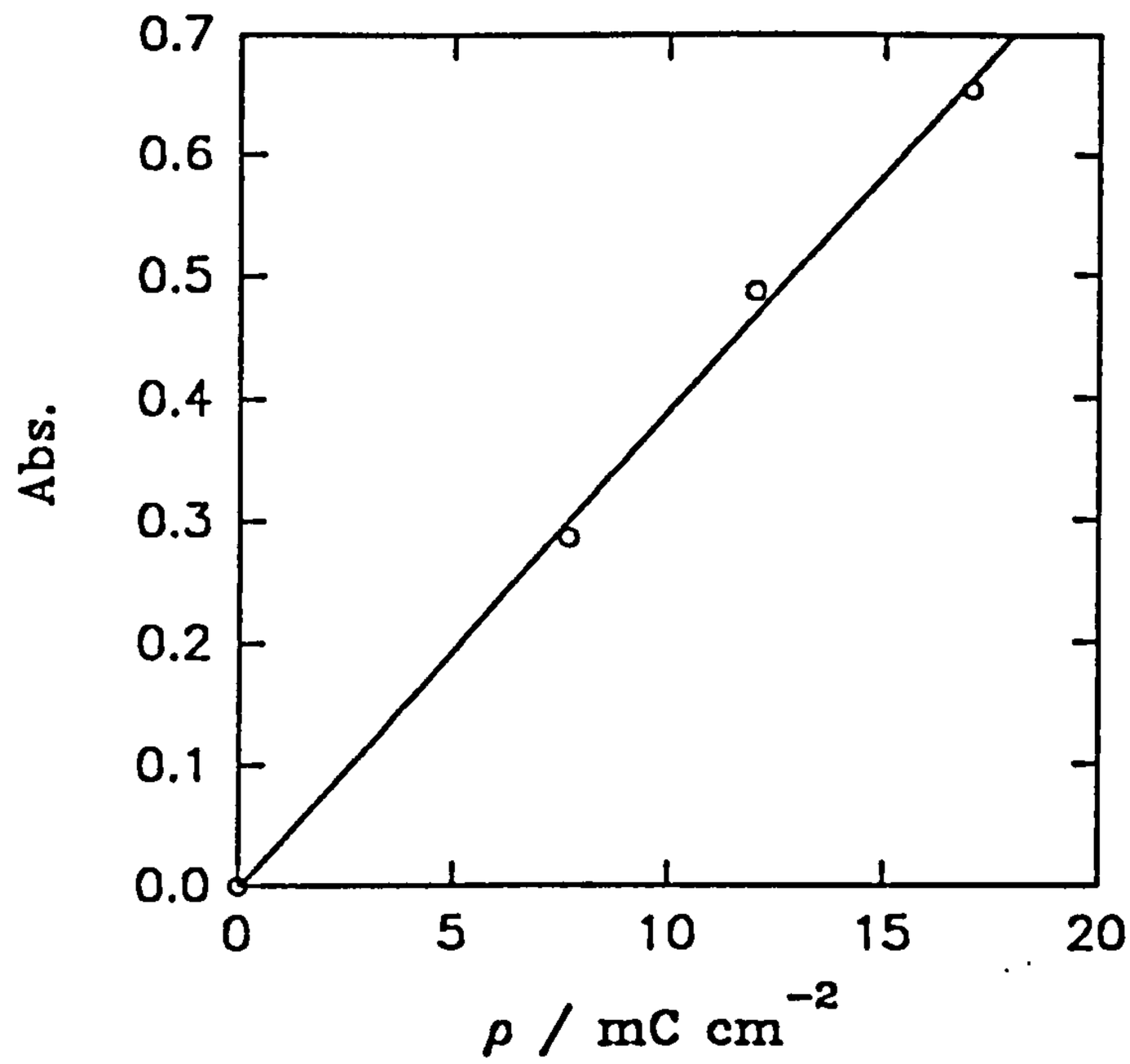

A potential step from 0.0 V to 0.9 V (vs. SCE) performed upon the film, figure 5.42, shows that species {B} is formed and almost completely depleted within the first 10 s. Species {C} begins to form almost immediately when there is a maximum concentration of species {B} present. The complete oxidation of the polymer to species {C} seems to be retarded after 10 s and is not completed after 60s which coincides with a retardation in the depletion of species {B}. This retardation is certainly not due to *iR* drop effects across the solution and is probably due to slow kinetics within the film caused by its resistance.

A potential step from 0.9 V to 0.0 V (vs. SCE) in contrast, figure 5.43, results in the total conversion to species {A} within 20 s. Most of species {C} is depleted in the first 5 s and most of species {B} is depleted in the first 10 s. It is interesting to note that there is some dynamic hysteresis observed between the two potential steps which is probably due to the differences in the conductivity of the two redox species {B} and {C}.

The UV/visible spectra of a poly(5-carboxyindole) film grown for 60 s were recorded in acetonitrile solutions containing TEAT (0.1 mol dm^{-3}) at potentials between -0.4 V and 1.6 V (vs. SCE) at 0.2 V intervals, figure 5.44. The first oxidation process for the formation of species {B} does not have a discernable peak as such but shows an increase in absorbance over a wide spectral range between 450 nm and 820 nm and an isosbestic point at $\lambda_i^{\{A\}-\{B\}} = 418$ nm. When species {C} is formed a $\lambda_{max}^{\{C\}} = 476$ nm is recorded and two isosbestic points are observed at $\lambda_{i,2}^{\{B\}-\{C\}} = 412$ nm and $\lambda_{i,1}^{\{B\}-\{C\}} = 658$ nm which are fairly similar to the previously reported values in aqueous solution. A peak associated with the fully reduced species {A} is also observed at $\lambda_{max}^{\{A\}} = 342$ nm.

Figure 5.42 The UV/vis absorbance vs. time (t) for a potentiometric step from 0.0 V to 0.9 V (vs. SCE) recorded at $\lambda_{max}^{\{C\}}$ = 458 nm and $\lambda_{max}^{\{B\}}$ = 722 nm for a film of poly(5-carboxyindole) (previously grown for t = 60 s on an ITO electrode)

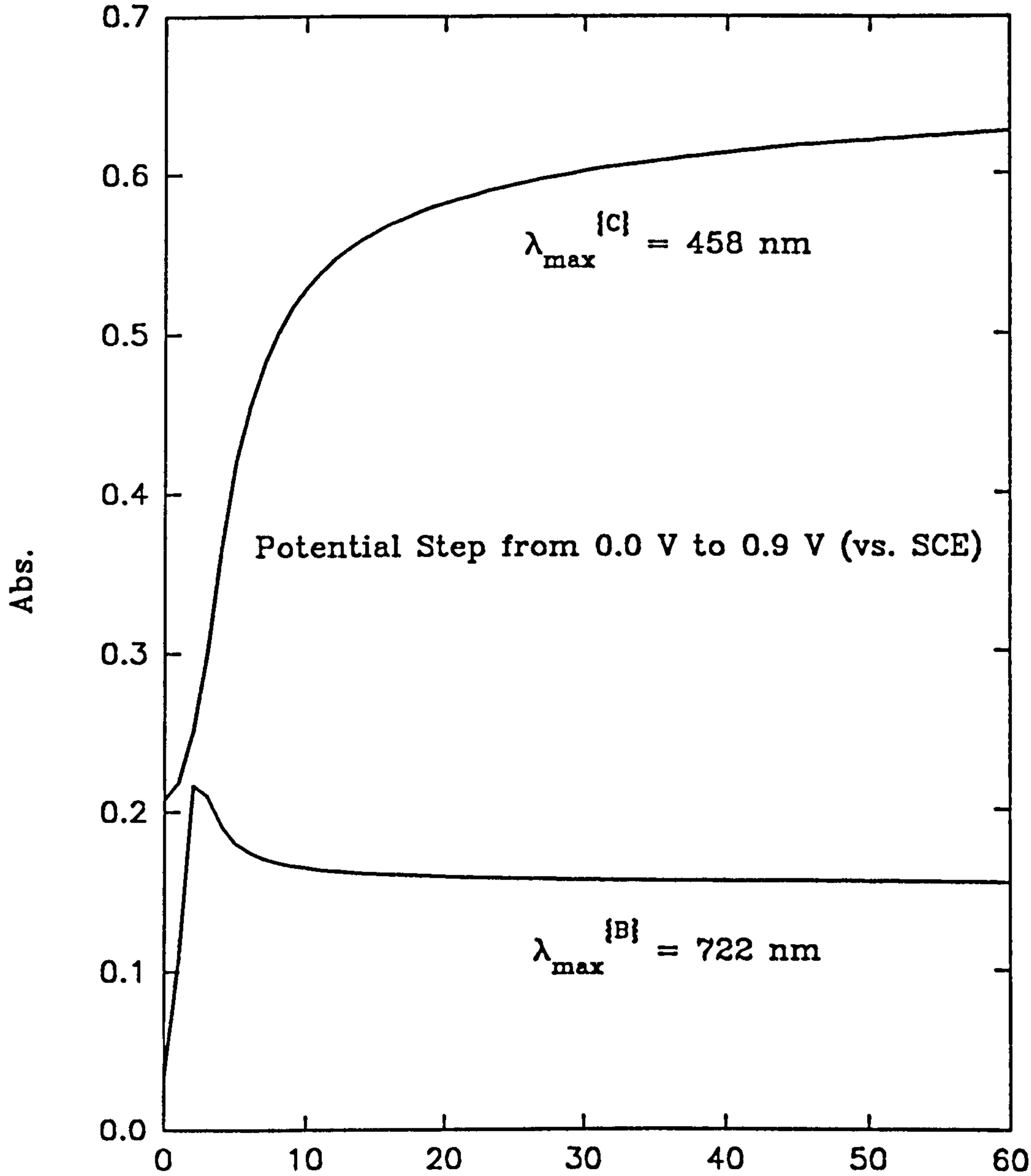

Figure 5.43 The UV/vis absorbance vs. time (t) for a potentiometric step from 0.9 V to 0.0 V (vs. SCE) recorded at $\lambda_{max}^{\{C\}} = 458$ nm and $\lambda_{max}^{\{B\}} = 722$ nm for a film of poly(5-carboxyindole) (previously grown for $t = 60$ s)

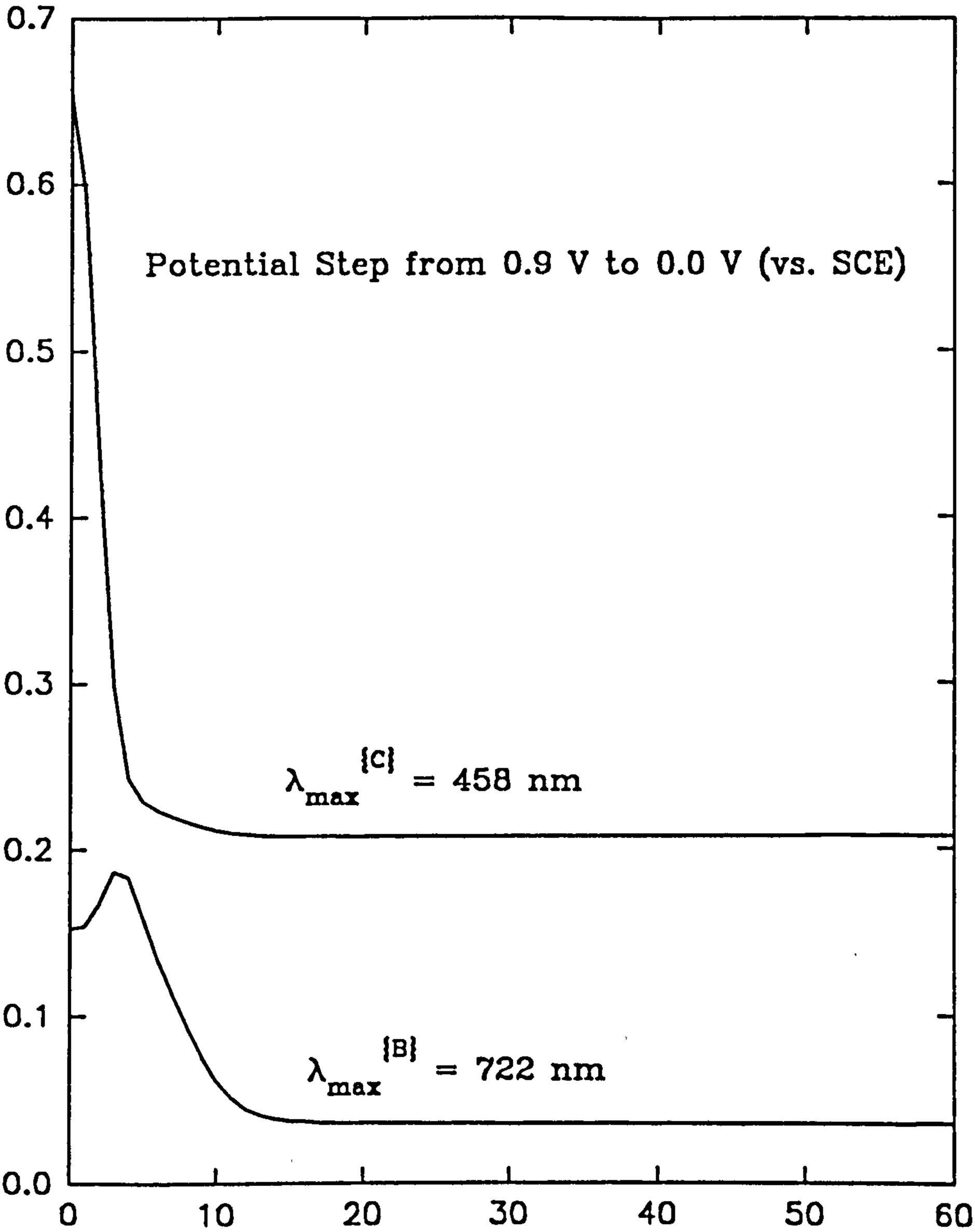

Figure 5.44 The UV/vis spectra of a poly(5-carboxyindole) film (previously grown for t = 40 s on an ITO electrode) recorded in acetonitrile containing TEAT (0.1 mol dm^{-3}) at stationary potentials between -0.4 V and 1.6 V (vs. SCE) at intervals of 0.2 V

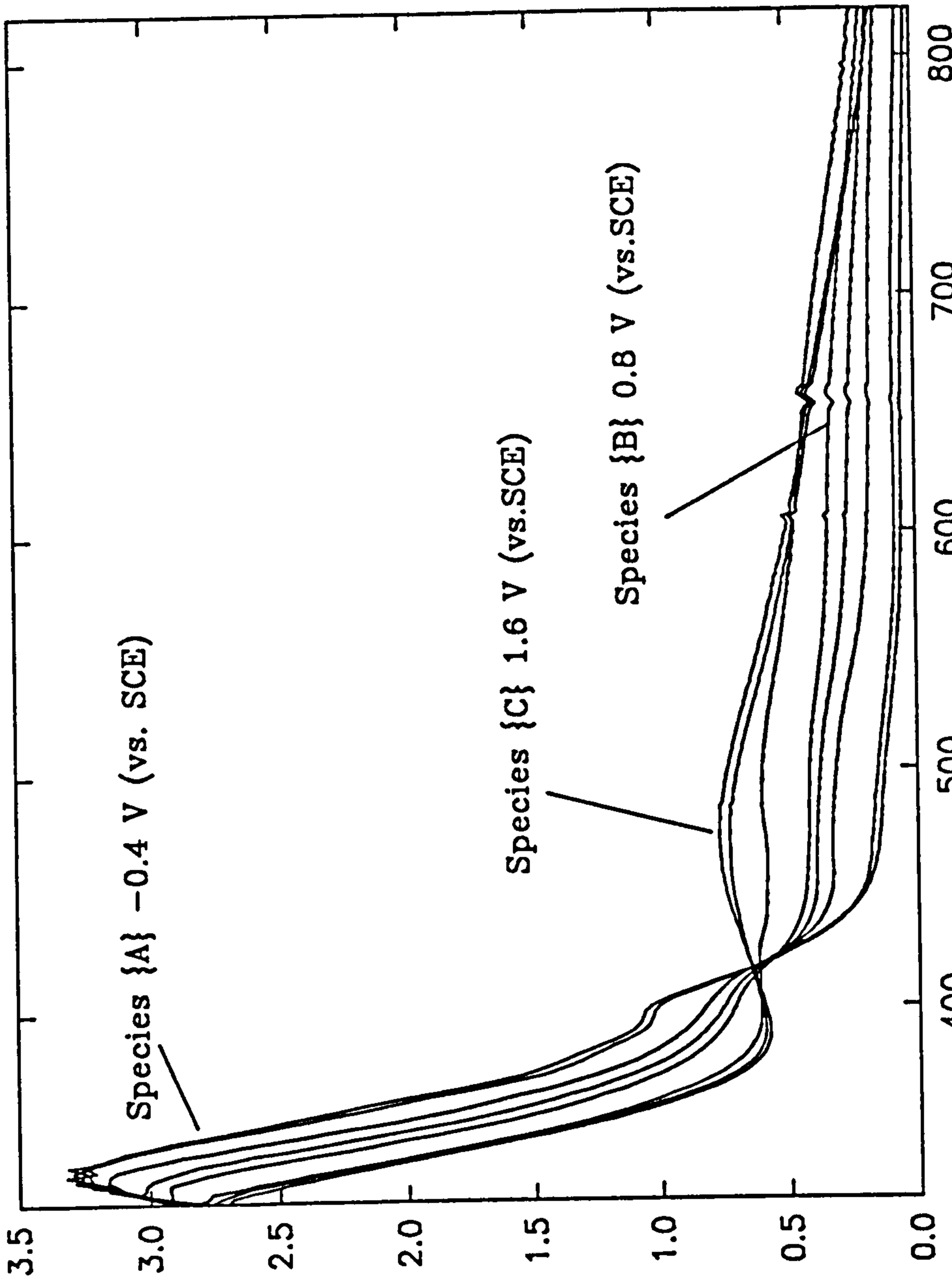

It seems that species {B} shows the greatest difference in its UV/vis spectroscopy in acetonitrile compared to that observed under aqueous conditions. This is not surprising since the electrochemistry observed by cyclic voltammetry in both solutions is quite different especially when the nature of the first oxidation process is considered. No major UV/vis studies were performed in acetonitrile solutions because of the film's relative instability in this media. Because of this the results reported above, which were performed in acetonitrile solutions, may have slight errors associated with them.

5.7 Impedance Spectroscopy of Poly(5-carboxyindole)

Impedance spectroscopy was performed on poly(5-carboxyindole) films, grown for 30 s, in degassed aqueous buffer solutions at pH 1.00, 3.25 and 5.00 chosen specifically to cover the different protonation states of the polymer, figure 5.28. The pH 3.25 and 5.00 solutions were McIlvaine buffers and the pH 1.00 solution was a concentrated citric acid solution. The films were held at -0.2 V and 0.2 V (vs. SCE) as well as at the mid-peak potential ($E^{\circ\prime}$) of the second oxidation process and at fully oxidised potentials at the particular pH values studied. The amplitude of the modulation was 10 mV (RMS) and the frequency range was from 50 mHz to approximately 100 Hz. The Nyquist plots recorded at 0.2 V (vs. SCE) and at the mid-peak potentials were similar to Nyquist plots of a resistance and capacitance in series.[107] The results obtained at pH 3.25 are typical of the standard results obtained, figure 5.45, the resistance being largely due to uncompensated solution resistance. Interpreting these results using equation 4.1 gives linear plots, figure 5.46, from which capacitance can be calculated.

Figure 5.45 The Nyquist plots for a film of poly(5-carboxyindole) (previously grown for t = 30 s on a platinum electrode (A = 0.385 cm^2)) held at 0.2 V (○) and 0.535 V (●) (vs. SCE) in aqueous pH 3.25 buffer (amplitude = 10 mV (RMS), frequency range - 50 mHz to 100 Hz)

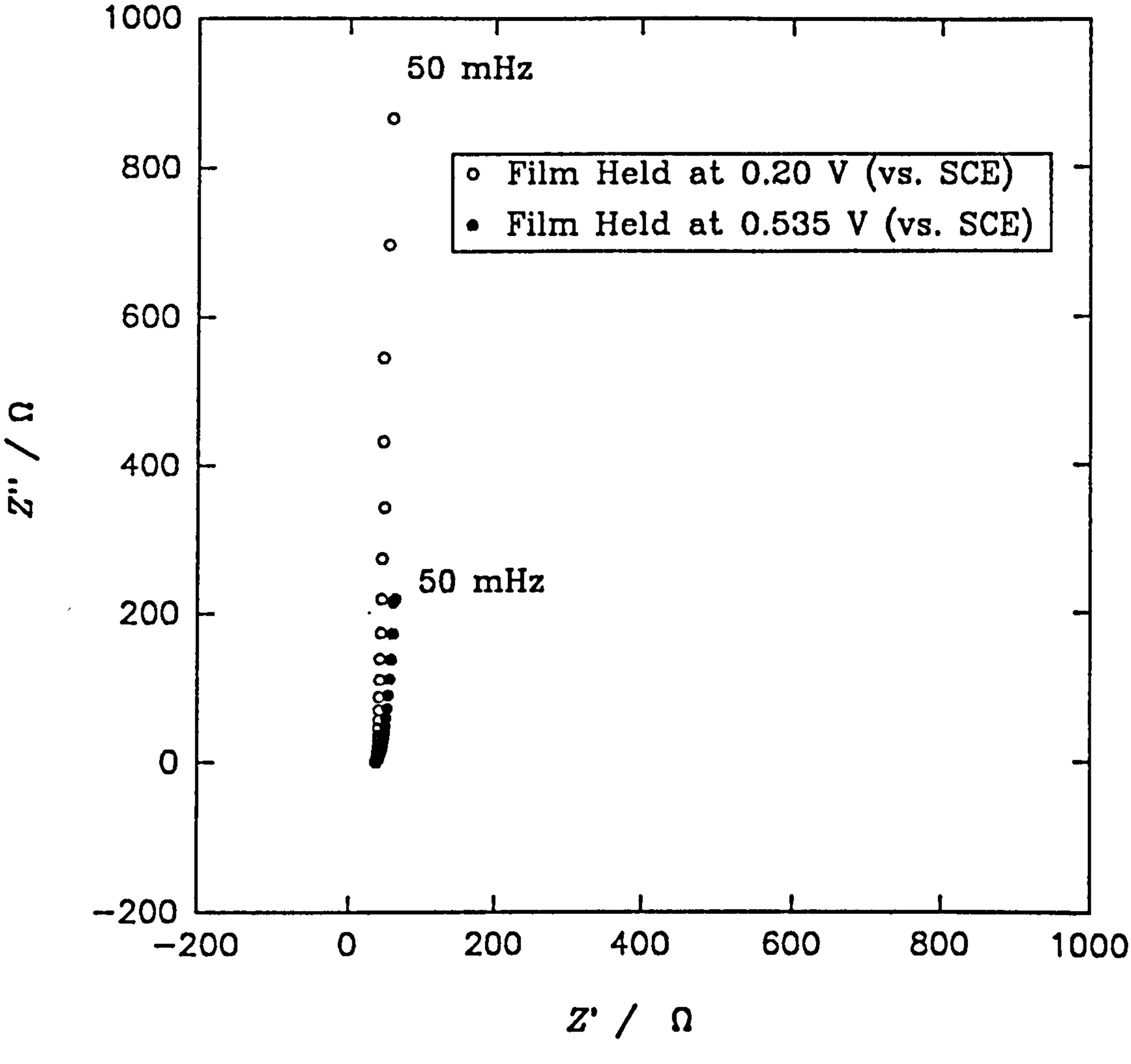

Figure 5.46 Interpretation of the data shown in figure 5.45 using equation 4.1

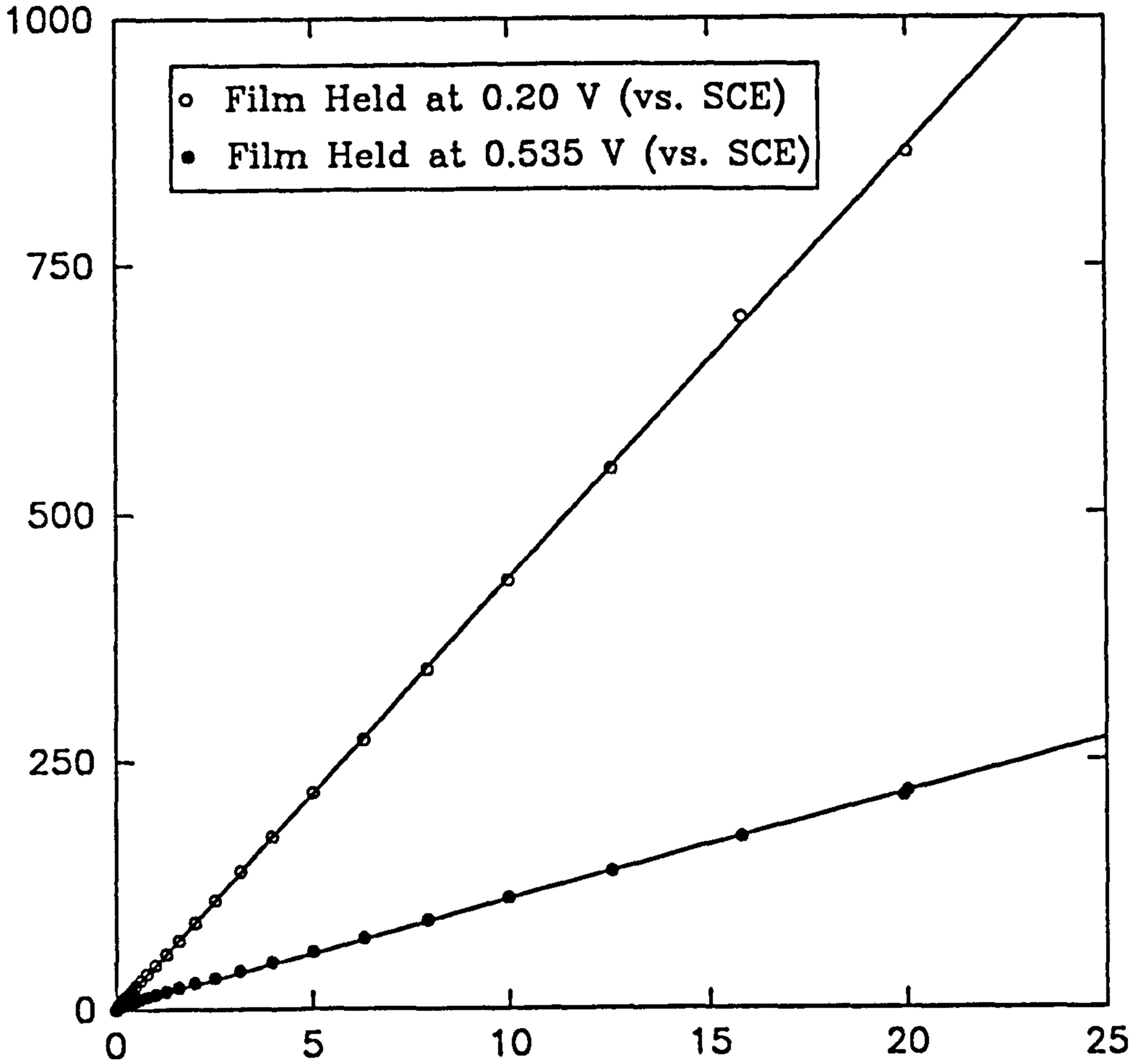

Table 5.3, shows the capacitances measured over the potential and pH ranges studied. For comparison the capacitances of a clean polished platinum disc electrode (A = 0.385 cm^2) held at 0.0 V (vs. SCE) were also studied in the three pH solutions by recording impedance spectra at frequencies of between 100 Hz to 500 Hz.

The results obtained for the clean platinum electrode were consistent with those expected for polycrystalline platinum. The capacitances recorded for poly(5-carboxyindole) at 0.2 V (vs. SCE) were consistent at all pH values within experimental error and are three orders of magnitude higher than the clean polished platinum electrode. The capacitances observed for poly(5-carboxyindole) at the mid-peak potential were approximately four times bigger than those recorded at 0.2 V (vs. SCE). When the films were either fully reduced at -0.2 V (vs. SCE) or in their fully oxidised state the measured capacitances were significantly reduced to values more comparable to those for clean polished platinum.

This data suggests that poly(5-carboxyindole) is electronically insulating in both its fully reduced and fully oxidised state but that it is also porous enabling the aqueous solution to contact with the underlying platinum electrode, this is supported by SEM data (appendix 2) provided by Dr. J. Farrington. Further confirmation of the resistance of a fully oxidised film of poly(5-carboxyindole) grown for 30 s, was gained by contacting with a drop of mercury. The film was found to be 10^3 times more resistive when removed from a pH 3.25 degassed aqueous solution in its fully oxidised state at 1.0 V (vs. SCE) than when it was removed from the same solution after being held at 0.4 V (vs. SCE). The resistance measured for the fully reduced film held at -0.1 V (vs. SCE) was found to be inconclusive presumably because of aerial oxidation.

Table 5.3 The capacitances of poly(5-carboxyindole) (previously grown for t = 60 s on a platinum electrode (A = 0.385 cm^2)) measured at -0.2 V, 0.2 V, the mid-peak potential ($E°'$) and fully oxidised potentials (vs. SCE) in aqueous pH 1.00, 3.25 and 5.00 buffer solutions

Electrode	Capacitance / mF cm^{-2}		
	pH 1.00	pH 3.25	pH 5.00
Clean Pt electrode 0.0 V	0.063	0.035	0.044
Coated Pt electrode			
-0.2 V	[a]	0.47	0.047
+0.2 V	9.5	9.5	10.7
mid-peak	40.0	37.0	37.0
fully oxidised	0.044	0.058	0.10

[a] Outside solvent limit.

Using the same assumptions that were made in section 4.4, (chapter 4), that the polymer is in the form of fibres which can be approximated to a continuous cylinder with radius r_{CYL}, the capacitance of the polymer was compared to the capacitance of the clean platinum electrode. The volume of a poly(5-carboxyindole), grown for 30s, was calculated to be $V_{TOT} = 5.0 \times 10^{-12}$ m^3 from a monomer volume estimated from molecular modelling to be $V_{MON} = 5.63 \times 10^{-29}$ m^3, taking the dopancy to be $\delta = 0.49$. When the capacitance of the poly(5-carboxyindole) film in pH 3.25 buffer at the mid-peak potential of the second oxidation process ($E^{\circ\prime}$ = 5.35 V (vs.SCE)) is compared to that of polished clean platinum at 0.0 V (vs. SCE), table 5.3, the effective area of the polymer compared to platinum is estimated to be $A_{EFF} = 0.041$ m^2. The radius of the cylinder is hence calculated to be $r_{CYL} = 1.2 \times 10^{-10}$ m or 1.2 Å which again is at the molecular level.

The results observed are consistent with the assumption that the second oxidation process behaves like an immobilised redox couple since when fully oxidised there are no sites available for electron hopping and resistive behaviour would be predicted. This was further investigated by studying a film of poly(5-carboxyindole), grown for 30 s before being introduced to aqueous conditions and placed in a degassed pH 3.25 McIlvaine buffer solution at a range of potentials from between 0.2 V to 1.1 V (vs. SCE), figure 5.47, using the impedance spectroscopy modulated amplitude and frequency values previously described.

For a simple immobilised redox couple a simple gaussian distribution for the capacitance with potential is predicted centred upon the redox potential ($E^{\circ\prime}$) of the couple (appendix 3). A simple gaussian is not observed because of the continued presence of species {A} at lower potentials, however a peak in capacitance is observed at E = 0.55 V (vs. SCE) which is approximately the $E^{\circ\prime}$ predicted from figure 5.28. Again very little hysteresis was observed since half the

Figure 5.47 The capacitance of a poly(5-carboxyindole) film (previously grown for t = 30 s at a platinum electrode (A = 0.385 cm^2) over a range of stationary potentials (vs. SCE) in aqueous pH 3.25 buffer

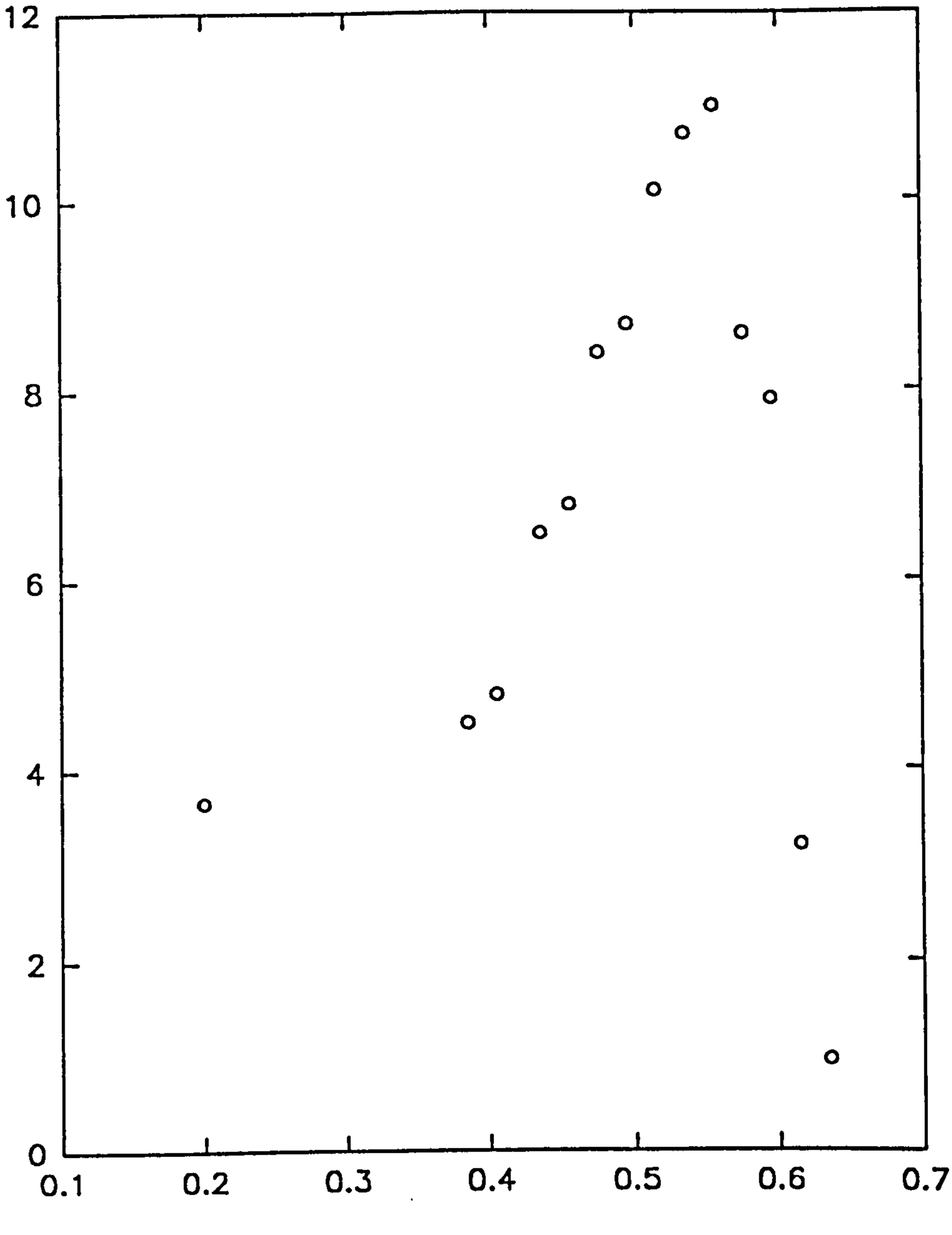

readings were taken after cathodic potential steps and the other half were taken after anodic potential steps.

The impedance spectroscopy of poly(5-carboxyindole) films grown for 15, 30 and 45 s, held at 0.535 V (vs. SCE), were studied using an ac modulation of 10 mV (RMS) from 50 mHz to approximately 100 Hz in degassed aqueous pH 3.25 McIlvaine buffer solution. The capacitances obtained gave a excellent linear relationship when plotted against Q_{CV}, figure 5.48 with a gradient of 5.1 V^{-1} cm^{-1} ($r = 0.999$, $n = 3$) showing that the capacitance measured depends upon the amount of material deposited upon the electrode.

5.8 Conclusion

The electrochemical polymerisation of a stable reproducible poly(indole) film has been achieved in acetonitrile solutions although stable aqueous electrochemistry was not observed.

Initial studies on the mechanism of polymerisation for poly(5-carboxyindole) have been described showing that the kinetics of polymerisation are potential dependent, zero order with respect to the concentration of 5-carboxyindole, at low rotation speeds, and that the polymerisation proceeds through a surface bound species.

The characterisation of the properties of poly(5-carboxyindole) has been much improved with chemical structural information provided by reflectance FTIR confirming the bonding at the 1 and 3 positions on the five membered ring. The structure of poly(indole) is thought to be through the same bonding positions as poly(5-carboxyindole) because of the similarities observed in the reflectance FTIR spectra.

Figure 5.48 The capacitance vs. Q_{CV} for films of poly(5-carboxyindole) (grown previously for t = 15, 30 and 45 s at a platinum electrode (A = 0.385 cm^2)) held at 0.535 V (vs. SCE) in degassed aqueous pH 3.25 buffer solution

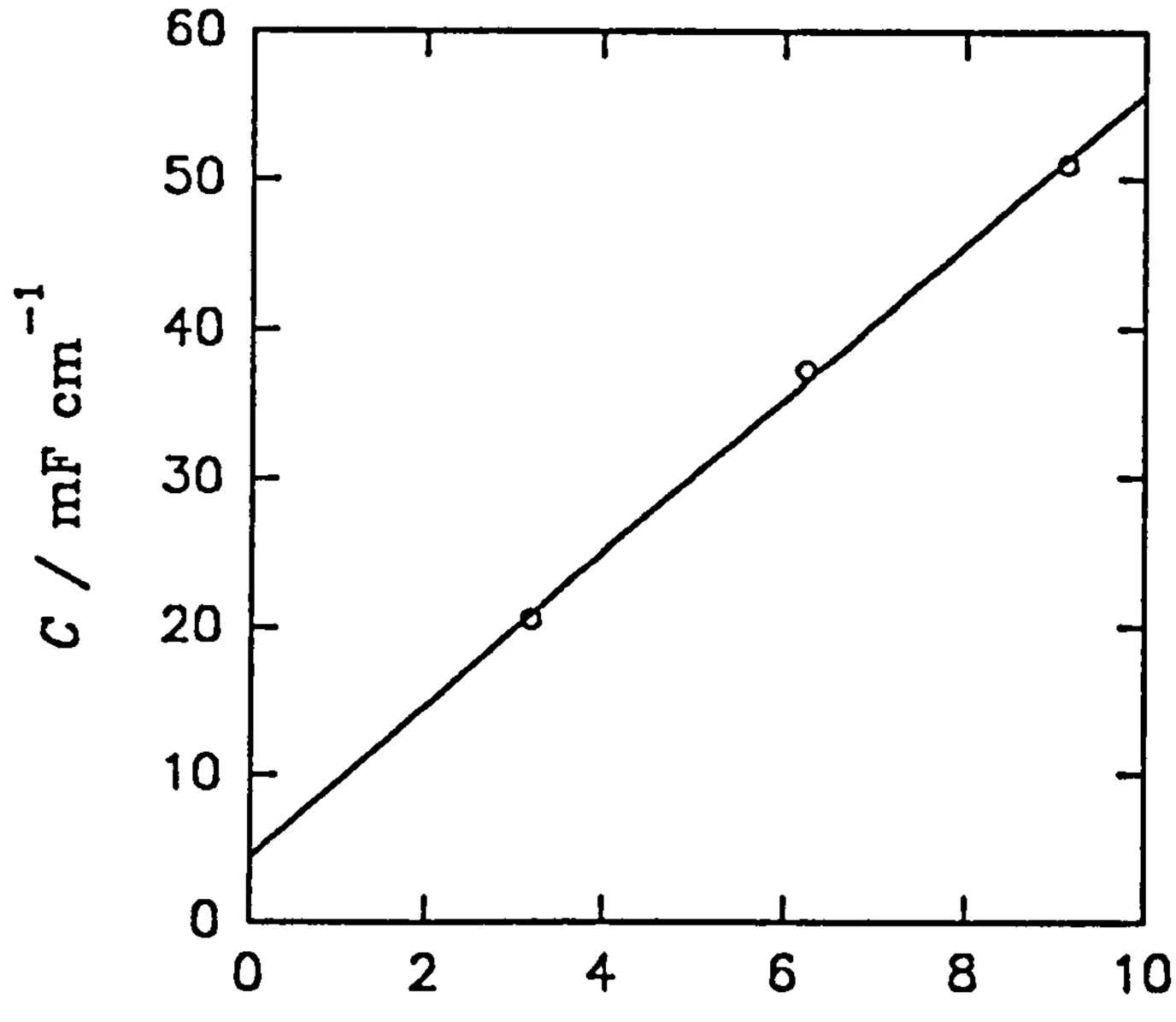

The aqueous electrochemistry of poly(5-carboxyindole) proved to be of particular interest with two distinguishable oxidation processes, the second having a pH dependency which could be attributed to self doping or partial self doping of the polymer upon deprotonation. The extent of the self doping was found to be dependent upon the pK_as of the partially oxidised polymer (pK_Y = 2.5) and the fully oxidised polymer (pK_X = 4.1). The nature of the oxidation processes and the two species {B} and {C} were characterised using UV/vis spectroscopy confirming that the second oxidation process behaved like a simple nernstian redox couple while the concentration of species {B} increased linearly with potential when species {A} was oxidised.

Impedance spectroscopy also confirmed that the second oxidation process behaved like a nernstian redox couple in addition to confirming that the polymer becomes electrically insulating at fully oxidised or reduced potentials. In this respect the polymer has similarities with poly(aniline)[21] which also displays variation in colour in its different oxidation states. The first oxidation process is however very different from poly(aniline) and still remains a very interesting phenomenon especially when its relationship to the second oxidation process is considered.

The main points that still remain unanswered are concerned with the nature of the first oxidation process and the structure of species {A}, {B} and {C}. The use of *in-situ* FTIR, e.s.r. and potentiodynamic UV/vis spectrometry would enable the chemical structure, spin density and kinetics of formation of all the species ({A}, {B} and {C}) to be determined. A quartz crystal microbalance (QCM) could be used to further investigate the complicated self doping and partial self doping effects suggested in the text, figure 5.28.

Chapter 6

General Conclusions

The electrochemistry of several chemically modified heterocyclic conducting polymers has been studied in conjunction with several other powerful analysis techniques. The major classes of heterocyclic conducting polymers namely poly(pyrroles), poly(thiophenes) and poly(indoles) have been covered with a particular emphasis placed upon carboxylic acid modifications.

Poly(pyrroles) have only briefly been studied but useful FT-IR data has been recorded suggesting that the covalently bound functionalities are affected by counter ion incorporation. The first conducting polymer incorporating a 15-crown-5 substituent has been reported (appendix 1). However, the electrochemistry of this polymer was found to be surprisingly independent of the alkali cation type present in electrolyte solutions. This has been attributed to steric restrictions within the polymer which prevent the complexation of cations with the crown ether substituent.

Poly(thiophenes) have been studied more intensely with particular emphasis placed upon poly(3-thiopheneacetic acid) which was found to undergo an extraordinary overoxidation process involving the acetic acid substituent. Some techniques to further modify the thiopheneacetic acid have been discussed but this remains an area which could potentially be expanded in order to introduce poly(thiophenes) into aqueous solutions. The use of carbodiimide chemistry opens up the area of biosensing. However this area is likely to be initially more successful using polymers which already display stable electrochemistry under aqueous conditions. Impedance spectroscopy has shown that the asymmetry observed in the poly(3-methylthiophene) cyclic voltammetry is thermodynamically based and not kinetic in nature.

Poly(indoles) have been studied intensely and this is the area in which the greatest advances have been made. Poly(indole) itself has been grown on platinum electrodes in the form of good quality and electrochemically reproducible films. The chemical structures of poly(indole) and poly(5-carboxyindole) have been characterised by FT-IR spectrometry confirming that bonding occurs at the 1 and 3 positions of the monomers. The electrochemical growth of poly(5-carboxyindole) has been further characterised using rotating disc and rotating ring disc experiments showing a marked potential dependence. In addition the polymerisation was found to be diffusion limited at low rotation speed and zero order with respect to the monomer concentration at high rotation speed. Only protons were detected at the ring, formed during the polymerisation at the disc and no evidence for soluble oligomeric by-products was found. This data suggests that the polymerisation is very efficient and proceeds via a surface bound site.

The electrochemistry of poly(5-carboxyindole) has been further characterised (appendix 2) with the pH response of the second redox process species {B} to {C} being interpreted as a nernstian redox couple which is confirmed by both UV/vis and impedance spectroscopy. The first oxidation process species {A} to {B} still remains largely uncharacterised although it is suggested that the incorporation of counter ions into the film is resisted mechanically, introducing an extra free energy term to the Nernst equation which results in an oxidation over a wider potential range.

Impedance spectroscopy performed upon poly(5-carboxyindole) suggests that the polymer is electronically insulating when fully oxidised or reduced. The maximum capacitance observed occurs at the $E^{\circ\prime}$ of the second oxidation process as would be expected from an immobilised redox couple (appendix 3).

Both poly(3-methylthiophene) and poly(5-carboxyindole) displayed impedance spectra which can be interpreted as a resistance and capacitance in series giving particularly large values for the capacitances. These values were interpreted as being due to the charging of the polymers at the molecular level. These results are not necessarily so surprising considering the very low frequencies used for the studies. It is also very important to define the interface at which the capacitance is acting. If the interface is defined as the traditional electrode/polymer interface it is hard to describe what the capacitance values reported actually mean. However, a more sensible interface to consider would be the polymer/solution interface, now the capacitances measured can easily be interpreted as a simple manifestation of the redox behaviour of the polymer with charge separation occurring between the chains and the counter ions.

There still remains much to be studied before a complete characterisation of poly(5-carboxyindole) and the other polymers mentioned in this thesis is attained. The polymers studied are so rich in their various properties that a list of all possible investigations which could be made would be impractical to report. However it would suffice to say that the area of conducting heterocyclic polymers is likely to remain a very fruitful area of interest.

References

1) H. Shirakawa and S. Ikeda, *Synth. Met.*, 1(1980)175.

2) S. Elemad, A. J. Heeger and A. G. A. MacDiarmid, *Rev. Phys. Chem.*, 33(1982)443.

3) H. Shirakawa and S. Ikeda, *J. Polym. Sci., Polymer Chem. Ed.*, 12(1974)11.

4) H. Shirakawa, E. J. Louis, A. G. Macdiarmid, C. K. Chiang and A. J. Heeger, *J. Chem. Soc., Chem. Commun.*, (1977)578.

5) D. O. Cowan and F. W. Wylgal, *Chemistry and Engineering*, (1986)28.

6) T. A. Skotheim (Ed), *Handbook of Conducting Polymers*, Vol. 2. Marcel Dekker. New York., 1986.

7) N. Basescu, Z-X. Liu, D. Moses, A. J. Heeger, H. Naarmann and N. Theophilou, *Nature*, 327(1987)403.

8) W. J Feast, in: T. A. Skotheim (Ed), *Handbook of Conducting Polymers*, Vol. 1. Marcel Dekker. New York., 1986 p1.

9) J. E. Frommer, *Acc. Chem. Res.*, 19(1986)2.

10) G. P. Gardini, *Adv. Hetrocyclic Chem.*, 15(1973)67.

11) K. K. Kazanawa, A. F. Diaz, W. D. Gill, P. M. Grant, G. B. Street, G. P. Gardini and J. F. Kwak, *Synth. Met..*, 1(1980)329.

12) K. K. Kazanawa, A. F. Diaz, R. H. Geiss, W. D. Gill, J. F. Kwak, J. A. Logan, J. F. Rabolt and G. B. Street, *J. Chem. Soc. Chem. Commun.*, (1979)854.

13) A. F. Diaz, K.K. Kazanawa and G. P. Gardini, *J. Chem. Soc. Chem. Commun.*, (1979)635.

14) A. Dall'Olio, Y. Dascola, V. Varacio and V. Bocchi, C. R. Acad. Sci., 267(1968)433.

15) P. R. Moses, L. Wier and R. W. Murray, *Anal. Chem..*, 45(1975)1882.

16) P. N. Bartlett, P. Tebbutt and R. G. Whitaker, *Progress in Reaction Kinetics*, 16(1991)55.

17) P. G. Pickup, *J. Electroanal. Chem.*, 225(1987)273.

18) J. W. Gardner and P. N. Bartlett (Ed), *Sensors and Sensory Systems for an Electronic Nose*, Kluwer Academic Publishers. Dordrecht, 1992.

19) F. Garnier, G. Tourillon, M. Gazard and J. C. Dubris, *J. Electroanal. Chem.*, 148(1983)299.

20) R. A. Bull, F-R. Fan and A. J. Bard, *J. Electrochem. Soc.*, 129(1982)1009.

21) A. F. Diaz and J. A. Logan, *J. Electroanal. Chem.*, 111(1980)111.

22) G. Schiavon, G. Zotti and G. Bontempelli, *J. Electroanal. Chem.*, 194(1984)327.

23) R. J. Waltman, A. F. Diaz and J. Bargon, J. Phys. Chem., 88(1984)4343.

24) G. Tourillon and F. Garnier, *J. Electroanal. Chem.*, 135(1982)173.

25) E. M. Genies, G. Bidan and A. F. Diaz, *J. Electroanal. Chem.* 149(1983)101.

26) S. Asavapiriyanot, G. K. Chandler, G. A. Gunawardena and D. Pletcher, *J. Electroanal. Chem.*, **177**(1984)229.

27) G. B. Street in: T. A. Skotheim (Ed), *Handbook of Conducting Polymers*, Vol. 1. Marcel Dekker. New York., 1986 p268.

28) F. Beck, P. Braun and F. Schloten, *J. Electroanal. Chem.*, **267**(1989)141.

29) A. F. Diaz and J. I. Castillo, *J. Chem. Soc. Chem. Commun.*, (1980)397.

30) R. J. Waltman, J. Bargan and A. F. Diaz, *J. Phys. Chem.*, **87**(1983)1459.

31) T. Inoue and T. Yamase, *Bull. Chem. Soc. Jpn.*, **56**(1983)985.

32) M. Takakubo, *J. Electroanal. Chem.*, **258**(1989)303.

33) K. Imanishi, M. Satoh, Y. Yasuda, R. Tsushima and S. Aoki, *J. Electroanal. Chem.* **242**(1988)203.

34) K. Imanishi, M. Satoh, Y. Yasuda, R. Tsushima and S. Aoki, *J. Electroanal. Chem.*, **260**(1989)469.

35) A. J. Downard and D. Pletcher, *J. Electroanal. Chem.*, **206**(1986)147.

36) F. Beck, P. Brown and M. Oberst, *Ber. Bunsenges. Phys. Chem.*,**91**(1987)967.

37) E. W. Tsai, S. Basak, J. P. Ruiz, J. R. Reynolds and K. Rajeshwar, *J. Electrochem. Soc.*, **136**(1989)3683.

38) A. R. Hillman and E. F. Mallen, *J. Electroanal. Chem.*, **220**(1987)351.

39) A. J. Downard and D. Pletcher, *J. Electroanal. Chem.*, **206**(1986)139.

40) S . Asavapiriyonant, G. K. Chandler, G. A. Gunawardena and D. Pletcher, *J. Electroanal. Chem.*, **177**(1984)229.

41) G. Zotti, G. Schiavon, A. Berlin and G. Payani, *Electrochimica Acta.*, **34**(1989)881.

42) A. Hamnett and A. R. Hillman, *J. Electrochem. Soc.*, **135**(1988)2517.

43) A. R. Hillman and E. F. Mallen, *J. Electroanal. Chem.*, **243**(1988)403.

44) A. T. Hubberd and F. C. Anson, *J. Electroanal. Chem.*, 4(1970)129.

45) S. W. Feldberg, *J. Am. Chem. Soc.*, **106**(1984)4671.

46) E. M. Genies and J. -M. Pernaut, *J. Electroanal. Chem.*, **191**(1985)111.

47) J. L. Bredas and G. B. Street, *Acc. Chem. Res.*, **18**(1985)308.

48) A. R. Bishop, D. K. Campbell and K. Fesser, *Mol. Cryst. Liq. Cryst.*, 77(1981)253.

49) J. Bredas, R. R. Chance and R. Sibley, *Phys. Rev. B.*, **26**(1982)5843.

50) J. Heinze, M. Störzbach and J. Mortensen, *Ber. Bunsenges Phys. Chem.*, **91**(1987)960.

51) K. Meerholz and J. Heinze, *Angew. Chem. Int. Ed. Engl.*, **29**(1990)692.

52) K. Meerholz and J. Heinze, *Synth. Met.*, 43(1991)2871.

53) W. J. Albery, Z. Chen, B. R. Horrocks, A. R. Mount, P. J. Wilson, D. Bloor, A. T. Monkman and C. M. Elliot, *Faraday Discuss. Chem. Soc.*, 88(1989)247.

54) G. Wegner and J. Rühe, *Faraday Discuss. Chem. Soc.*, 88(1989)333.

55) J. M. Pernaut, R. C. D. Peres, V. F. Juliano and M-A. De Paoli, *J. Electroanal. Chem.*, 274(1989)225.

56) F. F. Fan and A. J. Bard., *J. Electrochem. Soc.*, 133(1989)307.

57) T. Shimidzu, A. Ohtani, T. Iyoda and K. Honda, *J. Electroanal. Chem.*, 251(1987)323.

58) T. Shimidzu, A. Ohtani, T. Iyoda and K. Honda, *J. Electroanal. Chem.*, 224(1987)123.

59) C. M. Elliot, A. B. Kapelove, W. J. Albery and Z. Chen, *J. Phys. Chem.*, 95(1991)1743.

60) A. Patil, Y. Ikenou, F. Wudl and A . J. Heeger, *J. Am. Chem. Soc.*, 109(1987)1858.

61) A. Patil, Y. Ikenoue, N. Basescu, N. Colemeri, J. Chen, J. Wudl and A. J. Heeger, *Synth. Met.*, 20(1987)151.

62) N. Sunderson, S. Basch, M. Pomerantz and J. Reynolds, *J. Chem. Soc., Chem. Commun.*, (1987)621.

63) P. Audebert and G. Bidan, *J. Electroanal. Chem.*, 190(1985)129.

64) Q-Z. Zhou, C. J. Kolaskie and L. L. Miller, *J. Electroanal. Chem.*, 223(1987)283.

65) H. Harada, T. Fuchigami and T. Nonaka, *J. Electroanal. Chem.*, **303**(1991)139.

66) G. Tourillon and F. Garnier, *J. Electroanal. Chem.*, **161**(1984)407.

67) G. Kossmehl and M. Niemitz, *Synth. Met.*, **41**(1991)1065.

68) S. Sunde, G. Hagan and R. Ødegård, *Synth. Met.*, **43**(1991)2983.

69) S. Sunde, G. Hagan and R. Ødegård, *J. Electrochem. Soc.*, **138**(1991)2561.

70) J. Roncali, L. H. Shi, R. Garreau, F. Garnier and M. Lemaire, *Synth. Met.*, **36**(1990)267.

71) A. H. Schroeder, F. B. Kaufman, V. Patel and E. M. Engler, *J. Electroanal. Chem.*, **113**(1980)193.

72) A. H. Schroder and F. B. Kaufman, *J. Electroanal. Chem.*, **113**(1980)209.

73) A.F. Diaz, J. Castillo, K. K. Kanazawa, J. A. Logan, M. Salmon and O. Fanjardo, *J. Electroanal. Chem.*, **133**(1981)237.

74) M. Sato, S. Tanaka and K. Kaeriyama, *J. Chem. Soc., Chem. Commun.*, (1986)873.

75) K. Y. Jen, G. G. Miller and R. L. Elsenbaumer, *J. Chem. Soc. Chem.* Commun.,(1986)1346.

76) G. B. Street in: T. A. Skotheim (Ed), *Handbook of Conducting Polymers*, Vol. 1. Marcel Dekker. New York., 1986 p305.

77) A. R. Diaz and J. Bargonin: T. A. Skotheim (Ed), *Handbook of Conducting Polymers*, Vol. 1. Marcel Dekker. New York., 1986 p99.

78) N. J. Morse, D. Rosseinsky, R. J. Mortimer and D. J. Walton, *J. Electroanal. Chem.*, **255**(1988)119.

79) A. Hairmerl and A. Merz, *Angew. Chem., Int. Ed. Engl.*, **25**(1986)180.

80) P. Aubert, G. Bidan and M. Lapkowski, *J. Chem. Soc., Chem. Commun.*,(1986)887.

81) D. Delabouglise and F. Garnier, *New J. Chem.*, **35**(1990)233.

82) M. Bodanszky, *Principles of Peptide Synthesis*, Springer Verlag, New York, 1984.

83) D. Delabouglise and F. Garnier, *Synth. Met.*, **39**(1990)117.

84) P. N. Bartlett and J. Farrington, *J. Electroanal. Chem.*, **261**(1989)471.

85) T. Schalkhammer, E. Mann-Buxbaum, F. Pittner and G. Urban, *Sensors and Actuators B*, 4(1991)273.

86) P. R. Griffiths and J. A. DeHaseth, *Fourier Transform Infrared Spectrometry*, John Wiley, 1986 p1.

87) J. B. Lambert, H. F. Shurwell, D. Lightner and R. G. Cooks, *Introduction to Organic Spectroscopy*, Macmillan, 1987 p147.

88) P. A. Christensen and A. Hamnett, *Electrochimica Acta*, **36**(1991)1263.

89) H. Neugebauer, A. Neckel and N. Brinda-Konopik in: H. Kuzmany, M. Mehring and S. Roth (Ed), *Electronic Properties of Polymers and Related Compounds*, Springer Verlag (Berlin) 1986 p227.

90) G. B. Street in: T. A. Skotheim (Ed), *Handbook of Conducting Polymers*, Marcel Dekker 1986 p279.

91) J. L. Bredas and G. B. Street, *Acc. Chem. Res.*, 18(1985)309.

92) N. Colaneri, M. Nowak, D. Spiegel, S. Hotta and A. J. Heeger, *Physical Review B*, 36(1987)7964.

93) M. J. Nowak, S. D. D. V. Rughputh, S. Hotta and A. J. Heeger, *Macromolecules*, 20(1987)965.

94) A. O. Patil, A. J. Heeger and F. Wudl, *Chem. Rev.*, 88(1988)183.

95) C. H. Pyun and S. M. Park, *Anal. Chem.*, 58(1986)251.

96) D. E. Stilwell and S. M. Park, *J. Electrochem. Soc.*, 136(1989)427.

97) S. M. Hoier, D. S. Ginley and S. M. Park, *J. Electrochem. Soc.*, 135(1988)91.

98) J. Roncali, P. Marque, R. Garreau, F. Garnier and M. Lemaire, *Macromolecules*, 23(1990)1347.

99) J. Kankare and J. Lukkari, *Synth. Met.*, 43(1991)2839.

100) E. E. Bancroft, J. S. Sidwell and H. N. Blount, *Anal. Chem.*, 53(1981)1390.

101) D. D. Cunningham, A. Galal, C. V. Pham, E. T. Lewis, A. Burkhardt, L. Laguren-Davidson, A. Nkansah, O. Y. Ataman, H. Zimmer and H. B. Mark, *J. Electrochem. Soc.*, 135(1988)2750.

102) T. Amemiya, K. Hashimoto, A. Fujishima and K. Itoh, *J. Electrochem. Soc.*, 138(1991)2845.

103) J. Heinze, M. Storzbach and J. Mortensen, *Ber. Bunsenges. Phys. Chem.*, **91**(1987)960.

104) J. Roncali, F. Garnier, R. Garreau and M. Lemaire, *J. Chem. Soc., Chem. Commun.*, (1987)1500.

105) J. Roncali, R. Garreau, A. Yasser, P. Marque, F. Garnien and M. Lamaire, *J. Phys. Chem.*, **91**(1987)6709.

106) S. M. Dale, A. Glidle and A. R. Hillman, *J. Mater. Chem.*, **2**(1992)99.

107) R. Greef, R. Peat, L. M. Peter, D. Pletcher and J. Robinson, *Instrumental Methods in Electrochemistry*, Ellis Horwood 1985.

108) J. R. Macdonald and W. B. Johnson, *Impedance Spectroscopy Emphisizing Solid Materials and Systems*, Wiley, New York 1987.

109) J. Tanguy, N. Mermilliod and M. Hoclet, *J. Electrochem. Soc.*, **134**(1987)795.

110) R. A. Bull, F-R. Fan and A. J. Bard, *J. Electrochem. Soc.*, **129**(1982)1009.

111) S. H. Glarum and J. H. Marshall, *J. Electrchem. Soc.*, **134**(1987)143.

112) W. J. Albery and A. R. Mount, *J. Electroanal. Chem.*, **305**(1991)3.

113) A. R. Hillman, D. C. Loveday, M. J. Swann, S. Bruckenstein and C. P. Wilde, *J. Chem. Soc., Faraday Trans.*, **87**(1991)2047.

114) A. R. Hillman, M. J. Swann and S. Bruckenstein, *J. Phys. Chem.*, **95**(1991)3271.

115) G. Tourillon in: T. A. Skotheim (Ed), *Handbook of Conducting Polymers*, Marcel Dekker, New York, 1986 p 298.

116) A. P. Monkman and P. Adams, *Synth. Met.*, 41(1991)891.

117) T. A. Skotheim (Ed), *Handbook of Conducting Polymers*, Marcel Dekker, New York 1986.

118) U. Hayat, P. N. Bartlett, G. H. Dodd and M. H. Lewis, *J. Polym. Sci.,Part A, Polym. Chem.*, 26(1988)201.

119) G. Tourillon and F. Garnier, *J. Electroanal. Chem.*, 135(1982)173.

120) F. Garnier, G. Tourillon, M. Gazard and J. C. DuBois, *J. Electroanal. Chem.*, 148(1983)299.

121) J. Farrington, PhD Thesis, Univ. of Warwick, 1990.

122) A. J. Bard and L. R. Faulkner, *Electrochemical Methods, Fundamentals and Applications*, J. Wiley and Sons, New York, 1980.

123) P. H. Rieger, *Electrochemistry*, Prentice-Hall, New Jersey, 1987.

124) W. J. Albery and M. L. Hitchman, *Ring Disc Electrodes*, Oxford University Press, 1971.

125) W. J. Albery, *Electrode Kinetics*, Oxford University Press, 1975.

126) D. Pletcher, *A First Course in Electrode Processes*, The Electrochemical Consultancy, Romsey, 1991.

127) R. G. Whitaker, PhD. Thesis, University of Warwick, 1989.

128) R. M. C. Dawson, D. C. Elliott, W. H. Elliot and K. M. Jones, *Data For Biochemical Research*, Oxford University Press, New York, 1986.

129) J. A. Joule and G. F. Smith, *Heterocyclic Chemistry*, Van Nostrand Reinhold (UK), 1978.

130) A. R. Diaz and J. Bargan in: T. A. Skotheim (Ed), *Handbook of Conducting Polymers*, Marcel Dekker, New York 1986 p90.

131) T. Schalkhammer, E. Mann-Buxbaum, F. Pittner and G. Urban, *Sensors and Actuators* B, 4(1991)273.

132) H. W. Siesler and K. Holland-Moritz, *Infrared and Raman Spectroscopy of Polymers*, Marcel Dekker. New York 1980.

133) C. A. Ferreira, S. Aeigach, M. Delamar and P. C. Lacaza, *J. Electroanal. Chem.*, **284**(1990)351.

134) R. M. Izalt, J. S. Bradshaw, S. A. Nielson, J. D. Lamb and J. J. Christensen, *Chem. Rev.* **85**(1985)271.

135) J. Roncali, R. Garreau, D. Delabouglise, F. Garnier and M. Lemaire, *J. Chem. Soc., Chem. Commun.*, (1989)679.

136) J. Roncali, R. Garreau and M. Lemaire, *J. Electroanal. Chem.*, **278**(1990)373.

137) M. Anderson, P. O. Ekbald, T. Hjertberg, O. Wennerstrom and O. Inganas, *Polymer Communications*, **32**(1991)546.

138) D. Ofer and M. S. Wrighton, *J. Am. Chem. Soc.*, **101**(1988)4467.

139) W. J. Albery, F-B. Li and A. R. Mount, *J. Electroanal. Chem.*, **310**(1991)239.

140) F-B. Li and W. J. Albery, *Electrochemica Acta*, **37**(1992)393.

141) F-B. Li and W. J. Albery, *Langmuir*, **8**(1992)1645.

142) B. L. Whuler, G. Caple, A. Henderson, J. Francis, K. Contrell, S. Vogel and S. Gray, *J. Electrochem. Soc.*, **136**(1989)2769.

143) G. Mengoli, *Adv. Polym. Sci.*, **33**(1979)26.

144) R. J. Waltman, J. Bargan and A. Diaz, *J. Phys. Chem.*, **88**(1984)4343.

145) K. M. Choi, C. Y. Kim and K. H. Kim, *J. Phys. Chem.*, **96**(1992)3782.

146) T. F. Otero and J. Rodriguez, *J. Electroanal. Chem.*, **310**(1991)219.

147) S. Bruckenstein and J. W Sharkey, *J. Electroanal. Chem.*, **241**(1988)211.

148) F. Beck and M. Oberst, *J. Electroanal. Chem.*, **285**(1990)177.

149) E. F. Bowden, M. F. Dautartas and J. F. Evans, *J. Electroanal. Chem.*, **219**(1987)49.

150) P. Marque and J. Roncali, *J. Phys. Chem.*, **94**(1990)8614.

151) M. A. Vorotyntsev, L. I. Daikhin and M. D. Levi, *J. Electroanal. Chem.*, **332**(1992)213.

Appendix 1